Technische Universität München
Wissenschaftszentrum Weihenstephan
Lehrstuhl für Ökologische Chemie und Umweltanalytik

Development of a miniaturized immunochemical flow-injection system for on-site analysis of selected nitroaromatics and pesticides in water

Ioan Manuel Ciumasu

Vollständiger Abdruck der von der Fakultät Wissenschaftszentrum Weihenstephan für Ernährung, Landnutzung und Umwelt der Technischen Universität München zur Erlangung des akademischen Grades eines

Doktors der Naturwissenschaften (Dr. rer. nat.)

genehmigten Dissertation.

Vorsitzender: Univ.-Prof. Dr.rer.nat.habil. Wilfried Huber
Prüfer der Dissertation:
1. Univ.-Prof. Dr.rer.nat. Dr.h.c.(RO) Antonius Kettrup
2. Univ.-Prof. Dr.med.vet. Dr.med.vet.habil. Johann Bauer
3. Priv.-Doz. Dr.rer.nat. Petra Krämer

Die Dissertation wurde am 29.07.2005 bei der Technischen Universität München eingereicht und durch die Fakultät Wissenschaftszentrum Weihenstephan für Ernährung, Landnutzung und Umwelt am 09.11.2005 angenommen.

for my wife

Related research articles:

1. Ioan M. Ciumasu, Petra M. Krämer, Cristina M. Weber, Günther Kolb, David Tiemann, Stefan Windisch, Ines Frese, Antonius A. Kettrup. *A new, versatile field immunosensor for environmental pollutants. Development and proof of principle with TNT, diuron and atrazine*. Biosensors and Bioelectronics 21: 354-364. http://www.sciencedirect.com/science/journal/9565663

2. Petra M. Krämer, Elisabeth Kremmer, Cristina M. Weber, Ioan M. Ciumasu, Stephan Forster, Antonius A. Kettrup. *Development of new rat monoclonal antibodies with different selectivities and sensitivities for 2,4,6-trinitrotoluene (TNT) and other nitroaromatic compounds.* Analytical and Bioanalytical Chemistry 382: 1919-1933. http://www.springerlink.com/(cams0xblxzdzdfjaeuhfquca55)/app/home/isue.asp

Related oral presentations:

3. I. Frese (oral presenter), G.Kolb, D. Tiemann, P.M. Krämer, I.M. Ciumasu, C.M. Weber, 2003. *Development of an Optical Cell for an Automated Miniaturized Immunochemical Device for On-site Screening of Pesticides Residues in Water.* In: Proceedings of the Oral presentation at "Sensor 2003" International Trade Fair and Conference, 13-15 May 2003, Nuremberg, Germany. Further information on the conference at : http://www.sensorfairs.de/neu/SO3/index.html

4. G. Kolb (oral presenter), I. Frese, V. Hessel, I.M. Ciumasu, P.M. Krämer, H. Löwe, D. Tiemann, 2004. *An automated, portable immunochemical flow-injection system for on-site analysis of environmentally hazardous chemicals*. In: Proceedings of the Oral Presentation at Lab Automation 2004, 1-5 February 2004, San Jose, CA, USA. Further information on the conference at: http://labautomation.org/LA/LA04/conference

5. P.M. Krämer (oral presenter), I.M. Ciumasu, C.-M. Weber, A.A. Kettrup, D. Tiemann, I. Frese, G. Kolb, 2004. *Entwicklung eines neuen, tragbaren, automatisierten Einweg-immunosensors für eine Vor-Ort-Auswahl von mit Umweltschadstoffen belasteten Proben.* Abschlussveranstaltung des Graduiertenkollegs 'Analytische Chemie', 2.–4. Februar 2004, Blaubeuren.

Related posters:

6. P.M. Krämer, I.M. Ciumasu, C.M. Weber, G. Kolb, I. Frese, B. Werner, A.A. Kettrup. *Development of an automated miniaturized immunochemical device for on-site screening of pesticide residues in water*. Poster at "The 10th IUPAC International Congress on the Chemistry of Crop Protection", 4-9 August, 2002, Basel, Switzerland. Congress proceedings, Main Topic 6 – Residues and Consumer Safety, Subtopic 6a – Trends in Analytical Methods and Instrumentation, p 201;

7. I.M. Ciumasu, P.M. Krämer, C.M. Weber, G. Kolb, D. Tiemann, S. Windisch, I.Frese, A.A. Kettrup. *Single-use immunosensor for environmental pollutants. Proof of principle for nitroaromatics and pesticide.* The Eighth World Congress on Biosensors, 24-26 May 2004, Granada, Spain. Poster abstract (BS67) in the Congress Proceedings, Topic "Immunosensors".

8. P.M. Krämer, C.-M. Weber, I.M. Ciumasu, E. Kremmer, A.A. Kettrup. *Development of monoclonal antibodies for 2,4,6-trinitrotoluene and its metabolites 2-amino-4,6-dinitrotoluene and 4-amino-2,6-dinitrotoluene for their use in immunosensor.* The Eighth World Congress on Biosensors, 24-26 may 2004, Granada, Spain. Poster abstract (BS632) in the Congress Proceedings, Topic "Immunosensors".

ACKNOWLEDGEMENTS

This work was funded by the Bmbf (Ministry for Science and Education, Germany), project number FKZ 02WU0102. Bmbf also funded the work of the Institut für Mikrotechnik Mainz GmbH (IMM), the instrument manufacturer, project number FKZ 02WU0102.

The author feels grateful for the PhD studentship and the technical support provided by TUM, especially the Faculty of Nutrition, Agriculture and Environment, Department of Ecological Chemistry and Environmental Analysis as PhD student all along the research project (2001 – 2004) and for the finalization of the PhD thesis.

The author thanks GSF–National Research Centre for Environment and Health, Neuherberg, Germany, especially the Institute of Ecological Chemistry, for hosting this work and for insuring excellent research conditions during the research project.

The author thanks to Univ. Professor Dr. Antonius A. Kettrup for effective leadership and kind supervision of this PhD work.

The author thanks to the project leader, Dr. Petra M. Krämer, for fruitful and pleasant collaboration, and for precious help in forging a professional personality.

The author thanks Dr. Ing. Günther Kolb, Dipl.-Ing. David Tiemann and Dr. Ines Frese, from IMM (Institut für Mikrotechnik Mainz), for their close collaboration.

The author thanks Dr. Elisabeth Kremmer, from GSF – Institute for Molecular Immunology, for her collaboration during our research project.

The author thanks Dipl.-Chem. Hartmut Thomas from WASAG DECON GmbH, BioPlanta, Leipzig for amiable exchange of scientific info and experience.

The author expresses his gratitude for the friendly collaboration of all the technical and scientific staff from the GSF Institute for Ecological Chemistry, especially Dr. Sigurd Schulte-Hostede – provisional director of the institute, Mrs Cristina Mihaela Weber, Dr. Mariana Neamtu, Dr. Monica Pantiru, Dipl.-Ing. Annette Franke, Mr. Geza Cocsis, Ms. Sylvia Oberleitner, Ms. Sabine Röttmuller and Mr. Stephan Forster.

But most of all I thank my wife, Maria Cristina Antal, for being so lovely all these years of geographical quasi-separation.

Abbreviations and acronyms

Ab	Antibody / antibodies
AFM	Atomic force microscopy
Ag	Antigen / antigens
An	Analyte
ARIS	Apoenzyme reactivation immunoassay
BSA	Bovine serum albumine
CE	Capillary electrophoresis
CEC	Capillary electro-chromatography
CFI	Continuous flow immunosensor
CR	Cross-reactivity
CV	Cyclic voltametry
DCC	1,3-Dicyclohexyl carbodiimide
Dil.	Dilution
DL	Detection limit
DMF	Dimethyl formamide
DNP-glycine	N-(2,4-dinitrophenyl)-glycine
DNP-γ-AmBA	2,4-Dinitrophenyl-γ-aminobutyric acid
DNP-ε-AmCA	2,4-Dinitrophenyl-ε-aminocaproic acid
DNT	Dinitrotoluene
DOM	Dissolved organic matter
ECD	Electron capture detection
EDC	1-Ethyl-3-(3-dimethylaminopropyl) carbodiimide
ELISA	Enzyme-linked immunosorbent assay
EPA	Environmental protection agency (USA)
Eq.	Equation no
Fab	Fraction antigen binding (of the Ab molecule)
Fc	Fraction constant (of the Ab molecule)
FIA	Flow-injection analysis
Fig.	Figure no
FP	Field prototype (of the developed immunosensor)
FRET	Fluorescence resonance energy transfer
Gam	Goat anti-mouse IgG
GC	Gas chromatography
GSF	GSF – National Research Centre for Environment and Health, Neuherberg, Germany

HRMS	High resolution mass spectrometry
HPLC	High performance liquid chromatography
HRP	Horseradish peroxidase (E.C. 1.11.1.7)
IgG	Immunoglobuline
IC	Ion chromatography
IC_{20}	Analyte concentration producing 20% inhibition
IC_{50}	Analyte concentration producing 50% inhibition
ICP	Inductively coupled plasma
IDLIF	Indirect laser-induced fluorescence
Inc.	Incubation
Ip	Isoproturon
IMM	Institut für Mikrotechnik Mainz
IÖC	Institut für Ökologische Chemie - GSF
ITMS	Ion trap mass spectrometry
k_a	Association constant
k_d	Dissociation constant
KLH	Keyhole limpet hemocynine
LASER	Light amplification by stimulated emission of radiation
LC	Liquid chromatography
LP	Laboratory prototype (of the developed immunosensor)
µ-TAS	Micro-total-analysis-systems
mAb	Monoclonal antibody
MECK	Micellar electro-kinetic chromatography
MIMS	Membrane induction mass spectroscopy
MP	Skimmed milk, powder; used in solution
MPA	3-Mercaptopropanoic acid; mercaptan
MRL	Maximum residues level
MS	Mass spectrometry
MW	Molecular weight
NHS	N-hydroxysulfosuccinimide sodium salt
NMR	Nuclear mass resonance
NPD	Nitrogen-phosphorus detector
n	Number of measurements
NT	Nitrotoluene
OD	Optical density (absorbance reader)
PAN	Pesticide action network
PASA	Parallel affinity sensor array

PBS	Phosphate buffered saline
PBST	Phosphate buffered saline containing Tween 20
PMMA	Polymethylmethacrylate; acrylic glass; Plexiglas; Lucite (in USA)
POPs	Persistent organic pollutants
Pre-inc.	Pre-incubation of analyte before the enzyme-tracer
Prot A	Protein A
Prot A/G	Protein A/G
Prot G	Protein G
PTFE	Polytetrafluoroethene (plastics)
PVC	Polyvinyl chloride
RDX	Hexahydro-1,3,5-trinitro-1,3,5-triazine
READ	Reversed electron attachment detection
RLU	Relative light units
RP-HPLC	Reverse-phase HPLC
RT	Room temperature
SAM(s)	Self-assembled monolayer(s)
SEM	Scanning electron microscopy
SFA	Segmented flow analysis
SPE	Solid-phase extraction
SPMDs	Semipermeable membrane devices
SPME	Solid-phase microextraction
STM	Scanning tunnelling microscopy
TAT	2,4,6-Triaminotoluene
TMB	3,3',5,5'-Tetramethylbenzidine
TNT	2,4,6-Trinitrotoluene
TNP–glycylglycine	Trinitrophenyl-glycylglycine
TNP-α-AmBA	Trinitrophenyl-α-Aminobutyric acid
Tr	Enzyme-tracer
UV	Ultraviolet
w/v	Weight per volume
(n)x	(n) times
Y/m/d	Year / month / day
Zero dose	Reference; analyte (standard) concentration 0 µg l^{-1}

List of tables

Table 1. Chemicals and standards
Table 2. Composition of the used buffers
Table 3. Composition of the used substrates for HRP
Table 4. Catching proteins / antibodies
Table 5. Anti-analyte monoclonal antibodies, enzyme-tracers, and enzymes for producing enzyme-tracers
Table 6. Proteins, surfactants and buffers that were used as blocking solutions
Table 7. Materials and instruments
Table 8. Surfaces and volumes specific to each stage of the sensor development
Table 9. Cross-reactivities in TNT-ELISA, with the in-house produced enzyme-tracer TNP-Glycylglycine–HRP, as compared with the literature (Zeck et al., 1999)
Table 10. Methods used for the analysis of explosives and their degradation products in water and soil
Table 11. Nitroaromatic compounds used in ELISA, with molecular structures and measured cross-reactivity (CR)
Table 12. Comparative table with standard curve parameters obtained with various catching proteins in TNT-ELISA
Table 13. Automatic steps: Program for fluid handling and measurement of one chip
Table 14. Automatic steps: Program for preparation washing (for making the conduit air-free) before starting any measurement and after finishing all the measurements
Table 15. Automatic steps: Program for substrate set-up before measurements
Table 16. Automatic steps: Program for the washing of the ground plate in between measurements (to avoid inter-measurements contamination)

List of figures

Figure 1. Details (A) and portable box (B) of the temperature-controlled field prototype
Figure 2. Hypothetical standard curves (%Control)
Figure 3. Variable reaction speeds in the formation of Ab-Ag complexes towards equilibrium
Figure 4. Hypothetical example for the relative importance of direct inhibition, facilitated binding and feed-back inhibition of Tr, at a given moment of the incubation time
Figure 5. Hypothetical standard curves (%Control) with different relative importance of facilitated binding and feed-back inhibition of Tr

Figure 6. Combined representation of the inhibition dynamic with competing antigens (standard curve), and dissociation of Ab – An complexes formed before washing and Tr incubation

Figure 7. Combined representation of the inhibition dynamic with competing antigens (standard curve), and dissociation of Ab – An complexes formed before washing and Tr incubation

Figure 8. Laboratory sensor prototype

Figure 9. Field sensor prototype (portable box)

Figure 10. Field prototype – user interface

Figure 11. Golden structures in experimental glass vials (batch ELISA set-up)

Figure 12. Golden structures in glass vials detailed view of two structure types: A. Final version (Aspect 1); B. Earlier version (Aspect 0.5)

Figure 13. Golden structures detailed view of the final version

Figure 14. Single-use chips

Figure 15. Scheme of the incubation / measurement cell and of the detection principle

Figure 16. Standard curves, with TNT-ELISA, using the enzyme-tracers TNP-glycyl-glycine–HRP and DNP-γ-AmBA–HRP

Figure 17. Standard curves, optimization with TNT-ELISA, using the Tr DNP-γ-AmBA–HRP

Figure 18. Standard curves, with TNT-ELISA, using the enzyme-tracers TNP-α-AmBA–HRP, and DNP-ε-AmCA–HRP

Figure 19. Stability of the current Tr (TNP-Glycylgycine – HRP) in time, at +3°C, and at -28°C with the commercial SuperFreeze stabilizor

Figure 20. Standard curves, with 2,4,6-TNT and its main degradation products (◇) 2-amino-4,6-DNT and 4-amino-2,6-DNT

Figure 21. Standard curves, with TNT-ELISA, using two different coating reagents and an Ab concentration of 400 μg l^{-1}

Figure 22. Standard curves, with TNT-ELISA, using two different coating reagents and an Ab concentration of 285 μg l^{-1}

Figure 23. Standard curves, with TNT-ELISA, using three different coating reagents and an Ab concentration of 400 μg l^{-1}

Figure 24. Standard curves – TNT-ELISA optimizations, using Protein A/G and two Ab concentrations

Figure 25. Standard curves, with TNT-ELISA, using three different Ab concentrations which were applied directly on microtiter plate (no catching protein)

Figure 26. Standard curves, with fast TNT-ELISA, with three Ab concentrations which were immobilized via Gam

Figure 27. Standard curves, with fast TNT-ELISA, with three Ab concentrations which were immobilized directly on the wall of the microtiter plate wells

Figure 28. Standard curves, with TNT-ELISA on Gam, using standards in Milli-Q water and in 40 mM PBS

Figure 29. Standard curves, with TNT-ELISA on Protein A, using standards in Milli-Q water and in 40 mM PBS

Figure 30. Standard curves, with fast TNT-ELISA, using three different buffer molarities for the Tr solution

Figure 31. Standard curves, with fast TNT-ELISA, employing the usual buffer 40 mM PBS or 40 mM PBST (0.05%)

Figure 32. Standard curves, with TNT-ELISA, using three different buffers for the anti-TNT mAb solution. The Tr solution was prepared in 40 mM PBS

Figure 33. Standard curves, with TNT-ELISA, using three different buffers for the anti-TNT mAb solution. The Tr solution was prepared in 4 mM PBST

Figure 34. Standard curves, with TNT-ELISA, with the Tr in 40 mM PBS, containing three different concentrations of Tween 20: 0.00 %; 0.05 %; 0.50 %

Figure 35. Standard curves, with TNT-ELISA, applying washing with 4 mM PBST and 4 mM PBS. The antibody and Tr solutions were prepared in 40 mM PBS

Figure 36. Standard curves, with fast TNT-ELISA, applying washing with 4 mM PBST and 4 mM PBS. The antibody and Tr solutions were prepared in 40 mM PBS

Figure 37. Standard curves, with TNT-ELISA, applying washing with 4 mM PBST and 4 mM PBS. The antibody and Tr solutions were prepared in 4 mM PBST

Figure 38. Standard curves, with TNT-ELISA (incubations: mAb 120 min; TNT/Tr 30 min; H_2O_2 / TMB 10 min), applying washing with 4 mM PBST and 4 mM PBS. The antibody solution was prepared in PBST, but the Tr solution was prepared in 40 mM PBS

Figure 39. With TNT-ELISA, the standard curve maintained its parameters in insignificant variations at pH values between 4 and 10

Figure 40. With TNT-ELISA, the standard curve maintained its parameters in insignificant variations at pH 3 and pH 8

Figure 41. With TNT-ELISA, the standard curve maintained its parameters in insignificant variations with up to 5% 2-isopropanol in the standard solutions (in water)

Figure 42. With TNT-ELISA, the standard curve maintained its parameters in insignificant variations with up to 5% methanol in the standard solutions (in water)

Figure 43. With TNT-spiked LUFA soil, standard curve shifted moderately to the right by methanol extracts, and more significantly by isopropanol extracts

Figure 44. With TNT-spiked Merzenhausen soil, standard curve shifted moderately to the right by methanol extracts, and strongly (almost 2 orders of magnitude) by isopropanol extracts

Figure 45. With methanol extracts, the standard curve shifted moderately to the right in both soil types

Figure 46. Three-curve pattern with isoproturon-ELISA when each incubation step lasted 30 min

Figure 47. Three-curve pattern with isoproturon-ELISA when each incubation step lasted 10 min

Figure 48. Three-curve pattern with isoproturon-ELISA when each incubation step lasted 3 min

Figure 49. Three-curve pattern with diuron-ELISA when each incubation step lasted 10 min

Figure 50. Three-curve pattern with diuron-ELISA when each incubation step lasted 3 min

Figure 51. Three-curve pattern with atrazine-ELISA when each incubation step lasted 10 min

Figure 52. Three-curve pattern with atrazine-ELISA when each incubation step lasted 10 min

Figure 53. Three-curve pattern with TNT-ELISA when each incubation step lasted 10 min

Figure 54. In the immunoassay set-up (TNT+Buffer / washing / Buffer+Tr), some inhibition is visible (ca. 40-50 % controls), and this is similar at shorter and longer TNT incubations

Figure 55. In the immunoassay set-up (TNT+Buffer / washing / Buffer+Tr), some inhibition is visible (ca. 50-60 % controls), and this is similar at shorter and longer Tr incubations

Figure 56. In the immunoassay set-up (Buffer+Tr / washing / TNT+Buffer), some inhibition is visible (ca. 40-80 % controls), and this is getting better with longer TNT incubations

Figure 57. In the immunoassay set-up (Buffer+Tr / washing / TNT+Buffer), some inhibition is visible (ca. 30 % control), but it does not increase with longer TNT incubations

Figure 58. Two-slope standard curves with TNT-ELISA

Figure 59. Two-slope standard curve with isoproturon-ELISA, in format (Ip+Buffer / washing / Buffer+Tr)

Figure 60. Two-slope curves with TNT-ELISA in format (TNT+Buffer / washing / Buffer+ Tr). TNT was incubated 10 min

Figure 61. Facilitated binding of Tr in the presence of increasing concentrations of TNT, below the optimized detection (inhibition) limit of 0.1 µg l^{-1}

Figure 62. Facilitated binding of Tr in the presence of increasing concentrations of TNT, below the optimized detection (inhibition) limit of 0.1 µg l^{-1}

Figure 63. Facilitated binding of Tr, at shorter incubation time, in the presence of increasing concentrations of TNT, below 0.1 µg l^{-1}

Figure 64. Facilitated binding of Tr, at shorter incubation time, in the presence of increasing concentrations of TNT, below 0.1 µg l^{-1}

Figure 65. Facilitated binding of Tr, at shorter incubation time, in the presence of increasing concentrations of TNT, at all doses

Figure 66. Facilitated binding of Tr, at shorter incubation time, in the presence of increasing concentrations of TNT, at all doses

Figure 67. Facilitated binding of Tr, at shorter incubation time, in the presence of increasing concentrations of TNT, at all doses

Figure 68. Facilitated binding of Tr, at shorter incubation time, in the presence of increasing concentrations of TNT, at all doses

Figure 69. Feed-back inhibition occurring around the detection limit (IC_{20}) (between 0.001 – 0.01 µg l^{-1}) with the TNT assay (two different Tr)

Figure 70. Feed-back inhibition occurring just before the detection limit (IC_{20}) (between 0.001 – 0.01 µg l^{-1}) with the isoproturon assay

Figure 71. Standard curve obtained with isoproturon-ELISA, applying a very high sampling intensity (n = 60)

Figure 72. Standard curves obtained with isoproturon-ELISA, with moderately low (though common) sampling intensity (n = 3)

Figure 73. Standard curves for TNT (n =5), diuron (n = 3) and atrazine (n = 5), produced with fast ELISA

Figure 74. Standard curves produced with fast isoproturon-ELISA

Figure 75. Preliminary standard curve with different structure aspects (n = 1), obtained with TNT batch ELISA, in Eppendorf plastic vials

Figure 76. Standard curve with different structure aspects (n = 2), obtained with TNT batch ELISA, in glass vials

Figure 77. Standard curve with different structure aspects (n = 2), obtained with TNT batch ELISA in glass vials, blocking step with skimmed milk powder (1% (w/v), 1h at RT), in PBST 4 mM, applied after antibody immobilization

Figure 78. Standard curve (n = 3), obtained with TNT batch ELISA on small pyramids (structure aspect 0.5), with three different BSA concentrations in mAb solution

Figure 79. Standard curve (n = 3), obtained with TNT batch ELISA on tall pyramids (structure aspect 2), with three different BSA concentrations in mAb solution

Figure 80. Standard curve (n = 4), obtained with TNT batch ELISA on small pyramids (structure aspect 0.5) and taller pyramids (structure aspect 2), with 1% Casein in a separate incubation step after the mAb immobilization step

Figure 81. Standard curve (n = 2), obtained with TNT batch ELISA on taller pyramids (structure aspect 2), with 4 mM PBS / 4 mM PBST as washing buffers

Figure 82. Standard curve (n = 2), obtained with TNT batch ELISA on taller pyramids (structure aspect 2), with 4 mM PBS as washing buffer

Figure 83. Low dose hook (n = 2) obtained in TNT batch ELISA optimizations (here taller pyramids - structure aspect 2)

Figure 84. Standard curve (n = 2), obtained with TNT batch ELISA on taller pyramids (structure aspect 2), with 120 min / 10 min antibody (anti-TNT) incubation time

Figure 85. Inhibition pattern (n = 2), obtained with TNT batch ELISA on the same golden structure type that was applied in the biosensors chip, with covalent attachment vs. physical adsorption of Protein A/G

Figure 86. Comparison between the inhibition patterns obtained with TNT batch ELISA (n = 2) by the golden structures onto which Protein A/G was covalently attached anew ("new covalent") and two days earlier ("old covalent"; fig. 83)

Figure 87. Standard curves for TNT, diuron and atrazine, produced with batch ELISA. Standards and Tr (both in 40 mM PBS) were incubated together

Figure 88. Standard curves (n = 3), obtained with isoproturon batch ELISA on the golden structure type (structure aspect 1) that was employed in the sensor), with 1h / no An pre-incubation time

Figure 89. Standard curves (n = 3), obtained with isoproturon batch ELISA on the golden structure type (structure aspect 1) that was employed in the sensor, with 2x / 3x washing (with 4 mM PBST, 1ml/ vial)

Figure 90. Scheme of the experimental steps needed for measuring with the sensor prototype

Figure 91. Typically, the inhibition obtained by on-line measurements (n = 3) with the laboratory prototype was very poor

Figure 92. Typically, the inhibition obtained by on-line measurements (n = 2) with the field prototype was very poor

Figure 93. Inhibition obtained with off-line measurements (n = 1), in the mixed antigens format. For each chip type, one pair of chips (zero dose chip and inhibition chip) was measured each day, 4 days in a row

Figure 94. Inhibition obtained with 10 µg l^{-1}, by on-line measurements (n = 1), in the mixed antigens format, with both normal and high volume chips

Figure 95. Inhibition obtained with 100 µg l^{-1}, by on-line measurements (n = 1), in the mixed antigens format, with both normal and high volume chips

Figure 96. Inhibition obtained with 10 min vs. 5 min duration of the antigens incubation, by on-line measurements (n = 1), in the mixed antigens format

Figure 97. Inhibition obtained with 5 min vs. 2 min duration of the antigens incubation, by on-line measurements (n = 1), in the mixed antigens format

Figure 98. Inhibition obtained with the sequential saturation format (n = 1), by on-line measurements with the field prototype, with the Tr incubations of 1 / 3 / 9 min

Figure 99. Inhibition obtained with two different dilutions (1: 4,000 and 1: 6,000) of the Tr, by on-line measurements (n = 1), in the competitive saturation (mixed antigens) format

Figure 100. Preliminary standard curve obtained in three different days, by on-line measurements (n = 1), with the competitive saturation format.

Figure 101. Standard curves ELISA for TNT, diuron and atrazine, produced with the immunosensor field prototype

Figure 102. Standard curves with isoproturon in microtiter plate (n=6) and batch ELISA (n=3)

Figure 103. Pilot on-line measurements with the immunosensor (field prototype) with 100 µg l^{-1} TNT, with Protein A/G coated by covalent binding (n = 2) and by adsorbtion (n = 1)

Figure 104. Typical development of luminescence signal on competitively bound Tr on monoclonal anti-TNT antibody

Figure 105. Development of luminescence signal after coating with catching protein /antibody and anti-TNT mAb, in the absence of the Tr

Figure 106. Intensity of luminescence signal produced after coating with Gam decreases with higher process temperature longer (a) and store time (b)

Figure 107. Intensity of luminescence signal produced by antibodies is higher when antibodies bound TNT

Figure 108. Scheme of the conduit in the sensor platform (ground plate and chip)

Figure 109. The micromixer manufactured by IMM and incorporated into the developed biosensor: A) General view; B) Mixing principle; C) Lamellae detail

Figure 110. View of the developed sensor field prototype (lid on; in the GSF-IÖC laboratory)

Figure 111. View of a set of 10 chips which could be measured in one day

Figure 112. Example of two-dimensional titration with three concentrations of the anti-TNT antibody and eight dilutions of the enzyme-tracer TNP-glycylglycine – HRP: lower tracer dilutions

Figure 113. Example of two-dimensional titration with three concentrations of the anti-TNT antibody and eight dilutions of the enzyme-tracer TNP-glycylglycine – HRP: higher tracer dilutions

Figure 114. Standard curve and edge effect with TNT-ELISA

TABLE OF CONTENT

page

1. INTRODUCTION ……..... 21

1.1. Environmental pollution with nitroaromatics and pesticides …… 21

1.1.1. Pollution with TNT and its degradation products …….. 22

1.1.2. Pollution with pesticides …… 27

1.2. Field and laboratory approaches in environmental analytics ……... 28

1.3. Environmental analysis of nitroaromatics – state of the art …….. 30

1.4. The general objective of the thesis ……... 33

2. THEORETICAL FRAME ……... 36

2.1. Fundamentals of immunoassays ……..... 36

2.1.1. Antibody - antigen system dynamics ……... 36

2.1.2. Typical standard curves …… 39

2.1.3. The source of the complex behaviour in systems made up by one antibody and two antigens …… 41

2.2. Theoretical predictions on the immunoassay flexibility ……..…… 43

2.2.1. Case of concern …….. 43

2.2.2. Direct inhibition ……..... 43

2.2.3. Facilitated binding ……... 44

2.2.4. Low dose hook …… 45

2.2.5. Feed-back inhibition ……... 45

2.2.6. Interaction between direct inhibition, facilitated binding and feed-back inhibition ……..... 46

2.2.7. Standard curves with separated incubations of antigens …… 48

3. MATERIALS AND METHODS …… 52

3.1. **Materials** ……..... 52

3.1.1. Chemicals and standards …….. 52

3.1.2. Buffers and enzyme substrates ……..... 53

3.1.3. Proteins, antibodies and enzyme-tracers ……... 54

3.1.4. Materials and instruments …….. 55

3.1.5. Automated and miniaturized flow-injection analysis ……..... 56

3.1.6. Solid supports for antibody immobilization …….. 61

3.2. Methods ……... 65

3.2.1. General remarks …….. 65

page

3.2.2. Antibody immobilization …….… 65
3.2.2.1. Adsorption of coating proteins …….. 65
3.2.2.2. Covalent attachment of coating proteins …….… 66
3.2.3. Preparation of enzyme-tracers …….. 68
3.2.4. ELISAs on microtiter plates ……... 69
3.2.4.1. Competitive saturation ELISAs on microtiter plates …….. 69
3.2.4.2. Sequential saturation ELISAs on microtiter plates ……... 70
3.2.4.3. Further methods: soil TNT spiking, TNT extraction, and ELISA with soil extracts …….…71
3.2.5. Competitive saturation ELISAs on batch structures …….. 72
3.2.5.1. Selection of the material for structures ……... 72
3.2.5.2. Selection of the structure (pyramids) geometry …….… 73
3.2.5.3. General batch ELISA procedure …….. 74
3.2.5.4. Regeneration of the golden structures ……..……. 74
3.2.5.5. TNT batch ELISA ……... 75
3.2.5.6. Atrazine batch ELISA…….. 75
3.2.5.7. Diuron batch ELISA ……... 75
3.2.5.8. Isoproturon batch ELISA ……... 75
3.2.6. ELISAs by the immunosensor prototypes (demonstrators) …….. 75
3.2.6.1. Off-line preparation of the chips …… 75
3.2.6.2. Automated (on-line) measurements ……. 76
3.2.6.3. Chip regeneration …… 77
3.2.7. Data analysis ……... 77

4. RESULTS AND DISCUSSION …….… 78

4.1. Immunoassay design and flexibility ……... 78
4.1.1. TNT competitive assays …….… 78
4.1.1.1. Panel of new enzyme-tracers ……... 78
4.1.1.2. Stability of enzyme-tracers ……... 80
4.1.1.3. Assay performances with the new enzyme-tracers ……... 82
4.1.1.3.1. General assay performances ……... 82
4.1.1.3.2. Influence of the coating protein ……... 84
4.1.1.3.3. Influence of the reaction buffer …… 89
4.1.1.3.4. Influence of Tween 20 ……... 93
4.1.1.3.5. Further developments ……... 96

page

4.1.1.4. Influence of the physical parameters in TNT-ELISA ……..….. 97
4.1.1.4.1. Influence of temperature ……..... 97
4.1.1.4.2. Influence of pH ……..... 99
4.1.1.4.3. Influence of solvents ……... 101
4.1.1.5. Influence of soil matrix ……. 105
4.1.2. Patterns of reciprocal displacement between antigens …….. 108
4.1.2.1. Three-curve pattern with the isoproturon assay ……..... 109
4.1.2.2. Three-curve pattern with the diuron assay ……... 111
4.1.2.3. Three-curve pattern with the atrazine assay ……... 112
4.1.2.4. Three-curve pattern with the TNT assay …….. 114
4.1.3. Variation in the shape of the standard curve ……... 117
4.1.3.1. Intermediary inhibition plateau ……... 117
4.1.3.2. The low dose hook and the feed-back inhibition ……. 120
4.1.3.2.1. Curves obtained with sequential saturation …..... 121
4.1.3.2.2. Curves obtained with competitive saturation …… 126
4.1.3.2.3. Discussion ……. 128
4.1.3.3. Dependence on sampling intensity ……... 130

4.2. Optimized fast immunoassays on microtiter plates ……. 132
4.2.1. Fast ELISA with TNT, atrazine, diuron and isoproturon ……. 132
4.2.2. Troubleshooting in fast ELISA ……... 134

4.3. Optimizations of competitive saturation ELISA on batch structures …….. 135
4.3.1. General requirements for batch ELISA ……. 135
4.3.2. Batch ELISA developments with TNT ……... 136
4.3.3. Optimized batch ELISA with TNT, atrazine and diuron …….. 149
4.3.4. Batch ELISA developments with isoproturon ……... 150
4.3.5. Troubleshooting with batch ELISA ……. 152

4.4. Competitive immunoassays using the immunosensor prototype ……..... 153
4.4.1. Probing measurements with prototypes (demonstrators) …….. 153
4.4.1.1. General remarks on measuring with the sensor …….. 153
4.4.1.2. Measurements …….. 155
4.4.1.3. Preliminary standard curve with on-line measurements …..... 161
4.4.2. Optimizations and proof of principle with TNT, atrazine and diuron ……. 163
4.4.3. Further developments ……..……... 165
4.4.3.1. Developments with isoproturon …….. 165
4.4.3.2. Covalent immobilization of Protein A/G ……. 166

Page

4.4.4. Trouble shooting in sensor measurements ……..... 168
4.4.4.1. Background luminescence …….… 168
4.4.4.2. The low dose hook ……... 173
4.4.4.3. Unspecific binding of the enzyme-tracer ……... 174
4.4.4.4. Analyte adsorption to the channel wall …….. 174
4.4.4.5. Blocked channels and micromixer ……. 177
4.4.4.6. Lose rubber disks (air bubbles) ……..... 177
4.4.4.7. Unevenly drawing micromixer …… 178
4.4.4.8. Process temperature ……..... 180

5. SUMMARY AND OUTLOOK ……..... 181

6. LITERATURE ……... 186

7. ANNEXE

Annex 1. General properties of TNT, atrazine, diuron and isoproturon …….. 224
Annex 2. Methods used for the analysis of explosives and their degradation products in water and soil ……... 228
Annex 3. View of the developed sensor field prototype (lid on), and of a set of 10 chips ……..... 231
Annex 4. Nitroaromatic compounds used in ELISA, with molecular structures and measured cross-reactivity ……..… 232
Annex 5. Two dimensional titrations with anti-TNT mAb and the enzyme-tracer TNP-glycylglycine–HRP ……..... 235
Annex 6. Standard curve parameters obtained with various catching proteins in TNT-ELISA ……... 237
Annex 7. Specific programs for the automatic steps carried with the developed sensor …… 239
Annex 8. The edge effect observed with TNT-ELISA ……... 241

CURRICULUM VITAE …… 242

1. INTRODUCTION

1.1. Environmental pollution with nitroaromatics and pesticides

Social acknowledgement of the necessity that people take good care of the Earth is quite new. Until recently, our cultural heritage proclaimed humans "to be something apart from, even over and above, the beasts of the field." (Niles Eldredge). First, humans were akin with the entire living world. Then, humans created goods and instituted "dominion over the nature" (Eldredge, 1995).

Nowadays, we know very well that natural resources need adaptive management with rather tighten cost and benefit loops (Arrow et al., 2000; Farber and Griner, 2000), and that human economy can survive on long term only through careful cognition upon environment, and tool-codes of environmental management practice (Nash and Ehrenfeld, 1997; Chua, 1999).

Society began to understand well that short-sighted exploitation and irresponsible pollution of the environment is going to hit back. This happens, notably, because numerous man-made chemicals revealed complex toxicological effects on humans. Some good examples are the disorders of the human hormonal system (Keith, 1997; Hock et al., 2000a), and the destructions of ecosystems (Korte, 1980; Kettrup et al., 1991; Hulpke et al., 2000).

The concept of industrial hygiene became a recognized necessity (Harper et al, 1997), along with environmentally conscious design of chemical and technological development (Cano-Ruiz and McRae, 1998; Grübler et al., 1999; Adriaens et al., 2003). In many countries, large efforts are currently made for assessing the fate of man-made chemicals in nature, as well as their risks to humans and to environment (Stadlbauer, 1999; Draper, 2001; Jager et al., 2001; Sabljic and Peijnenburg, 2001).

Pesticides and nitroaromatics are two hard-weighing examples of persistent organic pollutants (POPs), both through their long history of use and misuse, and their problematic toxicological assessment and environmental sanitation. Each such pollutant makes a complex issue, requiring comprehension and long-sustained action towards cost-effective pollution assessment and cost-effective remediation.

POPs were subject to several international actions towards pollution limitations and alternative strategies (Mörner et al., UNEP, 2002) like the Stockholm Convention (into force since 17 May 2004), the U.N. Workshop to Develop a Global POPs Monitoring Programme to Support the Effectiveness Evaluation of the Stockholm Convention (Geneva, 24-27 May 2003) and the U.N. POPs Global Monitoring Programme.

In Europe, the EU drinking water directive (80/68/EC) and the water framework directive (2000/60/EC) have been the most important in driving water regulatory standards and analytical methodology (Schmitz, 2001; Oehmichen et al., 2003). The maximum permitted concentration is 0.1 µg l^{-1} for any individual pesticide, and a maximum total concentration of 0.5 µg l^{-1} for the total amount of pesticide residues (though these limits may undergo some changes).

For the sake of human and environmental health survey and action in Europe and in the world, huge efforts are currently made towards ever better analytical methods and approaches. Many pollutants priority lists are already in place, requiring acquisition and up-dating of analytical and toxicological data.

For all these, the classical laboratory methods need to be assisted by novatory, on-site techniques. Pioneer methods are already proving great potential, both in the field of analysis, e.g. biosensors for environmental pollutants (Rogers and Gerlach, 1999; Scheler et al., 2001; EWCB, 2004; Turner, 2005), and in the field of environmental remediation, e.g. biological and biotechnological remediation (Lau and DeLorenzo, 1999).

The scope and contribution of the present thesis is the development of a flexible analytical tool for on-site water analysis of such pollutants like nitroaromatics and pesticides. The developed analytical platform is a versatile biosensor which uses antibodies as recognition element. This prototype is a field (or laboratory) instrument onto which the ELISA technique is adapted, and oriented towards several choice pollutants: TNT, atrazine, diuron and isoproturon. In principle, the number of target analytes is limited only by the number of available, extant immunoassays (Hock et al., 2000b).

1.1.1. Pollution with TNT and its degradation products

TNT is a light-yellow solid used as high-explosive. Because of its high chemical stability and low sensitivity to impact, friction and temperature, TNT is relatively manufacture-, handling-, and storage-safe. Because of its properties (technical data in annex 1-A), TNT was the most widely used explosive in the 20th century. TNT is also used as an intermediate in the manufacture of dyestuff and photographic chemicals (Sax and Lewis, 1987). TNT can enter the environment from leachates at the disposal (or abandonment) sites and from production facilities (Opresko, 2005). Water polluted with TNT is also known as "pink water" or "red water", because of the characteristic reddish colour (US Dpt of the Army TM 5-814-8, 1987; Wu, 2001; Eriksson, 2003).

In the past, the explosive properties of mixtures containing TNT were employed in mining, or as gun-powder ("black-powder"). History recorded controlled preparation of TNT in 1863 by J. Wilbrand, first detailed study on TNT in 1870, first preparation of pure TNT in

1880, and establishment of the chemical structure in 1883 by Claus and Becker (Wisniak, 2000; Kelly, 2004). Manufacture of TNT started for the first time in 1891 in Germany, and was adopted in the German army in 1902. In 1912, TNT started to be used also in the USA army, but at present, TNT is no longer manufactured in the USA (Hwang et al, 1998). The first documented concerns and public actions about the environmental fate appeared around 1990, regarding the entrance of TNT in the food chains in the contaminated vegetation plots (Palazzo and Leggett, 1986; Harvey et al., 1997), and the contamination of the drinking water reservoirs (Schäfer, 2002; Eriksson, 2003).

1.1.1. A) Examples of polluted sites

In 1993, there were ca. 35,500 sites concerned with military-related pollution in Germany (Stadlbauer, 1997). The typical examples of areas polluted with TNT (and other explosives), are the ammunition plants.

One huge ammunition plant functioned between 1936 and 1945 at the Heeresmunitionsanstalt (MUNA) Nürnberg-Feucht, on ca. 300 ha. During the demilitarization period in 1946-1947, ca. 50,000 t ammunition was found in the area and subsequently destroyed. The area continued to be used by military. The strong soil pollution with TNT in the area is particularly concerning the neighbouring drinking water reservoirs (Schwendner, 1996), and this situation is not unique.

The ammunition plant "Werk Tanne" at Clausthal-Zellerfeld, Lower Saxony, one of the biggest manufacturing sites during World War II, was build by "Dynamit Nobel" in 1934-1939, on 120 ha, and it was destroyed in 1944-1945. Many years later, pollution with TNT continued to be extremely high, so that provisions for drinking water in the neighbour area had to be closed in 1991. Here, levels of contamination of 3,100 mg TNT / kg soil could be measured, and used for toxicological assessment (Schäfer, 2002). These sites also hosted some pilot studies aiming at removing TNT pollution via molecular degradation by microorganisms (fungi) (Michels, 1998).

Other two important sources of pollution were the explosives manufacture plants at Lichtenau-Hirschhagen (near Kassel), Hesse, and at Stadtallendorf (near Marburg), Hesse. The two sites are still a serious menace for people in the neighbourhood. These were the two largest explosives factories during World War II. The first, with hundred buildings spread over ca. 230 ha, produced ca. 135,000 t TNT between 1939 and 1945. Together, the two factories produced ca. 260,000 t TNT (the total production in this period in Germany was ca. 830,000 t TNT) (Scheider et al., 1996; Lemke, 1998). The former production plant in Lichtenau-Hirschhagen caused pollution of both soils and waters in the area, as well as

(in the late 80's) the groundwater, and it was subject for pilot sanitation studies (Warrelmann, 1996).

Another former explosive manufacture plant ("Carbonit") is at Leverkusen-Schlebusch, comprising a territory of ca. 84 ha, was already the subject of a sanitation program between 1993 and 1997 (AB Umweltanalytik, 1997; Radenberg and Sidiropulos, 1998).

The smaller former ammunition plant Elsnig, near Torgau, Saxony, was built in 1934-1935, and was later destroyed by the Soviets. There, soils and waters are strongly contaminated on ca. 8 km^2, which is very concerning, because these sites are close to the drinking water reservoir for the Halle/Leipzig area. Here, levels of contamination of 4,577 mg TNT / kg soil could be measured (Schäfer, 2002). Important pollution with TNT and other explosives exists at the former ammunition plants Stadtallendorf, Hesse, which was the largest in Europe during World War II, with some measured contamination levels of up to 15 mg TNT / kg soil; and at the storage facility for TNT at Hambüren, close to Celle (Lower Saxony), with some measured contamination levels of up to 350 mg TNT / Kg soil (Schäfer, 2002).

In the USA, the EPA national priority list contains 22 ammunition production and processing sites that are associated with areas that are strongly polluted with TNT and other nitroaromatics. In places, contamination with TNT is as high as 200 g / kg, which is much above the 10% threshold of explosive concentration – as established by the US Army Environmental Center (Hooker and Skeen, 1999; U.S. EPA NPL, 2005; Jenkins et al., 1996a). Explosives contamination also occurs at the military firing ranges, with soil contaminations usually ranging up to 75 mg / kg (Jenkins et al., 2001). Ca. 1,200 US army sites have pollution with TNT (Doppalapudi et al., 2000). An estimated ca. 0.82 million m^3 of soil is polluted with explosives at former ordnance sites and military proving grounds (Boyd and Bruce, 2002). Therefore, the US Army (its environmental divisions) surveys the pollution of soils and groundwaters with explosives and their degradation products (Pennington, 1999; Marion and Pelton, 2000).

1.1.1. B) Decontamination methods

Regarding its fate in nature, TNT generally undergoes transformation by sequential reduction of nitro groups to amino groups. Commonly observed reductive transformation products includes 2-amino-DNT, 4-amino-DNT, 2,4-diamino-NT and 2,6-diamino-NT. 2,4,6-Triaminotoluene (TAT) is also possible (Walsh et al., 1995; Brannon and Myers, 1997; Lendeman et al., 1998; Spanggord et al., 1997; Hawari et al., 1998; Schmidt et al., 1998; Vorbeck et al., 1998; Spanggord et al., 2000a,b; Zhang et al., 2000). It is known that

mobility of TNT in soils may be limited by its sorption into soils (U.S. EPA, 1990; Hundal et al., 2005) and by its coupling with the humic organic soil matrix (Dawel et al., 1997; Eriksson, 2003). Biological degradation by microorganisms is possible, though not easy.

Biological degradation of TNT is primarily a reductive process, but mineralization to CO_2 is extremely poor, and many of the degradation compounds are toxic (e.g. 2,4-DNT; 2,6-DNT, which are also manufacture intermediates, Stahl and Aust, 1993a; Hawari et al., 1998; Nishino et al., 1999; Stadlbauer, 1999). Poor mineralization of TNT to CO_2 during its biodegradation is probably due to the fact that bacteria use TNT primarily as a nitrogen source, and not as a carbon source, TAT being a metabolic dead end in certain conditions (Haeari et al., 1998; Wikström et al., 2000). At the same time, coupling of TNT with the humic matter appears as a common biodegradation pathway (Knicker and Müller, 2003). Combined abiotic and biotic degradation methods have a higher chance of TNT complete degradation, i.e. mineralization (Schrader and Hess, 2004).

Biological degradation of TNT and related nitroaromatics can take place through anaerobic (McCormick et al., 1976; Preuss et al., 1993; Daun et al., 1998; Lenke et al., 1998; Hofstetter, et al., 1999; Adrian and Campbell, 1999) or aerobic metabolic processes (Won et al., 1974; Carpenter et al., 1978; Stahl and Aust, 1993b; Gilcrease and Murphy, 1995; Warrelmann et al, 1996; Boopathy et al., 1997; French et al., 1998; Tope et al., 1999; Behrend and Heesche-Wagner, 1999). Such microorganisms are bacteria and fungi (Pasti-Grigsby, 1996; Meharg et al., 1997; Montpas et al., 1997; Kim and Song, 2000). Some algal and microbial TNT nitroreductase could even be isolated, purified and used for biological destruction of TNT (Wolfe et al., 1994; Oh et al., 2001). Spores of TNT degrading bacteria could be produced for usage as inoculum in TNT-polluted media (Sembries and Crawford, 1997). Anaerobic reduction of TNT to TAT can be enhanced by adding cosubstrates (like glucose or cathecol) for the enzymatic biodegradation (Hwang et al., 1998; Thiele et al., 2002).

These processes allow decontamination through cometabolic advanced degradation of TNT by amendments with microbial consortia (Tharakan and Gordon, 1999; Achtnich and Knackmuss, 2000; Beltz et al., 2001; Boyd and Bruce, 2002) for replacing incineration of TNT-polluted soil with anaerobic/aerobic composting (Bruns-Nagel et al., 1998; Achtnich and Lenke, 2001) or with decontamination-digestion by slurry reactors (Manning et al., 1994; Thorne and Leggett, 1999). A comprehensive review upon the biological degradation of TNT is provided by Esteve-Núñez et al., 2001.

Aquatic plants and the roots of some terrestrial higher plants can promote TNT degradation, but their potential is limited by various metabolical and toxicological effects (Mueller et al., 1995; Betts, 1997; Boyajian and Carreira, 1997; Thompson et al., 1998; Best

et al., 1997; 1999; 2004; Bhadra et al., 1999; Davis and Chou, 1996; Chekol and Vough, 200265; Schoenmuth, 2002; Thompson et al., 2003). Transgenic plants expressing microbial degradative enzymes of selected bacterial strains represent a high potential for remediation methods (French et al., 1999; Hooker and Skeen, 1999).

At present, granular activated carbon adsorption is the standard method in the US for treating wastewaters containing TNT (Hwang et al., 1998; Morley and Speitel, 1999), but in the past, open burning, detonation and incineration were generally used. Mild thermal degradation (Ecotechniek Bodem (Maarssen, NL), 1997), or oxidation in the presence of UV radiation (Wu, 2001) may also be applied under some particular conditions. TNT toxicity can be decreased, and remediation can be accelerated by activated carbon (Wu, 2001; Vasilyeva et al., 2001).

TNT can also be reduced to aminotoluenes by electrochemical treatments (Rieffler and Smets, 2000; Doppalapudi et al., 2000; Rodgers and Bunge, 2001). Alkaline hydrolysis can also result, under certain conditions, in a significant decay of TNT and its derivatives in contaminated soils, either as such (Emmrich, 2001; Wu, 2001) or combined with thermal or biological post-treatment (Saupe et al., 1998; Hawthorne et al., 2000). Abiotic reduction of TNT by Fe^{+2} and alkaline pH can also contribute to the TNT decay in soil (Brannon et al., 1998; Hoffman et al., 1999; Wu, 2001).

In surface waters, TNT may be broken down by sunlight (photolysis), with an estimated half-life of 1 to 6 months (Godejohann et al., 1998; Schmidt and Butte, 1999; Larson et al., 2000; Wu, 2001), but TNT can also reach groundwaters, hence the drinking water reservoirs (Harvey et al., 1997; Schäfer, 2002; Eriksson, 2003). Natural transport of TNT is limited by its low solubility in water and its strong variation of solubility with temperature: ca. 90 mg l^{-1} at 14°C; 130 mg l^{-1} at 20°C; 100 mg l^{-1} at 25°C and 190 mg l^{-1} at 33°C (Walsh et al., 1995; Wu, 2001; Eriksson, 2003). Despite this, TNT can leach as coupled with the dissolved organic matter (DOM). TNT tends not to accumulate at high levels in plants and animals (Phelan and Barnett, 2001; Eriksson, 2003).

1.1.1. C) Toxicological risks

TNT and its degradation products 2-amino-DNT and 4-amino-DNT are known to be toxic to wildlife among which some species are also important detritivores (e.g. *insects; fungi; worms*), which contribute to the natural circuits of organic matter in soils (Yinon, 1990; Johnson, 1998; Kratz and Riesbeck, 1998; Gong et al., 1999; Best et al., 2004).

Humans can be exposed to TNT by eating, drinking, touching or inhalation of contaminated soil, water, air or food. In humans, TNT is directed primarily to kidney, liver,

lungs and fat (in relation with the intake way), and it is excreted mainly through urine and bile (El-hawari et al., 1981; Weiss and Angerer, 2001).

Studies upon TNT toxicity are derived mainly from occupational medical studies and tests on animals (U.S. ATSDR, 1995; Opresko, 2005). The cytotoxicity and genotoxicity of nitroaromatic compounds is due to the bioactivation to metabolic intermediates that are highly reactive with proteins and DNA (Bakhtiar et al., 1997).

Accidental (acute) exposure to TNT can cause methaemoglobin-anaemia, breathing difficulties, cyanoses, headaches, blood hypotension, and even unconsciousness and coma. Chronic exposure to TNT gives, in addition, internal lesions and muscle pains (U.S. ATSDR, 1995).

Also, TNT is classified as potential carcinogen in Germany (class III B), and in USA (class C). Beside certain cytotoxicity in bacterial and mammal cells, TNT has also a mutagenic potential (Tan et al., 1992; Berthe-Corti et al., 1998). The recommended threshold TNT (toxicological) limit in drinking water is 1 µg l^{-1} in Germany, while in USA, the drinking water equivalent level (DWEL) is 20 µg l^{-1} (Schäfer, 2002; Opresko 2005).

1.1.2. Pollution with pesticides

For pesticides, the literature is very rich in studies and standardized information, and data banks exist for them. In the world, pesticides are reported as polluting virtually everything, from soils of Tibet (Fu et al., 2001) and the corral reefs (Hallock et al., 2004), to the human body fluids in Ghana (Ntow, 2001) and the supposedly healing medicinal herbs (Ahmed et al., 2001).

Many sources inform on sensitive data upon pesticides, as well as upon concrete actions against such pollution. For example, EU is already oriented towards a strategy of "sustainable" use of pesticides (Directive 91/414/EEC; Wattiez, 2002). Maximum residue levels (MRLs) for pesticides are set at the EU level for about 150 plant protection products; complete harmonization between the member states is expected by the end of 2005 (EU MRLs, 2004).

The Pesticide Action Network (PAN) published a catalogue of lists of pesticides with their harmful impacts, as well as a list with web addresses of governmental and non-governmental organizations, which provide technical information on pesticides and official regulations in the world (a list of the lists). PAN also provides a comprising survey on the costs to human and environment health of pesticides in water (PAN UK, 2000).

The pesticides that are subject to the analytical and methodological developments described in the present thesis are three well known herbicides (technical data in annex 1):

atrazine, diuron and isoproturon, all three present among the 33 compounds of the EU *List of Priority Substances* (Decision No 2455/2001/EC).

To acknowledge the threat that the mentioned three pesticides represent for the human health, it is enough to mention that they are still in use in many countries, especially in the under-developed world, despite the fact that they are toxic and have a serious potential or confirmed carcinogenicity. Thus, atrazine is indicated as possible human carcinogen by the U.S. EPA. Diuron is classified by EU as with possible risks of irreversible cancer effects, while it is acknowledged to cause cancer by U.S. EPA. Isoproturon is also classified by EU as with possible risks of irreversible cancer effects (PAN UK, 2001).

Atrazine is also identified as endocrine disruptor by EU and the World Wide Fund (WWF), and classified as potential endocrine disruptor by OSPAR (Oslo and Paris Commission for the Protection of the Marine Environment in the North-East Atlantic) (PAN UK, 2001).

Among the three target pesticides, atrazine is most concerning due to its combined widespread use and toxicity. For example, more than 37,000 tons of atrazine were used in agriculture in the US in 1997. Humans may be exposed to atrazine mainly in water, but it can travel by air currents. There are reports that atrazine was found at more than 300 km from the application site. Atrazine may have adverse effects upon human and animal health, its toxic effects being reported especially in the adult reproductive system and in the pre-adult stages of the organism development. Among such effects are perturbations of the reproductive physiology, incomplete ossification of skull and members, and neuro-behavioural modifications (U.S. ATSDR, 2003)

According to Pesticide Action Network, in 2000, atrazine, diuron and isoproturon frequently exceeded the drinking water standards (PAN UK, 2000), putting human health at risk. In soils, pesticides may be filtered and degraded, but these mechanisms are still poorly known (Burauel and Bassmann, 2005). All in all, the natural ecosystems and their self-depolluting mechanisms are strongly disturbed by the overall negative influence of certain pesticides upon aquatic (and soil) microorganisms (DeLorenzo, 2001; Hanazato, 2001).

1.2. Field and laboratory approaches in environmental analytics

The last decade witnessed an explosion in analytical methods and analytical performances. Precise identification and measurement of nitroaromatics and pesticides is carried out and further optimized by/with laboratory methods like HPLC; HPLC-NMR; GC; GC-ECD; GC-MS; IC; MIMS; CE; ICP/HRMS; plus analyte preconcentration methods (to avoid matrix effects), e.g. SPME (Clement et al., 2000; Richardson, 2001).

The economic dash brought a tremendous increase in the number of and amounts of artificial compounds introduced in environment through human activity. A huge amount of samples and analytes must be screened by alternative strategies, for many and very diverse scientific, economic and societal objectives. Effective management of pollution and remediation requires that relevance of analytical data and data models be maintained in functional limits through relatively fast and extensive sampling (Arrow et al., 2000; Farber and Griner, 2000; Lavine, 2000; Oks and Stein 2000; Martin, 2001).

Therefore, investigation of the extent and intensity of the pollution cannot be done exclusively with laboratory methods anymore. Instead, field analysis emerged as a necessary companion to laboratory analysis. The logistic and technical advantages of each of the two approaches began to attain complementarity towards more tailored analytical objectives (Clement et al., 2001).

Today, laboratory and field methods are rather viewed in terms of specific advantages and drawbacks. If compared with the field methods, laboratory methods are in general more precise, more accurate and better controlled. In exchange, laboratory methods are more resource consuming, require highly-qualified personnel, elaborate sample preparation (e.g. pre-extraction and stabilization) and (sometimes) sample prescreening. For example, EPA method 8330 (HPLC) for TNT is applied after prescreening with EPA method 4050 to see whether TNT is above 5 µg l^{-1} in water or 0.5 mg kg^{-1} in soil. With the HPLC method, the sample is sonicated 18 hrs in acetonitrile. Both mentioned EPA methods must be carried by highly qualified personnel (U.S. EPA Method 8330, 1994; U.S. EPA Method 4050, 1996).

In addition, sampling area is often very heterogeneously contaminated (requiring composite sampling and statistical adaptations), sampling being (as a matter of fact) an issue of its own (Martin, 2001). But, samples are usually taken by untrained personnel and the transport of the samples from the sampling site to the analytical laboratory may take many days or weeks, during which the sample content may change through natural degradation processes. For example, micro-organisms may grow and use some analytes for their biological needs. Such degradation processes are favoured by the transport and storage conditions (e.g. 4 - 20°C or higher), and by sample oxygenation during sampling (as it is the case with soils) (Jenkins et al., 1995a,b).

The importance of good sampling design and real-time sampling is maximal in the study of the fate of pollutants. The data should effectively meet the quality management requirements (U.S. EPA 5360 A1, 2000; U.S. EPA QA/R-2, 2001), even with highly heterogeneously distributed pollutions. When sampling errors and sampling denaturation during transport occur, the supposedly high-precision measurements actually produce both slow and misguiding surveys.

Also, the survey correctness / value depend not only on the measurement result, but on the time at which the result is produced and introduced in the decision circuit, i.e. on real-time analysis and decision. (Crockett at al., 1996a,b, 1999; Jenkins et al., 1996b; 1997a,b, 1998; Crumbing et al., 2001; Workman et al., 2001).

Field methods are not as highly precise analytical tools as their laboratory counterparts, but they are capable of producing real-time results. More, on-site analysis avoids biases due to sample storage and transport. Further, field methods usually employ minimal handling (requiring some limited training) as well as are often miniaturized (portable) instruments which need small amounts of reagents. Field instruments/methods may also be adapted with user-friendly interfaces and environmental-friendly materials.

Although the development of field methods may be at least as demanding as the laboratory ones, they commonly provide the user with lower cost per sample indices than the laboratory methods. Still, this is not necessarily a rule, the costs per sample being also a matter of the program size and strategy (Gottlieb et al., 1997; Wollin and Levsen, 1999; Crockett et al., 1999).

Nowadays, the best approach in pollution assessments of explosives or pesticides is to define flexible, on-site oriented strategies, with good data quality control. The precise objectives must be stated, and the decision criteria and the tolerable error rates must be defined.

In general, a pollution assessment involves the designation of a field-screening phase, followed by well targeted, precise laboratory analyses (Crockett et al., 1996a,b; Crockett et al., 1999). Nevertheless, while the domain of laboratory analyses is already well structured and highly functional, field-screening is still a poorly charted terrain, with many innovatory concepts and methods yet to gain reconnaissance.

1.3. Environmental analysis of nitroaromatics – state of the art

Reviewing the multitude of techniques and methods that are applied in the field of analytical chemistry and biochemistry is daunting, particularly with biosensors. In a wide practical perspective many approaches look promising, but one general conclusion that emerged with time is the need of versatility.

There is a trade-off between different analytical performances, notably sensitivity and precision versus simplicity and speed of analysis. Essentially, the best compromise must be found between the basic performances of a method and the many practical requirements like measurement time, temperature control, sensors' autonomy and price. The trick is to design flexible analytical techniques, which are affordable, easy to use and fast, but at the same time reliable.

Earlier physico-chemical approaches for the field screening of explosives were colorimetric methods, like detection of TNT, 2,4-DNT and RDX by using sodium /potassium hydroxide or sodium disulfide (Medary, 1992; Jenkins and Walsh, 1992). Later, the same principle was used to develop a sequential injection spectrophotometric method (Echols et al., 1999).

Currently, the conventional and accepted laboratory methods for the quantitative analysis of explosives are based on GC-MS (Bader et al., 1998; Psillakis et al., 2000) and HPLC (Jenkins et al., 1989; Schuster and Gratzfeld-Huesgen, 1993; U.S. EPA Method 8330, 1994).

Other methods are also available: GC (Eiceman, 2000); GC-ECD (Welsch and Block, 1996; Walsh and Ranney, 1998a,b; 1999; Alter et al., 1998; Jenkins et al., 2001), GC-ITMS (Barshick and Griest, 1998), GC-NPD (Hewitt and Jenkins, 1999); LC-MS (Cassada et al., 1999); LC with amperometric detection (Spiegel and Welsch, 1997; Hilmi et al., 1999); RP-HPLC with a UV detector (RP-HPLC-UV) (Spiegel and Welsch, 1997; Jenkins et al., 1998); HPLC-NMR (Godejohann, 1997); READ (Darrach et al., 1998); and two-dimensional HPLC (Köhne et al., 1998).

Analyte may also be pre-extracted / pre-concentrated (to circumvent matrix effects), e.g. SPE or SPME (Barshick and Griest, 1998). For better analytical discrimination of nitroaromatics, explosives in mixtures may be separated prior to e.g. HPLC analysis, using CEC (Bailey and Yan, 1998). In principle, CEC may also be miniaturized (Pyell, 1997).

Immunochemical techniques are also widespread, mainly due to their flexibility and affordability (Van Emon, 2001). These are immunoassays and immunosensors. Immunoassays are ligand binding assays which use antibodies and the antibody's corresponding antigen as binder and ligand (Tijssen, 1985). Biosensors are devices incorporating a biological sensing element connected to a transducer. The last converts an observed change (physical or chemical) into a measurable signal, usually an electronic signal whose magnitude is proportional to the concentration of a specific chemical or set of chemicals (Eggins, 1996). When the biological sensing element is an antibody, the biosensor is referred to as immuno-chemical sensor or immunosensor.

Immunosensors are affinity ligand-based biosensor solid-state devices in which the immunochemical reaction is coupled to a transducer (Rogers, 2000; Luppa et al., 2001). Immunoassays, and especially their biosensors applications, open the possibility to simplify the biochemical measurements, and carry reliable analyses outside the confines of the main laboratories, within a wide range of domains, objectives and analytical aspects (Torrance, 1998; Pearson et al., 2000). Immunosensors (like immunoassays) were first applied to clinical analysis (Stefan et al., 2000; Luppa et al., 2001; D'Orazio, 2003), but applications are already bourgeoning in the analysis of environmental pollutants, toxins, endocrine

disruptors and food contaminants (Baeumner, 2003; Rodriquez-Mozaz et al., 2003; Estevez-Alberola and Marco, 2004).

For explosives, various immunoassay systems were developed, among which are different test-kit formats, which have already been tested and validated (U.S. Method 4050, 1996; Craig et al., 1996; Jenkins et al., 1996a; Thorne and Myers, 1997; Eikenberg et al., 1997; Krämer, 1998b; Crocket et al., 1998; Wollin and Levsen, 1999), an immunofiltration screening test (Keuchel and Niessner, 1994), an apoenzyme reactivation immunoassay (ARIS) for TNT (Dosch et al., 1998), a fluorescence-based array immunosensor (Sapsford et al., 2002), and colorimetric/immunoassay test-kits (Myers et al., 1994).

One wide spread immunoanalytical approach is to employ a displacement technique, which is dependent upon the dissociation kinetics between the labelled analyte and the immobilized antibodies. Methods based on displacement approaches included colorimetric (dip-strips: Heiss et al., 1999), fluorescence (Goldman et al., 2003), and electro-chemical techniques (Buttner et al., 1997; Hilmi et al., 1999) or semipermeable membrane devices (SPMDs, Wang et al., 1999). Another promising direction was demonstrated with capillary-based continuous flow displacement immunosensors (Narang et al., 1997; Holt et al., 2002) that have polymers (PMMA) as immobilization surfaces for antibodies.

TNT could also be detected by membrane-based displacement flow immuno-assays (Rabbany et al., 1998; 2000); paramagnetic beads based electro-chemi-luminescence immunoassay (Wilson et al., 2003a,b), homogenous immunoassays based on microfabricated electrophoresis chips (Bromberg and Mathies, 2003); microfabricated chip using micellar electrokinetic chromatography (MEKC) and indirect laser-induced fluorescence (IDLIF) (Wallenborg and Bailey, 2000); or reversed-displacement immunoassays with fluorescent Cy5-labelled antibodies immobilized on a micro-affinity column incorporated into a flow system (Green et al., 2002).

Other nitroaromatics can be detected either with the above mentioned methods or with specific methods like electrochemical assays based on screen-printed carbon electrode (Honeychurch et al., 2003). When mixtures of explosives were present, multi-analyte detection of TNT and RDX was possible with a fibre optic immunosensor with a detection limit (DL) of 5 to 6 ng ml^{-1} (Bakaltcheva et al., 1999).

There are also developments of sensor systems based on electro-chemical detection (Krausa et al., 1996; Krausa, 1998), modular multi-functional surface-tethered components (Medintz et al., 2005), immobilized maltose binding protein (MBP) nitroreductase (Naal et al., 2002), phage display peptides (TNB-binding phage) incorporated in a flow system for TNT (Goldman et al., 2002), or entire organisms like mutant micro-algae (Altamirano et al., 2004) and goldfish (Wang et al., 1999).

Most of these methods have poor trade-offs between the analytical-practical requirements mentioned earlier (technical details in annex 2). The big challenge still remains a high performance, cost-effective field analysis.

One major tendency in environmental analysis is to combine an effective field screening with a high-performance laboratory technique. Nowadays, while HPLC and GC/MS techniques are the best analytical tools in the laboratory, immunochemical methods emerge as a top option for field screening.

Concerning immunosensors, first commercial types of field-use instruments were engineered by Research International (Woodinville, WA, USA) starting in 1997, albeit they did not report that there was a temperature-control build in.

FAST 2000 (Flow Assay Sensing and Testing system) (Kusterbeck and Charles, 1998; Charles et al., 2000; Kusterbeck and Shriver-Lake, 2000; Dindal et al., 2000; Gauger et al., 2001; Shriver-Lake et al., 2003) and *FAST 6000* are based on fluorescence displacement immunoassays (on permeable membranes containing the tagged analyte), and reach a DL between 1-10 ppb for explosives (TNT and RDX).

Analyte 2000 (Kusterbeck and Shriver-Lake, 2000; Van Bergen et al, 2000), is a fibre optic fluorometer based on competitive fluoroimmunoassay, and reaches a DL for explosives (TNT and RDX) between 10 mg l^{-1} in water and 100 mg l^{-1} in soil. *RAPTOR is* a fibre optic portable immunosensor for bacteria toxins (Anderson et al., 2000; Anderson and Rowe-Taitt, 2001).

Like with explosives, determination of pesticides in the environment (a much wider field than analysis of explosives) is performed in laboratories with established chromatographic methods like HPLC, LC-MS or GC-MS, as well as some immunochemical methods, such as immunoassays (including test-kits) and immunosensors (Krämer, 1996, 1998a; Renner et al, 1997; Strategic Diagnostics, 1997; Dankwardt, 1999, 2000; Gabaldon et al., 1999; Strachan et al., 2000; Schobel et al., 2000; Mallat et al., 2001).

1.4. The general objective of the thesis

This thesis describes the development and the proof of principle of a new portable, temperature-controlled, power-supply autonomous, field immunosensor for environmental applications (fig. 1), inspired by earlier developed immunochemical detection systems (Krämer et al., 1997; Meusel et al., 1998), and built by IMM GmbH, Mainz, Germany (Kolb et al., 2004).

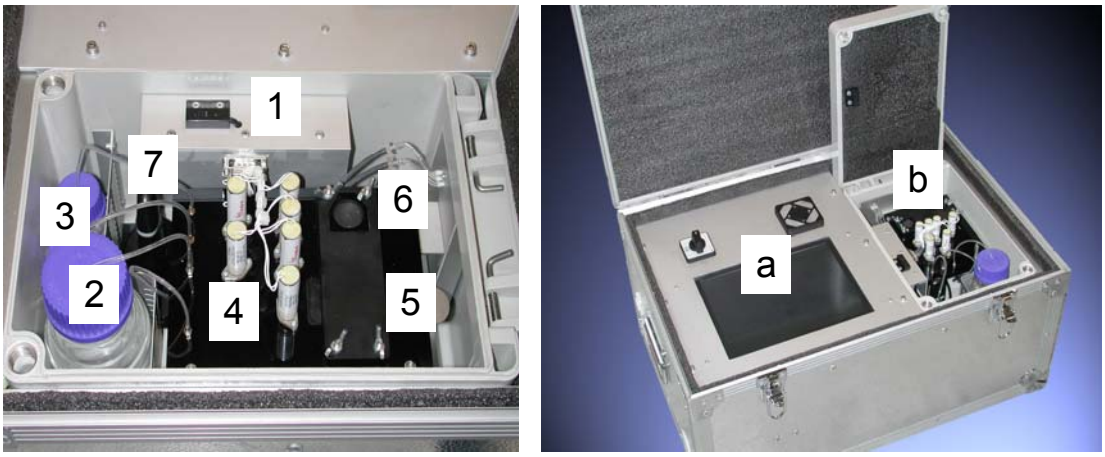

A B

Figure 1. Details (A) and portable box (B) of the temperature-controlled field prototype. (A) Details of the temperature-controlled part: 1) Peltier elements for temperature control; reservoirs for buffer 2) and substrate solutions 3); 4) black PMMA ground plate with valves, hosting the fluidic part and connections to the chip; 5) single-use chip (upside down) with sample reservoir (6), Tr, and golden structures (the last two are not visible); 7) USB stick for data storage. (B) The whole instrument within a box suitable to carry into the field: a) touch screen of computer, b) temperature-controlled part. Syringe pump with step motor is also incorporated, but not visible (after Ciumasu et al, 2005).

This instrument was developed and optimized using TNT as the key target. In addition, the pesticides diuron and atrazine were used to demonstrate the versatility of this platform. Finally, a newly developed isoproturon assay (Krämer et al., 2004a) was adapted towards the future usage of this field immunosensor.

Some generalities about the described development are given in the following lines. The biochemical development consisted in three steps. First, we studied the antibody - antigen dynamics in several immunoassays, and the potential for immunosensor applications. Second, we adapted the immunoassays from microtiter plate to batch structures (pyramids), i.e. out-of-chip structures. Third, we performed off-line and on-line analyses with the immunosensor prototypes (demonstrators): the laboratory prototype (LP) and the field prototypes (FP). In the later step, the solid support was represented by exchangeable chips containing the pyramid structures inside an incubation-measuring cell on the chip.

Monoclonal antibodies (mAbs) were immobilized via adsorption on a gold surface with numerous pyramidal structures. The recognition reaction was enhanced in three ways, 1) via the enzymatic reaction, 2) via the gold surface cover of pyramidal structures, and 3) via the detection of the chemiluminescence of the product through a very sensitive photomultiplier (situated directly above the pyramid tips).

Immunoreagents (enzyme-tracer – Tr and mAb) and the environmental sample (containing the analyte – An) are located in a single-use chip, which is replaced after each measurement. This exchangeable chip is the key to the versatility of the analytical system, because it can be prepared for any desired analyte.

Thus, the versatility of the ELISA technique is transferred to the biosensor platform. Transport of reagents is performed with an automated, miniaturized flow-injection system, which is the consistent part and applicable for all analytes. The chemiluminescence signal is inversely proportional to the amount of analyte present in the sample.

The versatility potential of the developed sensor concept is enhanced by using (1) a flow-injection system, thus providing fast and automatizable analyses (Tojanowicz, 2000; Fletcher et al., 2001); (2) miniaturization, since investigation of a large number of immunochemical systems and set-up combinations requires that the scale of each experiment should be as small as possible (Workman et al., 2001); (3) chemiluminescence-based detection system, which is highly amenable to analytical purposes, including in combination with flow-injection. Chemiluminescence is highly sensitive and does not require a light source, meaning less energy consumption, i.e. longer power-supply autonomy (Roda et al., 2000; Fletcher et al., 2001).

A proof of principle is provided for the explosive TNT and for the pesticides atrazine and diuron. The immunosensor development comprised also immunoassays developments and/or adaptations for the pesticide isoproturon.

2. THEORETICAL FRAME

2.1. Fundamentals of immunoassays

2.1.1. Antibody – antigen system dynamics

2.1.1. A) Antibodies as analytical tool

A bio-physical system made up by one free antigen (the analyte – An) and one labelled antigen (the tracer – Tr) that are competing for the limited binding sites of a monoclonal antibody (mAb) can be used for designing analytical tools like immunoassays. The core of this analytical approach is the reaction of recognition of antigens (Ag) by specific antibodies (Ab).

Antibodies (immunoglobulins) have been used in analysis for over 60 years (Miller, 2002a,b) and in enzyme immunoassays since the mid-sixties (Tijssen, 1985). They are the main components of the humoral immune system being secreted by lymphocytes B. There are several classes of immunoglobulins, but the present thesis is concerned with applications with antibodies from IgG class.

For analytical purposes, the Ab is produced by means of biotechnological techniques. The Ab is produced by eliciting an immune reaction towards an immunizing agent with known chemical structure (immunogen). Immunogens which are injected into the animal body (e.g. mouse or rat) should be large enough to elicit immunological response from the host organism and bear close chemical resemblance with the target antigen.

If a substance is chemically suited but too small (i.e. a hapten) to elicit immune response, it is conjugated to a large protein, like BSA or KLH. Usually, the chemical structures which are best for such immunizations are identified in a rather empirical way, by testing several substances which are chemically similar to the target Ag.

Recently, some attempts were also made to identify the best immunogen in a strictly reductionist approach, by trying to predict the functions of the potential immunogen using computer simulations (Kleinstein and Seiden, 2000; Garrett, 2003; Dasgupta and Balachandran, 2004).

However, this approach ignores the fact that immunogenicity depends on the complex situation represented by the biological potential of the host being immunized, i.e. the immunoglobulin gene repertoire, the self-tolerance, the production of cytokines, and many cellular and regulatory mechanisms which are practically impossible to control (Buchbinder et al., 1998; Van Regenmortel, 2004).

Following immunizations, the germ-line antibodies seem to allow a certain structural plasticity during the affinity maturation, so that affinity and specificity of the mature Ab is very much increased (Yin et al, 2003).

The technology of hapten-specific recombinant mAb, is based on the advent of recombinant DNA technology, and has the potential to produce Abs with specificities and affinities suited for various applications (Yau et al., 2003).

Other efforts attempt to employ molecularly imprinted polymers – the so called "plastic antibodies" – as alternative to the natural Ab molecules (Haupt and Mosbach, 1998; Knopp, 2000; Piletsky et al., 2001).

2.1.1. B) The antibody molecule

The fact that Abs are multi-chain proteins was established in 1959 by G.M. Edelman, while the four-chain structure of Abs was postulated in 1962 by R.R. Porter. For their work the two men were awarded the Nobel Prize in 1972 (Edelman 1972; Porter, 1972).

The whole molecule is made up by ca. 1330 amino acids. The structural unit of Abs is made up by two identical heavy chains (50 kDa each) and two light chains (25 kDa each). By papain digestion the Ab molecule is split into one Fc fragment (made of the constant portion of the heavy chains) and two Fab fragments (made of the variable region of both heavy and light chains).

In principle, the recognition (Ag-binding) sites of the Ab (i.e. the paratopes) are placed at the end of each of the two Fab fragments of the Ab molecule, and "recognize" a specific portion of the Ag molecule (i.e. the epitope). The interaction forces between Abs and Ag are non-covalent: hydrogen bonds, van der Waals forces, ionic bonds, and hydrophobic interactions. Extensive descriptions of the Ab structure and function are provided in the literature (Edelman 1972; Porter, 1972; Tijssen, 1985; Feldkamp and Carey, 1996; Raymond, 1999; Strandth, 2000).

More extravagantly, but very important, immunochemical engineering allows production of multivalent and bispecific (or "bifunctional") Ab, i.e. engineered molecules with two different types of binding sites against two different Ag (Pluckthun and Pack, 1997; DeSilva and Wilson, 2000; Hudson and Souriau, 2003; Kufer et al., 2004).

One common approach, in such analytical methods as immunoassays, is to immobilize the mAb on a solid support, e.g. test tubes, polystyrene microtiter plates, polymer membranes or gold films. Gaining strong momentum is the evolution of analytical methods like immunoassays into analytical instruments like immunosensors for the detection / measurement of chemicals / micro-organisms in environment / human body fluids.

In order to preserve the function and promote the orientation of the Ab recognition sites towards Ag (Vijayendran and Leckband, 2001), Abs are commonly immobilized through other proteins (including anti-Ab antibodies) which can adsorb physically to the solid support and also maintain the ability to bind the Fc fragment of the Ab. This is non-covalent binding. When necessary, Ab immobilization may involve covalent bonding as well.

2.1.1. C) The antibody – antigen reaction dynamics

The kinetics between Ab and Ag are governed by the law of mass action and the general laws of thermodynamics (Tijssen 1985; Schwesinger et al., 2000). According to the law of mass action, the rate of Ab-Ag complex formation is proportional to the concentration of the reactants. The reaction dynamics evolves towards equilibrium between the concentrations of free Ab / free Ag and Ab-Ag complexes (eq. 1).

$$\mathbf{Ab} + \mathbf{Ag} \underset{k_d}{\overset{k_a}{\rightleftharpoons}} \mathbf{Ab\text{-}Ag} \qquad \text{(eq. 1)}$$

The equilibrium (affinity) constant (K) equals the ratio between the association (k_a) and dissociation (k_d) rate constants. In principle, K may be established by measuring the concentrations of complexes and free reagents at equilibrium (eqs. 2; 3):

$$k_a\,[Ab]\,[Ag] = k_d\,[Ab\text{-}Ag] \text{ and} \qquad \text{(eq. 2)}$$

$$K = k_a / k_d = [Ab\text{-}Ag] / [Ab]\,[Ag] \qquad \text{(eq. 3)}$$

When two antigens, the An and the Tr, are competing for the given population of immobilized Ab, then there are two reactions influencing each other like in equation 4.

$$\mathbf{Ab} + \mathbf{An} \underset{k_d\,An}{\overset{k_a\,An}{\rightleftharpoons}} \mathbf{Ab\text{-}An} \qquad \text{(eq. 4)}$$

$$\mathbf{+}$$

$$\mathbf{Tr}$$

$$k_d\,Tr \uparrow \downarrow k_a\,Tr$$

$$\mathbf{Ab\text{-}Tr}$$

Thermodynamically, the reaction equilibrium depends on the association and dissociation rate constants, which in turn reflect the amount of entropy gain during bond formation and the free energy required to break an existing bond:

$$\Delta F° = -RT \ln K, \qquad \text{(eq. 5)}$$

where R is the gas constant (8.3 J/mol·degree) and T the absolute temperature.

An and Tr may have different diffusion rates, which often stand as limiting factors in the reaction dynamics. Differences in the diffusion rates of antigens are due to the differences in their molecular weights: some An are as small as few tens to few hundred Da (haptens) while Tr are much larger, e.g. above 40 kDa with the popular horseradish peroxidase (HRP) as conjugated enzyme.

Measurement of reaction constants is particularly exacting and usually they are not known. The k_a is very similar for various Ab-Ag systems where the Ag is a hapten (like most An in environmental samples), this being limited by the diffusion rates. The association rate for protein Ag (like any Tr) can be about 100 times lower, due to their slower diffusion. In contrast, k_d can vary from ca 10^{-4} for high affinity antibodies to 10^3 for low affinity antibodies (Tijssen, 1985).

The stability of the Ab-Ag complex depends on the affinity of the given Ab for a certain Ag. Affinity is the quotient of the association rate and dissociation rate between Ag and Ab. The half-life of the Ab-Ag complexes ($t_{1/2}$) can be measured using the dissociation rate constant. Usually, it ranges between 1 min – 1 day (Aalberse et al., 2001).

When Abs (or Ag) are immobilized on a solid surface, the stability of Ab-Ag complexes is enhanced by rapid re-association of the dissociated Ag in a confined interfacial reaction volume. This volume is known as "true reaction volume" (Butler, 2000) or as "unstirred layer" of the solution (Aalberse et al., 2001).

The overall stability is referred to as "avidity". This higher stability of the Ab-Ag complexes in solid-phase (heterogeneous) immunoassays makes possible the introduction of washing steps in the experimental at all. Without this higher stability, most of the Ab-Ag complexes would dissociate at washing, because the law of mass action requires new reaction equilibrium after the removal of the bulk Ag solution (Tijssen, 1985).

2.1.2. Typical standard curves

Typically, one given concentration of Tr is competing with different concentrations of An for the limited amount of Ag-binding sites of the antibodies. High concentrations of An can inhibit the binding of the Tr to the limited population of immobilized Ab. The end product of such an assay is a standard curve, also called inhibition curve, where the signal

produced by the Tr bound to antibodies is plotted against the log concentration of applied An (fig. 2).

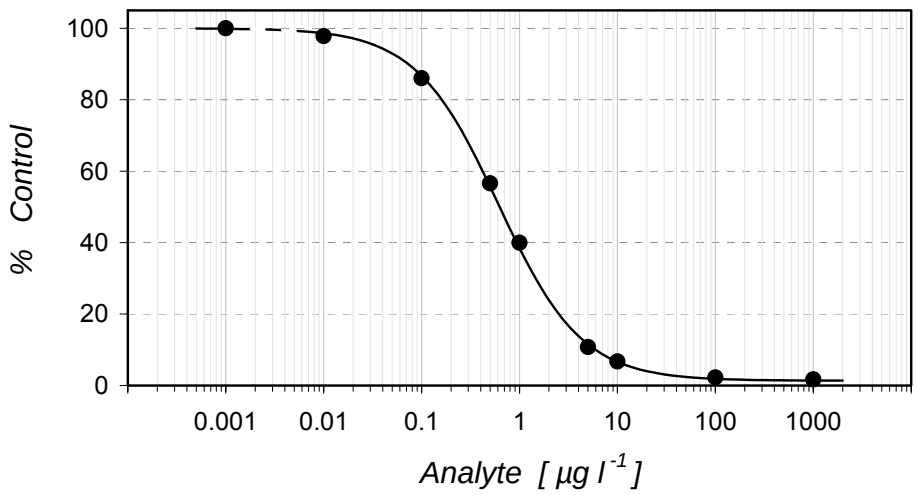

Figure 2. Hypothetical standard curves (%Control). The typical standard curve was fitted according to the 4-parameter equation (eq. 6), with the resulted parameters: A = 100; B = 1; C = 0.6 µg l^{-1}; D = 1. The zero dose is represented as 0.001 µg l^{-1} and separated from the first real concentration by a broken line.

The standard curve produced by an immunoassay can be fitted with the 4-parameter equation (eq. 6), to account for the sigmoid pattern of the signal inhibition:

$$y = \{[(A-D) / [1+(x/C)^B]\} + D, \qquad \text{(eq. 6)}$$

where y is the ordinate axis (signal); x is the abscise axis (An concentration); A is the highest value (on ordinate); D is the lowest value (on ordinate); B is the slope and C is the concentration at 50 % inhibition (IC_{50}). Standard curves are produced using either a specialized software program for microtiter plate absorbance reader, e.g. SoftMaxPro, or a general one, like MS Office Excel.

On the curve, "A" corresponds to the reference, also known as the "zero dose" (Tijssen, 1985). The "D" corresponds to the highest An concentration. The descending slope of the curve is known as the dose-response region. This curve segment allows quantitative analyses in samples with unknown concentrations of An. The limits of the dose response region can be used to make semi-quantitative estimations (screening).

Using standards, the assays are optimized for a slope parameter (B) of 1.0, which coincides with the best dose-response resolution. At this value for the slope parameter, An concentration range stretches over ca. 2 orders of magnitude.

The minimum concentration of An yielding a signal that is discernible from zero dose signal represents the detection limit (DL) of the assay. The DL may be established statistically or empirically (Shan et al., 2002).

Theoretically DL may be calculated from the standard deviation and the slope (Rodbard, 1978; Hayashi et al., 2005), i.e. subtracting from the zero dose signal a value that equals 3 times the standard deviation. In practice, the problem with this method is that the standard deviation is heavily variable with the number of measurements. In our development, it was needed above all, a rule to allow comparison between standard curves. For this reason, a more empirical and conservative method was used: DL was established at 20 % inhibition (IC_{20}), i.e. 80 % in the % control curve.

In principle, the signal begins to be discernibly lower when the An concentration is high enough to inhibit the binding of the Tr molecules. At a certain An concentration, the inhibition is maximal, i.e. reaching the value of background signal.

In many cases the slope is smoother (B < 1) or steeper (B >1). In principle, when the An and the Tr are incubated together, the slope gets steeper and shifts to higher An concentrations with longer incubation times and higher Tr concentrations (Weller, 1992).

In some cases, the slope is very abrupt. This phenomenon is due to the correlations between An / Tr dissociation rates and the length of the incubation times. Certain enzyme-tracers have lower dissociation rates because of hysteresis in dissociation, due to the multivalent attachment effect. Thus, if an Ag is fixed at two binding sites of an Ab, dissociation at one site is more likely followed by re-association than by dissociation of the second site (Aalberse et al., 2001).

This effect was addressed by many experimental studies. For example, artificial antibodies with multiple valencies have an improved strength of antigen binding (Kipriyanov et al, 1996). Vice versa, kinetic experiments proved faster displacement reactions with Fab fragments (i.e. one binding site) than with whole antibodies (i.e. two binding sites) (Gerdes et al., 1999).

2.1.3. The source of the complex behaviour in systems made up by one antibody and two antigens

In a one Ab – one Ag system, the speed of the formation of the Ab-Ag complexes is higher at earlier moments of the incubation time, because of higher concentrations of free reagents. This is predicted by the law of mass action, and observed experimentally (Weller, 1992). The overall speed (and time needed for reaching equilibrium) depends on association and dissociation rates.

In a one Ab – two Ag system, despite differences in k_a and k_d between An (haptens) and Tr (enzyme conjugates), the law of mass action dictates the concentrations of two Ag sum up. Because the reaction speed is higher/lower with higher/lower concentrations of Ag, at short Ag incubation times, the distance from equilibrium is longer/shorter when the total amount of Ag is higher/lower. The incubation time needed for reaching equilibrium may also change with different affinities and reagent concentrations.

In fig. 3 we represent three types of reaction speeds, with an Ag incubation time that is normalized with percentage. The three rectangular hyperbolas correspond to three different association speeds. The underlying dynamics can be described by methods that are analogue to the Michelis-Menten kinetics in enzymes, where the enzyme activity is replaced by the concentration of the Ab-Ag complex. More detailed mathematical description of the association dynamics, and for empirical results are given by Tijssen, 1985; Weller, 1992; Christopoulos and Diamandis, 1996 and Strandh, 2000.

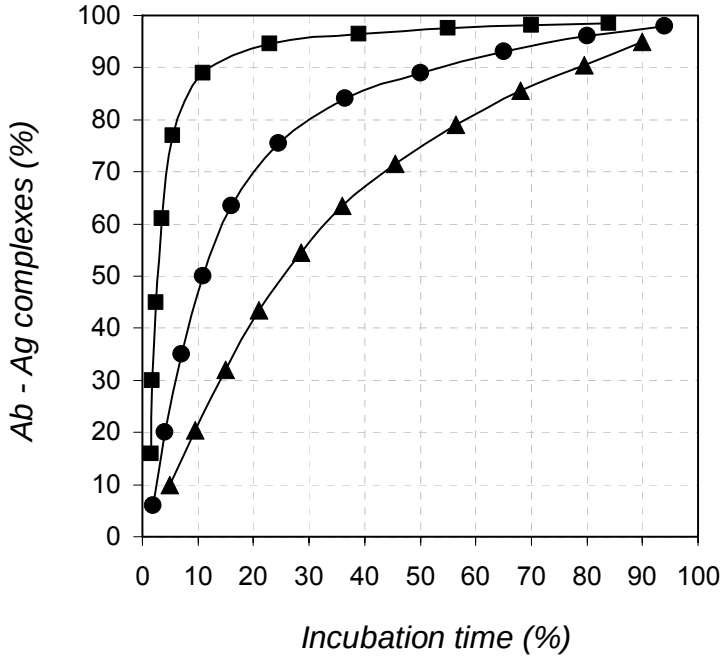

Figure 3. Variable reaction speeds in the formation of Ab-Ag complexes towards equilibrium: (■) fast reaction; (●) moderately fast reaction (▲) slow reaction. The maximum number of Ab-Ag complexes is limited by the number of Ab molecules. Here, the time needed for reaching is normalized by percentage.

Thus, supposing that 100 min of Ag incubation are needed for reaching equilibrium, after 10 min, the number of Ab-Ag complexes may attain 20, 50 or 90 % of the possible number of complexes, corresponding to different reaction speeds. Or, to put it differently,

half of the total number of Ab-Ag complexes is reached within ca 2.5 min in the fast reaction, within 10 min with the moderate reaction and within 25 min with the slow reaction.

The consequences of this situation are discussed in the following sub-chapter, together with a proposed theoretical framework that may explain the behaviour of the system made up by one Ab and two Ag in some limit experimental situations. Of central concern are the best performances of immunoassays that are required in immunosensor applications, like the design of Ag competition and the duration of the Ag incubation.

Experimental evidence upon the flexibility of the assays employed in the sensor development is presented in sub-chapter 4.1., together with the discussion of the specific consequences upon the success of the immunoassays transfer onto the sensor platform.

2.2. Theoretical predictions on the immunoassay flexibility

2.2.1. Case of concern

Of bedrock interest for the sensor development is the situation where one given concentration of Tr is incubated with various (increasing on a log scale) concentrations of An, the two Ag being in competition for the binding sites of a limited number of immobilized Abs.

In competitive heterogeneous immunoassays (immobilized antibody format) that are developed for field screening, one possible general approach is to prevent any direct contact between sample (standards) and Tr, by applying distinct incubation times for sample (An) and Tr solutions, separated by a washing step (sequential saturation analysis). The advantage of this set-up is the avoidance of any false positives coming from the incidence in the real sample of certain substances which impede upon the final enzymatic activity of the Tr.

The big risk is the dissociation, during the washing step, of a large number of the Ab-An complexes (formed after the incubation of An), leading to a poor precision at low An concentrations (Tijssen, 1985). Another possible design is by incubating together the sample/standard (An) and Tr (competitive saturation analysis), with the advantage of a better experimental precision (Tijssen, 1985), and with the risk of a high proportion of false positives.

2.2.2. Direct inhibition

At a given Ag incubation duration, at An concentrations higher than the detection limit, there is a direct inhibition of the Tr binding to Abs. From the detection limit upwards,

the number of An molecules dissociated from Abs is smaller than that of associated molecules. At An concentrations lower than the detection limit, the two numbers are equal. Direct inhibition is the very rational of heterogeneous immunoassays.

2.2.3. Facilitated binding

Usually, the two Ag have different rates of association and dissociation to Ab, as well as different diffusion rates. No matter how different the properties of the two Ag are, the law of mass action dictates that the speed of the reaction (i.e. Ab - Ag association) is dictated by the total amount of free Ag and free Ab.

One immediate consequence of the law of mass action is that the reaction speed is lower in the absence of one of the two Ag than when both Ag are present. In other words, the two Ag facilitate each other's binding to the given population of immobilized Ab. Basically, this phenomenon may be called "facilitated binding" of Ag. In the experimental conditions, beside direct inhibition, we have a case of "reciprocally facilitated binding" of the two Ag.

On the one hand, the speed of Tr binding increases with higher An concentrations. How much higher, depends on how many times the total Ag concentration increased with the addition of the An. The highest An concentration that is yet not producing direct inhibition will correspond to the fastest Tr binding. Therefore, the speed headway brought by An on the reaction between Ab and Tr is higher with higher An concentrations; logically, this speed is also higher with lower Tr concentrations.

On the other hand, the speed of An binding is higher at higher An concentrations and even higher when the Tr is also present. How much higher, depends on how many times the total Ag concentration increased with the addition of Tr. Therefore, the speed headway brought by Tr on the Ab - An reaction is higher with lower An concentrations and with higher Tr concentrations.

In a nutshell, at the portion of the standard curve that is below DL (e.g. 1 μg l^{-1}), the stronger facilitation of Tr binding by An occurs at higher concentrations of An and lower concentrations of Tr; while the stronger facilitation of An binding by Tr occurs at lower concentrations of An and higher concentrations of Tr.

In experimental conditions, the two separate facilitations overlap and their presence can be spotlighted by careful experimental designs, on the condition that short incubation times are being applied. Screening with a set of 3 or more different incubation durations (per experiment) is required for hitting close to the peak of maximum relative importance of facilitated binding of antigens.

The "facilitation turnover" is the ratio between the number of "facilitated Ag" molecules and the number of "facilitator Ag" molecules. The facilitation turnover varies with the changing concentrations of free and bound molecules of the two Ag, as the reaction approaches the equilibrium.

In the next sub-chapters are discussed the analytical consequences of the two types (orientations) of facilitated binding, at different facilitation intensities.

2.2.4. Low dose hook

One consequence of the facilitated binding of the Tr in the presence of An is the occurrence of a "low dose hook". This is a well-known, but poorly studied phenomenon, which consists in a characteristic "hooked" shape of the standard curve at An concentrations below / around the detection limit. To our knowledge, there is yet no study upon low dose hook in the competitive heterogeneous immunoassays with one immobilized Ab and two Ag, despite their wide use in environmental analysis.

With homogeneous assay systems (used more in clinical analysis, e.g. the "sandwich assays"), the low dose hook is better studied. In such assays, the low dose hook and the high dose hook are due to cooperative interaction between mixtures of Abs; or to other effects involving the An, the anchoring antibody and the labelled antibody, preventing optimal formation of the "sandwich" complexes (Fernando et al., 1992; Fernando and Wilson, 1992a,b; Selby, 1999; Stern, 2001).

In principle, facilitated binding of Tr should be experimentally discernible by incubating Tr with only that part (amount) of An solution that could bind in a simple Ab - An dynamic that took place in a previous incubation step followed by washing. The separated pre-incubation of An insures no facilitated binding of An in the presence of Tr. Thus, when the two Ag come to be incubated together, only that much An is present which could bind alone in the first incubation. Results obtained with such an experimental set-up are presented in sub-chapter 4.1.3..

2.2.5. Feed-back inhibition

At An concentrations below detection limit, the number of associated An molecules is equal to the number of dissociated molecules. In the presence of Tr, An binding is facilitated, that is the number of associating An molecules increases. Thus the number of associating An molecules can become higher than the number of dissociated molecules; hence inhibition may occur. Like this, we have a phenomenon of "feed-back inhibition": the

pool of Tr molecules facilitates (through total antigenic concentration) An binding, which lead to the occupation of some recognition sites by the pool of An molecules.

On the standard curve, this phenomenon may be visible in certain experimental conditions, notably at very short incubation times, as a short negative hook in the low dose plateau of the standard curve. In sub-chapter 4.1.3.2. of the thesis, we present experimental evidence for this phenomenon.

The relative importance of feed-back inhibition might be not significant as it is overlapping with facilitated binding of Tr and direct inhibition Tr. In the next section, we discuss the theoretical interaction between the three phenomena.

2.2.6. Interaction between direct inhibition, facilitated binding and feed-back inhibition

At a threshold concentration of An, the number of An molecules associating to Abs equals the number of An dissociating from Abs. At An concentrations above this threshold, we talk about direct inhibition of Tr. At An concentrations below this threshold, we can expect facilitated binding and feed-back inhibition.

These three phenomena overlap to various degrees, albeit the relative importance for the standard curve of each of them is quite different, both at a given incubation time and during the incubation time.

In fig. 4, we represent a most general case for the three phenomena and the way they limit each other in terms of percent of the total amount of recognition sites. This graphic representation is derived from that of Ab-Ag association dynamics in fig. 3 (being also a direct consequence of it).

Further, in fig. 5 we show a theoretical example of standard curves resulted from the interaction of the three phenomena.

In direct inhibition, a maximum ceiling is determined by the amount of immobilized (available) Ab. In facilitated binding and feed-back inhibition, maximum ceilings are determined by the facilitated binding turnovers. These are resultants of combinations of diffusion rates, affinities and distance from reaction equilibrium. In principle, they make an interesting subject for future mathematical modelling.

Facilitated binding and feed-back inhibition are consequences of the variation of reaction speed when the reaction is far from equilibrium. Facilitated binding of Tr will reach maximum importance (close to asymptote, in % of Ab involved) at very short incubation times. Moreover, above detection limit, the higher the An concentration the sooner facilitated binding of Tr is being cancelled by direct inhibition.

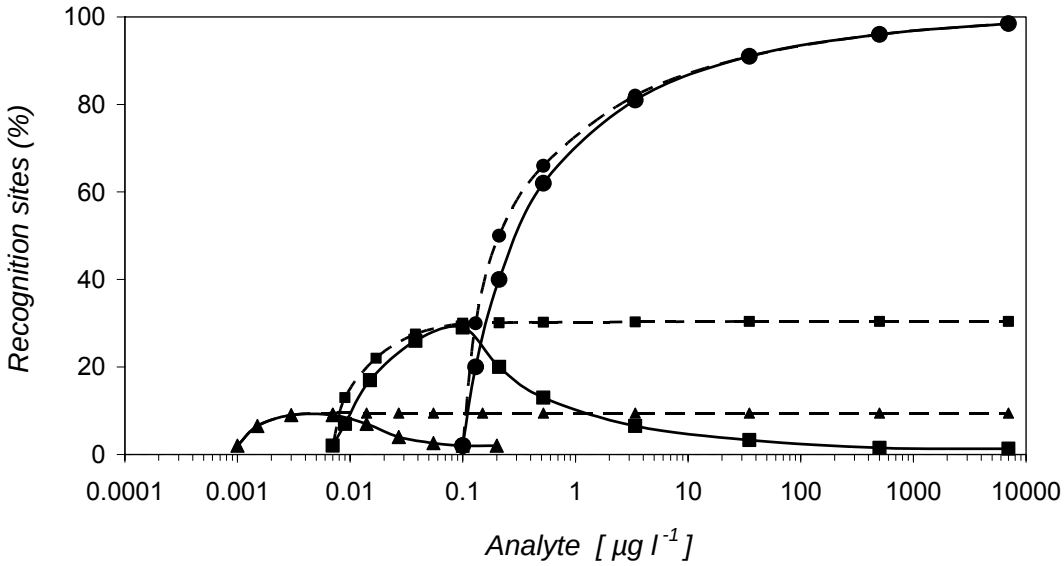

Figure 4. Hypothetical example for the relative importance of direct inhibition, facilitated binding and feed-back inhibition of Tr, at a given moment of the incubation time. Direct inhibition of Tr binding (●) begins at 0.1 µg l^{-1} and tends to an asymptote defined by the population of recognition sites. Facilitated binding of Tr (■) reaches a maximum below 0.1 µg l^{-1} and it is mitigated at higher An concentrations because the number of recognition sites potentially involved in facilitated binding is lowered by direct inhibition. Feed-back inhibition (▲) reaches a peak relative importance below 0.01 µg l^{-1}, and is lowered at the occurrence of facilitated binding. In all three cases, the broken line represents the hypothetical relative importance of each phenomenon in the absence of the other two. The height of the asymptote represents the potential percent of the immobilized mAb recognition sites involved in each phenomenon. The asymptote height, as well as the An concentration corresponding to the peak, may vary with different immunoassays and with different distances from equilibrium (related to Ag incubation duration).

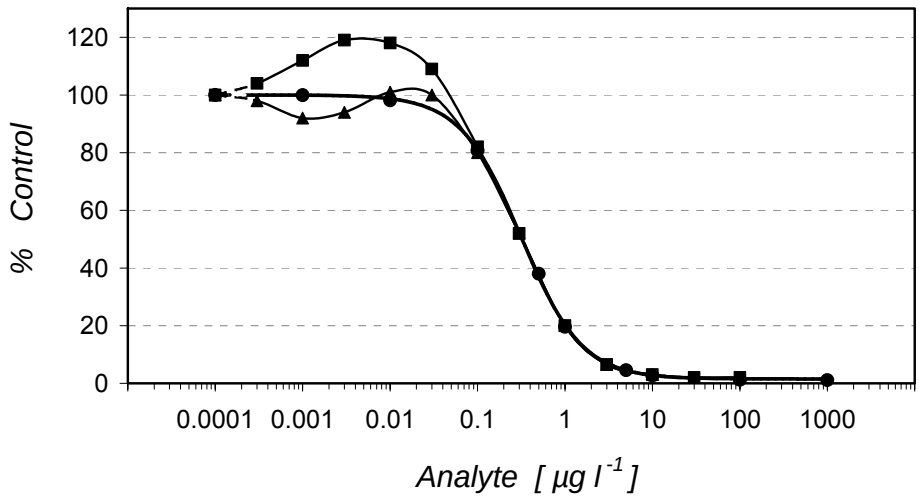

Figure 5. Hypothetical standard curves (%Control) with different relative importance of facilitated binding and feed-back inhibition of Tr. In order to account for direct inhibition of Tr at An concentrations above detection limit (here DL = 0.1 µg l^{-1}), the standard curve was fitted according to the 4-parameter equation (eq. 6) with the following resulted parameters: Standard curve with positive hook: A = 100; B = 1.25; C (IC_{50}) = 0.32 µg l^{-1}; D = 2. In the first hypothetical curve (●), there is no deviation from the sigmoid curve. In the second hypothetical curve (■), facilitated binding of Tr is visible below the detection limit as a positive hook, while the feed-back inhibition is not distinguishable. In the third hypothetical curve (▲), feed-back inhibition is visible below 0.01 µg l^{-1}, and a weak facilitated binding between 0.01 – 0.1 µg l^{-1}. The zero dose is represented as 0.0001 µg l^{-1} and separated from the first concentration by a broken line.

2.2.7. Standard curves with separated incubations of antigens

As mentioned earlier (sub-chapter 2.1.1.), when the Ab - Ag reaction takes place at the interface between a solid support and the solution, the Ab-Ag complexes are more stable than they would be in a bulk solution. This is making possible the introduction of washing steps separating the free Ag from bound Ag. Therefore, this is how heterogeneous immunoassays may exist at all (Tijssen, 1985).

In principle, the An and the Tr may be incubated either together in a competition step (<u>competitive saturation</u>), or separated by a washing step in a displacement format (<u>sequential saturation</u>).

In a displacement design, the resulted standard curve depends on the displacement pattern of the two Ag: which one can displace the other, how well and how fast. In such a design, the second Ag incubation is a sort of competition in which the bulk solution of the first Ag was removed after a certain time.

In such a competition, the amount of the first Ag involved in the competition depends on the dissociation of the first incubated Ag during the separation washing and the second incubation. Because it obeys to the law of mass action, the Ab-Ag reaction is reversible, a new equilibrium being established after any change of the reagent concentration. By washing, the bulk solution of the first incubated Ag is removed, and a dissociation dynamic will began immediately and continue during the incubation of the second Ag.

In standard curves, the extent of signal inhibition reflects the Ab-An association as related to (log) An concentration. The dissociation dynamic of An is symmetrical to the association dynamic: dissociation is slow at low concentrations of Ab-An complexes and fast at high concentrations.

In a sequential saturation format, when the first Ag is An, the shape of the standard curve will approximate the resultant obtained by overlapping a typical competition curve and the dissociation curve of the An (fig. 6). Thus, best inhibitions (of Tr by An) may occur at intermediary An concentrations on the dose-response region of the standard curve. At high affinities, the dissociation is weaker; hence the inhibition is better preserved.

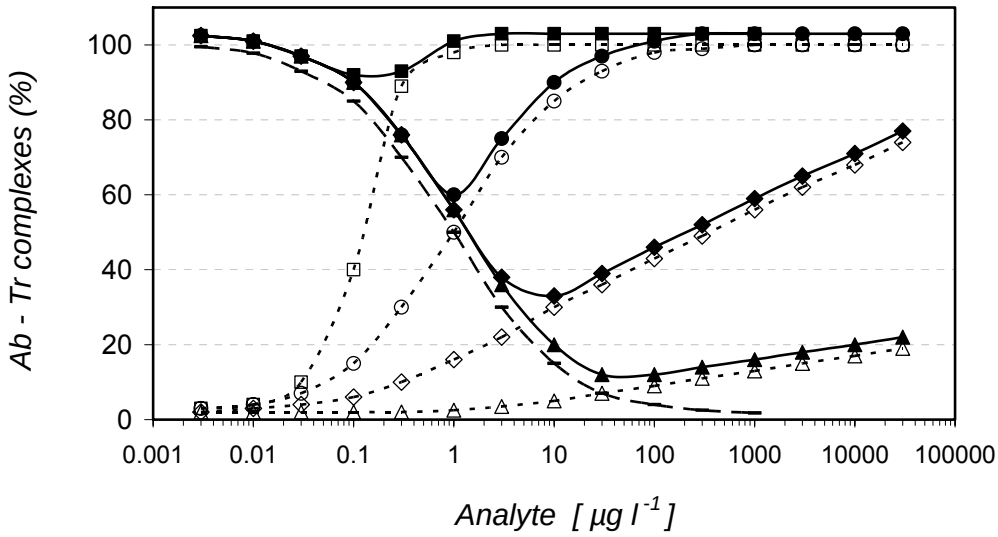

Figure 6. Combined representation of the inhibition dynamic with competing antigens (standard curve), and dissociation of Ab – An complexes formed before washing and Tr incubation. At a given incubation time of the first incubation, the number of Ab – An complexes is higher with higher An concentrations, and so is the dissociation speed during washing and second incubation. The dissociation is faster with lower Ab affinities for An (□;○) and lower with higher affinities (◇;△). The result on the final standard curve (●;■;◆;▲) is that maximum inhibition is reached with intermediate concentrations of An on the dose-response region of the standard curve. Thus, a new plateau can be established at different inhibition levels (%), which should be not mistaken for background signal.

An molecules dissociated at washing are lost from the system, except those in the true reaction volume (unstirred volume). These ones and those dissociated during the second incubation (buffer and Tr) will participate in the reaction and will produce inhibition at (applied) An concentrations of one to several orders of magnitude (fig. 7).

The steepness of the new inhibition slopes will be depending on the affinity constant of the Ab to the Ag (An) and the experimental parameters, notably incubation time.

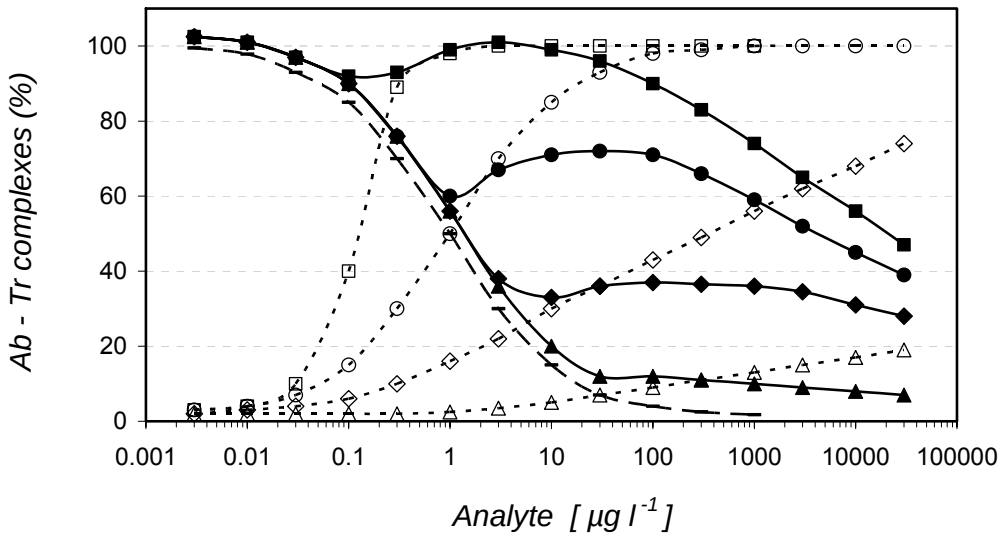

Figure 7. Combined representation of the inhibition dynamic with competing antigens (standard curve), and dissociation of Ab – An complexes formed before washing and Tr incubation. At a given incubation time of the first incubation, the number of Ab – An complexes is higher with higher An concentrations, and so is the dissociation speed during washing and second incubation. The dissociation is faster with lower Ab affinities for An (□;○) and lower with higher affinities (◇;△). The result on the final standard curve (●;■;◆;▲) is that maximum inhibition is reached with intermediate concentrations of An on the dose-response region of the standard curve. Thus, a new plateau can be established at different inhibition levels (%), which should be not mistaken for background signal.

The fact that washing is critical for the standard curve is a critical aspect in immunosensor developments, for two reasons. First, the concentration of An that is present in the measured sample is calculated on the basis of the previously obtained standard curve (calibration curve). So, the influence of washing and of the assay design must be known. Second, the reaction dynamic of the An in the sample may itself undergo the same influences of washing and assay design as the standard curve, but not necessarily in a very predictable manner.

Such peculiar curve shape as with the two-slope curves was experimentally obtained with different An. These results, together with An-specific displacement patterns, will be presented and discussed in chapter 4.1.3.1.

It should be mentioned here that curve shapes similar to the two-slope curve, i.e. double-sigmoid curves, are also known in the ELISA. But those have different causes, like the shared reactivity with two different Abs in a coating antigen format (Schütz et al., 1999).

Mathematical simulation of such dynamics is a subject of its own. In the present study, we limited ourself to expose the simple, qualitative predictions on the standard curve, which can be devolved from the law of mass action. For a discussion upon washing and the dissociation dynamics of the Ab-Ag complexes, one can consult Tijssen, 1985.

3. MATERIALS AND METHODS

3.1. Materials

3.1.1. Chemicals and standards

Table 1. Chemicals and standards

Substance	***Company***
N-hydroxysulfosuccinimide sodium salt (NHS)	Sigma-Aldrich Chemie GmbH, Schnelldorf, Germany
1,3-dicyclohexyl carbodiimide (DCC)	
3,3',5,5'-tetramethylbenzidine (TMB)	
water peroxide	
N,N-dimethyl formamide 99% (DMF)	Fluka (now Sigma-Aldrich Chemie GmbH)
dimethylsulfoxide 99% (DMSO)	
methanol; isopropanol; acetone	
glycerol	Roche Diagnostics, Penzberg, Germany
SuperSignal®ELISA Femto Maximum Sensitivity Substrate (luminescence), i.e. two solutions: (1) the substrate itself: H_2O_2 (2) the luminogen (luminol) + enhancer	
SuperFreeze™ Peroxidase Conjugate Stabilizer	Pierce, Rockford, IL, USA
NaH_2PO_4 (MW 137.99); Na_2HPO_4 (MW 177.99);	Merck, Darmstadt, Germany.
Na_2CO_3 (MW 105.99); $NaHCO_3$ (MW 84.01)	
NaCl (MW 58.44)	
TNP–glycylglycine; TNP–glycine; DNP–glycine	Research Organics, Cleveland, OH, USA.
TNP–α–aminobutyric acid	
DNP–ε–aminocaproic acid	
DNP–γ–aminobutyric acid	
TNT (annex 1-A); 2–amino–4,6–DNT; 4–amino–2,6–DNT; and all the other cross-reactant nitroaromatics (table 9 – sub-chapter 4.1.1.3.1; table 11 – Annex 4)	Dr. Ehrenstorfer, Augsburg, Germany; Institute of Industrial Organic Chemistry, Warsaw, Poland; Cerilliant Corporation, Austin, TX, USA.
atrazine (annex 1-B)	Riedel-de Haën, Seelze, Germany.
diuron (annex 1-C)	
isoproturon (annex 1-D)	

3.1.2. Buffers and enzyme substrates

Table 2. Composition of the used buffers

Buffers	***Salts***	***Per l***
130 mM sodium carbonate (pH 8.1)	$NaHCO_3$ (MW 84)	130 mM (10,92 g)
50 mM carbonate buffer (pH 9.6-9.8)	Na_2CO_3 (MW 105.99)	15 mM (1.59 g)
	$NaHCO_3$ (MW 84.01)	35 mM (2.94 g)
100 sodium acetate (pH 5.5)	Sodium acetate (82.04)	100 mM (8.2 g)
	Citric acid 1% (w/v) in water	ca. 50 ml
100 mM sodium citrate (pH 2.5)	Sodium citrate (MW 294.1)	100 mM (29,4 g)
	NaCl (MW 58,44)	100 mM (5,8 g)
	HCl (37%) for pH adjustment	ca. 24 ml
40 mM PBS (pH 7.5-7.6)	NaH_2PO_4 (MW 137.99)	5 mM (0,69 g)
	Na_2HPO_4 (MW 177.99)	35 mM (6,23 g)
	NaCl (MW 58.44)	100 mM (5.84 g)
4 mM PBS	NaH_2PO_4 (MW 137.99)	0.5 mM (0,07 g)
	Na_2HPO_4 (MW 177.99)	3.5 mM (0.62 g)
	NaCl (MW 58.44)	10 mM (0.58 g)
40 mM PBST	40 mM PBS	1 l
	Tween 20	0.5 ml
4 mM PBST	4 mM PBS	1 l
	Tween 20	0.5 ml

Table 3. Composition of the used substrates for HRP

Substrate / chromogen or luminogen (reading)	***Components***	***Amounts***	
H_2O_2 / TMB (absorbance)	100 Sodium acetate buffer	24.5 ml	per 25 ml
	H_2O_2 (1% in Milli-Q water)	0.1 ml	
	TMB (6 mg ml^{-1}, in DMSO)	0.4 ml	
SuperSignal®ELISA Femto (luminescence)	solution (1): luminol / enhancer	1:1 (v/v)	
	solution (2): H_2O_2		

3.1.3. Proteins, antibodies, enzyme-tracers and blockers

Table 4. Catching proteins / antibodies

Substance	***Company***
Goat anti-mouse IgG (Gam) unconjugated	Pierce, Rockford, IL, USA
Protein A; Purified®; Protein A/G Purified®Protein G recomb.	
Mouse anti-rat IgG (TIB 172, κ-specific)	in-house clone (E. Kremmer, GSF); commercially available through ATTC (American Type Culture Collection), Manassas, VA, USA

Table 5. Anti-analyte monoclonal antibodies, enzyme-tracers, and enzymes for producing enzyme-tracers

Substance	***Company***
anti-TNT mAb (mouse, A1.1.1, 10.6 mg ml^{-1})	Strategic BioSolutions, Inc. (SBS), Newark, DE, USA.
Peroxidase from horseradish (HRP; ca. 1000 U mg^{-1})	SERVA Electrophoresis GmbH, Heidelberg, Germany.
anti-atrazine mAb (mouse, AM5D1-3)	Karu et al., 1991.
enzyme-tracer for the atrazine assay ("atrazine-HRP conjugate", 65-IA01)	Fitzgerald Industries International Inc. (Concord, MA, USA).
anti-isoproturon mAb (rat, IOC 7E1)	Krämer et al., 2004a
enzyme-tracer for the isoproturon assay ("III-HRP")	
anti-diuron mAb (mouse, 481.3)	Karu et al., 1994.
enzyme-tracer for the diuron assay ("1-(5-carboxypentyl)-3-(3,4-dichlorophenyl)-1-metylthiourea – HRP")	Krämer et al., 1997

Table 6. Proteins, surfactants and buffers that were used as blocking solutions

Substance	***Company***
skimmed milk, powder (MP)	Fluka (now Sigma-Aldrich, Schnelldorf, Germany)
casein from bovine milk (powder)	
bovine serum albumin fraction V (BSA, powder)	Sigma-Aldrich Chemie GmbH, Schnelldorf, Germany.
Tween 20 (Polyoxylethylenesorbitan monolaurate, also generically known as Polysorbate 20, is a non-ionic surfactant commonly used in blocking solutions)	Fluka (now Sigma-Aldrich, Schnelldorf, Germany)
LowCross™ Buffer (commercial)	Candor Biosciences GmbH, Münster, Germany

3.1.4. Materials and instruments

Table 7. Materials and instruments

Materials and instruments	***Company***
Slide-A-Lyser® dialysis cassettes, needles, syringes and syringe filter-caps	Pierce, Rockford, IL, USA.
Milli-Q (MQ) filtration system for water demineralization (for buffers and solutions)	Millipore, Eschborn, Germany
microtiter plates (NUNC F-96 certified MaxiSorp™)	NUNC, Wiesbaden, Germany
NUNC Immunowash system for plate washing; vacuum pump	NUNC, Roskilde, Denmark; KNF Neuberger, Laboport, K&K Laborservice, Munich, Germany
ThermoMax or SpectraMax microtiter plate reader (absorbance)	Molecular Devices, Palo Alto, CA, USA
Centrifuge Heraeus Sepatech Biofuge 15	Heraeus, Hanau, Germany
Multipette® pipette with Combitips tips	Eppendorf, Hamburg, Germany
Multi-channel pipette and pipette tips	
Pipette Research: 1-10 µl; 10-100 µl; 100-1000 µl	
Safety cap tubes (plastic)	
Parafilm	Pechiney Plastic Packaging, Menasha, WI, USA
"Amilo" laptop (connected to the sensor), with Windows 2000 Professional, Microsoft tw MC, Intel ® and Celeron ™ processor 128.0 MB RAM	FUJITSU SIEMENS Computers

3.1.5. Automated and miniaturized flow-injection analysis

3.1.5. A) Principles

From a biochemical perspective, the immunosensor prototype developed by IMM Mainz, in collaboration with the Technical University Munich, is an application of the ELISA technique. Overall, the developed immunosensor is based on several engineering and analytical concepts, which will be depicted briefly in the next paragraphs.

Flow-injection analysis (FIA) emerged in 1975 (Ruzicka and Hansen, 1975) as an improved alternative to segmented flow analysers (SFA), and was started to be used in combination with enzymes and antibodies 15 years later (e.g. Schmid and Künnecke, 1990). FIA allowed better elimination of air bubbles from the analytical system, easier miniaturization, more precise injection of samples into the analytical system (details by Lachat Instruments).

Miniaturization is manufacture at greatly reduced scales. Through miniaturization, FIA expanded towards and into the field of microfluidics, which is the study and the application of flow phenomena near boundaries with micron-scale features (including flow in channel, over beads, etc; Sequeira et al., 2002).

A flow-injection analysis system is materially based on a manifold, i.e. an assemblage of pumps, rigid (channels) and flexible flow tubing, fluid mixers, injection valve, detectors, etc, in a given configuration. Conceptually, it consists of a functional assemblage of several components: propulsion system, conduit system, mixing systems, sample-injection system, detection system, and a data acquisition/processing/output system.

Success of flow-injection analysis is based on three basic principles: (1) reproducible handling of sample and reagents; (2) reproducible timing; and (3) controlled sample dispersion. These principles are respected because: the length and the geometry of the manifold tubing remain constant; the flow rate is constant during transport of sample and reagents; and because the analyses steps are automated.

The propulsion system realizes the delivery of carrier and reagent solutions. In our system it is a step-motor syringe pump which acts on vacuum principle. In other flow-injection systems, propulsion can be realised by a peristaltic pump or pumps (typically with the capacity to pump between four to eight carrier/reagent lines). Flow rates used in flow-injection analysis systems typically vary from 0.5 - 4 ml per min.

The conduit insures the physical fluid delivery. It consists of chemically unreactive tubing with an internal diameter of 0.3 -1.0 mm for maintaining laminar flow conditions and controlled dispersion of the sample zone.

Mixing systems (devices; mixers) are used to promote radial diffusion – hence mixing – of fluid reagents. Mixers usually consist of intertwining small-radius channels. Such mechanical systems facilitate secondary flows, i.e. on a primary flow, small disturbances of the flow direction, where the primary flow is the main two-dimensional flow.

Sample injection systems are used for introducing the sample into the flow system, and are correlated with the type of propulsion system employed by the flow-injection system.

Detection systems are used to sense changes in fluorescence, absorbance, chemiluminescence, atomic emission or absorption, infra-red absorption, electrical conductivity, electrode potential, diffusion current, pH, turbidity, mass, etc. The detection system renders the measured changes as quantified electrical signal, e.g. as a digital record.

The use of luminescence in analytical chemistry is based on the formation, from the An (or with is participation) of an excited species which emission spectrum provides analytical information. When the excited species is formed by the absorption of photons, the radiation emission is called fluorescence. When the excited species emitting radiation is formed chemically, the emission process is called chemiluminescence. At present, the field of luminescence detectors is already very developed, allowing a great flexibility in the FIA design (Roda et al., 2000; Trojanowicz, 2000).

The instrument control and acquisition/processing/output system integrates all the other components and insures correct measurement and quantification. Usually, the integration and control function is achieved using a computer with a proper analogue to digital board, and control/data acquisition software.

Commercial systems are fully or partially automated, and include on-board microprocessor systems for timing of operations.

3.1.5. B) General features of the developed immunosensor

The single-use chip and the ground plate represent the heart of the instrument. The instrument itself incorporates also an electric step-motor syringe pump, a chemi-luminescence detector, reagent reservoirs and a computer control unit with a touch-screen user interface (fig. 1A/B).

In addition, the prototype is a one-box instrument, portable, autonomous from external power supply (with build-in accumulator; 6 hours), and temperature-controlled (IMM Mainz, Germany; Kolb et al., 2004). The user has to insert the (previously prepared) chip onto the ground plate, fill-in the sample reservoir, turn on the built-in PC, chose the

desired run-program, close the temperature-control, light-proof box, and select the start button.

The system output is a set of signal values obtained by automated measurements, with programmable frequency, and displayed on a small screen, represented on logarithmic scale. On this screen the development pattern of the luminescent reaction is observed in time (one measurement at every 3 seconds). The data is stored as numbers and can be transferred into a common Office Excel format for further analysis.

The tested immunosensor contains a big polymeric block (16.6 x 12.6 x 1.1 cm) called "ground plate" (figs. 8 and 9), and a small polymeric exchangeable block called "disposable chip" (11.2 x 4 x 1 cm) (described in detail in the next subchapter), bearing engraved channels sealed (LASER-welded) with a cover layer of transparent PMMA. The diameter of the channels is 0.8 mm. The chip also bears three engraved and sealed chambers: the sample reservoir, the enzyme-tracer reservoir and the incubation/measuring cell. The scheme of the fluidics, together with all the main components of the system, is represented on the touch-screen user interface (fig. 10).

A micro-mixer (previously developed by IMM Mainz) may be used for mixing the two solutions of the commercial luminescence substrate. However, the micro-mixer is not essential, because the two solutions can be easily mixed before use, and the mixture is stable for 6 h at RT, even without light-protection.

The sample/standard solution is pumped (sucked) automatically from the 1 ml sample reservoir on the disposable chip. During our tests, we used to fill the sample reservoir manually, with a syringe. In principle, sample injection may be assigned to an auto-sampler for fully automated operations.

The immunosensor tested in our project employed a chemiluminescence detector, namely a photomultiplier (Hamamatsu Photonics K.K., Hamamatsu Photonics Deutschland GmbH, Herrsching, Germany), which measured light intensity (relative light units – RLU). The photomultiplier was attached under the ground plate and protected by a light-proofed box. The detector head was situated directly above the detection cell (of the disposable chip) in which the biochemical reaction took place, and recorded the produced chemiluminecence, through the transparent PMMA foil covering the chip.

According to the substrate vendor, the substrate's light emission wavelength is 425 nm, i.e. in the visible spectrum, at the violet / indigo border.

Figure 8.

Laboratory sensor prototype
(IMM Mainz, after Kolb et al. 2003)

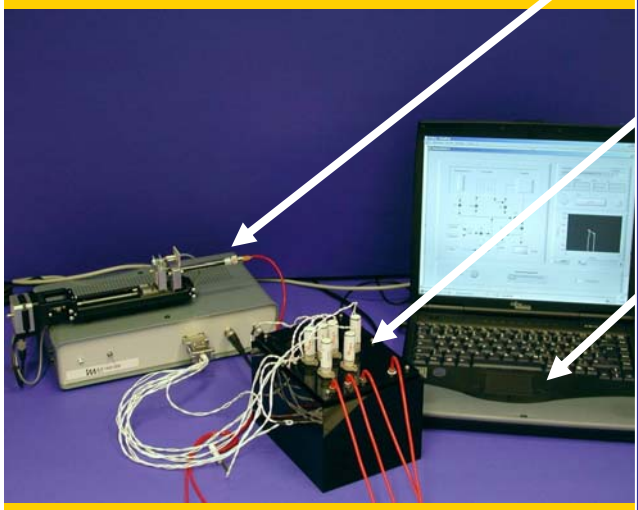

- **Pumping unit:** syringe with a step-motor
- **Luminescence detector** (Photomultiplier, light-proof)
- **Automated control and signal recording,** with a laptop (software: Labview)
- **Initially, no temperature-control**

Figure 9. **Field sensor prototype (portable box)**
(IMM Mainz, after Kolb et al. 2003)

- **Temperature-controlled and light proof part:** hosting the sensor conduit (ground plate and chip) and the reagent reservoirs (buffer and luminescence substrate)
- **Control unit:** incorporated PC with a *touch-screen* user interface
- **The accumulator and the pump are incorporated** though not visible

Figure 10. **Field prototype – user interface** (IMM Mainz, after Kolb et al. 2003)

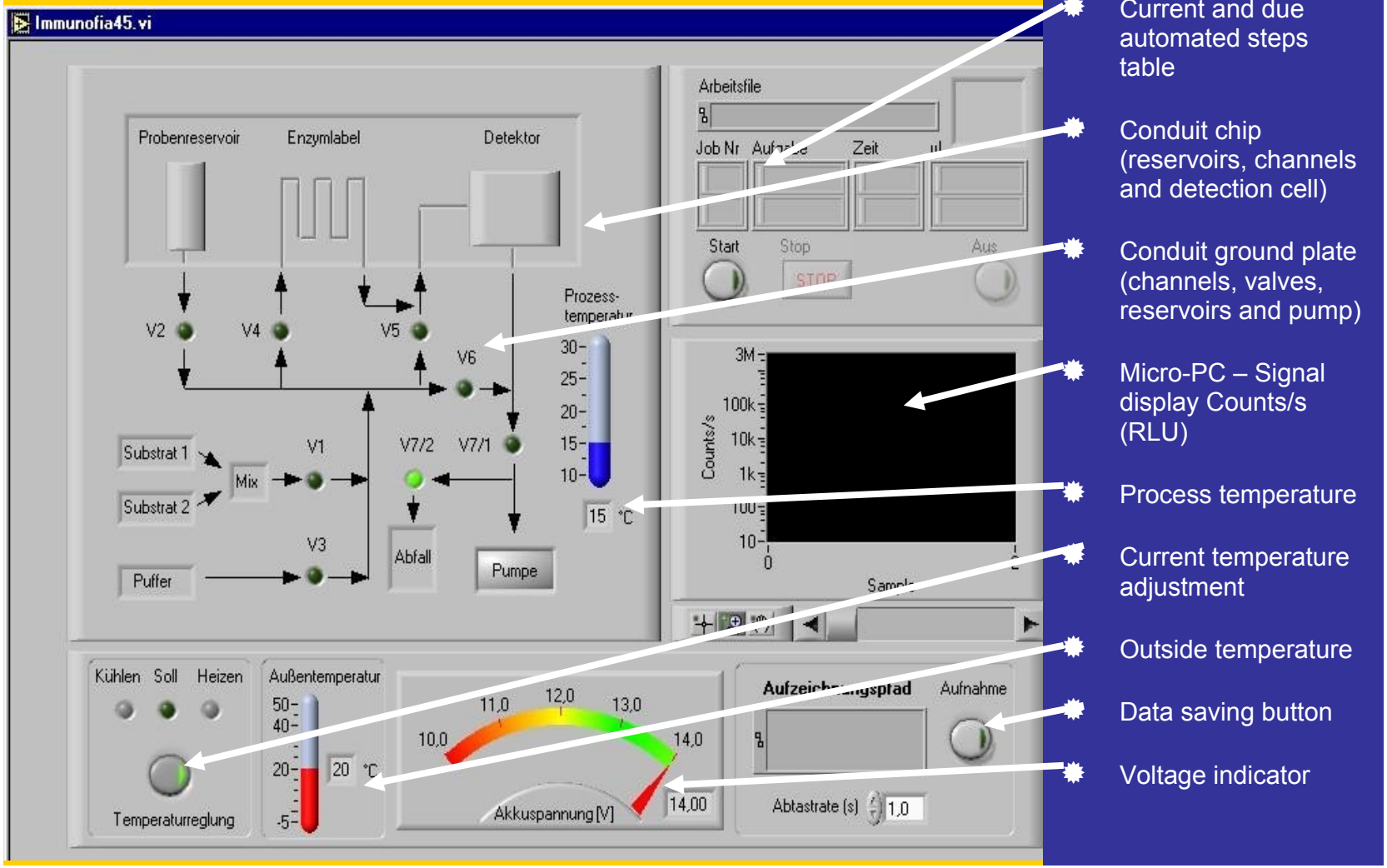

3.1.6. Solid supports for antibody immobilization and the immunosensor

Three types of solid supports and set-ups were employed for antibody immobilization (corresponding to three distinct steps of the transfer of the immunochemicals from ELISA to the immunosensor):

(a) microtiter plates (NUNC, 96 wells),

(b) 'batch structures' (in glass vials, but also possible in Eppendorf vials),

- which are the gold-covered structures, later incorporated into the disposable chip;
- each structure consisted in a certain number of micro-pyramids carved on the upper face of a PMMA (transparent) plastic disc, and covered with a thin layer of gold (by IMM Mainz, Germany);
- one structure per vial (fig. 11);

(c) structures incorporated into a disposable, but reusable chip.

Initially, it was checked which pyramid geometry was the best. All pyramids had square basis, and only the pyramid height was different: small (structure aspect 0.5), intermediate (structure aspects 1) and tall (aspect 2). The final (definitive) version was identified experimentally.

The final version (figs. 11, 12-A and 13) of the whole structure with pyramids (i.e. aspect 1) has the following dimensions: basic disc of 8 mm diameter and 3 mm height; the upper surface bears a gold layer covering 314 pyramids (intermediate height, aspect 1), each pyramid with an 'active optical surface' of 0.277 mm^2 (total active surface per structure: 86.978 mm^2).

Some earlier versions of the whole structures were square (fig. 12-B).

Figure 11. Golden structures in experimental glass vials (batch ELISA set-up)

Figure 12. Golden structures in glass vials detailed view of two structure types:

A. Final version (Aspect 1):

Round structure (for a round cell in chip)
Pyramids smaller, with intermediate height

B. Earlier version (Aspect 0.5):

Square structure (for a square cell in chip
Pyramids larger but with small height

Figure 13. Golden structures detailed view of the final version:

A. In the experimental glass vial
(The structure was left to vertical
for a better picture clarity):

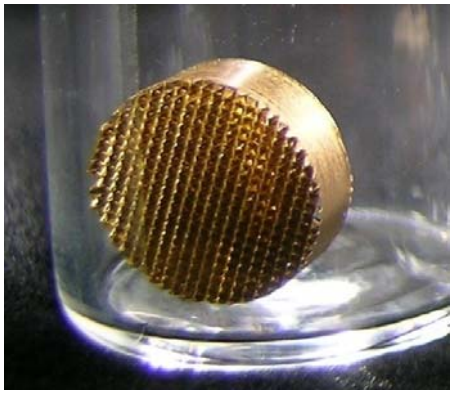

B. Out of the experimental space:

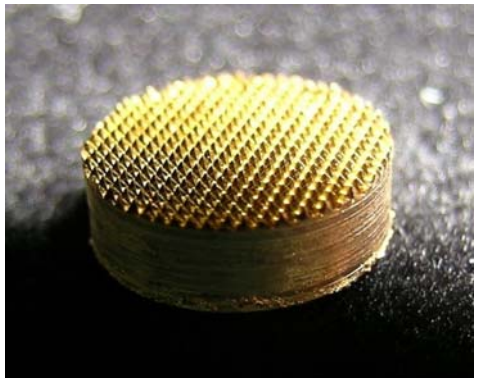

The single-use chip shelters an incubation / measurement cell (figs. 14 and 15; Frese et al., 2003), as well as the enzyme–tracer reservoir (ca. 0.7 ml) (fig. 14). On the side of the chip is the sample reservoir of ca 1 ml.

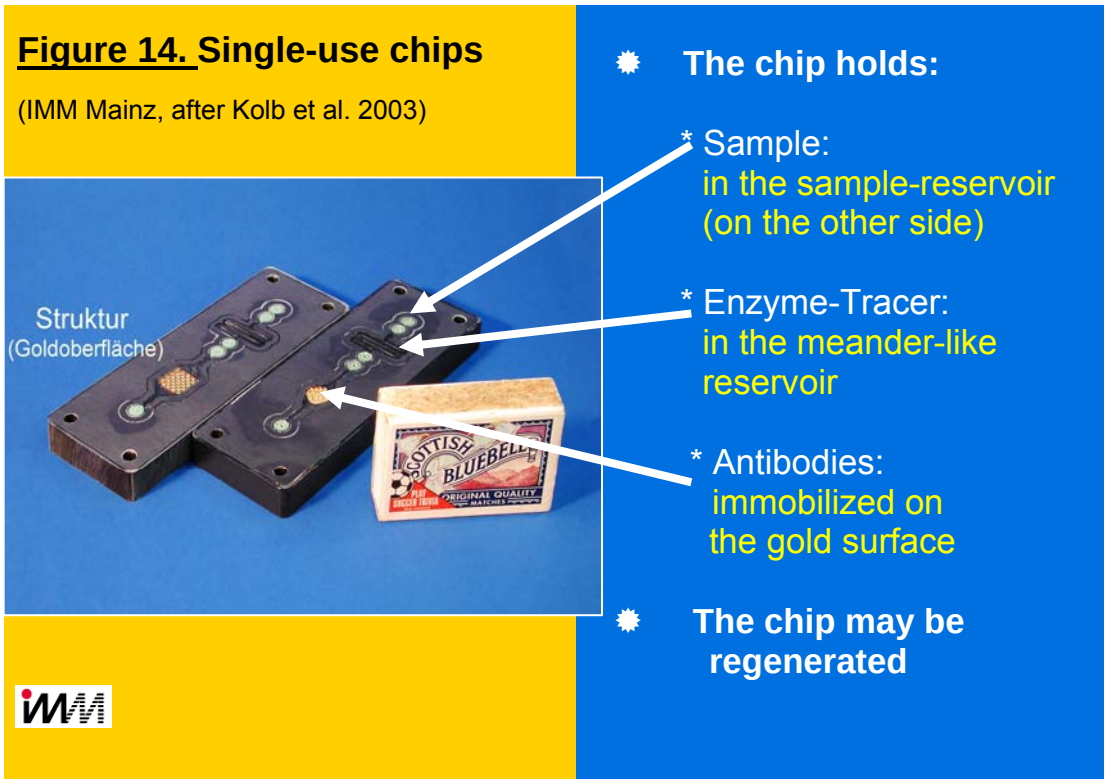

In the incubation / measurement part, the volume above pyramids is 9.478 µl, giving a volume per surface value of 0.11 µl mm^{-2}. By comparison, the corresponding ratio in a microtiter plate is ca. 10 x higher (1.08 µl mm^{-2}), while in a glass vial (batch) this ratio is ca. 100x higher (11.5 µl mm^{-2}), because 1 ml of volume is needed in vials. All these dimensions are presented in table 8.

The total volume of the incubation / measurement cell in the chip comprises, in addition to the volume (strictly) above the pyramids surface, two other volumes (in the direction of flow, in front of and behind the pyramids), which insure the fluids transport and the even flow over the pyramids.

Thus, the total volume of the incubation / measurement cell is ca. 30 µl. This may influence the speed of the chemical reactions to a certain extent (limited by the diffusion speed and the incubation time of the reagent molecules), but cannot be a serious source of variation, because the fluidics and the process temperature are automatically controlled.

Figure 15. Scheme of the incubation / measurement cell and of the detection principle (IMM Mainz, after Frese et al. 2003; Kolb et al. 2003)

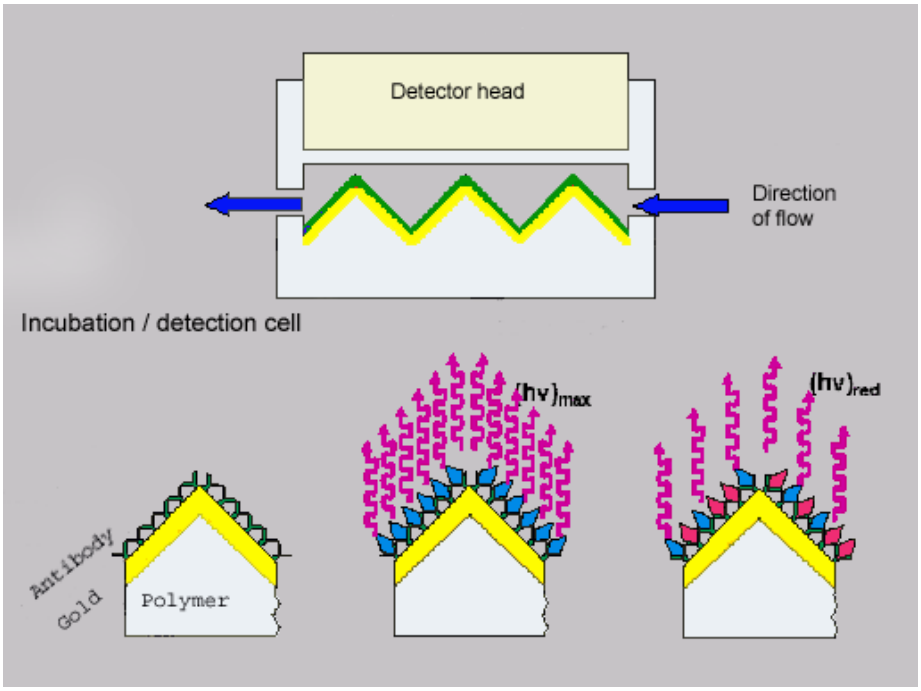

Table 8. Surfaces and volumes specific to each stage of the sensor development

	Conventional ELISA	Batch ELISA	Single-use chip
Set-up and adsorption surface	Polystyrene	Gold	Gold
Surface area	139 mm^2 (for 150 µl)	87 mm^2	87 mm^2
Maximum volume	150 µl	1,000 µl	9.5 µl
Volume per surface area	1.08 µl mm^{-2}	11.5 µl mm^{-2}	0.11 µl mm^{-2}
Antibody dilution	1: 35,000	1: 10,000	1: 1,000
Antibody volume	150 µl	1,000 µl	9.5 µl
Enzyme-tracer dilution	1: 2,000	1: 2,000	1:6,000
Enzyme-tracer volume	50 µl	300 µl	1/3 of 9.5 µl
Analyte volume	100 µl	600 µl	2/3 of 9.5 µl
Substrate / chromogen, or substrate / luminogen	H_2O_2 / TMB	H_2O_2 / TMB	Super Signal® (H_2O_2 / Luminol-Enhancer/)
Substrate volume	150 µl	1,000 µl	9.5 µl
Signal	Absorbance	Absorbance	Chemiluminescence

3.2. Methods

3.2.1. General remarks

The physical system of the developed sensor platform is quite different from the one employed in the traditional ELISA technique, which is based on the microtiter plate. Therefore, the success of the transfer of immunochemicals to the biosensor platform is being conditioned by the identification of those experimental conditions and set-ups which are suitable for the sensor platform. Such probing was done, during the sensor development, by experimenting with various methods of antibody immobilization, assay set-ups and assays physical parameters. The employed approaches and the methods are described in the next sections of this chapter.

3.2.2. Antibody immobilization

The monoclonal antibodies were immobilized by means of immobilized catching protein (Protein A, Protein G or Protein A/G) or catching (anti-species) antibodies (TIB 172 for anti-isoproturon antibody and goat anti-mouse IgG for all the others).

The catching protein/antibody may be immobilized by physical adsorption or by covalent attachment to the solid phase. Both methods are described in the next sub-chapters, as applied by us. The specific mAb could also be immobilized directly on the plate by physical adsorption, but using large amounts of antibodies.

The advantage of using a catching protein/antibody is that these molecules are Fc specific, leaving the Fab region, which bears the recognition sites (i.e. epitopes), free for antigen binding. This means that the layer of immobilized specific antibody is formed by molecules that are much more oriented, the proportion of blocked (by random adsorption to the solid phase) recognition sites being quasi-zero. Therefore, smaller amounts of An-specific antibody can be used, which usually leads to more sensitive (competition) assays.

3.2.2.1. Adsorption of coating proteins

Coating proteins were immobilized on the solid phase (microtiter plate, batch structures, and chip structures) by physical adsorption. A known concentration of coating protein/antibody solution in 50 mM carbonate buffer, pH 9.8, was incubated on the solid phase, either overnight at 3°C, or up to 2 h at RT. A usual concentration of catching protein/antibody was 2 µg l^{-1}. Details are provided in the experiments' descriptions for each An. Adsorption was used all along the sensor development.

3.2.2.2. Covalent attachment of coating proteins

Theoretically, covalent attachment of the coating protein/antibody has the advantage of stronger immobilization, coupled with the possibility of regeneration and re-use of the layer of immobilized molecules, for the immobilization of a new population of specific (monoclonal) antibody, either for the same An or for a different one (Quinn et al., 1999).

This approach involves the physical adsorption of thioalcanes to the (golden) solid surface via sulphur atoms, followed by covalent attachment of the catching protein/antibody to the alkane chain. This physical bond is thought to be very strong and has already wide applications in miniaturization technology like µ-TAS and biosensors, e.g. for functionalizing gold electrodes and gold bands.

In practice, the feasibility of this approach depends on the properties of the thioalcanes (including stability), and on the features of the self-assembled monolayer (SAM) of molecules which these compounds form on metal surfaces like gold (Au).

A thioalcane molecule, $HS(CH_2)_nX$, consists of a thiol group HS at one end, an alkyl chain $(CH_2)_n$ in the middle, and a tail group X at the end. The HS group of each molecule adsorbs very strongly to a (presumably) clean gold surface, so that a group of molecules form a SAM. In such a layer, the alkyl chains interact with each other via Van der Waals forces. The molecule tails is the reactive end, and can be used for covalent attachment of other molecules to the thioalcane monolayer (Engquist, 1996; Suo and Kim, 2001; Dijksma, 2001).

In principle, either catching proteins/antibodies or specific antibodies or only Fab fragments may be covalently bound to thioalcanes. But for our single-use chip immunosensor it was more advantageous to try to covalently bind catching proteins, hence allowing greater analytical flexibility: The layer catching protein can be regenerated and be used as platform for different antibodies, according to the desired An.

We explored this approach by designing a method, drawn upon Li et al. (1996) and Gobi and Mizutani (2001), consisting in covalent immobilization of Protein A/G through SAMs of 3-mercapto-propanoic acid (MPA) adsorbed onto the golden structures (batch and in the chip). In following lines we describe the applied procedures for batch structures and for chip structures, respectively.

Procedure (steps) for batch structures:

1. <u>Gold surface cleaning</u>
   a. Gold surface (IMM structures) incubated in 10 % H_2SO_4 (v/v), 10 min; each golden structure in one glass vial of 5 ml capacity, 2 ml solution per vial; in clean glass vials of 4 ml capacity;

b. Rinsed with Milli-Q water, 1 x 2 ml + 1 x 3 ml + 4 x 4 ml, then transferred to new glass vials;
c. Rinsed with Milli-Q water, 3 x 3 ml; then transferred to new glass vials.

2. Gold surface activation

d. Clean structures incubated in aqueous solution of 60 mM MPA (6.368 mg ml^{-1} in water; MW 106.14 g mol^{-1}), 2h, RT; 3 ml per vial;
e. Rinsed thoroughly with Milli-Q water (to remove excess MPA): 1 x 1ml + 1 x 4ml + 4 x 1ml + 4 x 4ml; then transferred to new glass vials, and used for covalent binding.

3. Covalent binding on MPA-SAM (in the same glass vials as in step 2)

f. Activated structures were incubated in solution of Protein A/G, in the presence of EDC at 4°C. For this, a solution of ca. 8 mg ml^{-1} EDC in PBS 40 mM (pH 7.0) was made; then a solution of 4 µg/mL (1: 500) of Protein A/G in PBS 40 mM was made; then the two solution were mixed 1:1 (by addition EDC solution over the Protein A/G solution); finally, the mixture was added on the golden structure – 3 ml per vial, and incubated overnight at 3°C. EDC concentration in the mixture was 20 mM (3.834 mg ml^{-1} = ca. 4 mg ml^{-1}). Protein A/G concentration in the mixture was: 2 µg ml^{-1} (1: 1,000 from the stock solution);
g. Then the structures were washed with PBST 4 mM: 1 x 1ml + 3 x 4ml PBST 4 mM;
h. Then, Protein A/G immobilized on the golden structures, the structures were ready for ELISA (starting with immobilization o the commercial anti-TNT mAb by the covalently bound Protein A/G);
i. Then the ELISA procedure was carried on as described in sub-chapter 2.3.5.

Procedure (steps) for chip structures:

1. Gold surface cleaning

j. Gold surface (IMM structures) cleaned with regeneration buffer (a watery solution of 100 mM Sodium citrate, adjusted to pH 2.5 with HCl) and buffer and lots of ultrapure water. For the sake of chip integrity, no H_2SO_4 (nor any other strong cleaners like piranha solution).

2. Gold surface activation

k. A solution of 600 mM MPA in water was incubated in the incubation cell of each chip, for 2 hours at RT;

l. This concentration of MPA is 10 times the concentration used in batch structures – though it looked like not all of it dissolved. However, the amount of thioalcane per golden structure is about the same in batch structures, because the volume in the chip is about 10 times smaller than the one applied in batch structures;
m. After incubation, each chips was thoroughly washed with Milli-Q water (50 ml per chip; with a 5 ml syringe), to remove the excess MPA.

3. Covalent binding on MPA-SAM

n. One end of the thioalcane is the S-H group; the other is the COOH group, which will be coupled to Protein A/G in the presence of NHS and EDC;
o. A solution of 240 µg EDC + 66 µl NHS in 3 ml PBS 40 mM was mixed with 3 ml Protein A/G 40 µg ml^{-1}, in portions of 0.75 ml EDC-NHS + 0.75 ml Protein A/G. After each portion was mixed, the mixture was immediately injected with a syringe into the incubation cell of each of the four chips. Incubation of EDC-NHS-Protein A/G mixture lasted 20 min at RT, followed by transfer to 3°C overnight. For comparison between covalent binding and adsorption, the same amount of Protein A/G was then left in other two chips at incubation at 3°C, overnight in carbonate buffer (no 3-MPA and EDC-NHS treatment, just simple adsorption procedure);
p. The next morning, all 6 chips were washed with 4 mM PBST prior to being used for immobilization of the commercial anti-TNT mAb (by the covalently bound Protein A/G) and the on-line measurements with the immunosensor field prototype;
q. The procedure of the on-line measurement is described in chapter 3.2.6.

The main difference in the covalent binding procedure for batch structures and for chip structures is that NHS is used only in the procedure for the chip. In principle, NHS is not necessary because we applied a one-step coupling, meaning that the unstable amine-reactive intermediate resulted from coupling of EDC to MPA is instantaneously reacting with (a COOH group of) Protein A/G molecules. NHS would be necessary for the stabilization of the amine-reactive intermediate in two steps procedures. However, given all the very small volumes handling that is necessary for chip manipulation, we used NHS (together with EDC) to insure proper coupling during the respective procedure.

3.2.3. Preparation of enzyme-tracers

A battery of six Tr for nitroaromatic compounds as haptens were produced by covalent conjugation of hapten to HRP, via N-hydroxy-succinimide esters (Tijssen, 1985;

Schneider and Hammock, 1992). For each hapten, 15 µmol NHS and 30 µmol DCC, were dissolved in 130 µl DMF. The hapten (3 µmol) was activated by dissolving it in the DMF-NHS-DCC at RT; the mix was stirred about 12 min at RT, until the precipitate was clearly visible, then the solution was centrifuged 10 min at 5,000 rpm, and the supernatant was added slowly to a solution of 2 mg horseradish peroxidase in 3 ml 130 mM sodium carbonate buffer, pH 8.1. Reaction vials were transferred to (3°C) and left over night under continuous stirring. The next day, conjugate solution was dialysed against 130 mM sodium carbonate buffer, pH 8.1, with Slide-A-Lyser® cassettes.

The dialyzed conjugate was diluted 1:3 in SuperFreeze™ and stored in the freezer (-27ºC). In total, six conjugates were produced by this method and tested as Tr: TNP–glycine–HRP; TNP–glycylglycine–HRP; TNP–α–AmBA–HRP; DNP–glycine–HRP; DNP–γ–AmBA–HRP; DNP–ε–AmCA–HRP.

After conjugation, each Tr was verified for specific binding to the commercial anti-TNT antibody. This was done by applying two-dimensional titration of the antibody and tracer dilutions, with the zero dose and one standard concentration (e.g. 10 µg l^{-1} TNT) (annex 5).

3.2.4. ELISAs on microtiter plates

3.2.4.1. Competitive saturation ELISA on microtiter plates

The coating antibody solution (anti-species mAb) was immobilized via physical adsorption. The solution of coating antibody (usually 2 µg ml^{-1}) in 50 mM carbonate buffer, pH 9.6, was incubated on microtiter plates, 200 µl/well, either over night at 3°C or 2 h at RT. Microtiter plates incubated with capture antibodies were brought to RT, washed (3 times), and dried. After washing with 4 mM PBST, pH 7.6 (phosphate buffered saline, including 0.05 % v/v Tween 20), the An-specific mAb (1: 35,000 or 303 ng ml^{-1} in 40 mM PBS, pH 7.6) was added and incubated at RT, for 2 h (except when otherwise stated and justified). After another washing (3 times) and drying, the plate was ready for the inhibition step.

Standard solutions (different concentrations from 0.001 to 1,000 µg l^{-1}; 100 µl/well) and the corresponding Tr (50 µl/well; e.g., optimised dilution for TNP-glycylglycine 1: 2,000) were incubated together between 5–30 min, at RT. Plates were washed again, and the substrate for the enzyme reaction was added (150 µl/well; H_2O_2 / TMB in 100 mM sodium acetate buffer, pH 5.5), and incubated for 10–30 min. The enzymatic reaction was stopped with 50 µl/well of 2M H_2SO_4. Plates were read with an ELISA absorbance reader (SPECTRAmax or THERMOmax) at 450 (reference 640 nm).

Using the commercial anti-TNT mAb A1.1.1 and our in-house produced Tr, the competitive ELISA was described and optimised for sensitivity, specificity, pH, solvent tolerance, incubation times and Tr stability.

Similarly, different ELISAs were performed and further optimized using mAbs against atrazine (Karu et al., 1991), diuron (Karu et al., 1994), and isoproturon (Krämer et al., 2004a). For these assays, coating proteins were Protein A, Protein G or Protein A/G, 2 µg ml^{-1}, goat anti-mouse or mouse anti-rat (TIP-172), 2.4 or 2.0 µg ml^{-1}, respectively.

The dilutions of mAb were 1: 4,000 (600 ng ml^{-1}) in the atrazine-ELISA, 1: 4,000 (from the culture supernatant) in the diuron-ELISA, and 1: 20,000 (75 ng ml^{-1}) in the isoproturon-ELISA. The dilutions of the corresponding Tr were 1: 2,000 in the atrazine- and isoproturon- ELISAs, respectively, and 1: 4,000 in the diuron-ELISA.

3.2.4.2. Sequential saturation ELISA on microtiter plates

The coating antibody solution (anti-species mAb) was immobilized via physical adsorption. The solution of coating antibody (usually 2 µg ml^{-1}) in 50 mM carbonate buffer, pH 9.6) was incubated on microtiter plates, 200 µl/well, either over night at 3°C or 2 h at RT. Microtiter plates incubated with capture antibodies were brought to RT, washed (3 times), and dried. After washing with 4 mM PBST, pH 7.6 , the An-specific mAb (in 40 mM PBS, pH 7.6) was incubated on the capture antibody at RT, for 2 hours (except when otherwise stated and justified). After another washing (3 times) and drying, the plate was ready for the inhibition step.

In displacement ELISA, the antigens (An and Tr) were not incubated in one step together but in two steps of equal duration (3 – 30 min) and separated by a washing step: sequential saturation. In each of the two steps, one of the two antigens was replaced by a corresponding volume of buffer, so that the separate concentration of the remaining antigen was the same as in the competition format. Plates were washed again, and the substrate for the enzyme reaction was added (150 µl/well; H_2O_2 / TMB in 100 mM sodium acetate buffer, pH 5.5), and incubated for 10–30 min. The enzymatic reaction was stopped with 2M H_2SO_4, 50 µl/well. The microtiter plates were read with the absorbance reader.

In certain sequential saturation set-ups, the antigens incubation steps were repeated three times in a row. In one set-up, the An was first incubated in three episodes in a row, separated by a single washing. The washing between episodes of incubation of the same antigen was single, instead of the usual triple washing, because we wanted to minimize the dissociation of the Ab-Ag complexes. A lower dissociation was also needed for a good additive effect in the binding pattern. This additive effected resulted in the amplified visibility of the features of the standard curve at very short incubation times: 10-120 s. This was the

rationale behind the repeated incubation. Then, after a triple washing step, the Tr was incubated only one time. In another set-up, the set formed by the first and the second incubation steps of the antigens was repeated 3 times in a row.

3.2.4.3. Further methods: soil TNT spiking, TNT extraction, and ELISA with soil extracts

Methanol and 2-isopropanol were used in the establishment of a soil extractions method and protocol from spiked standardized soil. Methanol is already known as a very successful solvent for soil extractions, together with acetone (Jenkins et al., 1996a) and acetonitrile (Jenkins et al., 1989; U.S. EPA Method 8330, 1994; Alter et al, 1998; Walsh and Ranney, 1998a,b, 1999), but all three are highly toxic. On the contrary, 2-isopropanol, which displayed a lower but promising extracting efficiency as methanol, it is much less toxic. Thus, soil extractions with 2-isopropanol will be more environment- and user-friendly, with good extraction properties. Isopropanol is also used in laboratory methods as technical solvent (Walsh and Ranney, 1998b).

For exploration of the influence of the soil matrix, we developed a relatively easy soil spiking and soil extraction method, which we will describe in the next paragraphs. Then, standard curves were produced with the soil extracts, assuming the same An concentration in the soil extracts as the spiked concentration (100 % recovery). By comparing these extraction-standard curves with the standard curves the general influence of matrix could be assessed.

The observed matrix influence on the TNT assays is the combined result of two phenomena: (1) An recovery (in %), connected with an apparent loss of assays sensitivity and (2) destructive effects of soil matrix (humic acids, etc) upon the bioreagents' structure-function.

The effect of solvent upon the assay might be avoided by applying high TNT spiking concentrations; this also allows a very strong reduction of the percent of solvent used in ELISA, by diluting the soil extracts with Milli-Q water.

Two types of standardised soils (air-dried) were spiked. The first soil was from "Landwirtschaftliche Untersuchungs- und Forschungsanstalt" – LUFA mollisol type-nr 2.2 (Speyer). The second soil was from *Merzenhausen* (Institut für Radioagronomie des Forschungszentrums Jülich (Prof. Dr. F. Führ).

Both soils are from the A_p horizon, i.e. the upper layer (1-30 cm) of the topmost mineral horizon (A) in the soil. This is where humus accumulates, so that it generally has the highest content in organic matter. Horizon A is also a zone of leaching where water

transports dissolved and suspended materials down into the lower layers; and where the highest amount of biological activity occurs.

Standard LUFA soil 2.2 is a loamy sand (SC) from the 1 – 30 cm soil depth layer, with 2.27 ± 0.28 % organic C; 9 ± 2 % N; pH 6.1 ± 0.2; water-holding capacity [g H_2O kg^{-1}] 480 ± 40; and cation exchange capacity 90 ± 20 mval kg^{-1} (Eikenberg, 1999).

Merzenhausen soil is a kind of alluvial silt (ML), with 0.98 % organic C; 0.08% N; pH 7.2; water-holding capacity [g H_2O kg^{-1}] ca. 460; and cation exchange capacity ca. 114 mval kg^{-1} (Eikenberg, 1999).

For spiking, three target concentrations of TNT in soil were chosen: 2.0 mg kg^{-1}; 0.5 mg kg^{-1}; and 0.0 (zero) mg kg^{-1}. Thus, known amounts of each of the three TNT solutions (in acetonitrile) were spread onto a thin layer of each of the two types of soil (6 spiked soils in total) and allowed the acetonitrile to evaporate under the fume-hood. Then the soils were mechanically homogenized in capped, clean glass bottles (of 100 ml capacity), with a vertical rotating mixer (Gerhard Rotierapparat RA20), for 24 hours at moderate speed.

Afterwards, TNT was extracted from each of the 6 spiked soils by applying two solvents in parallel: methanol and 2-isopropanol. In capped, clean glass vials (of 80 ml capacity), 5 g from each soil with 10 ml solvent by 15 min hand shaking; then the sediment was allowed to settle down for 20 min and the supernatant was collected and filtered with filter-capped plastic syringes and stored in labelled, brown glass vials (of 7 ml capacity) at 3°C.

Next day, the extracts were used in the TNT-ELISA – competitive saturation. The soil extracts were used like the standards, function of the known concentration of TNT spiked. The curve shift will indicate the combined effect of soil and extraction efficiency (recovery). Because precise measurement in soils was beyond the scope of the present thesis, the ELISA with soil extracts aimed only at (1) probing the method of fast extraction and (2) observing the general influence of soil matrix on the TNT assay.

3.2.5. Competitive saturation ELISAs on batch structures

3.2.5.1. Selection of the material for structures

Prior to deciding the structure (pyramids) geometry, it was important to determine which one, between gold and plastic, is the best material for the immobilization of the immunoreagents. Prior to any optimization, using a well established atrazine assay, intensities (efficiencies) of physical adsorption of the catching protein (Protein A) on plastic and golden surfaces were compared. Golden surface displayed higher adsorption; henceforth, we did all the subsequent tests on the golden structures.

3.2.5.2. Selection of the structure (pyramids) geometry

Before measurements could be carried out in the single-use chip, it was important to choose the right design and surface for the actual detection cell. Here, different criteria had to be met: 1) good binding of the bio-recognition element; 2) low unspecific binding of the Tr; 3) optimum surface area to ensure a sufficient signal; 4) optimum fluidics; 5) resilience of the gold layer to repeated immunoassay procedures and surface regenerations. Therefore different types of structures, out of which one would have later to serve within the sensor, had been tested.

Regarding points 1), 2) and 3), several types of structures were screened for antibody binding performances (the more binding, the better) and for unspecific binding, mainly caused by the Tr (the less binding, the better). All three issues were also related to the washing efficiency in each type of structure.

Regarding point 4), the computer simulations of the fluidics (at flow rates of 200 – 400 µl / min) was performed by IMM Mainz and proved that the best fluidics (flow spatial distribution and liquid replacement) corresponded to the round (instead of square) general shape, with a diameter of 8 mm. Our tests with the laboratory prototype confirmed the simulations, and allowed to establish an optimum combination of technical parameters. Thus, it was established that the best flow-rate is 300 µl / min, corresponding to the fastest safe operational speed of the flow-injection system (hence shorter injection times – faster analysis). At higher flow-rate, implying higher under-pressure imposed by the sucking step-motor pump, the reagent automated manipulation got corrupted.

The major problem was that air was inevitably penetrating into the flow system by the connections between the exchangeable chip and the ground plate. For proper system functioning and correct experimentation, the flow system must be air-free. In addition, the simulations performed by IMM Mainz showed that the flow over the pyramids is characterized by the fact that the bulk of the fluid passes by the top of the pyramids. Higher flow rates can only strengthen this flow pattern. This implies that washing is less efficient at the basis of the pyramids, and that higher flow rates are not desirable if good washing efficiency is to be preserved.

Regarding point 5), resistance of the gold layer through series of repeated experiments was determined by the current micro-manufacture quality limitations. Thus lower resistance was with higher pyramids because of the lower quality of micro-manufacture of the higher pyramids.

3.2.5.3. General batch ELISA procedure

After optimization on the microtiter plates, the ELISA procedure for each target An was adapted to the batch ELISA format, where the wells of the microtiter plate were replaced by the gold covered discs with numerous pyramid structures, which were placed and treated individually in glass vials.

The coating antibodies/proteins (anti-species mAbs or Protein A/G; 1 ml solution per vial) were set-up in 50 mM carbonate buffer, pH 9.6, and incubated at 3 °C, overnight (alternatively, 2 h at RT). The next day, structures were allowed to come to RT (15 min), the coating protein solution was removed, and the structures were washed 3 times with 1 ml of 4 mM PBST. After this, the An-specific mAb (in 40 mM PBS, pH.7.6) was incubated (usually 2 h) at RT, then this antibody solution was removed (washing not needed) and replaced by a solution made from skimmed milk powder (MP), 1% (w/v, in 40 mM PBS, pH, 7.6), 30 min at RT (blocking step). Following another washing, for the competition step, the An standards (in 40 mM PBS) were added onto the immobilized antibody before the Tr (40 mM PBS, pH 7.6).

During competition, the vials were incubated at RT and slowly moved with a microtiter plate shaker. After competition and another washing, the signal was obtained by incubating the structures in 1 ml per vial of substrate /chromogen solution for HRP (H_2O_2 / TMB) in 100 mM sodium acetate buffer, pH 5.5, 30 min (alternatively, up to 90 min) at RT, in the dark. In order to minimize unspecific binding, the structures can be quickly (but gently) transferred to clean glass vials before substrate incubation. After substrate incubation, 150 µl of incubated substrate/chromogen solution was transferred from each vial to a microtiter plate and the enzyme reaction was stopped with 2 M H_2SO_4, 50 µl/well before absorbance reading.

3.2.5.4. Regeneration of the golden structures

After reading, the structures were rinsed with Milli-Q water, and their surface was regenerated by washing first 3 times with regeneration buffer (100 mM sodium citrate, pH 2.5), 1 ml/vial, then three times with Milli-Q water, 1 ml/vial. After the first washing with water, the structures were transferred to clean glass vials and washed again two times with Milli-Q water. The regenerated structures were either stored in air at RT or used for another experiment. The structures could be regenerated and reused for at least 50 times.

3.2.5.5. TNT batch ELISA

The coating protein was Protein A/G (alternatively, goat anti-mouse IgG) for mouse mAb A1.1.1; coating (applied) concentration was 4 µg ml^{-1}. The recognition antibody was anti-TNT mAb A1.1.1, 2 µg ml^{-1}, 2 h at RT (alternatively, down to 10 min). After the blocking step, the TNT standards and the Tr solution (TNP-glycylglycine–HRP, 1: 2,000) were incubated together on the structures, 10 min.

3.2.5.6. Atrazine batch ELISA

As coating antibody, goat anti-mouse IgG, 4 µg ml^{-1}, was used. The recognition antibody was anti-atrazine mAb AM5D1-3 (cell culture supernatant 1: 2,000), 2 h at RT. After the blocking step, the atrazine standards and the Tr solutions (1: 2,000) were incubated together on structures, 10 min.

3.2.5.7. Diuron batch ELISA

The coating antibody was goat anti-mouse IgG, 2 µg ml^{-1}. The recognition antibody was anti-diuron mAb 481.1 (cell culture supernatant 1: 2,500); it was incubated for 2 h at RT. After the blocking step, the diuron standards and the Tr solutions (1: 4,000) were incubated together on structures, 10 min.

3.2.5.8. Isoproturon batch ELISA

The coating antibody was mouse anti-rat TIB 172, 2 µg ml^{-1}. The An-selective antibody is the anti-isoproturon rat mAb IOC 7E1 (75 ng ml^{-1}), and it was incubated for 2 h at RT. After the blocking step, the isoproturon standards and the Tr solutions (1: 200) were incubated together on structures, 30 min.

3.2.6. ELISAs by the immunosensor prototypes (demonstrators)

3.2.6.1. Off-line preparation of the chips

All off-line fluid handling on the chips was carried out with a simple single-use syringe with a needle (standards) or without (all the rest). The chips (incubation cell) were incubated: 1) with the appropriate catching protein at RT; 2) with the corresponding An-specific mAb; and 3) with 1% (w/v) MP dissolved in 40 mM PBS. Finally, the chips were

washed with 4 mM PBST, 1 ml/chip. At this point, the chips were either used immediately for measurements, or they were labelled and stored in the freezer (after removing the liquid from the chip as much as possible).

3.2.6.2. Automated (on-line) measurements

Before proceeding to on-line measurements, a minimum preparation of the instrument was required, i.e. some automatic steps carried out with a rinsing-chip, after which the system was air-free and the substrate was in place for automated injection.

The chip should be at RT and air-free at the beginning of the on-line measurement. Once the Tr reservoir on the chip was filled with Tr solution, the chip was inserted onto the ground plate and the sample reservoir filled with the standard (or sample) solution, the control software (provided by IMM Mainz and written by us with the Software programme *Labview*) was opened and the automated sequence of injection and incubation steps was started.

A short technical description of the automatic sequences of steps is provided in annex 9: measurement program (table 13); system washing before and after measurement (table 14); program for substrate/luminogen solution set-up before measurements (table 15).

For the sake of proper temperature-control (22°C) and insulation from outer light, once the sample injection was finished, the instrument had to be kept closed (picture in annex 3, fig. 110).

Basically, the automated sequence steps reproduced the ELISAs optimized on microtiter plates, but within adapted parameters: washing, sample and Tr injection (mixed on-line), mixture incubation, washing, substrate (mixture) injection and incubation, and washing. The mixture of the two solutions of the commercial substrate was stable 6 hours at RT; after this time interval, the substrate mixture must be renewed.

The luminescence signal (for calculations and fitting) was taken semi-automatically at the end of substrate incubation. However, the whole signal development and washing was followed on a small screen in order to detect any experimental disturbances. This was the first check of the correctness of the measurement, and consisted in observing whether the signal development showed the usual shape (well established by us) or not.

The second check was the visual observation of the chip after it was taken off the ground plate at the end of the measurement: the Tr reservoir and the incubation-measurement cell should be air-free.

Between two subsequent measurements, there was a system-washing step (3 min) with the rinsing chip, aiming at preventing contamination (with An) between measurements.

Until now, the instrument did not display the concentration of the target An, but renders a count number used (usually every 3 sec) in its calculation (e.g., with MS Excel).

3.2.6.3. Chip regeneration

In principle, the chips should be used only once. However, given the present production costs, we regenerated them with the same regeneration buffer used in batch ELISA and thorough rinsing with Milli-Q water. After regeneration, the chips could be prepared again (antibody immobilization) for any desired target An (or group of An) and stored frozen (until now, up to three days) until another measurement.

3.2.7. Data analysis

Standard curves were produced using either the specialized commercial software program for microtiter plate absorbance reader (SoftMaxPro, Molecular Devices, Palo Alto, CA, USA).) or a general Office Excel (Microsoft), on the theoretical basis described in chapter 2.1.2., eq. 6.

4. RESULTS AND DISCUSSION

4.1. Immunoassay design and flexibility

4.1.1. TNT competitive assays

4.1.1.1. Panel of new enzyme-tracers

Anti-TNT mAb were commercially acquirable, but no corresponding Tr was available commercially. In order to produce enzyme-tracers for the different immunochemical methods for TNT (ELISA, batch ELISA, and single-use immunosensor), six different haptens were conjugated to HRP and tested in conventional ELISA (sub-chapter 3.2.3).

All six enzyme-tracers displayed binding and inhibition to a certain extent with mAb A1.1.1. First, four of them were considered further: TNP–glycylglycine–HRP, DNP-γ-AmBA–HRP, TNP–α–AmBA–HRP, and DNP–ε–AmCA–HRP.

After additional optimizations, TNP–glycylglycine–HRP was established as the best Tr for mAb A1.1.1, because it showed the highest absorbance, the best test midpoint, and the lowest background. It was therefore used for all further optimizations (e.g., cross-reactivity studies) and formats (batch ELISA and immunosensor).

Standard curves are shown with the following four new enzyme-tracers: TNP-glycylglycine–HRP (fig. 16); DNP-γ-AmBA–HRP (figs. 16 and 17); TNP-α-AmBA – HRP (fig. 18); DNP-ε-AmCA – HRP (fig. 18).

The standard curves with the enzyme-tracers others than the main one can also be optimized. Here shown are two optimization curves with the Tr DNP-γ-AmBA–HRP (fig. 17)

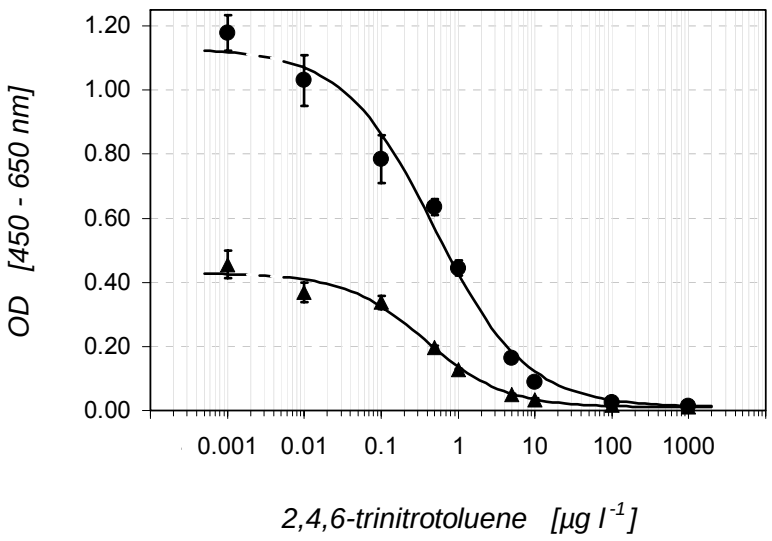

Figure 16. Standard curves, with TNT-ELISA, using the enzyme-tracers (●) TNP-glycylglycine–HRP and (▲) DNP-γ-AmBA–HRP. Applied Ab concentration: 285 µg l^{-1}. Applied Tr dilution: 1: 2,000. The following values of the curve parameters were obtained (n = 3):

(●) A = 1.13; B = 0.73; C (IC_{50}) = 0.50; D = 0.01; R^2 = 0.990;

(▲) A = 0.43; B = 0.85; C (IC_{50}) = 0.37; D = 0.01; R^2 = 0.988.

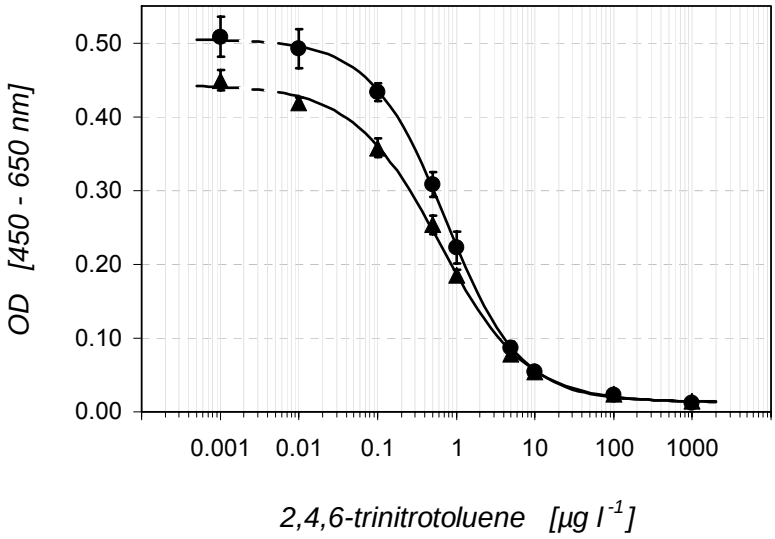

Figure 17. Standard curves, optimization with TNT-ELISA, using the Tr DNP-γ-AmBA–HRP. Applied Ab concentrations higher than in fig 16: (●) 400 µg $l^{-1}$and 333 (▲) µg l^{-1}. Applied Tr dilution lower than in fig. 16: 1: 1,500. The following values of the curve parameters were obtained (n = 3):

(●): A = 0.50; B = 0.91; C (IC_{50}) = 0.74; D = 0.01; R^2 = 1.000;

(▲): A = 0.44; B = 0.79; C (IC_{50}) = 0.62; D = 0.02; R^2 = 0.999.

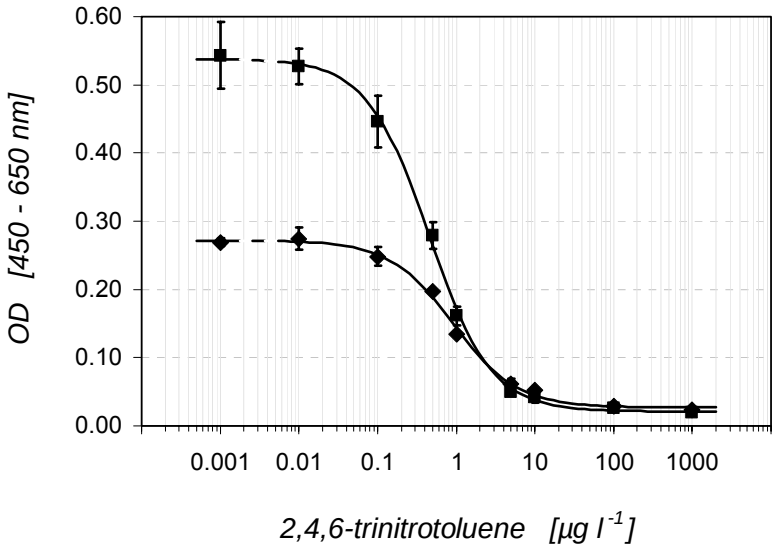

Figure 18. Standard curves, with TNT-ELISA, using the enzyme-tracers (◆) TNP-α-AmBA–HRP, and (■) DNP-ε-AmCA–HRP. Applied Ab concentration: 285 µg l^{-1}. Applied Tr dilution: 1: 1,000. The following values of the curve parameters were obtained (n = 3):

(◆): A = 0.27; B = 1.07; C (IC_{50}) = 0.92; D = 0.03; R^2 = 0.997;

(■): A = 0.54; B = 1.10; C (IC_{50}) = 0.45; D = 0.02; R^2 = 0.999.

4.1.1.2. Stability of enzyme-tracers

The hapten–HRP conjugate used as the best Tr showed pronounced instability at +3°C. Catalytic properties of the Tr could be maintained by storing it at -28°C after mixing it with the commercial peroxidase conjugate stabilizer SuperFreeze™, one volume Tr for two volumes of SuperFreeze (fig 19).

The pronounced instability of the Tr may be due to the fact that the hapten itself is moderately unstable at +3°C, therefore it is necessary to be stored at ca. -20°C. This discussion applies equally to the entire panel of enzyme-tracers produced by us.

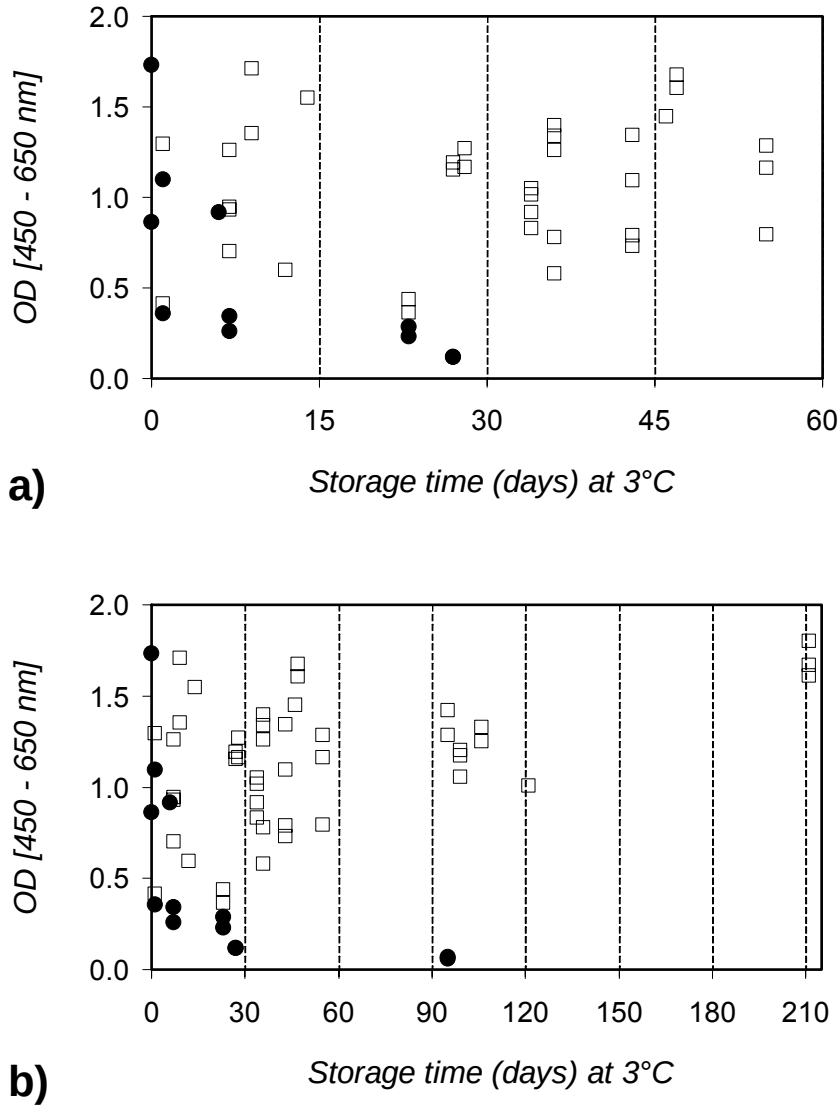

Figure 19. Stability of the current Tr (TNP-Glycylgycine – HRP) in time, at +3°C (●) and at -28°C with the commercial SuperFreeze stabilizer (□). The signal intensity (measured absorbance: optical density - OD) produced by the Tr (with some variations in experimental conditions, notably RT) is represented for 2 months **(a)** and for 7 months **(b)**. At +3°C, after one month the signal intensity (enzyme activity) dropped almost completely. On the contrary, at -28°C and with SuperFreeze stabilizer, the enzyme activity maintained, and even increased slightly with time (as predicted by the stabilizer manufacturer).

4.1.1.3. Assay performances with the new enzyme-tracers

4.1.1.3.1. General assay performances

With the optimized TNT-ELISA on microtiter plates, using Gam as coating antibody, anti-TNT mAb A1.1.1, and TNP-glycyl-glycine–HRP as Tr, the following performance characteristics of the standard curve were obtained:

- detection limit (DL; IC_{20}) between 0.1–0.2 µg l^{-1};
- linear dose-response region (IC_{20}–IC_{80}) from 0.1 to 10 µg l^{-1};
- test midpoint (IC_{50}) between 0.3 and 1 µg l^{-1};
- curve slope (B): in general 0.9 – 1.1;
- high specificity (low cross-reactivities) for TNT (table 9).

In the literature, "specificity" and "selectivity" are sometimes used as synonyms. However, one can argue that the degree of "specificity" means how well one individual component of a given multi-component system can be measured undisturbedly. Instead, the degree of "selectivity" means how well a number of components of interest can be measured simultaneously (Danzer, 2001), e.g. like with PASA system for triazines (Winklmair et al., 1999).

With a view to our final practical purpose (which is screening of a target An: TNT), because we applied one assay for one An, we use the term "specificity" to designate the technical parameter "cross-reactivity" (CR), i.e. the influence of an An-like component (also called "cross-reactant") upon the sensitivity of an immunoassay for a given An.

However, from a biochemical point of view, because these anti-TNT mAb have CR, they should not be considered "specific" (for TNT), but "selective" (for TNT). Thus, for the anti-TNT mAb employed by us, "specificity" to TNT is understood as "the highest level of selectivity" and the subsequent application use in the analysis of TNT.

The effect of cross-reactivity upon the measured result is usually a positive bias (false positives), which can sometimes vary with some experimental parameters like incubation time and temperature (Vining, 1981; Miller and Levinson, 1996). Less common, cross-reactivity can determine a negative bias (false negatives) in certain immunoassays (Jortani et al., 1997; Valdes and Jortani, 2002). Therefore, detailed verification of cross-reactivity with optimized commercial immunosensors is recommendable.

For the present immunosensor development, cross-reactivities have only been checked for the newly developed TNT assay. CR of any cross-reactant was calculated using the following equation:

$$CR\ (\%) = 100*(IC_{50}\ TNT\ /\ IC_{50}\ \text{test compound}) \qquad \text{(eq. 7)}$$

The most relevant cross-reactivities are: tetryl 25.6%; TNB 13.1%; 2-amino-DNT 5.2% (fig. 20); and 2,4-DNT 3.2%. The CR for different nitroaromatic compounds obtained with the Tr TNP-glycylglycine–HRP were similar to those published earlier by Zeck et al. (1999), who used the same antibody but a different Tr (table 9).

In addition to environmentally relevant nitroaromatic compounds, also the haptens for the Tr were determined, which revealed the highest CR for TNP-glycylglycine, namely 12.2%.

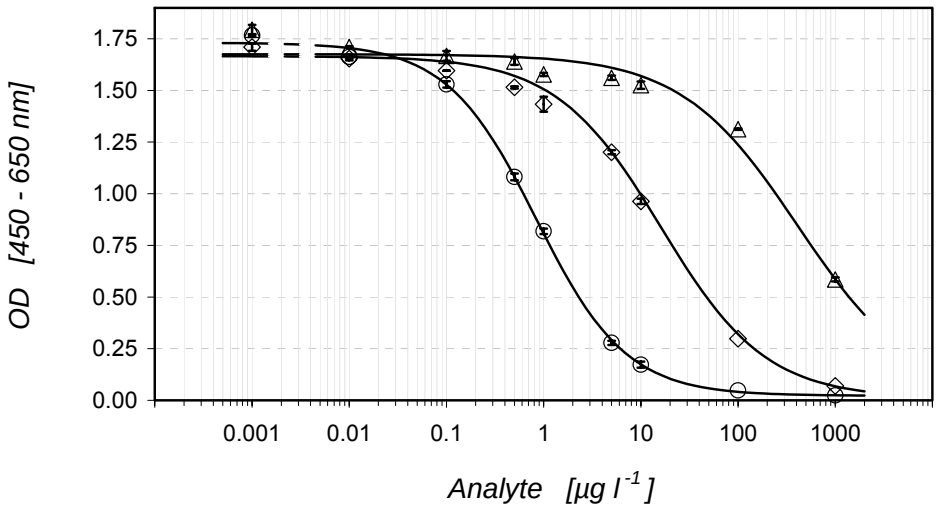

Figure 20. Standard curves, with (○) 2,4,6-TNT and its main degradation products (◇) 2-amino-4,6-DNT and (△) 4-amino-2,6-DNT. The applied antibody concentration was 285 µg l^{-1}. The applied Tr (TNP-glygylglycine–HRP) dilution: 1: 1600. The following curve parameters values were obtained (n = 2): (○) 2,4,6-TNT: A = 1.73; B = 0.94; C (IC_{50}) = 0.84; D = 0.02; R^2 = 0.99;
(◇) 2-amino-4,6-DNT: A = 1.67; B = 0.81; C (IC_{50}) = 16.1; D = 0.01; R^2 = 0.99; CR = 5.2%
(△) 4-amino-2,6-DNT: A = 1.68; B = 0.73; C (IC_{50}) = 415; D = 0.01; R^2 = 0.99; CR = 0.2%

The general parameters of the standard curve were preserved through different experimental set-ups. Thus, the TNT-assay:

a) runs with different coating reagents or with the antibody coated directly on the microtiter plate (details in sub-chapter 4.1.1.3.2);
b) runs with An in 40 mM PBS and in Milli-Q water (details in sub-chapter 4.1.1.3.3);
c) runs with a fast format, in which every incubation step lasted 10 min: catching protein 10 min instead of 2h at RT, anti-TNT antibody 10 min instead of 2h at RT, competing antigens 10 min instead of 30 min, and chromogen/substrate 10 min (usually) up to 30 min (details in sub-chapters 4.1.1.3.2; 4.1.1.3.3; 4.1.1.3.4.).

The format of short duration of incubation was also successfully extended to the immunoassays for atrazine, diuron and isoproturon (sub-chapters 4.2.) Furthermore,

incubation times for An / Tr mixture can be as low as 3 min, and the assays tolerated wide variations of the physical parameters (sub-chapters 4.1.1.4.; more on the experimental flexibility of these four immunoassays, in sub-chapter 4.1.2.).

Table 9. Cross-reactivities in TNT-ELISA, with the in-house produced enzyme-tracer TNP-Glycylglycine–HRP, as compared with the literature (Zeck et al., 1999).

Analyte	CR [%] (in-house)	CR [%] (Zeck et. al., 1999)
2,4,6-Trinitrotoluene	100.0	100.0
Tetryl	25.6	22.0
1,3,5-Trinitrobenzene	13.1	17.0
2,4-Dinitroaniline	7.2	6.3
2-Amino-4,6-dinitrotoluene	5.2	6.4
2,4-Dinitrotoluene	3.2	2.1
3,5-Dinitroaniline	1.1	1.4
1,3-Dinitrobenzene	0.3	0.5
2,6-Dinitroaniline	0.3	–
4-Amino-2,6-dinitrotoluene	0.2	0.1
2,6-Dinitrotoluene	0.1	0.2
2,4-Diamino-6-nitrotoluene	0.01	–
2-Nitrotoluene	0.01	–
3-Nitrotoluene	0.01	–
4-Nitrotoluene	0.01	–
Nitrobenzene	0.01	–

4.1.1.3.2. Influence of the coating protein

Potentially, four coating proteins can be used for the commercial (mouse) anti-TNT mAb: Gam, Protein G, Protein A/G and Protein A. With our TNT assay, the best results were obtained when the mAb was immobilized via Gam (figs. 21; 22).

Nevertheless, valid curves (despite much lower signal) could also be obtained with Protein G (fig. 21) or Protein A/G (fig. 22; 24), but not with Protein A, which allowed only a very low (i.e. worthless) signal – (fig. 23).

When the Ab was directly adsorbed on the wall of the microtiter plate (fig. 25), the standard curve was compromised with the lowest used Ab concentration: extremely low

signal and correlation coefficient (R^2) < 0.95. But, when the standard curve was not compromised (still enough Ab), the signal (optical density) is a quarter from that of the better curve.

As expected, when the specific Ab is not immobilized via a catching protein, huge amount of specific Ab is needed (4-5 times more) to obtain valid curves. As expected, the same pattern was obtained with fast assay format (figs. 26; 27).

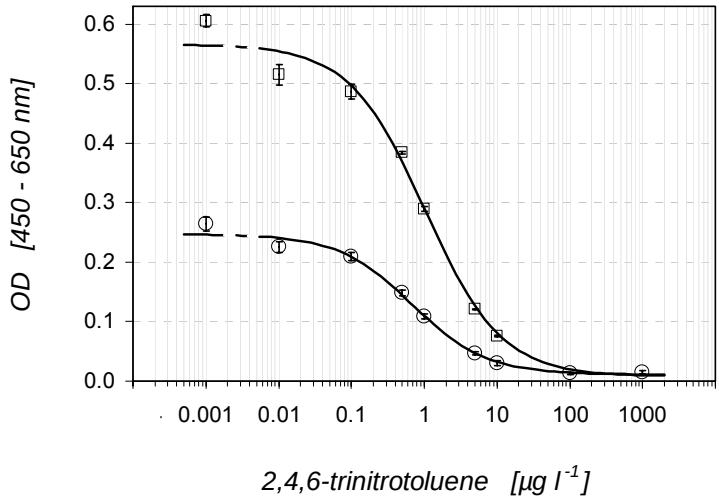

Figure 21. Standard curves, with TNT-ELISA, using two different coating reagents and an Ab concentration of 400 µg l^{-1}. The applied Tr dilution was 1: 2,000. The following curve parameters values were obtained (n = 3):

(□) Goat anti-mouse: A = 0.57; B = 0.83; C (IC_{50}) = 1.04; D = 0.01; R^2 = 0.992;

(△) Protein G: A = 0.25; B = 0.86; C (IC_{50}) = 0.68; D = 0.01; R^2 = 0.994.

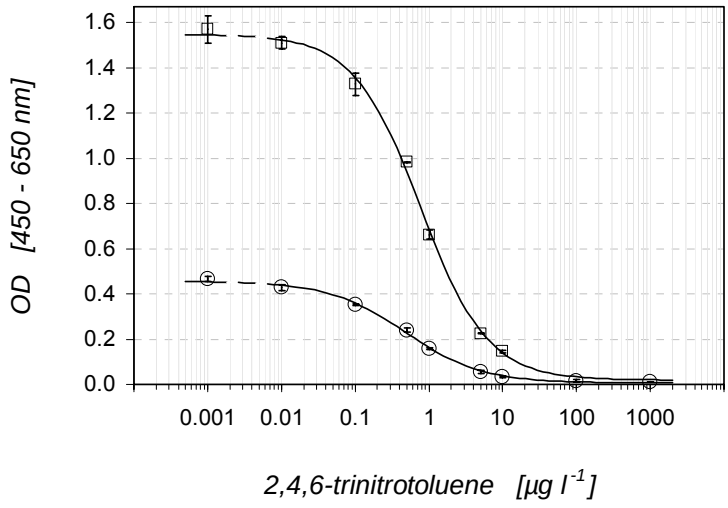

Figure 22. Standard curves, with TNT-ELISA, using two different coating reagents and an Ab concentration of 285 µg l^{-1}. The applied Tr dilution was 1: 2,000. The following curve parameters values were obtained (n = 3):

(□) Goat anti-mouse: A = 1.55; B = 0.96; C (IC_{50}) = 0.77; D = 0.02; R^2 = 0.999;

(○) Protein A/G: A = 0.46; B = 0.84; C (IC_{50}) = 0.47; D = 0.01; R^2 = 0.998.

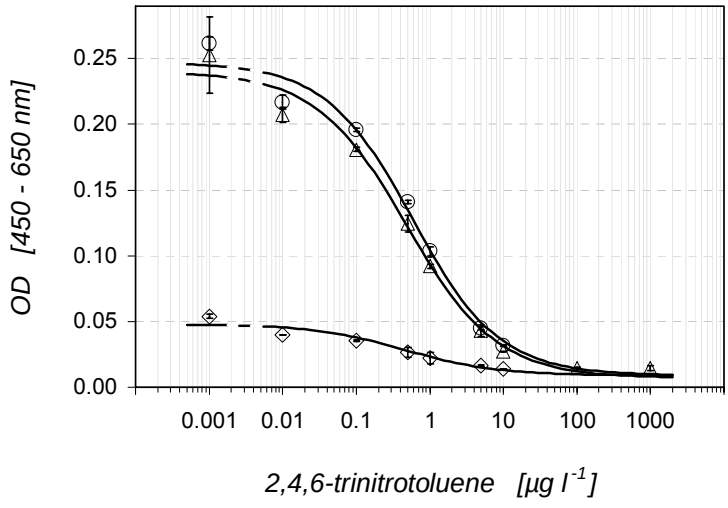

Figure 23. Standard curves, with TNT-ELISA, using three different coating reagents and an Ab concentration of 400 µg l^{-1}. The applied Tr dilution was 1: 2,000. The following curve parameters values were obtained (n = 2):

(○) Protein A/G: A = 0.25; B = 0.74; C (IC_{50}) = 0.58; D = 0.01; R^2 = 0.991;

(△) Protein G: A = 0.24; B = 0.71; C (IC_{50}) = 0.48; D = 0.01; R^2 = 0.989;

(◇) Protein A: A = 0.05; B = 0.70; C (IC_{50}) = 0.45; D = 0.01; R^2 = 0.982.

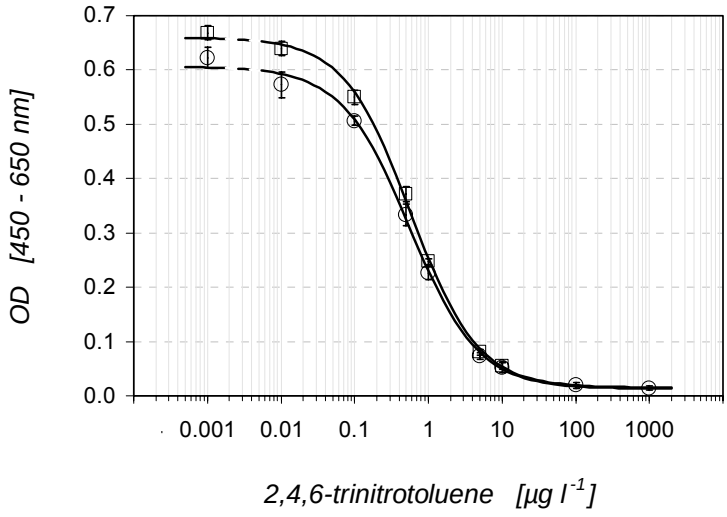

Figure 24. Standard curves – TNT-ELISA optimizations, using Protein A/G and two Ab concentrations. The applied Tr dilution was 1: 1,500. The following curve parameters values were obtained (n = 3):

(□) 400 µg l^{-1}: A = 0.66; B = 0.96; C (IC_{50}) = 0.57; D = 0.02; R^2 = 0.999;

(○) 333 µg l^{-1}: A = 0.61; B = 0.94; C (IC_{50}) = 0.56; D = 0.01; R^2 = 0.998.

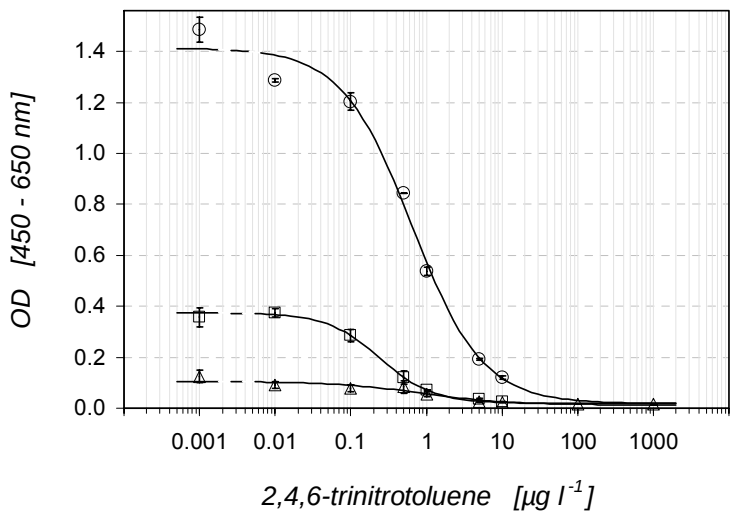

Figure 25. Standard curves, with TNT-ELISA, using three different Ab concentrations which were applied directly on microtiter plate (no catching protein). The applied Tr dilution was 1: 2,000. The following curve parameters values were obtained (n = 2):

(○) 2 000 µg l^{-1}: A = 1.41; B = 0.94; C (IC_{50}) = 0.65; D = 0.02; R^2 = 0.992;

(□) 1 000 µg l^{-1}: A = 0.37; B = 1.23; C (IC_{50}) = 0.24; D = 0.02; R^2 = 0.998;

(△) 667 µg l^{-1}: A = 0.11; B = 0.76; C (IC_{50}) = 0.87; D = 0.01; R^2 = 0.936.

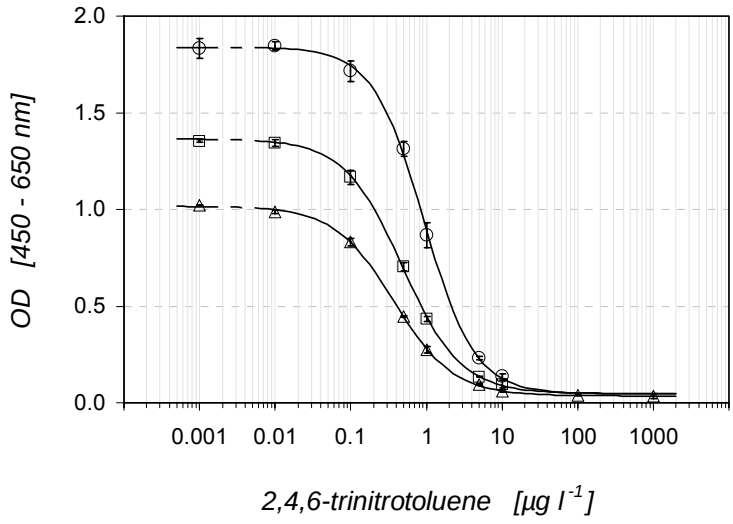

Figure 26. Standard curves, with fast TNT-ELISA, with three Ab concentrations which were immobilized via Gam. The applied Tr dilution was 1: 2,000. The following curve parameters values were obtained (n = 2):

(○) 2 000 µg l^{-1}: A = 1.84; B = 1.29; C (IC_{50}) = 0.92; D = 0.05; R^2 = 0.999;

(□) 500 µg l^{-1}: A = 1.36; B = 1.13; C (IC_{50}) = 0.48; D = 0.05; R^2 = 1.000;

(△) 285 µg l^{-1}: A = 1.02; B = 1.10; C (IC_{50}) = 0.40; D = 0.04; R^2 = 1.000.

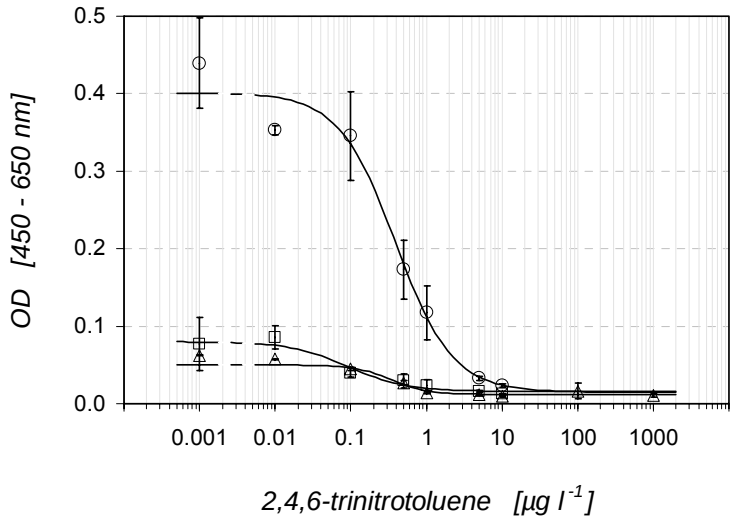

Figure 27. Standard curves, with fast TNT-ELISA, with three Ab concentrations which were immobilized directly on the wall of the microtiter plate wells. The applied Tr dilution was 1: 2,000. The following curve parameters values were obtained (n = 2):

(○) 2 000 µg l^{-1}: A = 0.40; B = 1.15; C (IC_{50}) = 0.39; D = 0.02; R^2 = 0.986;

(□) 500 µg l^{-1}: A = 0.08; B = 1.13; C (IC_{50}) = 0.09; D = 0.02; R^2 = 0.953;

(△) 285 µg l^{-1}: A = 0.05; B = 1.81; C (IC_{50}) = 0.34; D = 0.01; R^2 = 0.950.

4.1.1.3.3. Influence of the reaction buffer

The standard curve did not change significantly when TNT was incubated in Milli-Q water instead of 40 mM PBS (mAb and Tr in 40 mM PBS), when the coating protein was Gam (fig. 28). When Gam was replaced by Protein A, the signal decreased with both curves, and with An in water it was by ca. 30 % than with An in 40 mM PBS (fig. 29).

So, when the amount of immobilized anti-TNT mAb was lower (as indicated by the lower ODs obtained with Protein A), the negative effect of zero salt molarity in the An solution is stronger).

The signal of the standard curve decreased significantly when the Tr was incubated in 20 mM or 4 mM PBS instead of the usual 40 mM PBS (TNT in Milli-Q water) (fig. 30).

The signal of standard curves did not change significantly (in intensity) when the anti-TNT mAb was incubated in the 40 mM PBST instead of the (usual) 40 mM PBS (fig. 31).

Therefore, what really affected the Tr (hence the standard curve) was the buffer molarity, and not the Tween 20, at least not at the 0.05% (v/v) content (the usual % of Tween 20 in 4 mM PBST).

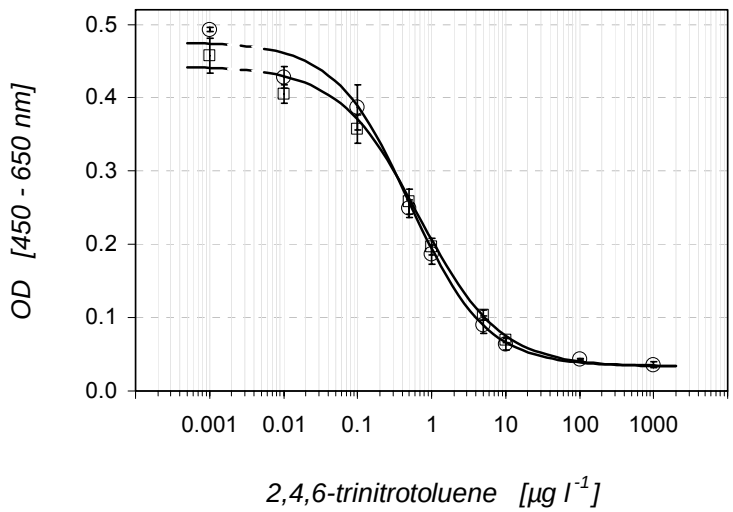

Figure 28. Standard curves, with TNT-ELISA on Gam, using standards (○) in Milli-Q water and (□) in 40 mM PBS. Incubations: mAb 2h; TNT/Tr 30 min; H_2O_2 / TMB 10 min. The following curve parameters values were obtained (n = 3):

(○) TNT in water: A = 0.44; B = 0.80; C (IC_{50}) = 0.68; D = 0.03; R^2 = 0.997;

(□) TNT in PBS: A = 0.48; B = 0.85; C (IC_{50}) = 0.52; D = 0.03; R^2 = 0.994.

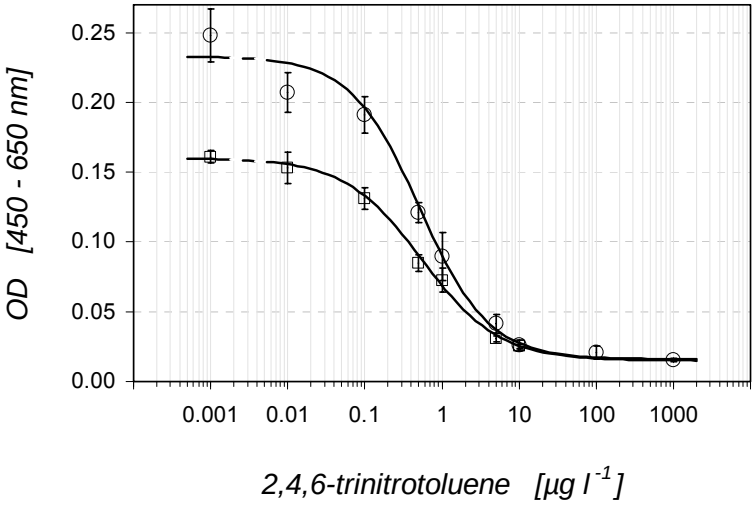

Figure 29. Standard curves, with TNT-ELISA on Protein A, using standards (○) in Milli-Q water and (□) in 40 mM PBS. Incubations: mAb 2h; TNT/Tr 30 min; H_2O_2 / TMB 10 min. The following curve parameters values were obtained (n = 3):

(○) TNT in water: A = 0.16; B = 0.87; C (IC_{50}) = 0.55; D = 0.02; R^2 = 0.999;

(□) TNT in PBS: A = 0.23; B = 0.97; C (IC_{50}) = 0.51; D = 0.02; R^2 = 0.989.

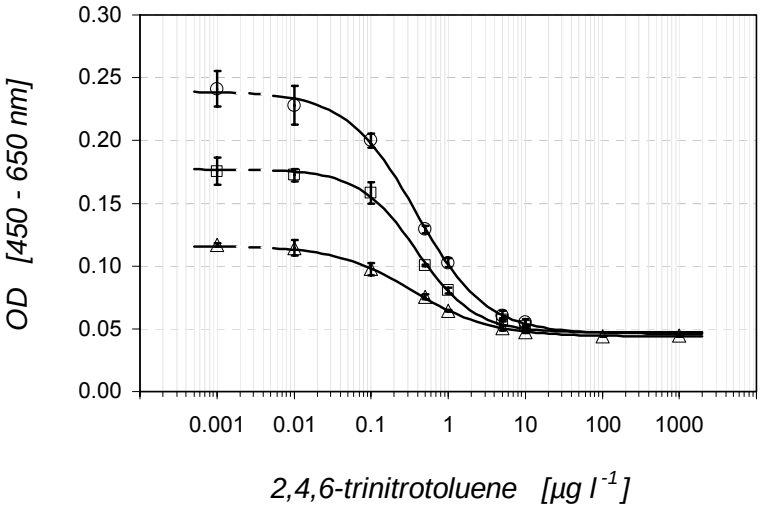

Figure 30. Standard curves, with fast TNT-ELISA, using three different buffer molarities for the Tr solution. Incubations: mAb 10 min; TNT/Tr 10 min; H_2O_2 / TMB 10 min. The following curve parameters values were obtained (n = 2):

(○) mAb in PBS 40 mM: A = 0.24; B = 0.96; C (IC_{50}) = 0.39; D = 0.05; R^2 = 0.999;

(□) mAb in PBS 20 mM: A = 0.18; B = 1.16; C (IC_{50}) = 0.39; D = 0.04; R^2 = 0.998;

(△) mAb in PBS 4 mM: A = 0.12; B = 0.87; C (IC_{50}) = 0.35; D = 0.04; R^2 = 0.999.

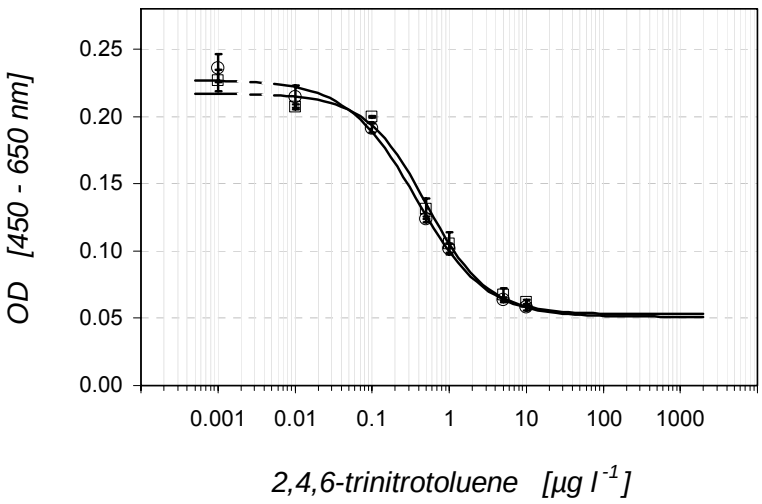

Figure 31. Standard curves, with fast TNT-ELISA, employing the usual buffer 40 mM PBS or 40 mM PBST (0.05%). Incubations: mAb 10 min; TNT/Tr 10 min; H_2O_2 / TMB 10 min. The following curve parameters values were obtained (n = 3):

(○) Tracer in 40 mM PBS : A = 0.23; B = 0.97; C (IC_{50}) = 0.37; D = 0.05; R^2 = 0.999;

(□) Tracer in 40 mM PBST: A = 0.22; B = 1.10; C (IC_{50}) = 0.50; D = 0.05; R^2 = 0.996.

The standard curves did not change significantly when the anti-TNT mAb was incubated in 4 mM PBS instead of the usual 40 mM PBS: neither with the Tr in 40 mM PBS (fig. 32), nor with the Tr in 4 mM PBST (fig. 33).

Similarly, the standard curves did not change significantly when the anti-TNT mAb was incubated in 4 mM PBST instead of the usual 40 mM PBS, neither with the Tr in 40 mM PBS (fig. 32), nor with the Tr in 4 mM PBST (fig. 33).

In conclusion for this sub-chapter, the washing buffer 4mM PBST could be used both for reagent preparation-incubation (Tr and antibody) and for washing. Like this, the application of the developed assay on a flow-injection sensor platform is very much simplified, the 4 mM PBST buffer becoming a "general buffer" in the biosensor platform.

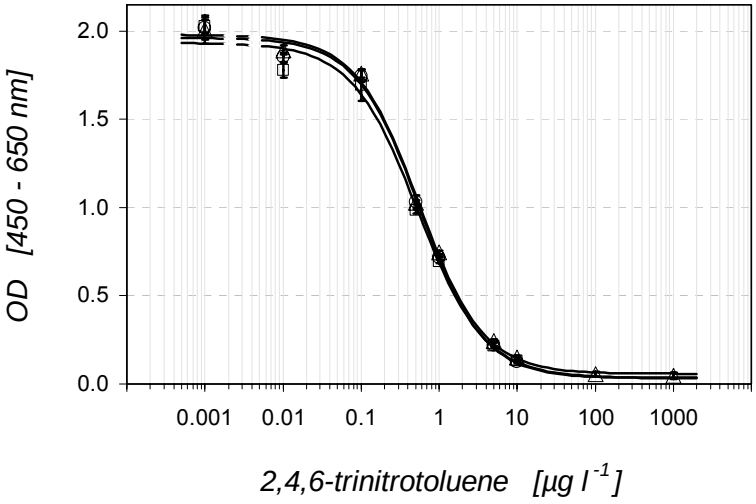

Figure 32. Standard curves, with TNT-ELISA, using three different buffers for the anti-TNT mAb solution. The Tr solution was prepared in <u>40 mM PBS</u>. The following curve parameters values were obtained (n = 2):

(○) mAb in 40 mM PBS : A = 1.96; B = 1.07; C (IC_{50}) = 0.57; D = 0.03; R^2 = 0.997;

(□) mAb in 4 mM PBS : A = 1.93; B = 1.03; C (IC_{50}) = 0.53; D = 0.04; R^2 = 0.995;

(△) mAb in 4 mM PBST: A = 1.98; B = 1.06; C (IC_{50}) = 0.56; D = 0.06; R^2 = 0.998.

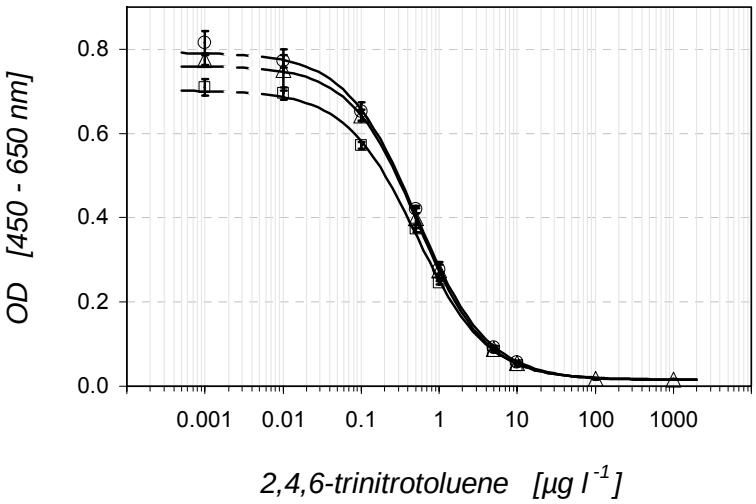

Figure 33. Standard curves, with TNT-ELISA, using three different buffers for the anti-TNT mAb solution. The Tr solution was prepared in <u>4 mM PBST</u>. The following curve parameters values were obtained (n = 2):

(○) mAb in 40 mM PBS : A = 0.79; B = 0.95; C (IC_{50}) = 0.51; D = 0.02; R^2 = 1.000;

(□) mAb in 4 mM PBS : A = 0.70; B = 0.96; C (IC_{50}) = 0.51; D = 0.02; R^2 = 0.999;

(△) mAb in 4 mM PBST: A = 0.76; B = 1.00; C (IC_{50}) = 0.53; D = 0.02; R^2 = 1.000.

4.1.1.3.4. Influence of Tween 20

Tween 20 has a certain negative effect on the Tr. If added into the Tr solution, it determines a lower signal in the standard curves, but the curves are still acceptable with Tween 20 concentrations of 0.05 % (v/v) (as in the usual washing buffer) and 0.5 % (v/v) (fig. 34).

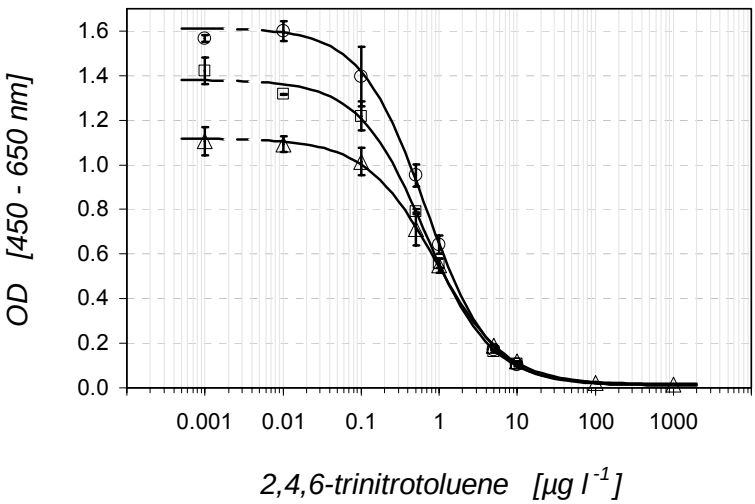

Figure 34. Standard curves, with TNT-ELISA, with the Tr in 40 mM PBS, containing three different concentrations of Tween 20: 0.00 %; 0.05 %; 0.50 %. Incubations: mAb 120 min; antigens 30 min; H_2O_2 / TMB 10 min. The following curve parameters values were obtained (n = 2):

(○) 0.00%: A = 1.61; B = 1.04; C (IC_{50}) = 0.67; D = 0.01; R^2 = 1.000;

(□) 0.05 %: A = 1.38; B = 1.02; C (IC_{50}) = 0.66; D = 0.02; R^2 = 0.999;

(△) 0.50 %: A = 1.12; B = 0.77; C (IC_{50}) = 0.92; D = 0.01; R^2 = 1.000.

Further in this sub-chapter, an experimental confirmation is provided that surfactant Tween 20, usually used in 4 mM PBST, is needed in the transfer of the TNT-ELISA onto the flow-injection immunosensor platform.

In the TNT-ELISA, when the washing steps are performed with 4 mM PBS instead of 4 mM PBST, the standard curve is completely wrecked, both with the usual incubation times (fig. 35) and with the fast format (each incubation time lasting 10 min) (fig. 36).

When the antibody and the Tr solutions were prepared in 4 mM PBST, washing with 4 mM PBS instead of 4 mM PBST does not lead to curve destruction (the curve parameters and fittings are valid), despite a strong reduction of the OD values (fig. 37).

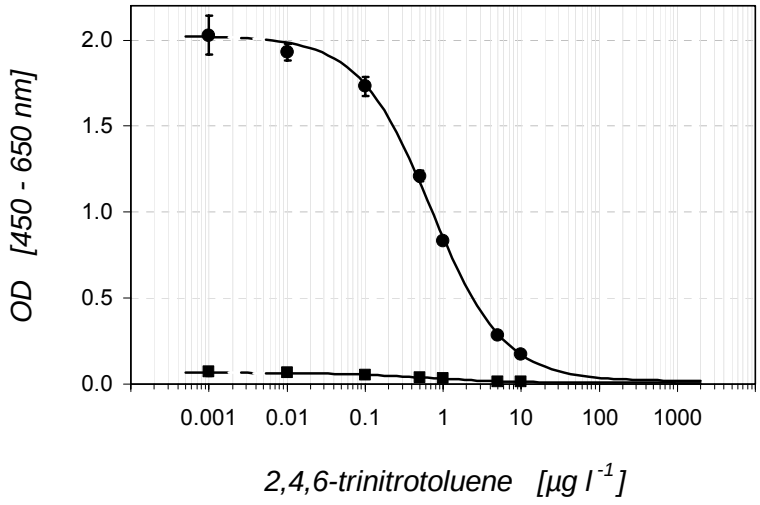

Figure 35. Standard curves, with TNT-ELISA, applying washing with 4 mM PBST and 4 mM PBS. The antibody and Tr solutions were prepared in 40 mM PBS (as usual). Incubations: mAb 120 min; TNT/Tr 30 min; H_2O_2 / TMB 10 min. The values of the curve parameters are (n = 3):

(●) washing with 4 mM PBST: A = 2.02; B = 0.94; C (IC_{50}) = 0.70; D = 0.02; R^2 = 0.999;

(■) washing with 4 mM PBS : A = 0.07; B = 0.77; C (IC_{50}) = 0.64; D = 0.01; R^2 = 0.989.

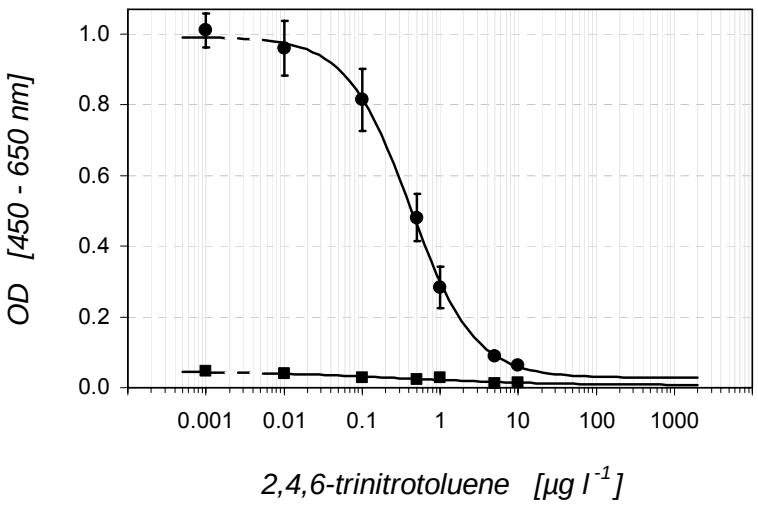

Figure 36. Standard curves, with <u>fast</u> TNT-ELISA, applying washing with 4 mM PBST and 4 mM PBS. The antibody and Tr solutions were prepared in 40 mM PBS (as usual). Incubations: mAb 10 min; TNT/Tr 10 min; H_2O_2 / TMB 10 min. The values of the curve parameters are (n = 3):

(●) washing with 4 mM PBST: A = 0.99; B = 1.07; C (IC_{50}) = 0.42; D = 0.03; R^2 = 0.999;

(■) washing with 4 mM PBS : A = 0.05; B = 0.45; C (IC_{50}) = 0.33; D = 0.01; R^2 = 0.954.

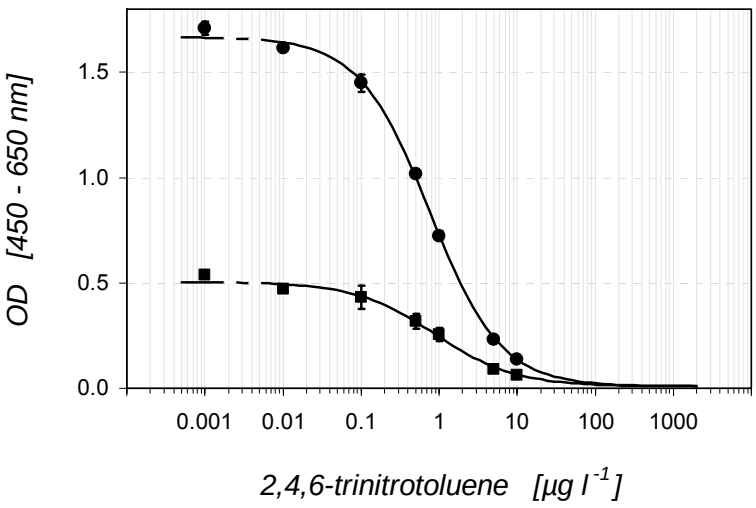

Figure 37. Standard curves obtained with TNT-ELISA, applying washing with 4 mM PBST and 4 mM PBS. The antibody and Tr solutions were prepared in 4 mM PBST (the usual washing buffer). Incubations: mAb 120 min; TNT/Tr 30 min; H_2O_2 / TMB 10 min. The following values of the curve parameters were obtained. (n = 3):

(●) washing with 4 mM PBST: A = 1.67; B = 0.96; C (IC_{50}) = 0.76; D = 0.01; R^2 = 0.999;

(■) washing with 4 mM PBS : A = 0.51; B = 0.85; C (IC_{50}) = 0.89; D = 0.01; R^2 = 0.996.

When only the antibody solution was prepared in 4 mM PBST while the Tr solution was prepared in 40 mM PBS (as usual), washing with 4 mM PBS instead of 4 mM PBST does not lead to curve destruction, despite a strong reduction of the OD values. However the OD values are much lower than with both antibody and Tr solutions in 4 mM PBST (fig. 38).

When Tween 20 is absent from both the washing buffer and from the antibody and Tr solutions, the standard curve is completely destroyed, and the OD reduced to ca. 3 %.

When Tween 20 is absent from the washing buffer but present in the both the antibody and Tr solution, the OD is reduced to ca. 30 %.

When Tween 20 is absent from the washing buffer and from the Tr solution but present in the antibody solution, the OD is reduced to ca. 15 %.

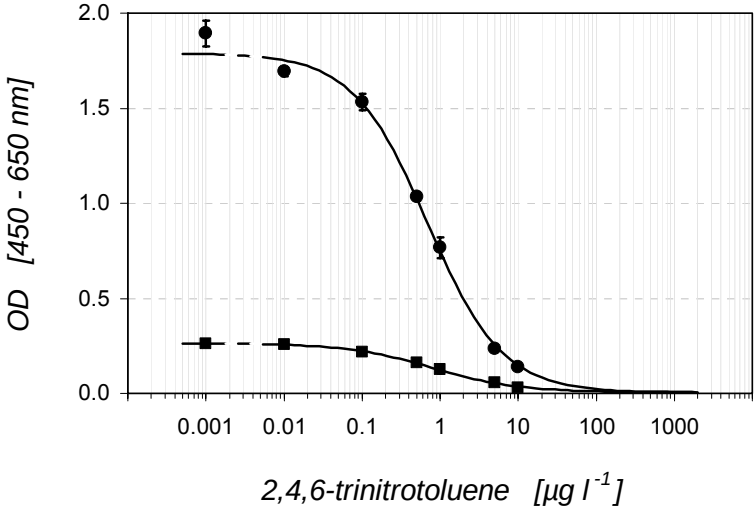

Figure 38. Standard curves, obtained with TNT-ELISA (incubations: mAb 120 min; TNT/Tr 30 min; H_2O_2 / TMB 10 min), applying washing with 4 mM PBST and 4 mM PBS. The antibody solution was prepared in PBST, but the Tr solution was prepared in 40 mM PBS. The following values of the curve parameters were obtained (n = 3):

(●) washing with 4 mM PBST: A = 1.78; B = 0.91; C (IC_{50}) = 0.69; D = 0.01; R^2 = 0.998;

(■) washing with 4 mM PBS : A = 0.26; B = 0.80; C (IC_{50}) = 0.79; D = 0.01; R^2 = 0.999.

Regarding the 4 mM PBST buffer, the conclusion is that high buffer molarity may not be necessary in the general buffer used in the sensor platform, but a minimum (0.05 %) content of Tween 20 is needed.

Despite the facts that low buffer molarity has a significant negative impact on the Tr, and that Tween 20 has a certain negative impact on the Tr, preparing the antibody and the Tr solutions in 4 mM PBST help maintain the validity of the standard curve when the washing buffer contains no Tween 20.

4.1.1.3.5. Further developments

In order to insure a safe transition from the development to the commercial phases of the immunosensor, in parallel with the commercial (mouse) anti-TNT antibody A1-1-1 used for the sensor development, a series of new (rat) antibody were produced (Krämer et al, 2004b; Krämer et al, 2005). Although these antibody developments are beyond the focus of the present thesis, it is worth mentioning them. Only to give an example, one rat anti-TNT antibody (clone DNT4 4G4) reached a test midpoint (IC_{50}) of 0.35 µg l^{-1} (n = 18), which is comparable with (if not better than) the commercial mouse anti-TNT (clone A1-1-1) antibody which attained 0.3 - 1 µg l^{-1}. This good correspondence in sensitivity insured excellent conditions for the application of the new anti-TNT antibody on the immunosensor platform

that we developed with the commercial A1-1-1 antibody. The most sensitive and selective rat monoclonal antibody obtained against 2-amino-4,6-DNT (clone DNT2 4B4) displayed a test midpoint (IC_{50}) of 8.5 µg l^{-1} (n = 15).

4.1.1.4. Influence of the physical parameters in TNT-ELISA

For any immunoassay or immunosensor developed for pollution screening in environmental samples (like natural waters or soil extracts), a description of the physical parameters limiting the analytic performances of the assay is necessary. The most important aspect is the preservation of (structure and) activity of the bioreagents (enzymes and antibodies).

A basic requirement is that the experimental conditions are as close as possible to the natural environment of the bioreagents, and that the physical limits are established experimentally. In general, immunoassays are performed at 20 – 40 °C, in aqueous buffers with known composition and pH.

Optimal buffers are employed for different reactions: coating of catching proteins (50 mM carbonate buffer, pH 9.6-9.8); antibody immobilization on the catching proteins and competition steps (40 mM PBS, pH 7.5-7.7); indicator reaction (for the HRP-H_2O_2-TMB system: 100 mM sodium acetate, pH 5.5).

Some ELISA practitioners perform the competition (immune recognition step) at 37°C (*in vivo* temperature for the antibodies) and other temperatures for the indicator reaction (depending on the optimum temperature for the employed enzyme).

With our TNT assay, all experiments were carried out at RT. Also required in ELISA practice is that unspecific binding of the Tr be prevented by blockers. All along the described development, we used the washing buffer PBST 4mM. Occasionally, we also used proteins like BSA, casein and skimmed milk powder, 1% (w/v) or lower, in PBS 40 mM, as blocking solutions.

4.1.1.4.1. Influence of temperature

Immunoassays are strongly dependent on temperature, mainly because (1) the molecular structures and the catalytic properties of enzymes maintain at optimum within rather narrow temperature limits; (2) the molecular structure and the reactivity of antibodies maintain and are optimum at certain temperature, not necessarily those of the enzymes employed together with them; (3) the degrading time of enzymes and antibodies depend on the process temperature; and (4) the immunochemical reaction is dependent on the diffusion rates of the reagent, namely it is slower with lower temperatures.

ELISA practitioners know that variations of only 3°C may lead to significant changes in immunoassay performances, and impose a control of the process temperature. The rates of many reactions catalysed by enzymes increase (in the sub-maximum domains) by a factor of 2 over a range of 10°C.

The temperature effects may cause signal differences between plates and inside the same plate, like the edge effect, due to uneven distribution of incubation temperatures between edge and central wells of the microtiter plate (Tijssen, 1985; Schneider et al., 1995; Esser, 1997; Miller et al., 2002a,b). With the developed TNT assay, the edge affect reached about 10% of the absorbance signal at zero dose (details in annex 10, fig. 114).

Upon the analytical performances of immunoassays, temperature exerts both direct influences (such those invoked earlier) and concerted with incubation time and the presence of cross-reactants in the standards / the sample. Thus, the measured cross-reactivities may change with temperature and with the length of the incubation time (Miller and Levinson, 1996).

Equilibrium constants may vary with temperature. But when the equilibrium constants (at a given temperature) are different for An and cross-reactant, cross-reactivity will vary with the temperature change. Further, as reaction rates vary with temperature, the reaction equilibrium tends to move to shorter times with higher temperatures. (Miller and Levinson, 1996; Stöcklein et al, 1998).

In some immunoassays, the presence of cross-reactants in the sample determines an increase of the time needed to reach equilibrium. Consequently, decreasing the incubation time may lower the affinity (Stöcklein et al., 1998) and increase the cross-reactivitiy for some compounds (Vining et al., 1981). So, the trick of increasing the temperature (and so be able to decreasing the incubation time) may induce unexpected changes in the observed specificity.

All these effects are not easily predictable (if at all) and must be quantified empirically for each immunoassay.

While cross-reactivities were not central to our investigations towards the proof of principle of the sensor, we studied the general immunoassays flexibility with the competition between An and Tr, especially at short incubation times. Nevertheless, as short incubation times are usually needed in immunosensors, cross-reactivity changes associated with short incubation times should be acknowledged in any present or future commercial immunosensor.

Our off-line explorations and optimizations have been carried on at RT. Therefore, the parameters of the standard curves varied to a moderate extent. However, the correctness and the relevance of the results was maintained by performing multiple and parallel zero dose measurements during every step of the sensor development, i.e. with

microtiter plates ELISA, batch ELISA and laboratory sensor prototype (which had, initially, no temperature-control).

With microtiter plates, edge effect was circumvented by leaving the edge rows of the microtiter plates out of calculations. Few exceptions from this rule were only allowed in certain probing experiments.

4.1.1.4.2. Influence of pH

The pH, i.e. the logarithmic index for the hydrogen ion concentration (eq. 8) in samples or standards, is a limiting factor for the immunoassays functioning.

$$pH = \log_{10} (1/[H^+]), \text{ at } 25°C \qquad \text{(eq. 8)}$$

A pH of 7 is usually thought of as normal. Most of the rivers have pHs between 6.5 and 8.5, but the pH of each river depends on local geological peculiarities, notably the river bed (Sigg et al., 2001).

For example, some water samples taken to our laboratory from Danube and its tributary Isar (on the German territory), had pHs around 7.7 all of them. But many natural waters (rivers, lakes, soil waters, seas) are slightly acidic, with a pH of 5.6 because atmospheric carbon dioxide dissolves into water to produce a weak acid, the carbonic acid (Wharton, 2002).

Strong acids and alkalis, not only prevent enzyme functioning, but also induce conformational changes and destroy the proteins and other vital biomolecules, like monoclonal antibodies, which have an isoelectric point of 5-9 (Stöcklein, 1998; Stern, 2001).

However, under experimental (hence controlled) conditions, the assessed range of pH tolerance may be quite wide. The pH tolerance of the TNT assay was tested at RT, and it was found that the parameters of the standard curve were preserved between 4 –10 (fig. 39).

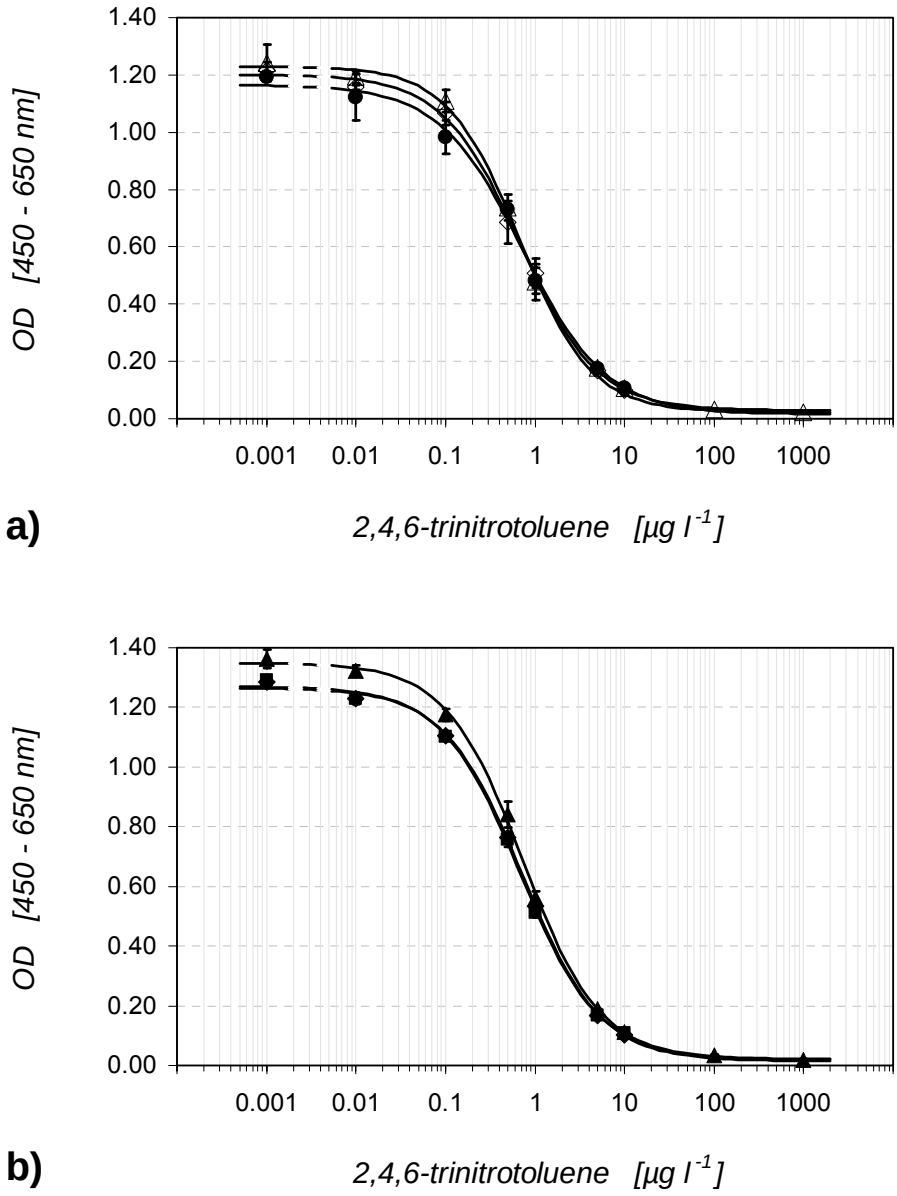

Figure 39. With TNT-ELISA, the standard curve maintained its parameters in insignificant variations at pH values between 4 and 10. The following values of the curve parameters correspond to graphs a) and b) (n = 2):

a) pH 5 (◇): A = 1.20; B = 1.00; C (IC_{50}) = 0.67; D = 0.03; R^2 = 0.999;
a) pH 7 (●): A = 1.17; B = 0.93; C (IC_{50}) = 0.73; D = 0.02; R^2 = 0.998;
a) pH 9 (△): A = 1.23; B = 1.08; C (IC_{50}) = 0.67; D = 0.03; R^2 = 0.999;
b) pH 4 (◆): A = 1.27; B = 1.00; C (IC_{50}) = 0.72; D = 0.02; R^2 = 1.000;
b) pH 7 (●): A = 1.27; B = 0.99; C (IC_{50}) = 0.68; D = 0.02; R^2 = 0.999;
b) pH 10 (▲): A = 1.35; B = 1.01; C (IC_{50}) = 0.74; D = 0.02; R^2 = 0.999.

At pH values of 4; 5; 6; 7; 8; 9 and 10, no significant differences were observed in the standard curve's maximal absorbance (A), slope (B), test midpoint (C; IC_{50}), background (D) or the correlation coefficient (R^2). R^2 was always above the "must be" limit of 0.95, usually above 0.99.

The above values show that our TNT-ELISA worked very well at pH from 3 orders of magnitude below 7 and 3 orders of magnitude above 7. The comparison between one exceptionally acid (pH 3) and one common situation (pH 8) showed no major shift in the parameters of the standard curve. (fig. 40). Very acidic conditions may occur at some heavily polluted sites.

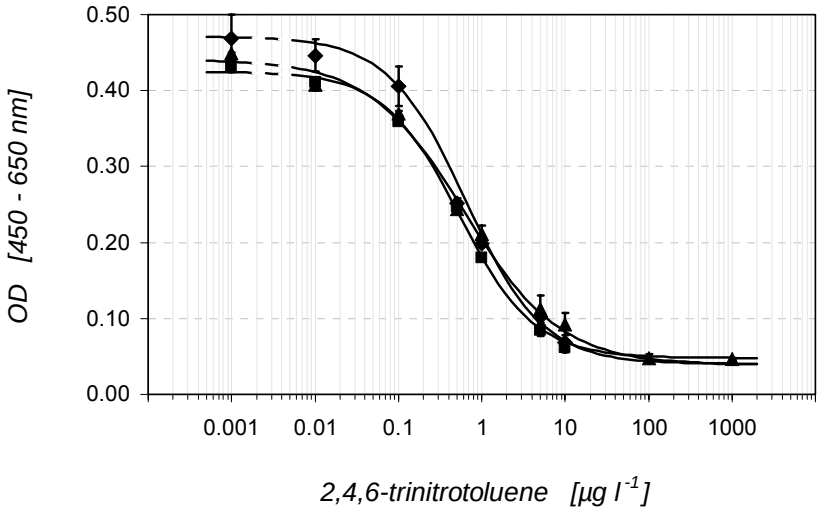

Figure 40. With TNT-ELISA, the standard curve maintained its parameters in insignificant variations at pH 3 and pH 8. (The signal in fig. 39 is higher than here, because at the time of that experiment, the best method for the stabilization of the Tr was already identified and applied – details in subchapter 4.1.1.2.). The following values of the curve parameters have been obtained (n = 3):

pH 3 (◆): A = 0.47; B = 0.94; C (IC_{50}) = 0.64; D = 0.04; R^2 = 0.998;
pH 7 (●): A = 0.43; B = 0.96; C (IC_{50}) = 0.53; D = 0.05; R^2 = 0.996;
pH 8 (▲): A = 0.44; B = 0.76; C (IC_{50}) = 0.62; D = 0.04; R^2 = 0.995.

4.1.1.4.3. Influence of solvents

In analytics, the choice of solvent is largely dependent on past experience, manufacturers' guidelines, standard methods recommended by governmental agencies, or on procedures based on calculating solvent efficiency with the Hildebrand solubility parameter (Fitzpatrick and Dean, 2002).

In immunoassays, the solvent must meet two basic requirements: (1) to insure good extraction of the An from the matrix, and (2) to be well tolerated by the biological reagents.

In general, ELISA can tolerate up to 10 % of solvent (Williams, 1996; Penalva et al., 1999; Niessner and Knopp, 2002), but some immunoassays tolerate even more (Setford, 1999, Setford et al., 2000).

It has also been reported that assay tolerance to solvents increases when the assay is performed at low temperatures, e.g. 4°C (Katagiri et al., 1999).

In general, organic solvents determine drops in assays sensitivity, occasionally even changes in the antibody specificity. It is thought that antibody and enzyme molecules retain their activity because of the film of water that surrounds them (the "hydration shell effect"), unless this thin layer is being removed by hydrophilic solvents, i.e. with high dissolvability in water (or by non-ionic detergents like Tween 20). A general negative correlation between solvent percent and antibody binding was observed experimentally (Weetall, 1991; Bang Laboratories, Inc., 1997; Stöcklein et al., 1998; Penalva et al., 1999; Horachek and Skladal, 2000, Setford, 2000).

These negative effects may be mitigated by performing ELISAs in flow conditions (immunosensors), where the contact time between the solvent and the immunoreagent is shorter. In such analytical platforms, higher solvent contents than those employed in conventional ELISA may be applied if needed (Penalva et al., 1999; 2000).

When only antibody fragments are used, the fragments can be (much) stabilized against the negative effects of solvents through the introduction of an interdomain disulfide bond (Strachan et al., 2000).

Sometimes, solvents enhance some desired characteristics of the enzymes, e.g. tolerance to extreme pHs (Klibanov, 2001). Also, the affinity may be increased by using solvents with high hydrophobicities, i.e. less soluble in water (Russell et al., 1989; Stöcklein, 1995; Setford et al., 1999; Horacek and Skladal, 2000).

In immunoassays, most used solvents are methanol and acetone, and sometimes other solvents like acetonitrile, ethanol, diethyl ether, benzene or hexane (Penalva et al., 1999; Setford, 2000). With a flow immunosensor, Penalva et al. (1999) obtained with organic solvents (the best was methanol) lower sensitivities, but higher specificities.

In certain conditions, organic phase immuno-sensing of less water-soluble An (like TNT) allow minimal sampling preparation in the field. Our TNT-assay was mainly directed towards biosensor applications in water analysis, but applications with aqueous - organic solvent phase (like with some hydrophobic An or/in soil extractions) remained a potential direction for future applications. Therefore, we checked (in microtiter plates) the basic tolerance of the TNT-assay to the concentration (%) of certain solvents in the standards: the commonly used (but quite toxic) methanol and the less used (but less toxic) 2-isopropanol.

The TNT-assay tolerated up to 5 % of solvent in the sample/ standard, i.e. either 2-isopropanol (fig. 41) or methanol (fig. 42).

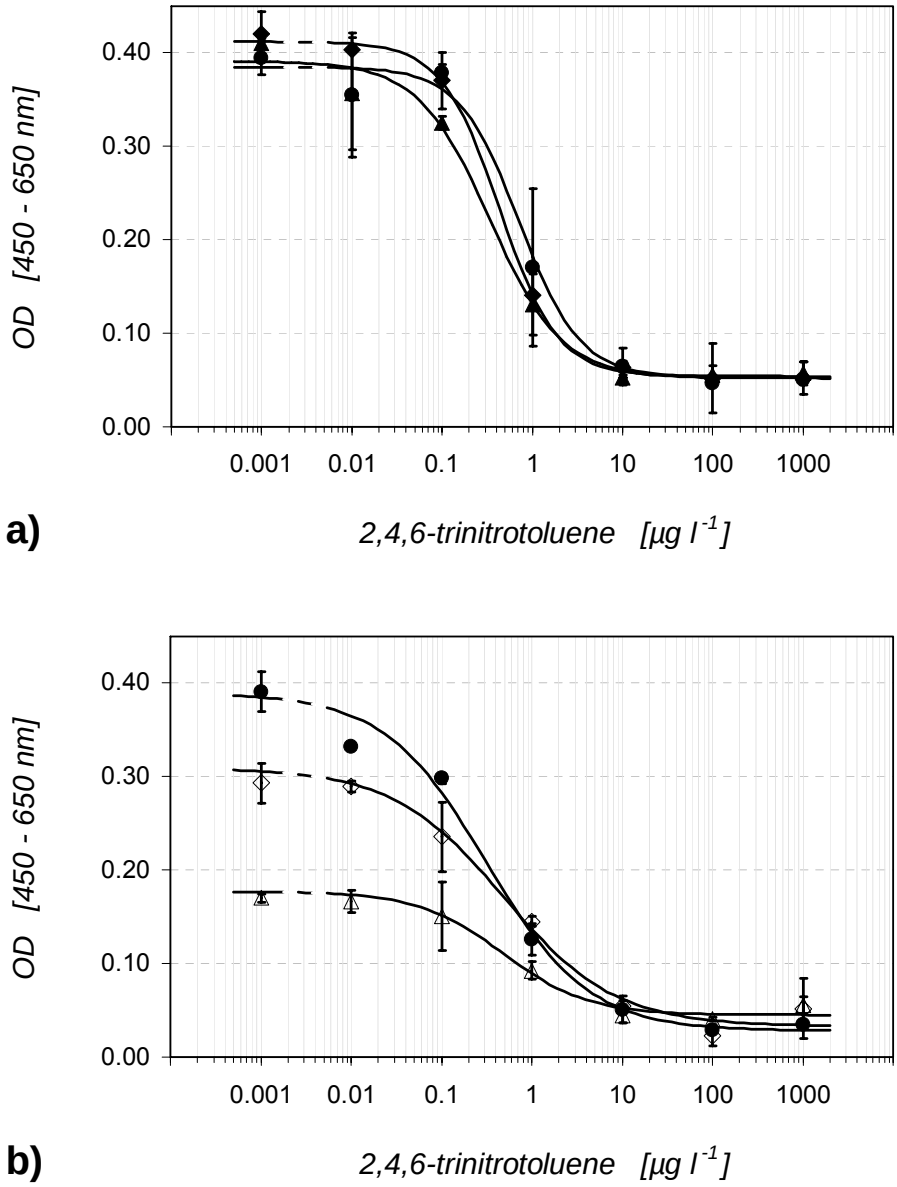

Figure 41. With TNT-ELISA, the standard curve maintained its parameters in insignificant variations with up to 5% 2-isopropanol in the standard solutions (in water). The following values of the curve parameters correspond to graphs a) and b) (n = 2):

a) 0.0% (●): A = 0.39; B = 1.30; C (IC_{50}) = 0.72; D = 0.05; R^2 = 0.990;

a) 0.5% (◆): A = 0.41; B = 1.35; C (IC_{50}) = 0.44; D = 0.05; R^2 = 0.999;

a) 1.0% (▲): A = 0.39; B = 1.09; C (IC_{50}) = 0.34; D = 0.05; R^2 = 0.991;

b) 0.0% (●): A = 0.39; B = 0.77; C (IC_{50}) = 0.31; D = 0.03; R^2 = 0.988;

b) 5.0% (◇): A = 0.31; B = 0.71; C (IC_{50}) = 0.49; D = 0.03; R^2 = 0.991;

b) 10.0 % (△): A = 0.12; B = 0.93; C (IC_{50}) = 0.48; D = 0.05; R^2 = 0.986.

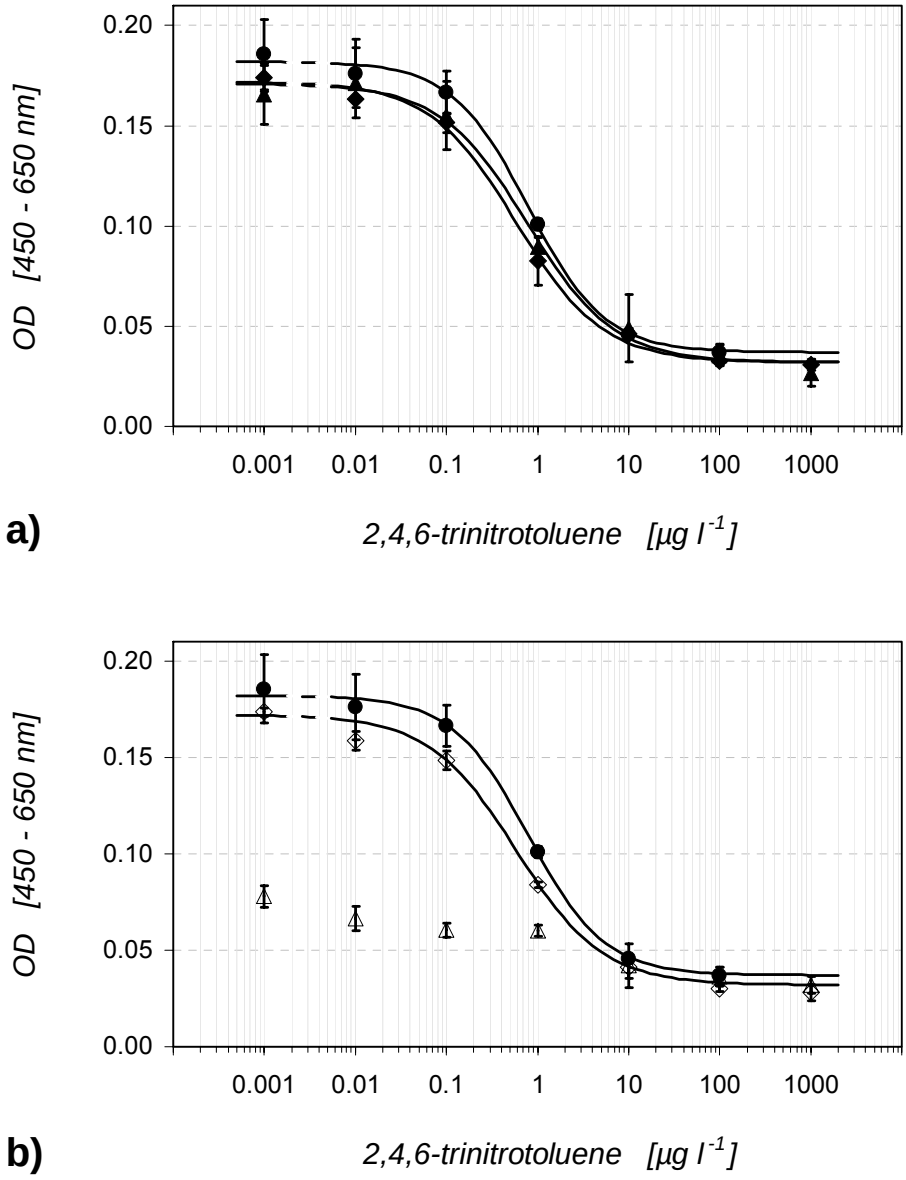

Figure 42. With TNT-ELISA, the standard curve maintained its parameters in insignificant variations with up to 5% methanol in the standard solutions (in water). The following values of the curve parameters correspond to graphs a) and b) (n = 2):

a; b) 0% (●): A = 0.18; B = 1.04; C (IC_{50}) = 0.79; D = 0.04; R^2 = 0.999;
a) 0.5% (◆): A = 0.17; B = 0.92; C (IC_{50}) = 0.58; D = 0.02; R^2 = 0.997;
a) 2.0% (▲): A = 0.17; B = 0.91; C (IC_{50}) = 0.77; D = 0.03; R^2 = 0.995;
b) 5.0% (◇): A = 0.17; B = 0.89; C (IC_{50}) = 0.64; D = 0.02; R^2 = 0.997;
b) 10.0 % (△): A = 0.10; B = 0.16; C (IC_{50}) = 1.01; D = 0.01; R^2 = 0.999.

At 5% solvent, the optical density was visibly lower, but still acceptable. At 10% solvent, the optical density was strongly diminished, and (all) the standard curve was significantly degraded. With 0.5 - 5 % of solvent in watery standards, no large differences

were observed in the standard curve's optical density (A), slope (B), test midpoint (C; IC_{50}), background (D) or the correlation coefficient (R^2). R^2 was always above the "must be" limit of 0.95, usually above 0.99.

4.1.1.5. Influence of soil matrix

Some pollutants (for example TNT) have poor solubility in water. To help solubilization one can add surfactants in solution (Albro, 1979). But surfactants may alter (at certain percentages) the tertiary structure of the antibody and the Ab-Ag interaction. The alternative is the use of organic solvents (Niessner, 2001; Stern 2001).

Humic substances or heavy metals present in the sample matrix may alter the structure and function of enzymes and of antibodies. Humic acids can also fix nitroaromatics in soils (Keuchel et al., 1993; Walsh et al., 1995; Dawel et al, 1997; Bruns-Nagel et al., 2000; Thiele et al., 2002), and special methods may be needed for measuring (by immunoassay) the nitroaromatics that are bound to humic acids (Pfortner et al, 1998a,b; Achtnich et al., 1999).

Sometimes matrix substances can be separated from the matrix, or can be complexated, for example by employing BSA in a TNT-ELISA (Keuchel et al., 1993).

Beside humic acids, other high molecular, organic components, like lignosulfonic acids, may disturb immunoassays. Also inorganic ions (e.g. Al^{3+}, Fe^{3+}) and oxidizing agents (Cl_2, O_3, ClO_2) used in water treatment may perturb the immunoassay well functioning, usually by impeding upon the function of the antibody or/and of the Tr (Niessner, 2001).

These factors induce an increased number of false positives. However, opposite effects may also occur. For example, the activity of HRP can increase by up to 40% in the presence of certain cations like Ca^{2+}, due to the stabilizing role of Ca^{2+} upon the protein structure (Ruppert et al., 1992).

It is worth acknowledging that, in certain assays, some negative influences upon the HRP structure might be compensated by the capacity of anti-HRP antibodies to promote HRP refolding (Ermolenko et al., 2002) or by increased thermal stability that follows enzyme immobilization (Miller, 2000b).

With our experiments, the % recovery (extraction efficiency) of the spiked concentration of TNT by extraction of TNT from TNT-spiked soils depended on the spiking concentration, solvent type and soil type.

Only the spiking concentration of 2 mg kg^{-1} allowed significant recovery. In general, low % recovery from soils is, to be expected, with low spiked TNT concentration (Harvey et al., 1997), and with not so efficient (for TNT) solvents (or with water) (Psillakis et al., 2000).

The general influence of soil matrix and extraction efficiency (% recovery) is shown with the standard curves produced with the soil extracts, which are supposed to contain ca. 2 mg l^{-1} TNT (from the soils spiked with 2 mg kg^{-1}). The recovery is calculated as (IC_{50} obtained with the standards / IC_{50} obtained with the soil extract)*100.

With the LUFA soil (fig. 43), the obtained recovery was ca 36.8 % with methanol and 27.2 % with isopropanol. With the Merzenhausen soil (fig. 44), the obtained recovery was 33.3 % with methanol and 1.6 % with isopropanol.

TNT extraction from the spiked soils was more efficient with methanol than with isopropanol in both types of soil. Notably, the extract with isopropanol displayed some recovery with the LUFA soil, but very poor recovery with the Merzenhausen soil, i.e. ca 17 times less than with LUFA soil. On the contrary, with fresh methanol extracts, higher recoveries could be measured with both soils (fig. 45), i.e. up to 80 % with LUFA soil and up to 55 % with Merzenhausen soil.

The results obtained with spiked soils are meant to open future biosensor applications in soil screenings for TNT. The data obtained on extractions with the two solvents provide basic information on the joint influence of soil matrix and extraction method (especially regarding the employed solvent).

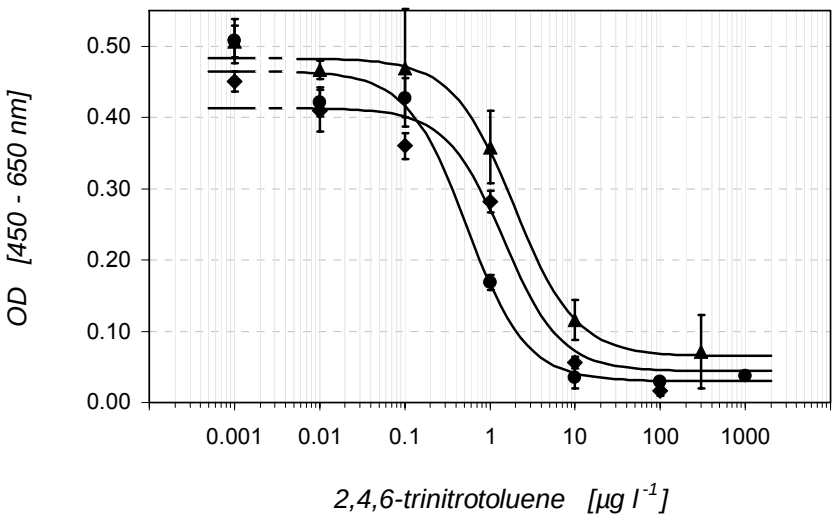

Figure 43. With TNT-spiked LUFA soil, standard curve shifted moderately to the right by methanol extracts, and more significantly by isopropanol extracts. The following values of the curve parameters were obtained:

standards (n = 4) **(●):** A = 0.47; B = 1.24; C (IC_{50}) = 0.53; D = 0.03; R^2 = 0.98;

methanol extracts (n = 4) **(◆):** A = 0.41; B = 1.29; C (IC_{50}) = 1.44; D = 0.04; R^2 = 0.97;

isopropanol extracts (n = 4) **(▲):** A = 0.48; B = 1.20; C (IC_{50}) = 1.95; D = 0.07; R^2 = 0.97.

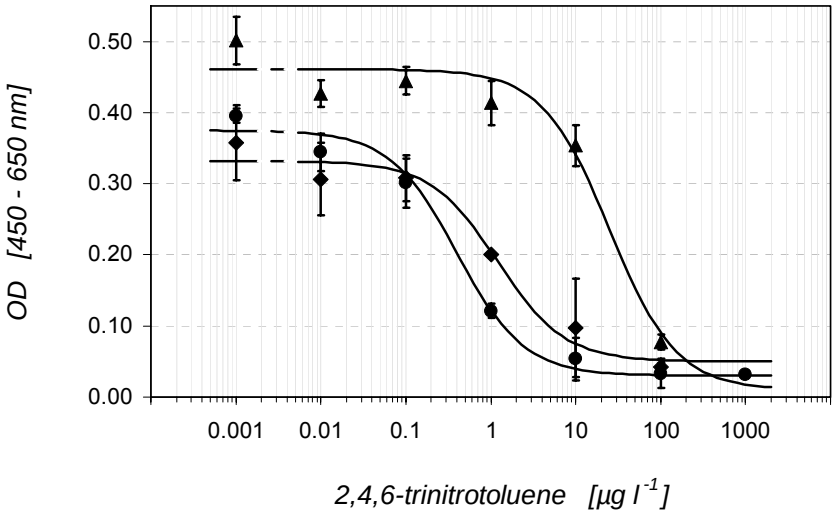

Figure 44. With TNT-spiked <u>Merzenhausen</u> soil, standard curve shifted moderately to the right by <u>methanol extracts</u>, and strongly (almost 2 orders of magnitude) by <u>isopropanol extracts</u>. The following values of the curve parameters were obtained:

standards (n = 4) **(●):** A = 0.38; B = 1.1; C (IC_{50}) = 0.40; D = 0.03; R^2 = 0.98;

methanol extracts (n = 4) **(◆):** A = 0.33; B = 1.1; C (IC_{50}) = 1.20; D = 0.05; R^2 = 0.98;

isopropanol extracts (n = 2) **(▲):** A = 0.46; B = 1.1; C (IC_{50}) = 25.0; D = 0.01; R^2 = 0.97.

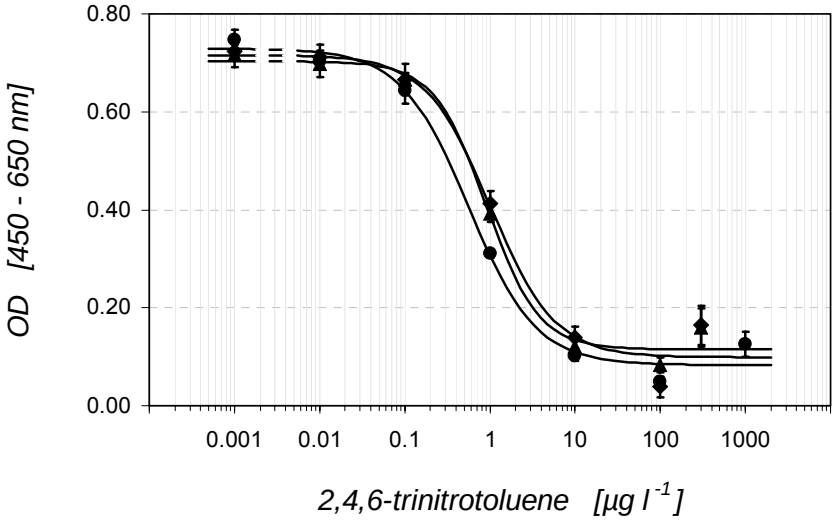

Figure 45. With <u>methanol extracts</u>, the standard curve shifted moderately to the right in both soil types. The following values of the curve parameters were obtained:

standards (n = 4) **(●):** A = 0.73; B = 1.10; C (IC_{50}) = 0.56; D = 0.08; R^2 = 0.99;

extracts <u>LUFA</u> soil (n = 4) **(◆):** A = 0.70; B = 1.41; C (IC_{50}) = 0.90; D = 0.12; R^2 = 0.99;

extracts <u>Merzenh.</u> soil (n = 4) **(▲):** A = 0.72; B = 0.14; C (IC_{50}) = 1.01; D = 0.10; R^2 = 0.98.

For future adapted methods, warm extractions might be considered, since it has been shown that extractions can be accelerated and improved at temperatures higher than RT, including by automated, fast procedures (Dionex Corporation, 1997; Alter et al., 1998). Beside methanol, other solvent with good extraction efficiencies for TNT are hexane and acetone (Bordelon et al., 1996).

It should be kept in mind that recovery values or indices (%) should be obtained with fresh soil spiking and extractions, i.e. before the spiked An gets degraded to a significant extent. Extensive information is available in the literature about the degradation of TNT and related explosives in soils, as well as the threat presented by such pollutants upon soils health and productivity. An evaluation of the ecotoxicological threat of explosives to the habitat function of soil is provided by Schäfer, including LUFA soils (Schäfer, 2002).

4.1.2. Patterns of reciprocal displacement between antigens

Real samples might contain substances that would destroy the enzymatic properties of the tracer enzyme. During the sensor development, the theoretical possibility to avoid the Tr coming into contact with the sample was experimentally investigated (in microtiter plate formats). This was done with the TNT assay, by testing the antigens reciprocal displacement dynamics: sequential saturation format, as opposed to the basic competitive saturation format. In principle, with sequential saturation, the sample and the Tr are separated by a washing step, instead of being incubated together as in the competitive saturation format.

To resume the predictions of the law of mass action in a system made up by one antibody and two antigens, in sequential saturation assays, the curve shape will depend on the differences in association and dissociation rates of antibodies with the two antigens. When the first incubated antigen is the An (standards), the standard curve will result from overlapping the competitive saturation curve with the An dissociation curve (sub-chapter 2.2.8.; figs. 6; 7).

The pattern of displacement between An and Tr was tested producing on the same microtiter plate, a combination of (1) one competitive saturation curve (Ag incubations: An+Tr / washing / Buffer+Buffer) and two sequential saturation curve, i.e. (2) one curve with An being incubated first (Ag incubations: Buffer+An / washing / Buffer+Tr), and (3) one curve with Tr being incubated first (Ag incubations: Buffer+Tr / washing / Buffer+An). This kind of pattern has been called "the three-curve pattern", and it was obtained for each of the tested immunoassays.

A well fitted standard curve in a heterogeneous immunoassay has a sigmoid shape. In the three-curve pattern, the competitive saturation curve was like any other inhibition

curve with the optimized ELISAs, but the two sequential saturation curves lost the sigmoid shape and also some sensitivity (IC_{50}). Typically, each sequential saturation curve displayed an intermediary plateau. In this chapter we present such curves, as obtained experimentally.

With sequential saturation curves, beside modifications in the curve shape, another general feature was that the differences, i.e. the curve properties changed with the incubation order of the two antigens of an immunoassay. The three-curve pattern was different in each of the studied immunoassay.

4.1.2.1. Three-curve pattern with the isoproturon assay

When isoproturon was incubated first and the Tr second, the standard curve was similar to the competitive saturation curve, except for an apparently high background which increased at shorter antigen incubation times. In percent control, this was ca. 25 – 40 % of the signal with 30 min (fig. 46); ca. 25 – 35 % with 10 min (fig. 47) and ca. 45 – 50 % with 3 min (fig. 48).

When the Tr was incubated first and isoproturon second, the standard curve displayed no significant inhibition at any incubation time (figs. 46; 47; 48). The competitive saturation curve has a better sensitivity with longer incubation times: the IC_{50} is 0.18 µg l^{-1} with 30 min incubation, 0.36 µg l^{-1} with 10 min and 0.68 µg l^{-1} with 3 min.

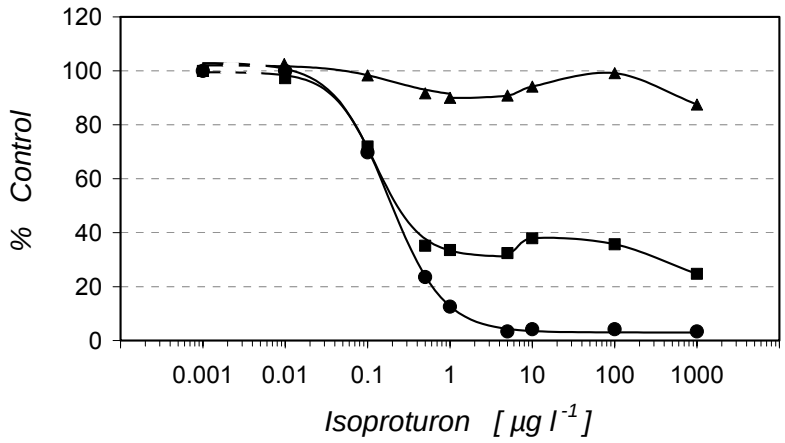

Figure 46. Three-curve pattern with isoproturon-ELISA when each incubation step lasted <u>30 min</u>. The shape of the standard curve (n = 2) varies with the sequence of the antigens incubation: (●) An+Tr / washing / Buffer+Buffer; (■) An+ Buffer / washing / Buffer+Tr; (▲) Buffer+ Tr / washing / An+Buffer. The standard curve with competitive saturation (●) was fitted according to the 4-parameter equation (eq. 6), with the resulted values of the curve parameters: A = 103; B = 1.3; C = 0.18 µg l^{-1}; D = 3. The zero dose is represented as 0.001 µg l^{-1} and separated from the first real concentration by a broken line.

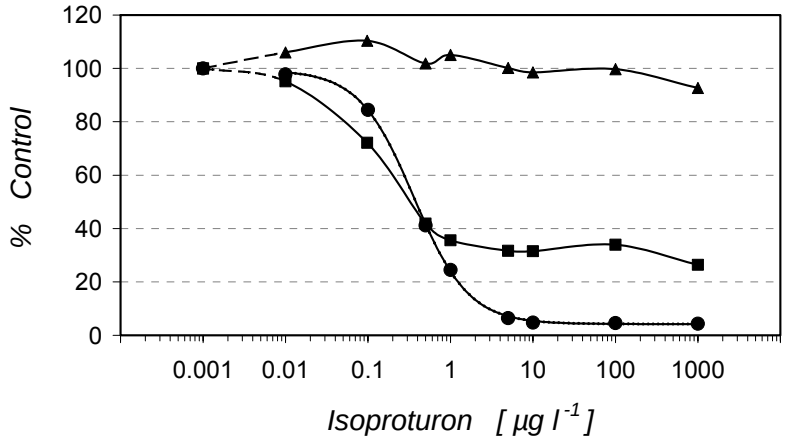

Figure 47. Three-curve pattern with isoproturon-ELISA when each incubation step lasted 10 min. The shape of the standard curve (n = 2) varies with the sequence of the antigens incubation: (●) An+Tr / washing / Buffer+Buffer; (■) An+ Buffer / washing / Buffer+Tr; (▲) Buffer+Tr / washing / An+Buffer. The standard curve with competitive saturation (●) was fitted according to the 4-parameter equation (eq. 6), with the resulted values of the curve parameters: A = 100; B = 1.3; C = 0.36 µg l^{-1}; D = 4. The zero dose is represented as 0.001 µg l^{-1} and separated from the first real concentration by a broken line.

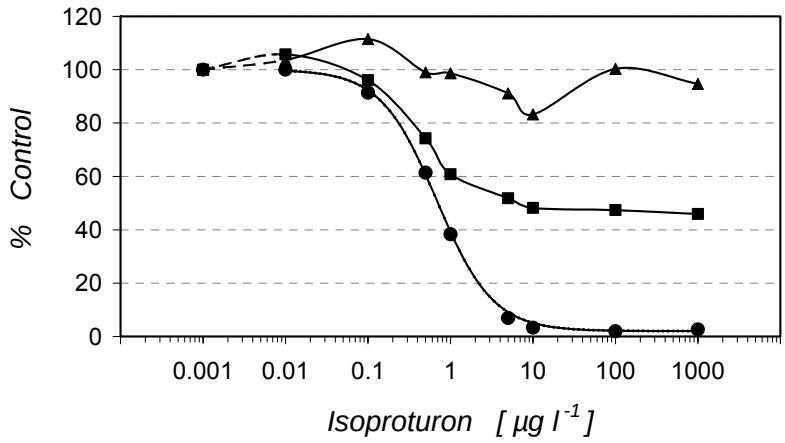

Figure 48. Three-curve pattern with isoproturon-ELISA when each incubation step lasted 3 min. The shape of the standard curve (n = 2) varies with the sequence of the antigens incubation: (●) An+Tr / washing / Buffer+Buffer; (■) An+ Buffer / washing / Buffer+Tr; (▲) Buffer+Tr / washing / An+Buffer. The standard curve with competitive saturation (●) was fitted according to the 4-parameter equation (eq. 6), with the resulted values of the curve parameters: A = 100; B = 1.3; C = 0.68 µg l^{-1}; D = 2. The zero dose is represented as 0.001 µg l^{-1} and separated from the first real concentration by a broken line.

4.1.2.2. Three-curve pattern with the diuron assay

When diuron was incubated first and the Tr second, the inhibition curve was largely degraded, especially by displaying a very poor inhibition. When the Tr was incubated first and diuron second, the inhibition curve was similar to the competition curve, except for a lower sensitivity and a higher background, which was ca 20 % in the sequential saturation curve and ca 10 % in the competition curves.

With competitive saturation the curves sensitivities were similar when antigen incubation lasted either 10 or 3 min. The sequential saturation curve was slightly more sensitive at the longer incubation time.

When each antigen was incubation 10 min (fig. 49), IC_{50} was 1.3 µg l^{-1} in the competitive saturation curve, and 2.9 µg l^{-1} in the sequential saturation curve. When each antigen was incubated 3 min (fig. 50), IC_{50} was 1.5 µg l^{-1} in the competitive saturation curve, and 4.8 µg l^{-1} in the sequential saturation curve. The sequential saturation curves were less steep: B = 0.8 both at 10 and 3 min separated incubation of antigens, while in the competitive saturation curves B = 1 - 1.1.

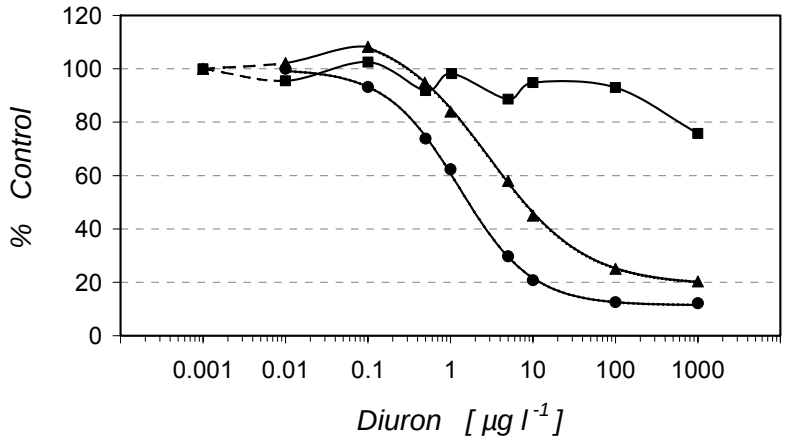

Figure 49. Three-curve pattern with diuron-ELISA when each incubation step lasted 10 min. The shape of the inhibition curve (n = 2) varies with the sequence of the antigens incubation: (●) An+Tr / washing / Buffer+Buffer; (■) An+ Buffer / washing / Buffer+Tr; (▲) Buffer+Tr / washing / An+Buffer. The obtained standard curves were fitted according to the 4-parameter equation (eq. 6), with the resulted values of the curve parameters: competitive saturation (●): A = 100; B = 1; C = 1.3 µg l^{-1}; D = 11; sequential saturation (▲): A = 115; B = 0.8; C = 2.9 µg l^{-1}; D = 19. The zero dose is represented as 0.001 µg l^{-1} and separated from the first real concentration by a broken line.

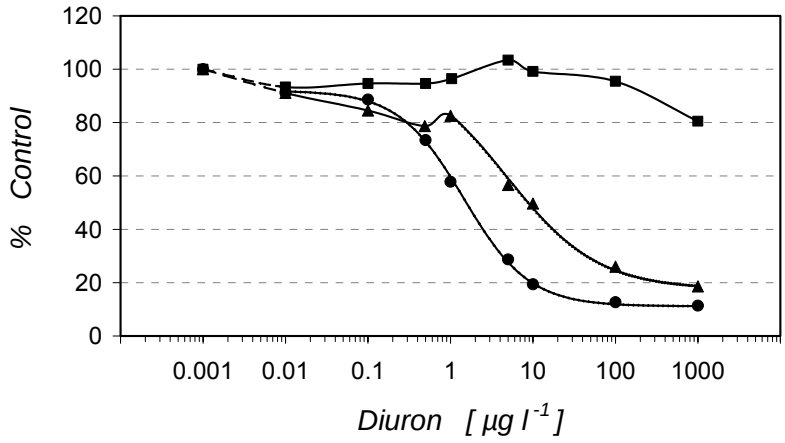

Figure 50. Three-curve pattern with diuron-ELISA when each incubation step lasted 3 min. The shape of the inhibition curve (n = 2) varies with the sequence of the antigens incubation: (●) An+Tr / washing / Buffer+Buffer; (■) An+ Buffer / washing / Buffer+Tr; (▲) Buffer+Tr / washing / An + Buffer. The obtained standard curves were fitted according to the 4-parameter equation (eq. 6), with the resulted values of the curve parameters: competitive saturation (●): A = 92; B = 1.1; C = 1.5 µg l^{-1}; D = 11; sequential saturation (▲): A = 102; B = 0.8; C = 4.8 µg l^{-1}; D = 18. The zero dose is represented as 0.001 µg l^{-1} and separated from the first real concentration by a broken line.

4.1.2.3. Three-curve pattern with the atrazine assay

With sequential saturation, the curve destroyed, no matter which Ag was incubated first. With competitive saturation, a standard curve was obtained both when each incubation step lasted 10 min (fig.51) and when it lasted 3 min (fig. 52).

The sensitive of the curve was not very different with 10 / 3 min incubation of Ab, albeit it was a bit better with 3 min (IC_{50} = 4.6 µg l^{-1}) than with 10 min (IC_{50} = 5.8 µg l^{-1}).

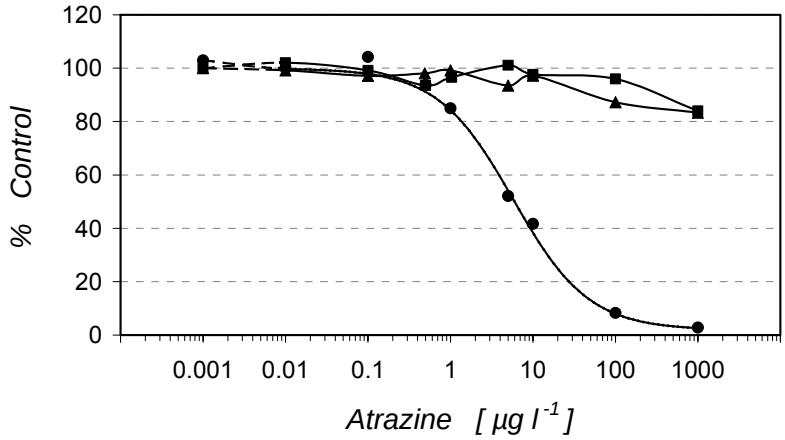

Figure 51. Three-curve pattern with atrazine-ELISA when each incubation step lasted 10 min. The sigmoid shape of the inhibition curve (n = 2) was completely corrupted with both sequential saturations: (■) An+ Buffer / washing / Buffer+Tr; and (▲) Buffer+Tr / washing / An + Buffer. With competitive saturation (●) (An+Tr / washing / Buffer+Buffer), the obtained standard curve was fitted according to the 4-parameter equation (eq. 6), with the resulted values of the curve parameters: A = 100; B = 1.0; C = 5.8 µg l^{-1}; D = 2. The zero dose is represented as 0.001 µg l^{-1} and separated from the first real concentration by a broken line.

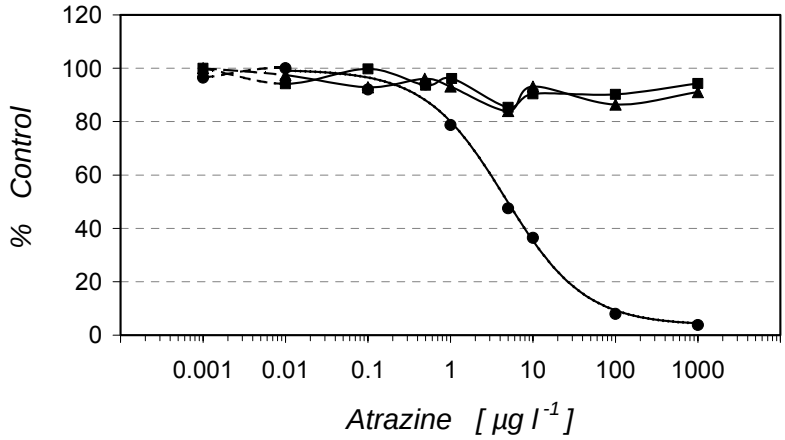

Figure 52. Three-curve pattern with atrazine-ELISA when each incubation step lasted 3 min. The sigmoid shape of the inhibition curve (n = 2) was completely corrupted with both sequential saturations: (■) An+ Buffer / washing / Buffer+Tr; and (▲) Buffer+Tr / washing / An + Buffer. With competitive saturation (●) (An+Tr / washing / Buffer+Buffer), the obtained standard curve was fitted according to the 4-parameter equation (eq. 6), with the resulted values of the curve parameters: A = 100; B = 0.9; C = 4.6 µg l^{-1}; D = 4. The zero dose is represented as 0.001 µg l^{-1} and separated from the first real concentration by a broken line.

4.1.2.4. Three-curve pattern with the TNT assay

When TNT was incubated first and the Tr second, the inhibition curve was largely degraded, especially by losing most inhibition.

When the Tr was incubated first and TNT second, the inhibition curve was similar to the competition curve, except for a clearly higher background and a lower sensitivity (fig. 53). When TNT was incubated first, inhibition was not improved, neither with longer An incubations – despite differences in the slope steepness (fig. 54) –, nor with longer Tr incubation time (fig. 55).

When the Tr was incubated first, inhibition improved with longer An incubation (fig. 56), but not with longer Tr incubation time (fig. 57). All these curves show that a certain inhibition exists (i.e. ca 30-80 % controls) with sequential saturation, depending on the incubation durations. However, a satisfactory standard curve can be obtained only with competitive saturation.

The three-curve pattern obtained with the TNT assay, imply that the displacement approach would not be suitable for an immunosensor platform. Therefore, in such an instrument, it is recommendable that a competitive saturation set-up be applied and optimized, instead of a sequential saturation one.

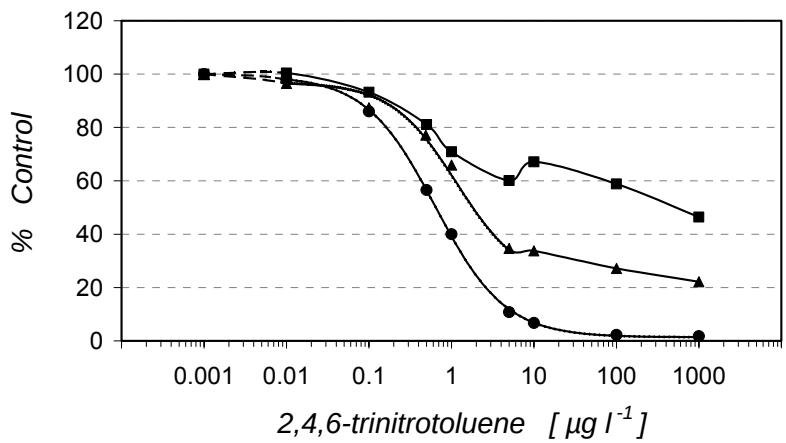

Figure 53. Three-curve pattern with TNT-ELISA when each incubation step lasted 10 min. The shape of the inhibition curve (n = 2) varies with the sequence of the antigens incubation: (●) An+Tr / washing / Buffer+Buffer; (■) An+Buffer / washing / Buffer+Tr; (▲) Buffer+Tr / washing /+ Buffer. The obtained standard curves were fitted according to the 4-parameter equation (eq. 6), with the resulted values of the curve parameters: competitive saturation (●): A = 99; B = 1; C = 0.6 µg l^{-1}; D = 1; sequential saturation (▲): A = 197; B = 1.1; C = 4.8 µg l^{-1}; D = 22. The zero dose is represented as 0.001 µg l^{-1} and separated from the first real concentration by a broken line.

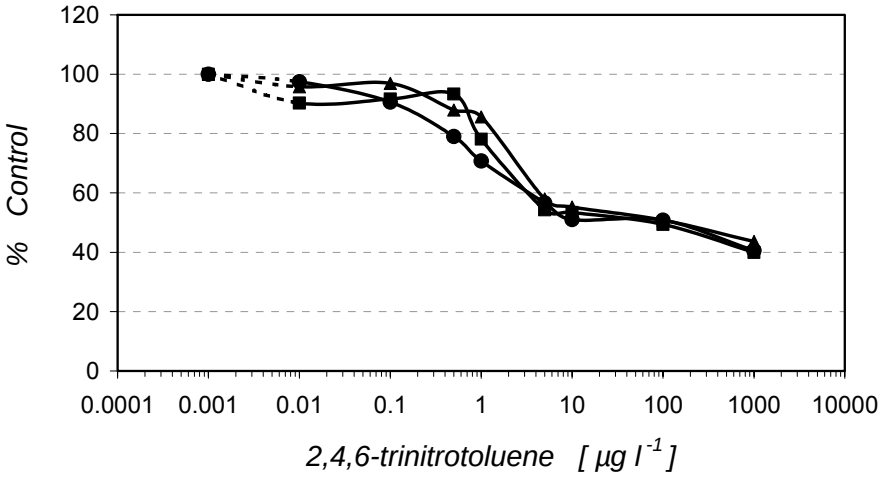

Figure 54. In the immunoassay set-up (TNT+Buffer / washing / Buffer+Tr), some inhibition is visible (ca. 40-50 % controls), and this is similar at shorter and longer TNT incubations. After TNT was incubated 1 min (▲); 2 min (■) or 3 min (●), the Tr was incubated 3 min (RT). The zero dose is represented as 0.001 µg l^{-1} and separated from the first real concentration by a broken line.

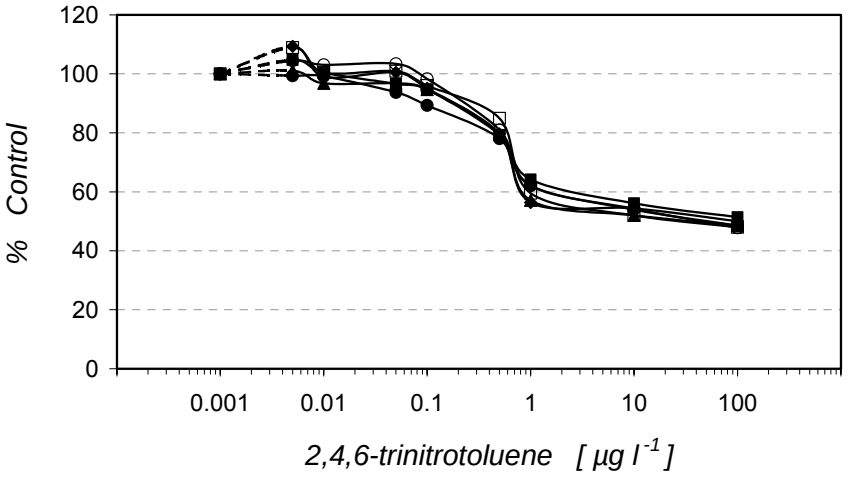

Figure 55. In the immunoassay set-up (TNT+Buffer / washing / Buffer+Tr), some inhibition is visible (ca. 50-60 % controls), and this is similar at shorter and longer Tr incubations. After TNT was incubated 10 min (RT), the Tr was incubated: 0.5 min (□); 1 min (○); 1.5 min (▲); 2.0 min (◆); 2.5 min (■); 3 min (●). The zero dose is represented as 0.001 µg l^{-1} and separated from the first real concentration by a broken line.

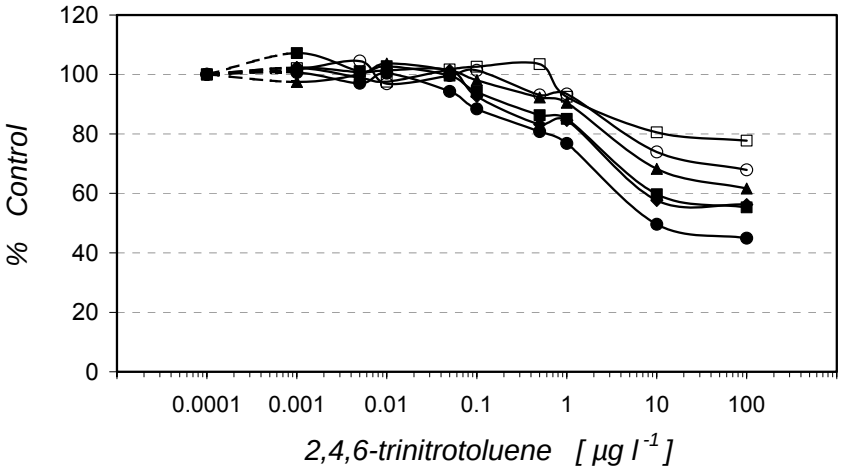

Figure 56. In the immunoassay set-up (Buffer+Tr / washing / TNT+Buffer), some inhibition is visible (ca. 40-80 % controls), and this is getting better with longer TNT incubations. After the Tr was incubated 10 min (RT), TNT was incubated: 1 min (□); 2 min (○); 3 min (▲); 4 min (◆); 5 min (■); 6 min (●). The zero dose is represented as 0.0001 µg l^{-1} and separated from the first real concentration by a broken line.

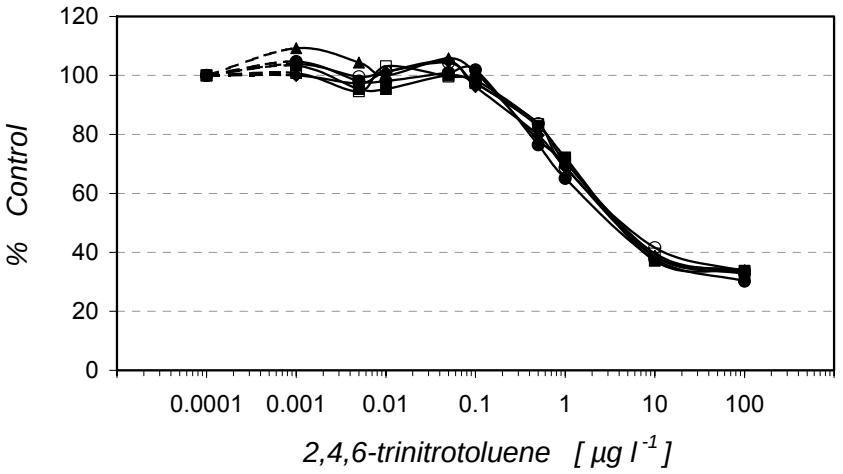

Figure 57. In the immunoassay set-up (Buffer+Tr / washing / TNT+Buffer), some inhibition is visible (ca. 30 % control), but it does not increase with longer TNT incubations. After the Tr was incubated: 1 min (□); 2 min (○); 3 min (▲); 4 min (◆); 5 min (■); 6 min (●), TNT was incubated 10 min (RT). The zero dose is represented as 0.0001 µg l^{-1} and separated from the first real concentration by a broken line.

4.1.3. Variation in the shape of the standard curve

4.1.3.1. Intermediary inhibition plateaus

Widening the range and the number of measured concentrations of An (by using 2-3 microtiter plates for each curve) confirmed that the high signal measured below 1,000 µg l^{-1} An was not a mere high background, but an intermediary plateau in the middle of the usual dose-response slope (fig. 58).

The same particular shape was obtained with the isoproturon assay (isoproturon incubation followed by washing and Tr incubation) except that the intermediary plateau was lower: ca. 20% instead of ca. 40% with the corresponding TNT sequential saturation format (fig. 59).

In the TNT assay, incubation format TNT 10 min / washing / Tr 2.5-20 min, the shape of the two-slope curve did not change significantly with different incubation times for Tr (fig. 60). In this experiment, the intermediary plateau was lower with shorter incubation times.

The shape of the experimentally obtained two-slope curve has some interesting properties. First, there is a general tendency that can be noticed in all curves presented so far: the intermediary plateau is more orderly fitted when lower and vice versa. The reason for this may be that higher intermediary plateaus occurs with higher An dissociation rates, in which case, the reaction dynamic is more sensitive to experimental conditions like semiautomatic washing.

Second, as one can notice in figs. 58, 59 and 60, the resulted two halves of slope had symmetrically strayed (from B = 1) steepness, the lower doses slope being steeper and the higher doses ones being less steep.

For example, in fig. 58, with one two-slope curve (format: TNT+Buffer / washing / Buffer+Tr), the slope is 1.4 (i.e. 1+0.4) with low doses and 0.6 (i.e. 1-0.4) with high doses. With the other curve (format: Buffer+Tr / washing / TNT+Buffer), the slope is 1.25 (i.e. 1+0.25) with low doses and 0.75 (i.e. 1-0.25) with high doses.

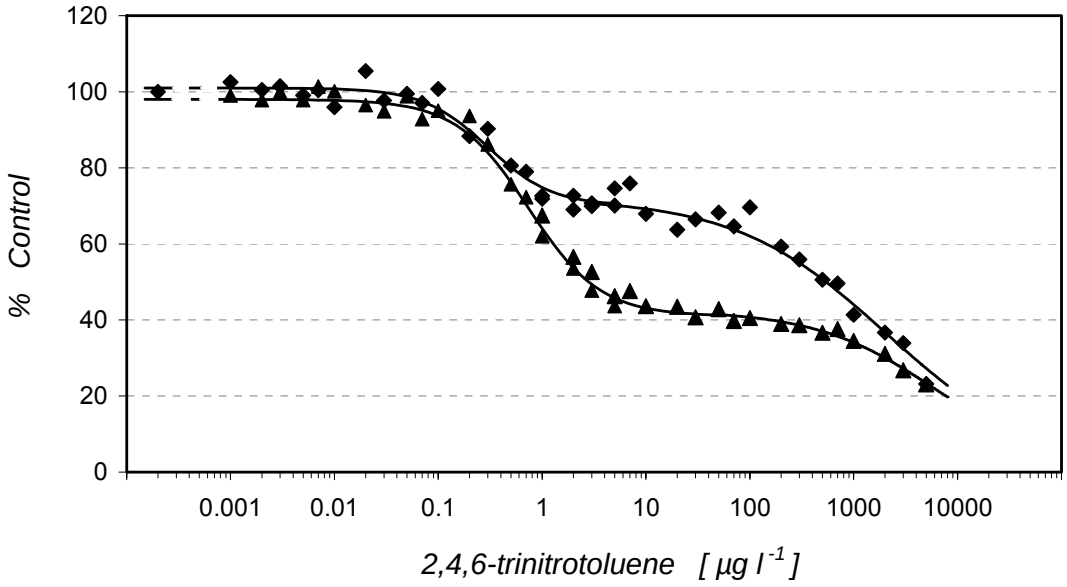

Figure 58. Two-slope standard curves with TNT-ELISA. All incubations took place at RT (21-22°C). The zero dose is represented as 0.0002 µg l^{-1} and separated from the first real concentration by a broken line. The obtained standard curve slopes were fitted according to the 4-parameter equation (eq. 6) (n = 2). In format (TNT+Buffer / washing / Buffer+Tr) (◆), the intermediary plateau is higher and shorter. In format (Buffer+Tr / washing / TNT+Buffer) (▲), the intermediary plateau is lower and longer. The resulted values of the curve parameters are:

(◆) low doses slope: A = 101; B = 1.4; C = 0.3 µg l^{-1}; D = 70;
(◆) high doses slope: A = 70; B = 0.6; C = 2050 µg l^{-1}; D = 1.
(▲) low doses slope: A = 98; B = 1.25; C = 0.74 µg l^{-1}; D = 41;
(▲) high doses slope: A = 42.5; B = 0.75; C = 6150 µg l^{-1}; D = 1.

This slope pattern suggests that a sort of specific complementary (and compensatory) dynamics takes place in the two curve portions, which must be correlated to the peculiar displacement dynamics in the low doses and high doses portions of the curve. Basically, the cause of this symmetrical deviation from the slope (i.e. from B = 1) may be the specific reaction dynamic in the sequential saturation format, as already described in sub-chapter 2.2.8..

Thus, at the end of the applied incubation time, the distance from reaction equilibrium is different in the two curve regions. In the region with higher An concentrations, more An from the Ab-An complexes dissociated, during the washing step, because the dissociation initial speed was higher. The dissociation speed was higher because a higher concentration of such complexes formed initially. Further, the concentration of complexes was higher because the association speed is higher with higher An concentrations.

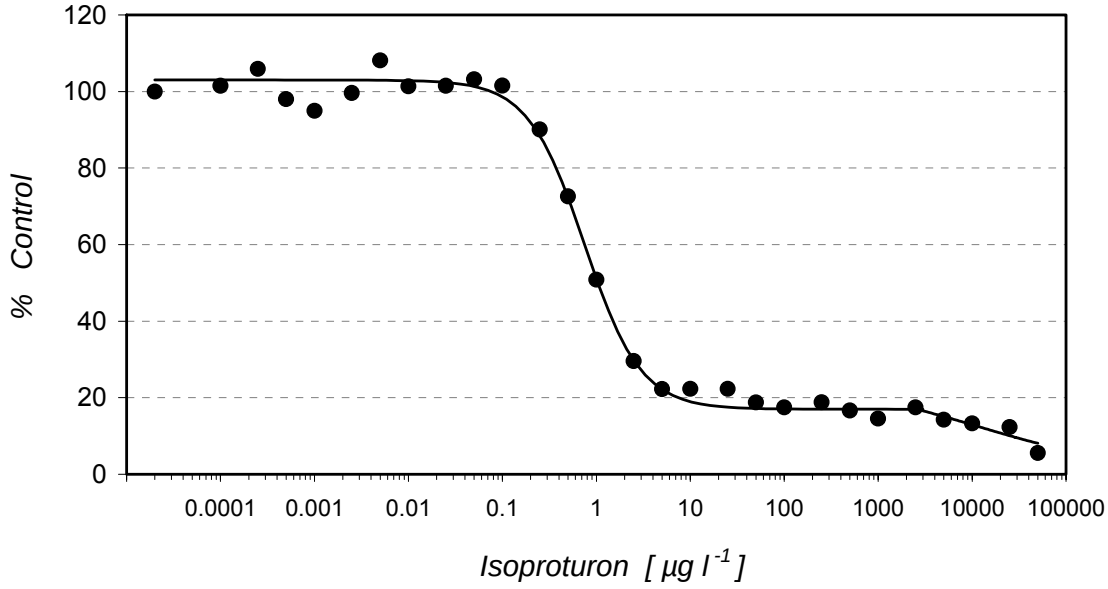

Figure 59. Two-slope standard curve with isoproturon-ELISA, in format (Ip+Buffer / washing / Buffer+Tr). The obtained standard curve slopes were fitted according to the 4-parameter equation (eq. 6) (n = 2). The resulted values of the parameters for low dose slope are: A = 103; B = 1.45; C = 0.8 µg l^{-1}; D = 17; and for the high dose slope: A = 24; B = 0.55; C = 11500 µg l^{-1}; D = 1. The zero dose is represented as 0.00002 µg l^{-1} and separated from the first real concentration by a broken line.

As a consequence, more An was removed from the system during the washing step, leading to lower initial An concentrations. In the end, in the area of high An concentrations, the lower An concentrations determined lower reaction speed, which determined a bigger distance from the reaction equilibrium, which resulted in the slope deviations mentioned above.

Third, the size of the intermediary plateau comprised 2-3 orders of magnitude of An concentrations, with the following tendency: the lower the plateau signal (% control) the longer it is.

Sometimes the intermediary plateau is hooked, and the tendency is to be more hooked when it is higher and more flat or even with a slight slope when it is low.

The obtained two-slope patterns support the theoretical prediction (sub-chapter 2.2.8, figs. 6 and 7) that the washing step employed in the sequential saturation analysis leads to the disruption of the standard curve by the occurrence of an intermediary plateau on the inhibition slope of the standard curve.

The obtained two-slope curves basically show the role of washing in assays with opposite displacement patterns (shown in sub-chapters 4.1.2.1. and 4.1.2.4).

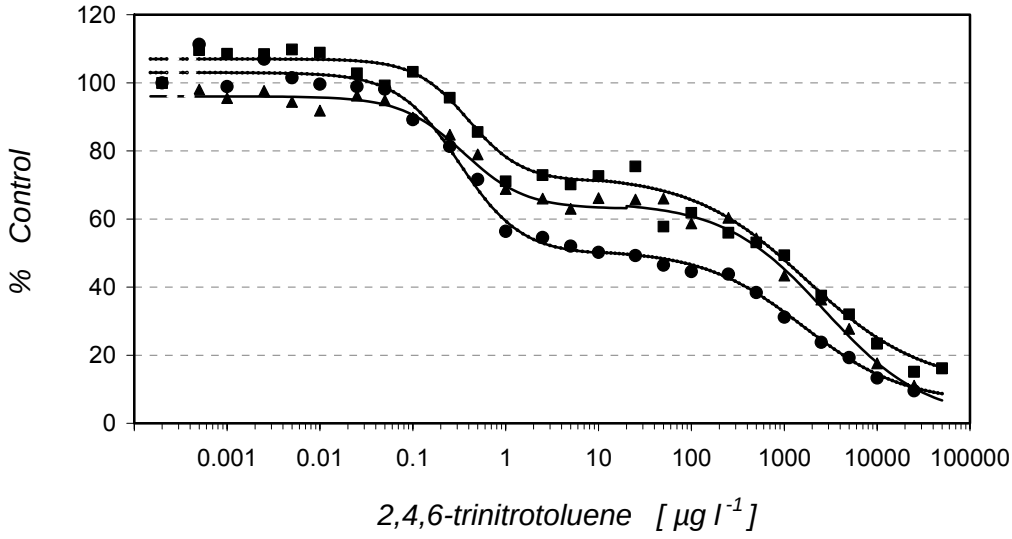

Figure 60. Two-slope curves with TNT-ELISA in format (TNT+Buffer / washing / Buffer+ Tr). TNT was incubated 10 min. Tr was incubated either 2.5 min (●); 5 min (■) or 20 min (▲). All incubations took place at RT (21-22°C). The zero dose is represented as 0.0002 µg l^{-1} and separated from the first real concentration by a broken line. The obtained standard curves - slopes were fitted according to the 4-parameter equation (eq. 6). The resulted values of the curve parameters are (n = 2):

(●) low dose slope: A = 103; B = 1.3; C = 0.3 µg l^{-1}; D = 50;
(●) high dose slope: A = 51; B = 0.8; C = 1600 µg l^{-1}; D = 6;
(■) low dose slope: A = 107; B = 1.5; C = 0.4 µg l^{-1}; D = 71;
(■) high dose slope: A = 73; B = 0.7; C = 1750 µg l^{-1}; D = 11;
(▲) low dose slope: A = 96; B = 1.3; C = 0.4 µg l^{-1}; D = 63;
(▲) high dose slope: A = 65; B = 0.8; C = 2750 µg l^{-1}; D = 6.

4.1.3.2. The low dose hook and the feed-back inhibition

As predicted in sub-chapter 2.2.4., low dose hook and feed back inhibition are due to facilitated binding of Ag, itself a theoretical consequence of the law of mass action.

In this chapter, we will experimentally demonstrate facilitated binding, as well as low dose hook and feed back inhibition, using sequential saturation and competitive saturation analyses.

This was done with immunoassays developed against the explosive TNT (Ciumasu et al., 2005; Zeck et al., 1999) and the pesticide isoproturon (Krämer et al., 2004a).

4.1.3.2.1. Curves obtained with sequential saturation

4.1.3.2.1. A) Incubation format: An / washing / Tr

At the optimized mAb dilution of 1: 35,000 and an Tr dilution of 1: 8,000, after incubations times of 20; 40; 60; 80; 100; 120 seconds for TNT (repeated 3 times), followed by washing and incubation times of 10; 20; 30; 40; 50; 60 seconds for Tr, a facilitated binding effect is visible with all incubations times (fig. 61).

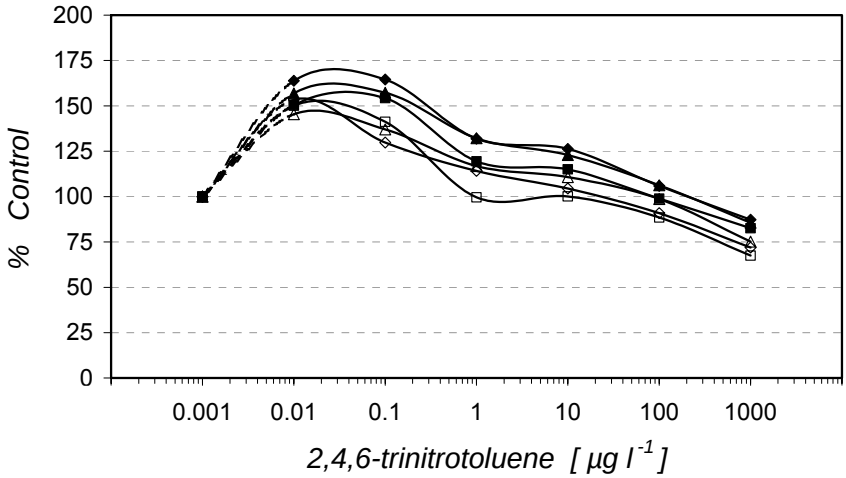

Figure 61. Facilitated binding of Tr in the presence of increasing concentrations of TNT, below the optimized detection (inhibition) limit of 0.1 µg l^{-1}. mAb 1:35 000. Tr 1:8 000. n = 2. The antigens were incubated separately, first An (followed by washing) then Tr, incubation at variable incubation times: (▲) 20s/10s; (◆) 40s/20s; (■) 60s/30s; (△) 80s/40s; (◇) 100s/50s; (□) 120s/60s. The zero dose is represented as 0.001 µg l^{-1} and separated from the first concentration by a broken line.

The amplitude of the resulted hook is already high at (157 % of the zero dose value) at the shortest incubation time of 20s/10s, it is increasing further towards a maximum (164 % of the zero dose value) at the incubation times of 40s/20s, and it goes down to 145 – 150 % with longer incubation times (120s/60s). In this graph, one can identify a tendency of the facilitation peak to move towards higher An concentrations at lower incubation times.

The addition to the duration of antigens incubation and the An concentration, the facilitation effect depends on the antibody and Tr concentrations. Facilitation effect is weaker at higher (here by a factor of 2) Tr concentration (fig. 62), and at higher applied (here by a factor of 3.5) antibody concentration (fig. 63).

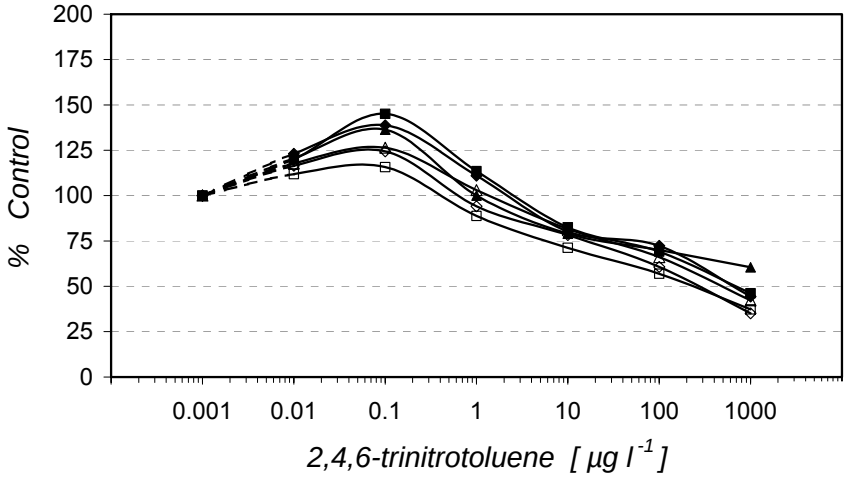

Figure 62. Facilitated binding of Tr in the presence of increasing concentrations of TNT, below the optimized detection (inhibition) limit of 0.1 µg l^{-1}. mAb: 1: 35,000. Tr: 1: 4,000. n = 2. The antigens were incubated separately, first An (followed by washing) then Tr, incubation at variable incubation times: (▲) 20s/10s; (◆) 40s/20s; (■) 60s/30s; (△) 80s/40s; (◇) 100s/50s; (□) 120s/60s. The mean zero dose is represented as 0.001 µg l^{-1} and separated from the first concentration by a broken line.

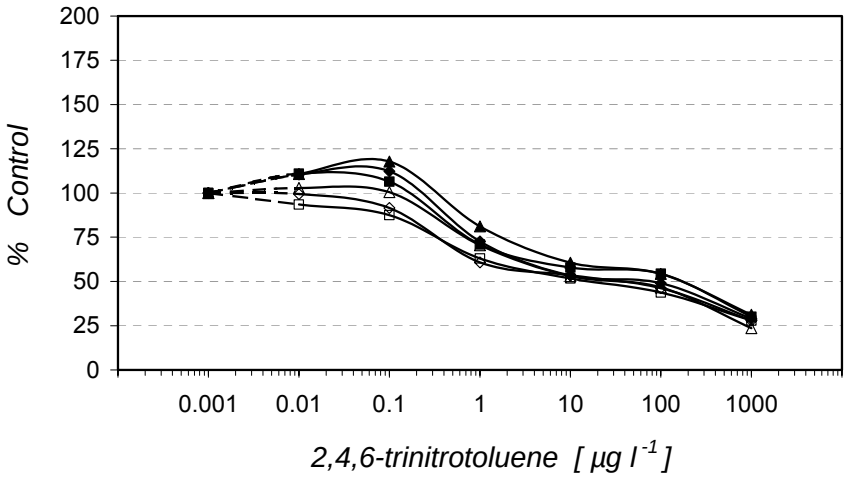

Figure 63. Facilitated binding of Tr, at shorter incubation time, in the presence of increasing concentrations of TNT, below 0.1 µg l^{-1}. mAb: 1:10,000. Tr: 1:8,000. n = 2. The antigens were incubated separately, first An (followed by washing) then Tr, incubation at variable incubation times: (▲) 20s/10s; (◆) 40s/20s; (■) 60s/30s; (△) 80s/40s; (◇) 100s/50s; (□) 120s/60s. The zero dose is represented as 0.001 µg l^{-1} and separated from the first concentration by a broken line.

With mAb 1: 35,000 and Tr 1: 4,000 (fig. 62), the facilitation strength increases with TNT concentration and it reaches it's highest at 0.1 µg l^{-1} TNT.

The amplitude of the resulted hook is already high (136 % of the zero dose value) at the shortest incubation time of 20s/10s, it is increasing further towards a maximum (145 %

of the zero dose value) at the incubation times of 60s/30s, after which it is attenuated gradually with longer incubation times, down to 112% at 120s/60s.

With mAb 1: 10,000 and Tr 1: 8,000 (fig. 63), the facilitation is weaker and only with the lower incubation times. The amplitude of the resulted hook is maximum (118 % of the zero dose value) at the shortest incubation time of 20s/10s, it is dropping towards zero at the incubation times of 80s/40s; at incubation times longer than this, facilitation seems to be replaced by a weak inhibition, even below 0.1 µg l^{-1} (feed-back inhibition). Again, there is a tendency of the facilitation peak to move towards higher An concentrations at lower incubation times.

In fig. 64, the dilutions are the same as in fig. 62 (mAb 1: 35,000; Tr tracer 1: 4,000), but instead of incubating 3 times the TNT before washing and incubation one time with tracer, we repeated 3 times the incubation sequence TNT /3x washing/ Tr / 1x washing. With these experimental conditions, the resulted hook is 2.5 times higher.

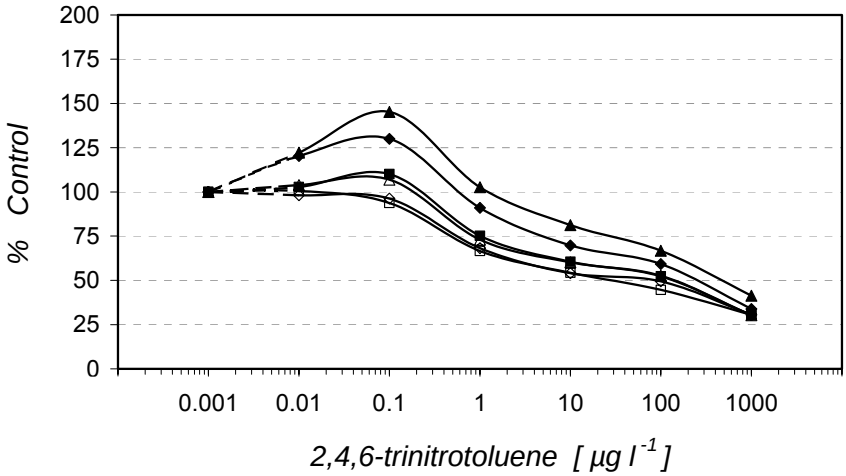

Figure 64. Facilitated binding of Tr, at shorter incubation time, in the presence of increasing concentrations of TNT, below 0.1 µg l^{-1}. mAb: 1: 35,000. Tr: 1: 4,000. n = 2. The antigens were incubated separately, first An (followed by washing) then Tr, incubation at variable incubation times: (▲) 20s/10s; (◆) 40s/20s; (■) 60s/30s; (△) 80s/40s; (◇) 100s/50s; (□) 120s/60s. The sequence An /3x washing/ tracer/ 1x washing was repeated 3 times. The zero dose is represented as 0.001 µg l^{-1} and separated from the first concentration by a broken line.

Thus, when the Tr is incubated 3 times the phenomenon of facilitated binding repeated itself 3 times (also, some tracer dissociated during the two washing). The hook was lost at 3x 100s/50s, with no inhibition below 0.1 µg l^{-1} (feed-back inhibition) like in fig. 63.

4.1.3.2.1. B) Incubation format: Tr / washing / An

In another set-up, we incubated first the tracer along different durations (10; 20; 40; 80; 160; 320 seconds), then we washed 3 times and incubated TNT 10 min. (RT was 26-28°C). With such a set-up and dilutions mAb 1: 50,000 and Tr 1: 2,000, the facilitation effect is visible all along the curve, up to ca 30 % at the shortest tracer incubation time (fig. 65).

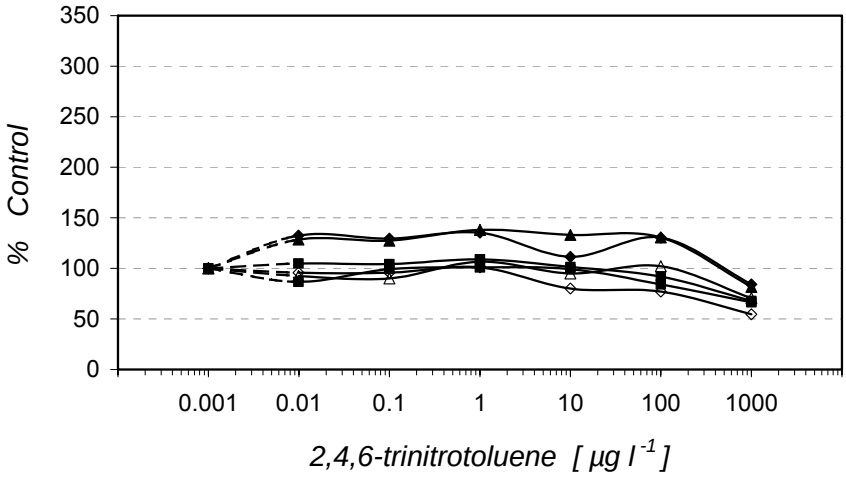

Figure 65. Facilitated binding of Tr, at shorter incubation time, in the presence of increasing concentrations of TNT, at all doses. mAb: 1: 50,000. Tr (hapten TNP-glycylglycine; CR = 12 %): 1: 2,000. n = 2. The antigens were incubated separately, first An 10 min (followed by washing), then Tr (▲) 10s; (◆) 20s; (■) 40s; (△) 80s; (◇) 160s; (□) 320s. The zero dose is represented as 0.001 µg l^{-1} and separated from the first concentration by a broken line.

With an identical set-up, but with an Tr that is recognized by the antibody by about 40 times less than the usual tracer, the facilitation is hugely stronger, i.e. up to 250 – 300 % (fig. 66). The hapten of this Tr (2,4-DNP-ε-aminocaproic acid) has a cross-reactivity to TNT of 0.3 %, while the usual tracer (TNP-glycylglycine) has a cross-reactivity of 12 % (sub-chapter 4.1.1.3.1., table 9).

With the usual Tr, the maximal facilitation is reached already at the lowest concentration (0.01 µg l^{-1}) and it stays high until 100 µg l^{-1}. With the poorly recognized tracer, the facilitation strength reaches a peak at 0.1 µg l^{-1} and then it is dropping like in the experiments with the Tr incubated after An.

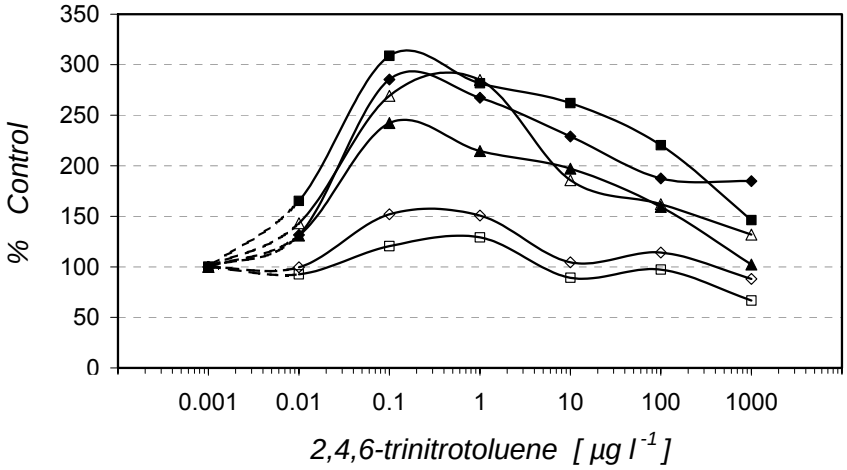

Figure 66. Facilitated binding of Tr, at shorter incubation time, in the presence of increasing concentrations of TNT, at all doses. mAb: 1: 50,000. Tr (hapten DNP-ε-AmCA; CR = 0.3 %): 1: 1,000. n = 2. The antigens were incubated separately, first An 10 min (followed by washing), then Tr (▲) 10s; (◆) 20s; (■) 40s; (△) 80s; (◇) 160s; (□) 320s. The zero dose is represented as 0.001 µg l^{-1} and separated from the first concentration by a broken line.

In identical conditions with those in fig. 65 but with 10 times more concentrated antibody incubated on the microtiter plate, the facilitation is a bit stronger, and the maximum is shifted towards higher concentrations of An after which it is clearly decreasing (fig. 67).

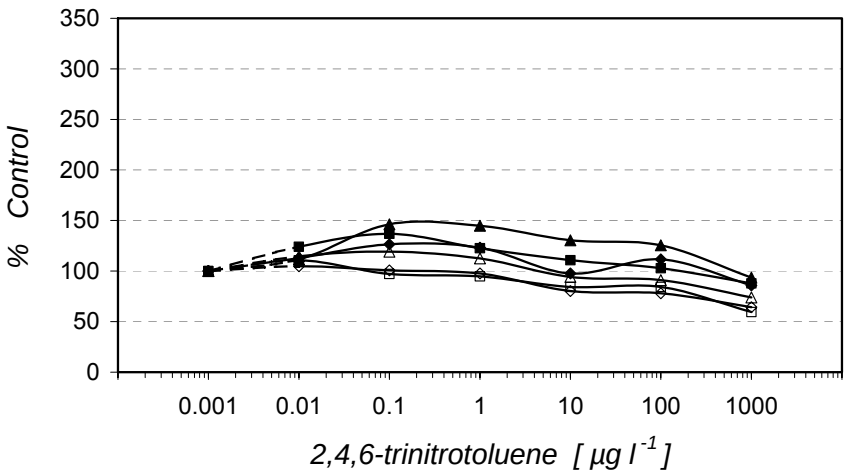

Figure 67. Facilitated binding of Tr, at shorter incubation time, in the presence of increasing concentrations of TNT, at all doses. mAb: 1: 5,000. Tr (hapten TNP-glycylglycine; CR = 12 %): 1: 2,000. n = 2. The antigens were incubated separately, first An 10 min (followed by washing), then Tr (▲) 10s; (◆) 20s; (■) 40s; (△) 80s; (◇) 160s; (□) 320s. The zero dose is represented as 0.001 µg l^{-1} and separated from the first concentration by a broken line.

With the low affinity tracer (like in fig. 66) and 10 times more concentrated antibody applied on the microtiter plate, the facilitation is weaker and the high peaks at shorter incubation times are strongly shifted to the higher concentrations of An (tendency which is just opposite to that in low antibody density) (fig. 68).

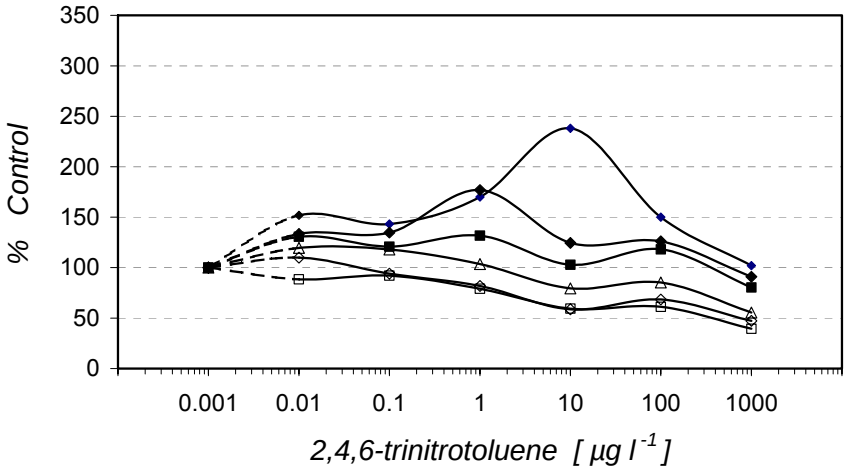

Figure 68. Facilitated binding of Tr, at shorter incubation time, in the presence of increasing concentrations of TNT, at all doses. mAb: 1: 5,000. Tr (hapten DNP-ε-AmCA; CR = 0.3 %): 1: 1,000. n = 2. The antigens were incubated separately, first An 10 min (followed by washing), then Tr (▲) 10s; (◆) 20s; (■) 40s; (△) 80s; (◇) 160s; (□) 320s. The zero dose is represented as 0.001 µg l^{-1} and separated from the first concentration by a broken line.

4.1.3.2.2. Curves obtained with competitive saturation

In experimentally obtained standard curves with TNT and isoproturon, feed-back inhibition was visible as deviations (around the detection limit) from the sigmoid shape.

A lower affinity in the Tr's hapten should determine a feed-back inhibition that is both weaker and shifted towards higher concentrations of An. In fig. 69, this prediction was confirmed experimentally (by employing two different Tr, with different affinities, in two different experiments with the same TNT assay format: TNP-glycylglycine–HRP and DNP-γ-AmCA–HRP.

Similarly, a lower affinity in the applied standard (the target An or a cross-reactant) yields a feed-back inhibition that is both weaker and shifted towards higher An concentrations. This was confirmed experimentally, as well, with the isoproturon assay, by applying isoproturon and diuron, the last one having a cross-reactivity of 4.5 % (fig. 70).

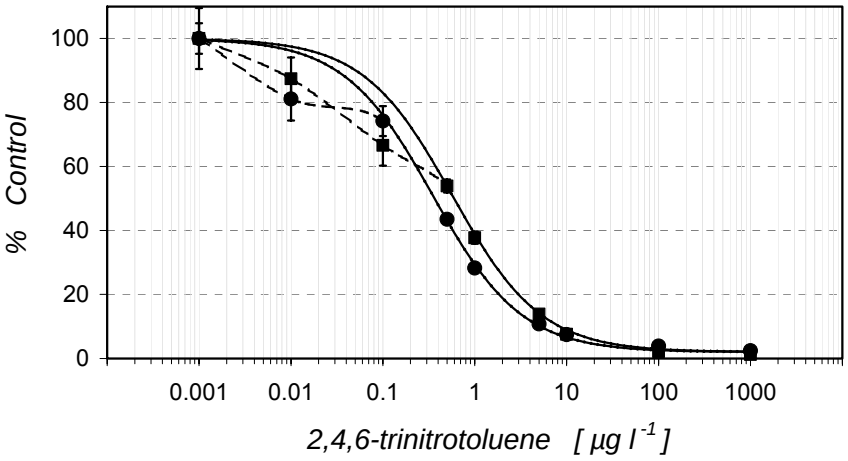

Figure 69. Feed-back inhibition occurring around the detection limit (IC_{20}) (between 0.001 – 0.01 µg l^{-1}) with the TNT assay (two different Tr). The continuous lines represent the fitted curves, according to the 4-parameter equation (eq. 6). The broken lines connect the values remained outside the fitting curve, indicating feed-back inhibition in the vicinity of DL (IC_{20}). In the fitted curves, the resulted parameters are (n = 3): (●) with the general Tr (TNP-glycylglycine–HRP; hapten CR % = 12 %): A = 100 (a priory); B = 0.9; C = 0.35 µg l^{-1}; D = 2; maximum negative hook of ca 20 % at 0.01 µg l^{-1}; (■) with a lower-affinity Tr (DNP-g-AmBA–HRP; hapten CR = 0.5 %): A = 100 (a priori); B = 0.9; C = 0.57 µg l^{-1}; D = 2; maximum negative hook of ca 15 % at 0.1 µg l^{-1}. The zero dose is represented as 0.001 µg l^{-1}, and is separated from the first real concentration by an interrupted line.

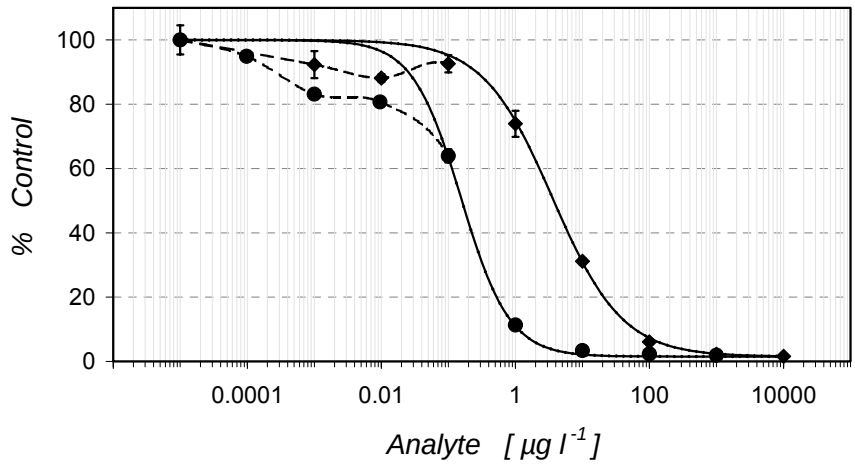

Figure 70. Feed-back inhibition occurring just before the detection limit (IC_{20}) (between 0.001 – 0.01 µg l^{-1}) with the isoproturon assay. The continuous lines represent the fitted curve, according to the 4-parameter (eq. 6). The broken lines connect the values remained outside the fitting curve, indicating feed-back inhibition in the immediate vicinity of DL (IC_{20}). In the fitted curves (n = 2), the resulted parameters are (n = 3): for isoproturon (●): A = 100; B = 1.2; C = 0.155 µg l^{-1}; D = 1.5; negative hook of 19 %; for diuron (CR = 4.5 %) (◆): A = 100 (a priori); B = 0.84; C = 3.6 µg l^{-1}; D = 1.5; negative hook of 12 %. The zero dose is represented as 0.00001 µg l^{-1}, and is separated from the first real concentration by an interrupted line.

Feed back-inhibition, like the low dose hook, has the potential to cause inaccurate fittings of the standard curve, hence subsequent analytical drawbacks (discussion in the next paragraphs).

4.1.3.2.3. Discussion

As shown in sub-chapter 2.2.8., the law of mass action actually predicts that the experimentally obtained standard curve is the consequence of a dynamical equilibrium between facilitated binding, direct inhibition and feed-back inhibition. At given incubation times, binding to antibody can vary a lot. Also, the Ab - Ag reaction is dependent on the diffusion rates of each Ag between the bulk volume and the reaction volume. For example, TNT has a much higher diffusion rate, because it has a molecular weight of only 227, compared to 40,000 of the HRP – a prolate ellipsoid with an axial ratio of 3 to 1 (Brunet et al., 1994).

Logically, facilitated binding and feed-back inhibition may be detectable only at An concentrations that produce weak or no direct inhibition (in principle below IC_{50}). At such An concentrations, facilitated binding and feed-back inhibition may cancel each other to various extents, in a fragile equilibrium. This equilibrium is dependent on small-to-moderate variations in the experimental conditions (like RT; incubation time; plate shaking, i.e. mass transport) and the physical properties of the reagents (diffusion rates; association / dissociation rates).

In sequential saturation assays, bellow / around 0.1 µg l^{-1} TNT (which is also the detection limit of the TNT assays), higher concentrations of TNT are associated with higher tracer binding. This indicates that there is a phenomenon of facilitated binding of Tr in the presence of low concentrations of An. In certain experimental conditions, this phenomenon can determine the occurrence of a low dose hook.

This low dose hook could be diminished by applying higher antibody concentrations (of course, at the expense of sensitivity), higher concentrations of Tr, high affinity Tr and/or longer incubation times.

In the sequential saturation assay, <u>incubation formats An / washing / Tr</u>, there is the general trend of a stronger hook with shorter incubation times, and direct inhibition starting at the same concentration as in the competitive saturation assay (ca 0.1 µg l^{-1}).

At certain incubation times, feed-back inhibition was replacing facilitated binding of Tr, suggesting that with slightly different conditions, one or another of the two phenomena prevail.

Further in the sequential saturation assay, at certain higher An concentrations, the relative strength of the hook effect becomes smaller than direct inhibition. A common

tendency is that there is a stronger hook just before the down-slope of the curve. Thus, the ascending portion of the hook is where the facilitation of the Tr becomes stronger than the feed-back inhibition of the Tr, and the descending portion of the hook is where the facilitation of the Tr binding gets lower than the inhibition of the Tr binding.

When the sequential incubation was repeated three times, there was an additive effect of facilitated binding of the Tr: the hook got 2.5 times higher.

With incubation formats Tr / washing / An, some of the Tr bound in the first step dissociated at washing (and it was lost) or during the subsequent An incubation. However, the total antigen concentration was higher at An incubation, leading to more binding of the Tr when the An was present.

This effect was even stronger when a lower affinity tracer was used, because such an Tr dissociates faster, its binding being more dependent on the presence of An. In this case, not only that the amount of bound Tr is much lower in the absence of An molecules (as in zero dose measurements), but the maximum facilitation effect occurs at higher An concentrations (than it happens with higher affinity Tr).

Using a more concentrated solution of antibody had two end effects: the facilitation hook was weaker and the facilitation peak shifted towards higher An concentration. The first effect may be explained by higher reaction speeds with more antibodies in zero dose measurements, which is reducing the differences in reaction speed leading to facilitated binding. The second effect is a consequence of the first: at higher antibody concentrations, maximum difference in the reaction speed (fig. 3, sub-chapter 2.1.3.) is conditioned less by the speed lag in the presence of no (or very low) An concentrations and more by the speed advantage provided by the presence of some higher (at detection limit) An concentrations.

In the TNT and the isoproturon assays, competitive saturation, feed-back inhibition (of the enzyme tracer binding) was also revealed. Feed-back inhibition consisted in a moderate decrease of the signal before or around the detection limit known for each assay. With lower affinity in the Tr, or with lower affinity An, feed-back inhibition was both weaker and shifted towards higher concentrations of An.

Facilitated binding and feed-back inhibition of the Tr have opposite effects. When they are of equal relative importance (in terms of percent of occupied recognition sites on the immobilized antibody population), they cancel each other. When they don't cancel each other, they may determine a low dose hook. In the current immunoassays practice, the low dose hook is usually moderate, hence ignored.

But unlike in classical immunoassays, the phenomena which determine the low dose hook are critical in automated biosensors, where the ratio volume/surface is very different than in the microtiter plates and the contact between bulk volume and reaction volume is

better. Other physical conditions are also changed in immunosensors: shorter incubation times, competition design and washing regime.

Virtually, the automatic curves produced by the computer (of a commercial immunosensor) may be seriously corrupted by the low dose hook and by feed-back inhibition. This is because, typically, the low dose inflection point of the sigmoid will be masked by the low dose hook / feed-back inhibition.

Consequently, when the low dose hook occurs, the slope parameter (B) would be much over-estimated: the displayed value will be usually well above 1.0. For the same reason, the zero dose value (A) would also be slightly over-estimated: the displayed value will be visibly above 100 %.

Symmetrically, when the feed-back inhibition occurs, the slope parameter (B) would be much under-estimated: the displayed value will be usually well below 1.0. For the same reason, the zero dose value (A) would also be slightly under-estimated: the displayed value will be visibly below 100 %.

In addition, lower values for these two curve parameters will induce a certain bias in the estimation of other parameters: the midpoint (C), the width of the dose – response interval, the detection limit, the general curve calibration and the concentration of An calculated on the basis of it.

In addition, some biosensor applications (including ours) require a switch between different measurement systems, e.g. from absorbance to luminescence, implying different Tr dilutions. As a consequence, (and like it was the case with our sensor development,) all immunochemicals applied in such biosensor systems need to be re-optimized and may provide analytical performances that are quite different from the ones initially expected.

As a general conclusion, the shape of the standard curve is the result of a dynamical equilibrium between low-dose hook, direct inhibition and feed-back inhibition of the Tr.

In the next sub-chapter it will be shown that even with robust, highly optimised immunoassays, like the isoproturon assay, moderate curve variations (at low doses) may occur at low sampling intensities.

4.1.3.3. Dependence on sampling intensity

This sub-chapter deals with the influence of sampling intensity (i.e. number of measurements) on the accuracy of curve fitting with a robust ELISA: the isoproturon assay. By "sampling intensity" we understand both the number of An (standard) concentrations and number of measurements per An concentration.

With the isoproturon assay used in the sensor development and proof of principle, we fitted a standard curve with a high number of measurements, i.e. *n* = 60 (fig. 71). This was done during a statistical study which is not discussed in the present thesis. What is relevant for the present thesis is that, when the number of measurements is lower so that multiple curves are produced instead of a single one, the resulted standard curves may partially lose the sigmoid shape (fig. 72).

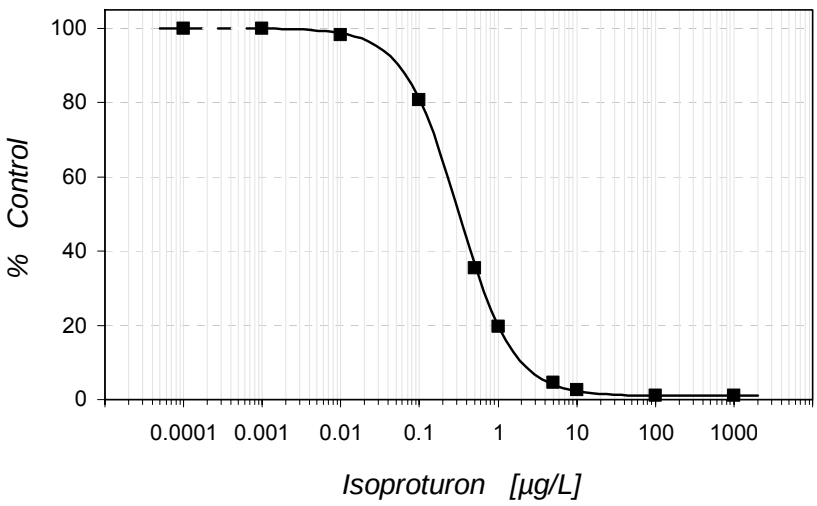

Figure 71. Standard curve obtained with isoproturon-ELISA, applying a very high sampling intensity (n = 60). The zero dose is represented as 0.0001 µg l^{-1}. The fitted average values are perfectly fitted on the sigmoid, with the following values of the curve parameters: A = 100; B = 1.25; C (IC_{50}) = 0.32; D = 1.

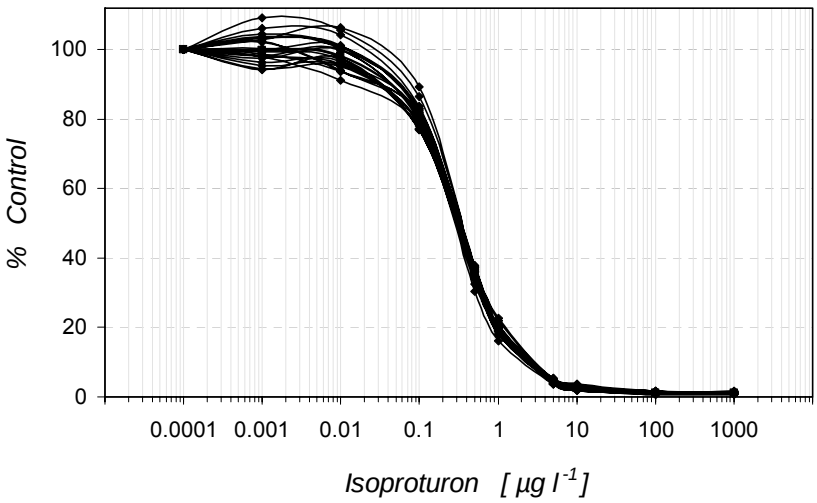

Figure 72. Standard curves obtained with isoproturon-ELISA, with moderately low (though common) sampling intensity (n = 3). The curves are superimposed onto the general curve (n = 60). The curve shapes are shown, instead of curve fitting. In the upper plateau region, the signal value varies between 94 - 109 %. The zero dose is represented as 0.0001 µg l^{-1}.

Attention must be payed to the fact that the standard deviation is not enough measure of the sampling intensity effects, for two reasons. First, when *n* is obtained with several plates, standard deviation from the biochemical process may be masked by the inevitable variations between plates. In this case, curve representation by % control (no standard deviation) is more appropriate. Second, standard deviation with high *n* provides, as such, no indication upon the curve variation with low *n.*

Variations from the single curve shape occurred especially in the lower concentrations range, e.g. positive and negative low dose hooks. The explanation we propose for this specific pattern was basically discussed in the chapter on low dose hook. In a nutshell, what causes this variation the curve shape is the fact that, at low doses, there is very sensitive equilibrium between antigens reciprocal facilitations and feed-back inhibitions, which may be easily influenced by tiny variations of the experimental conditions.

As a possible conclusion, the behaviour of each immunoassay transferred onto an immunosensor platform must be well known, especially the signal variations at low doses. Otherwise, potential misfittings of the calibration curve cannot be anticipated.

For the stage of sensor proof of principle, the intensity of sampling and the bio-physical dynamics of the Ab - Ag system have mainly a guiding role along the assays transfer and probing onto the biosensor platform. Therefore, single measurements were sufficient for our biosensor development and proof of principle. However, on the long run, a future commercial version of the developed immunosensor should tackle the error potential of single measurements.

4.2. Optimized fast immunoassays on microtiter plates

4.2.1. Fast ELISA with TNT, atrazine, diuron and isoproturon

All competition assays employed in our sensor development could be optimized for fast analyses on microtiter plates, indicating a very good potential for fast on-line measurements. On the basis of the observed immunoassays flexibility (sub-chapter 4.1.2.), the TNT-assay, the diuron assay and the atrazine assay could be optimized for an Ag incubation step of 10 minutes and even 3 minutes.

With later measurements with the sensor, 10 minutes was the minimum duration of the competition step needed to obtain acceptable standard curves. In fig. 73 we show standard curves obtained on microtiter plates with those fast assays that were successfully transferred to the sensor platform, i.e. ELISAs for TNT, diuron and atrazine.

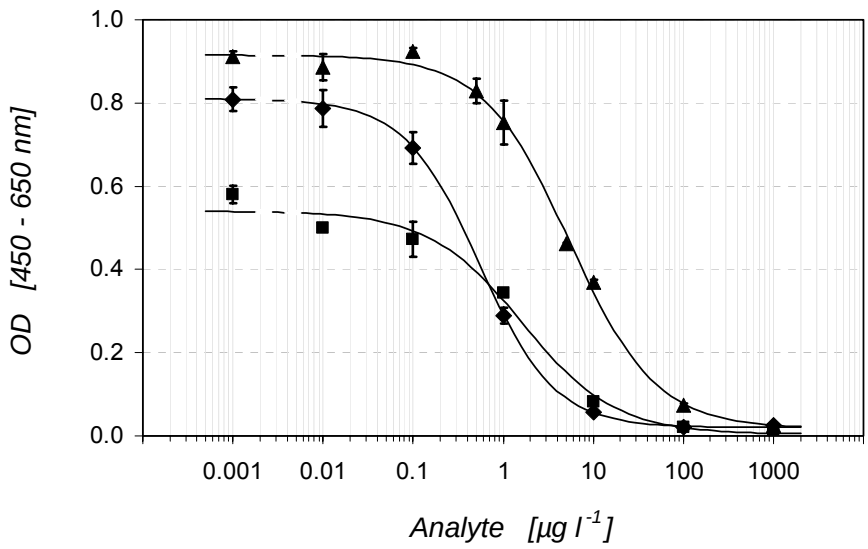

Figure 73. Standard curves for TNT (n =5), diuron (n = 3) and atrazine (n = 5), produced with <u>fast</u> ELISA. Standards and the Tr (both in 40mM PBS) were incubated together 10 min at RT (21-24°C) onto the immobilized mAb; H_2O_2 / TMB incubated 10 min at RT (21-24°C). The zero dose (in 40 mM PBS) is represented as 0.001 µg l^{-1} and separated from the first real concentration by an interrupted line. The standard curve was fitted with to the 4-parameter equation (eq. 6), with the following resulted parameters:

(◆) TNT: A = 0.81; B = 1.04; C (IC_{50}) = 0.5 µg l^{-1}; D = 0.02; DL (IC_{20}) = 0.2 µg l^{-1};

(■) Diuron: A = 0.54; B = 0.84; C (IC_{50}) = 1.6 µg l^{-1}; D = 0.01; DL (IC_{20}) = 0.3 µg l^{-1};

(▲) Atrazine: A = 0.92; B = 0.91; C (IC_{50}) = 5.5 µg l^{-1}; D = 0.02; DL (IC_{20}) = 1.2 µg l^{-1}.

With the isoproturon assays a very high background (in %) could not be avoided with 3 min competition step (fig 74). Apparently, the isoproturon assays, which is the most sensitive we used in our development, actually is not as amenable to the transfer on the developed immunosensor platform as the earlier mentioned three assays.

In the sub-chapter upon assays flexibility, we also noticed that the An/Tr displacement pattern (i.e. the three-curve patterns) in the isoproturon assay was different than the pattern with the TNT-, diuron- and atrazine- assay.

All these suggest that the isoproturon assay has some different values of the bio-physical dynamic parameters, and new approaches might be necessary for its successful transfer to the immunosensor platform.

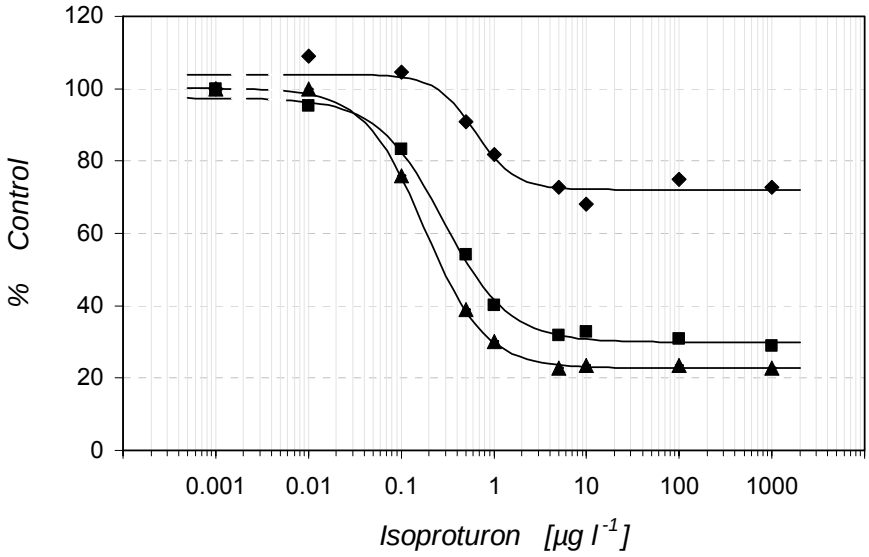

Figure 74. Standard curves produced with fast isoproturon-ELISA. Standards and the Tr (both in 40 mM PBS) were incubated together 30 min; 10 min or 3 min at RT (21°C) onto the immobilized mAb; HRP substrate/chromogen incubated 10 min at RT (21°C). The zero dose is represented as 0.001 µg l^{-1} and separated from the first real concentration by an interrupted line. The standard curve was fitted with to the 4-parameter equation (eq. 6), with the following values of the curve parameters (n =2): (▲) 30 min: A = 100.1; B = 1.33; C (IC_{50}) = 0.18 µg l^{-1}; D = 22.7; DL (IC_{20}) = 0.08 µg l^{-1};
(■) 10 min: A = 97.4; B = 1.23; C (IC_{50}) = 0.28 µg l^{-1}; D = 29.9; DL (IC_{20}) = 0.12 µg l^{-1};
(◆) 3 min: A = 104; B = 2.01; C (IC_{50}) = 0.70 µg l^{-1}; D = 72.1; DL (IC_{20}) = 1.1 µg l^{-1}.

4.2.2. Troubleshooting in fast ELISA

The most important trouble specific to fast ELISAs is the low dose hook. As seen in sub-chapter 4.1.3.2, low dose hook tends to occur especially at shorter incubation times. However, longer incubation time for the competing antigens is not the only possibility to avoid low dose hook.

To surpass this undesired effect, we propose that one can simply convert the standard/sample low doses into higher (enough) doses. Thus, one can add a known amount of An to every sampled that is to be analysed (the same amount needed to reach the maximal hook), and to the zero dose measurements, and then subtract it from the measured concentration of An.

Another main source of error with fast ELISAs is fast handling of reagents. Automation can help a lot in removing this error, like it is actually done during on-line measurements with the sensor we developed. (This is necessary especially with shorter incubations, because then the Ab-Ag reaction is not yet in the equilibrium.) Also necessary

are, obviously, good knowledge upon general troubleshooting in ELISA, good manual skills and general experience of the experimenter.

Fast ELISAs may also meet important modifications of cross-reactivities. Such changes can occur at very short incubation times, especially in conjunction with temperature (details in sub-chapter 4.1.1.3.). Cross-reactivities of an assay might also vary with different combinations of temperature and solvent content (%) of the sample (Katagiri et al., 1999). Such changes must be taken into account and measured with future commercial versions of the immunosensor, starting from the core developments described in this thesis.

4.3. Optimizations of competitive saturation ELISA on batch structures

4.3.1. General requirements for batch ELISA

Batch ELISA on structures was adapted from microtiter plates formats by adjusting the applied volumes and concentrations of reagents. The reagent volumes used in batch ELISA were higher than in the wells of the microtiter plates so that the structure itself was completely immersed in the solution and the solution layer above the pyramids was high enough to allow fast diffusion of the reagent molecules through the vial and to the surface of the pyramids.

The capture antibodies were immobilized by physical adsorption to the gold structure surface. In the vials, all solutions were added carefully with a Multipette® and removed with a Pasteur pipette.

At certain experimental steps, especially before the addition of substrate, the structures were changed to new clean vials, but the structures never touched anything else than the glass vials. This was done in an attempt to avoid any cross contaminations or structure damage; no handling instrument was used for their transfer between vials.

Washing proved to be critical, because of the pyramids geometry on the structure surface. Therefore, washing had to be evenly efficient (as much as possible) across the pyramidal surface and the structures in each vial. The standard amount of washing in batch ELISA was three times 1 ml of washing buffer (4 mM PBST, pH 7.6) per vial. Less washing (e.g. two times) prevented to obtain a valid standard curve. More washing was not necessary.

4.3.2. Batch ELISA developments with TNT

Among all employed assays, the TNT-assay was used as the main exploratory tool in batch ELISA. With this assay we identified the best structure geometry (pyramids number and pyramids dimensions).

Initially, we performed batch TNT-ELISA in plastic (Eppendorf) vials, and noticed that the inhibition tendency was present in all types of surface structures (polished, i.e. no pyramids, small pyramids, intermediate pyramids and tall pyramids), but the unspecific binding of the Tr was a serious problem (fig. 75).

Later, we performed the batch ELISA only in glass vials, which allowed better washing. In order to block the unspecific binding (adsorption) of the Tr to the golden surface of the pyramids, we used higher antibody concentration (thus allowing a maximum density in the population of immobilized antibodies) and lower concentrations of Tr (thus diminishing the chance of unspecific adsorption of Tr to gold). With this strategy, the unspecific signal diminished significantly, and the curve sensitivity was very good, with an IC_{50} of around 1 µg l^{-1} (fig. 76).

In order to fight the unspecific binding of the Tr and the reproducibility of the inhibition curves with batch TNT-ELISA, we tried several blockers: skimmed milk powder (fig. 77), and also BSA and casein.

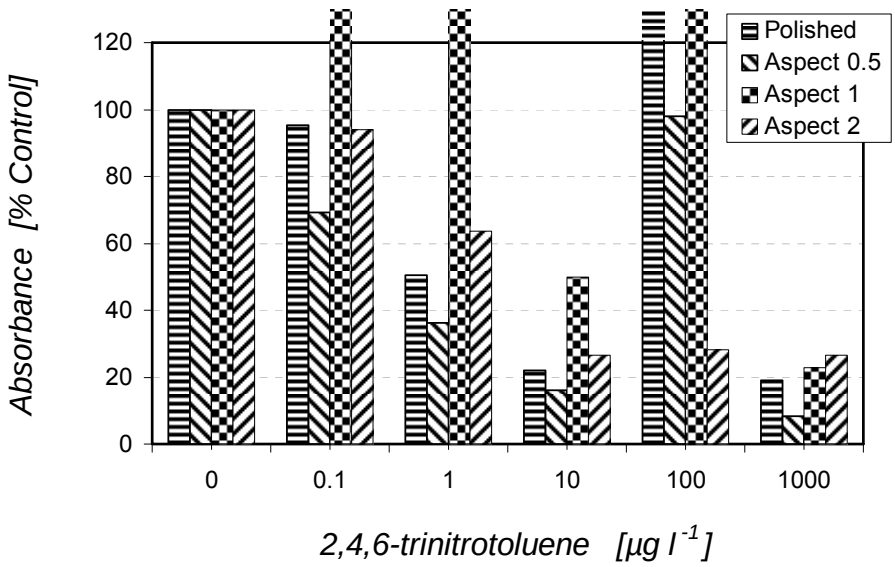

Figure 75. Preliminary standard curve with different structure aspects (n = 1), obtained with TNT batch ELISA, in Eppendorf plastic vials. The amount of incubated antibody is 0.091 µg / structure (Ab solution: 303 µg l^{-1}, 0.3 ml / structure). The dilution of the applied Tr was 1: 2,000. The high occurrence of outrageous values indicates strong unspecific binding.

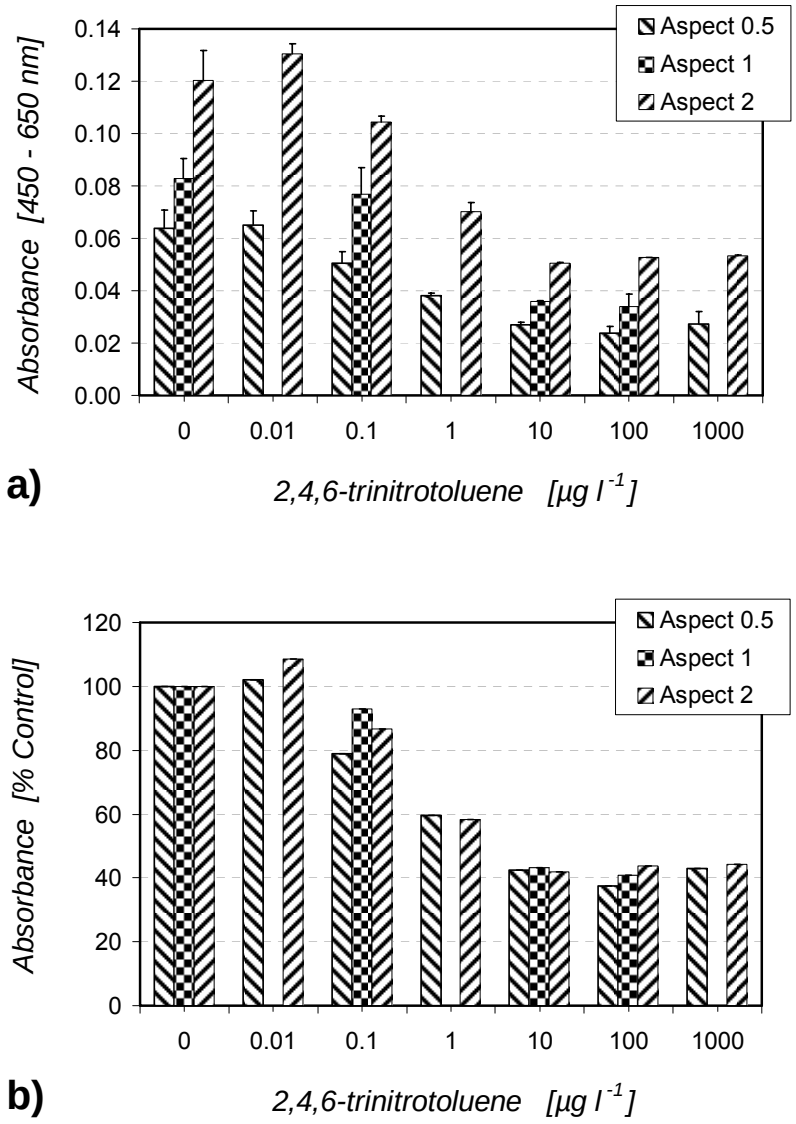

Figure 76. Standard curve with different structure aspects (n = 2), obtained with TNT batch ELISA, in glass vials. The amount of incubated antibody is 1.06 µg / structure (Ab solution: 1,060 µg l^{-1}, 1 ml / structure). The dilution of the applied Tr was 1: 20,000. Unspecific binding is high but more predictable (low standard deviations).

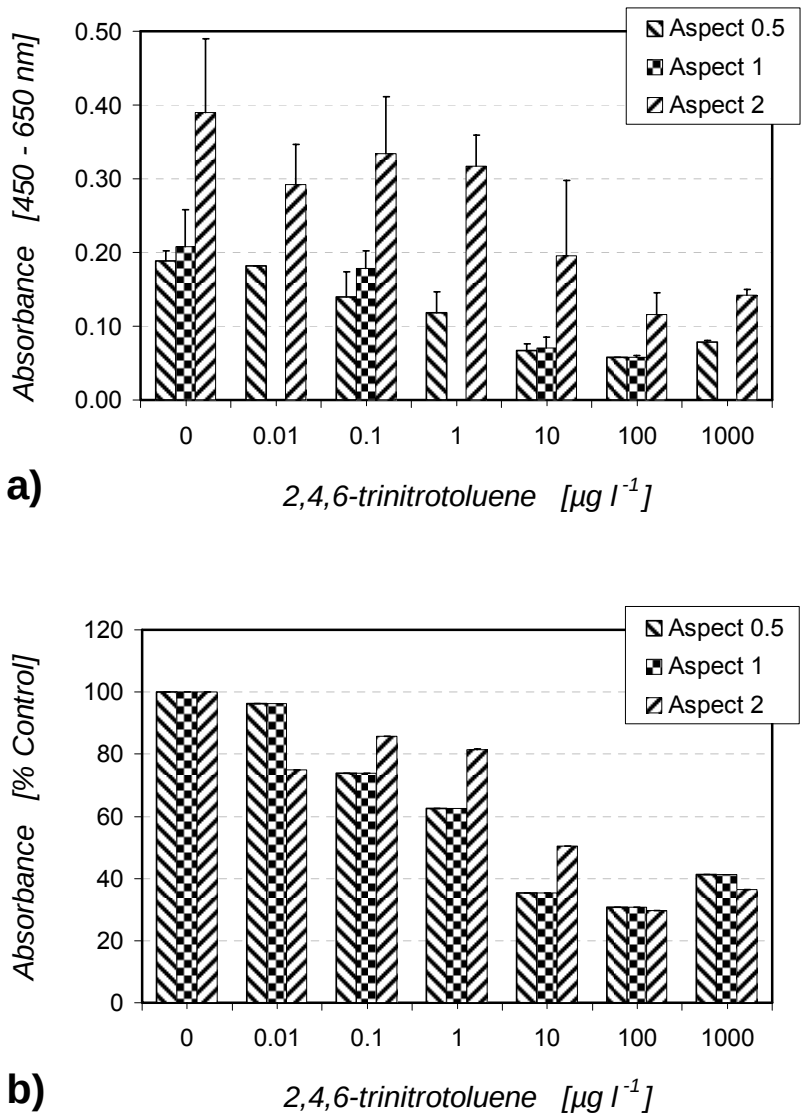

Figure 77. Standard curve with different structure aspects (n = 2), obtained with TNT batch ELISA in glass vials, blocking step with skimmed milk powder (1% (w/v), 1h at RT) in PBST 4 mM, applied after antibody immobilization. The amount of incubated antibody is 0.53 µg / structure (Ab solution: 530 µg l^{-1}, 1 ml / structure). The dilution of the applied Tr was 1: 4,000. Unspecific binding is still high, but more with taller pyramids (aspect 2). In small (structure aspect 0.5) and intermediate (structure aspect 1) pyramids, the unspecific signal is high but more predictable.

The effect of the blocking with solutions of proteins was correlated with the surface geometry of the structures, i.e. the height of the pyramids. Thus the most effective BSA concentration was 1% (w/v), but its efficiency was negatively correlated with the height of the pyramids (figs. 78 and 79). We explain this correlation by the influence of two aspects: higher total surface structures with taller pyramids (structure aspect 2); and the less effective washing associated (via surface geometry) with taller pyramids.

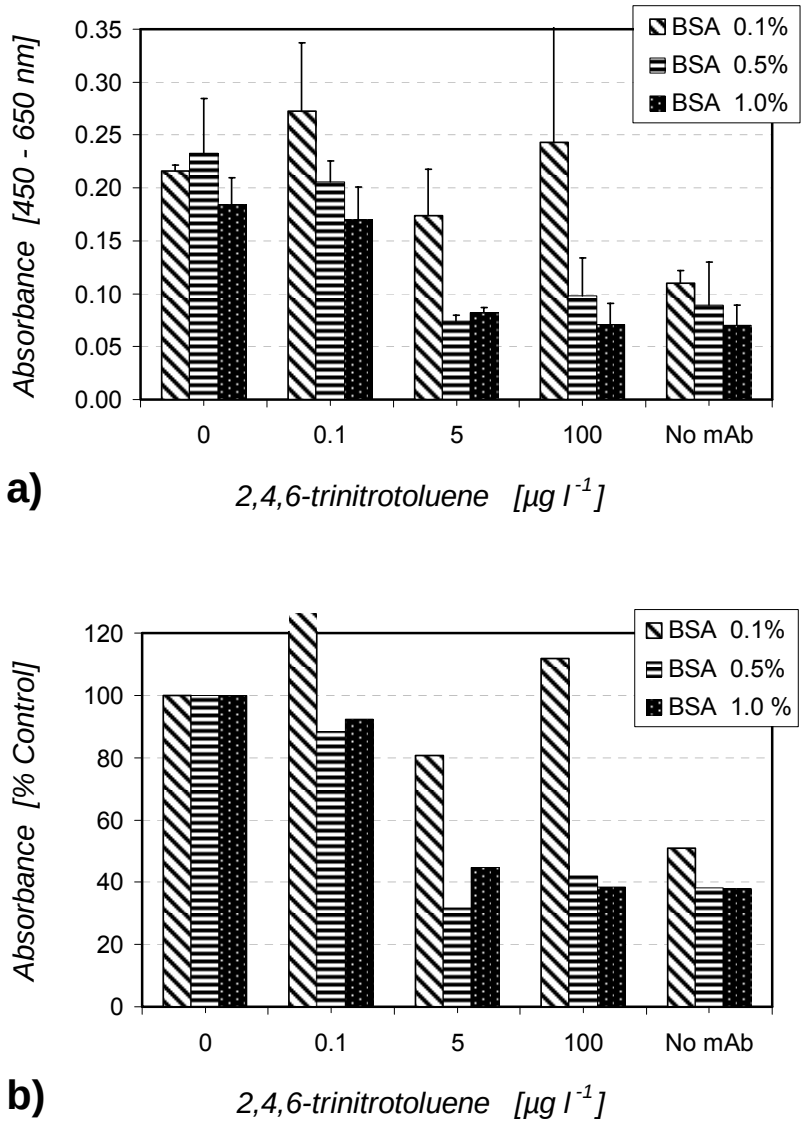

Figure 78. Standard curve (n = 3), obtained with TNT batch ELISA on small pyramids (structure aspect 0.5), with three different BSA concentrations in mAb solution. The amount of incubated antibody was low 0.091 µg / structure (Ab solution: 91 µg l^{-1}, 1 ml / structure). The dilution of the applied Tr was 1: 2,000. The signal pattern indicates that unspecific binding is lower with the higher BSA concentration.

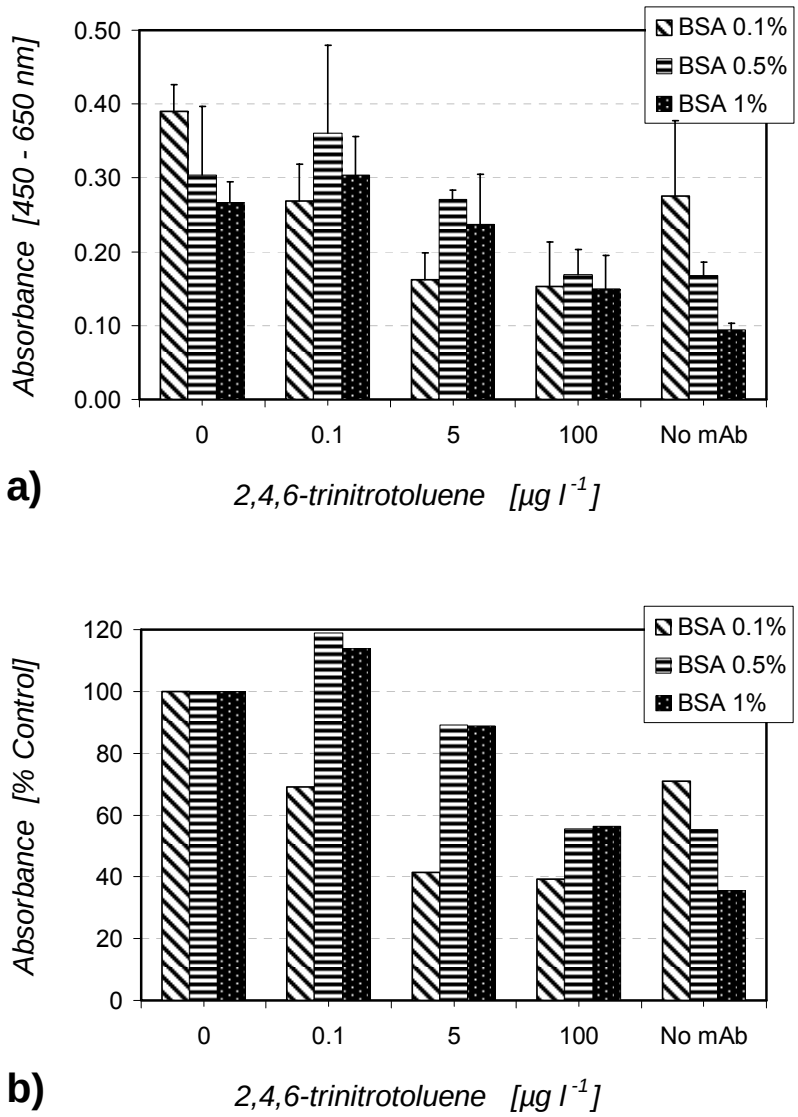

Figure 79. Standard curve (n = 3), obtained with TNT batch ELISA on tall pyramids (structure aspect 2), with three different BSA concentrations in mAb solution. The amount of incubated antibody was low 0.091 µg / structure (Ab solution: 91 µg l^{-1}, 1 ml / structure). The dilution of the applied Tr was 1: 2,000. The signal pattern indicates that unspecific binding is lower with the higher BSA concentration, and higher than with squat pyramids (structure aspect 0.5).

The same 1% (w/v) concentration was effective for casein, but more with small pyramids (structure aspect 0.5) (fig. 80).

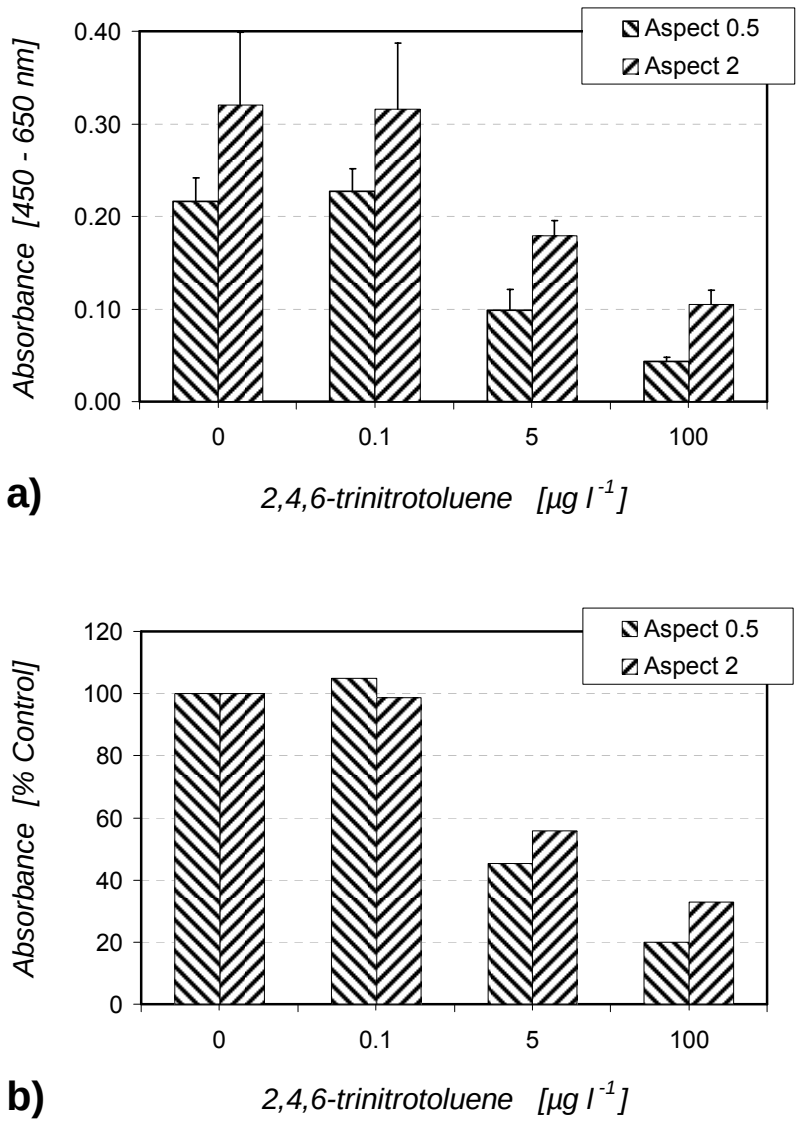

Figure 80. Standard curve (n = 4), obtained with TNT batch ELISA on small pyramids (structure aspect 0.5) and taller pyramids (structure aspect 2), with 1% Casein in a separate incubation step after the mAb immobilization step. The amount of incubated antibody was low 0.091 µg / structure (Ab solution: 91 µg l^{-1}, 1 ml / structure). The dilution of the applied Tr was 1: 2,000. The signal pattern indicates that unspecific binding is lower with small pyramids (structure aspect 0.5).

Besides blocking steps with proteins as blockers, the surfactant Tween 20 was also required in the washing buffer (fig. 81), just as in the microtiter plate format. In addition, when 4mM PBS (no Tween 20) was used instead of 4 mM PBST, we observed that the unspecific signal produced by the binding to the glass walls of the vials, in which the structures were incubated (one structure per glass vial), was negligible (fig. 82). Again, it was observed that unspecific signal was stronger with the taller pyramids (structure aspect 2). The last curve discussed above also reflects the tendency of the signal to be higher at

the highest An concentrations. We observed this phenomenon quite often during our development and, as it is visible on the graph, this effect is stronger when unspecific binding of the curve is high.

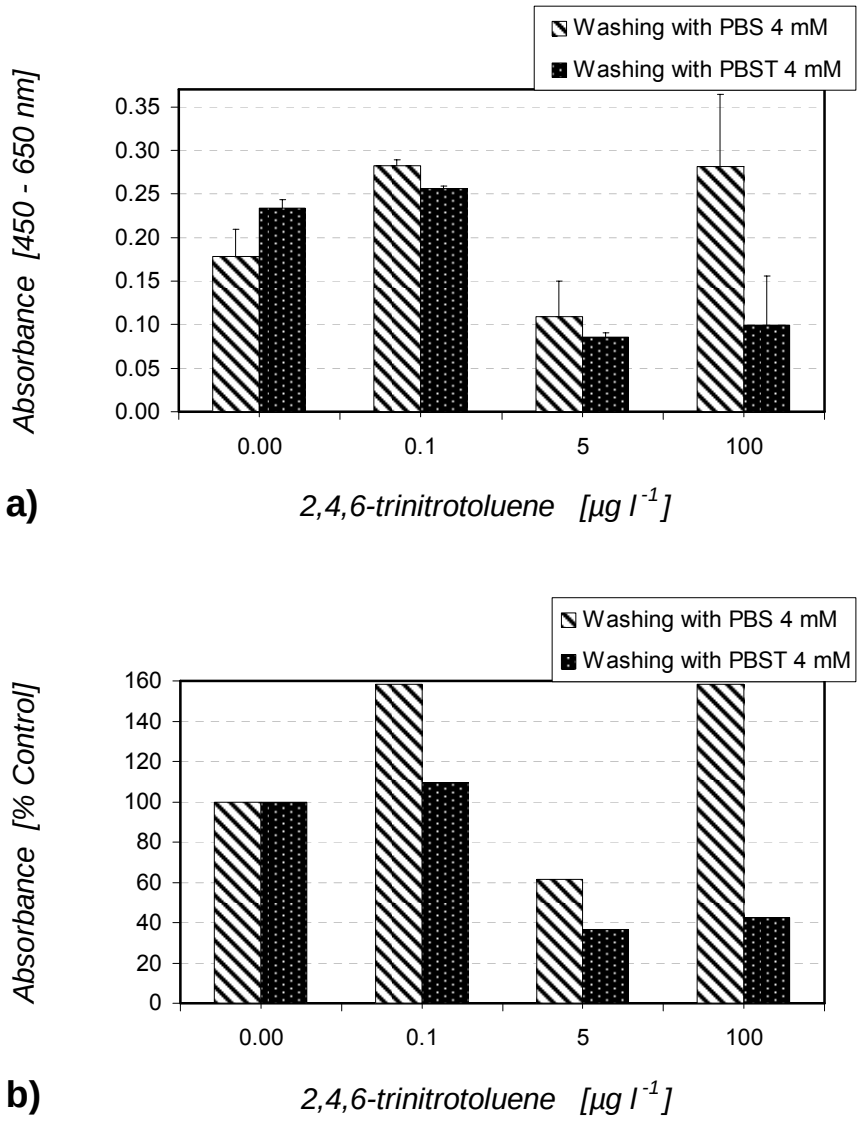

Figure 81. Standard curve (n = 2), obtained with TNT batch ELISA on taller pyramids (structure aspect 2), with 4 mM PBS / 4 mM PBST as washing buffers. The amount of incubated antibody was low 0.091 µg / structure (Ab solution: 91 µg l^{-1}, 1 ml / structure). The dilution of the applied Tr was 1: 2,000. The signal pattern indicates that unspecific binding is higher when the washing buffer does not contain Tween 20.

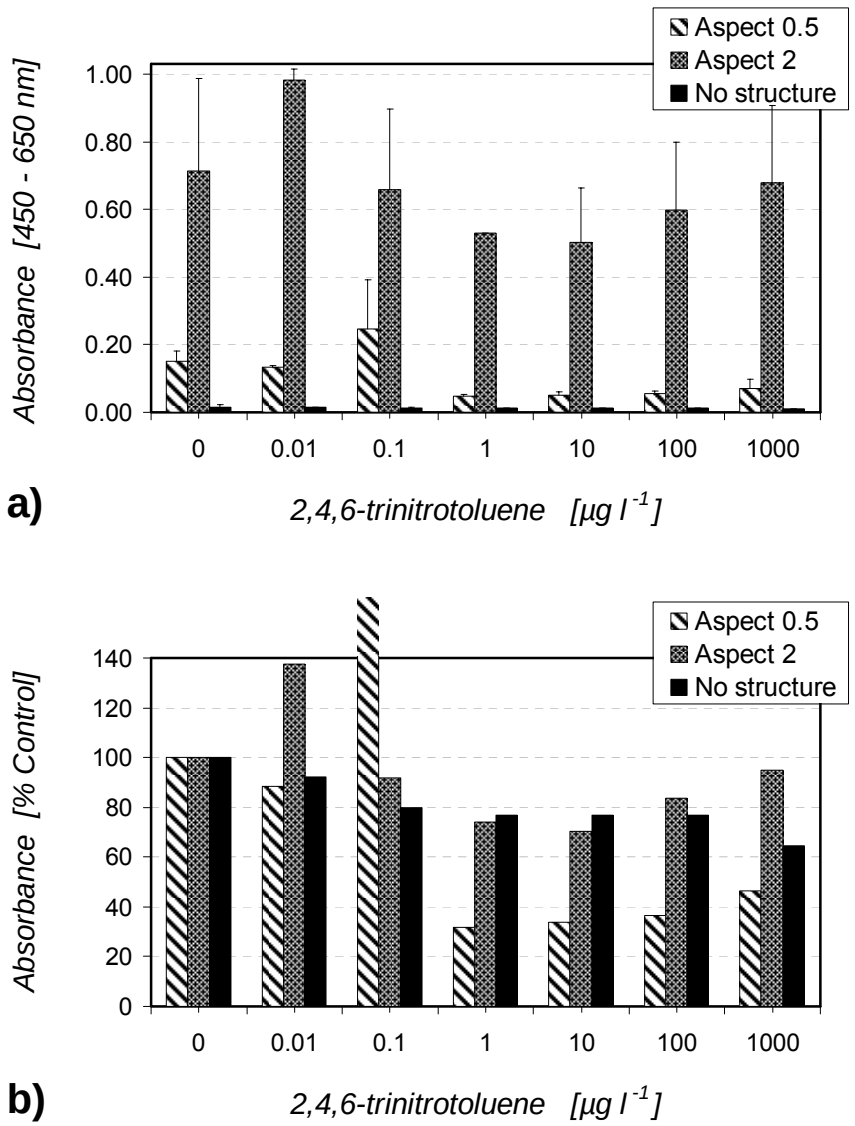

Figure 82. Standard curve (n = 2), obtained with TNT batch ELISA on taller pyramids (structure aspect 2), with 4 mM PBS as washing buffer. The amount of incubated antibody was low 0.091 µg / structure (Ab solution: 91 µg l^{-1}, 1 ml / structure). The dilution of the applied Tr was 1: 2,000. The signal pattern indicates that (1) unspecific binding is very high when the washing buffer does not contain Tween 20; that (2) the signal due to the glass vials is neglectable; and that (3) there is tendency that the unspecific binding increases with the highest An concentrations at the tail of the standard curve.

The mechanisms of unspecific binding are still in debate, as well as the blocking mechanism by proteins and surfactants. In principle there are two different possible causes (Schneider et al., 1995). In the first case, unspecific signal is due to unspecific binding of the Tr to the patches of the solid phase that are not occupied by antibodies; therefore, the blocker protein molecules are just filling in these patches before the Tr molecules would do it; independently, a surfactant is modifying the electrostatic properties of the surface.

In the second case, a small percent of the Tr (or An) molecules would bind, by weak forces (like the van der Waal interactions) to other portions of the antibody molecules than the specific recognition site. In this case, the protein blockers would spatially block the access of the Tr to the bulk of the antibody molecules; surfactants influence the unspecific Ab - Ag interactions by modifying the electrostatic properties at the surface of the antibody and Tr molecule.

In batch ELISA, blocking both with proteins and surfactant was required.

Regarding the flexibility of the batch ELISA, with the TNT assay, two aspects are remarkable. First, a moderate low dose hook was sometime visible in along the optimization of batch ELISA (fig. 83). Second, the antibody could be incubated either 2h or 10 min (fig. 84).

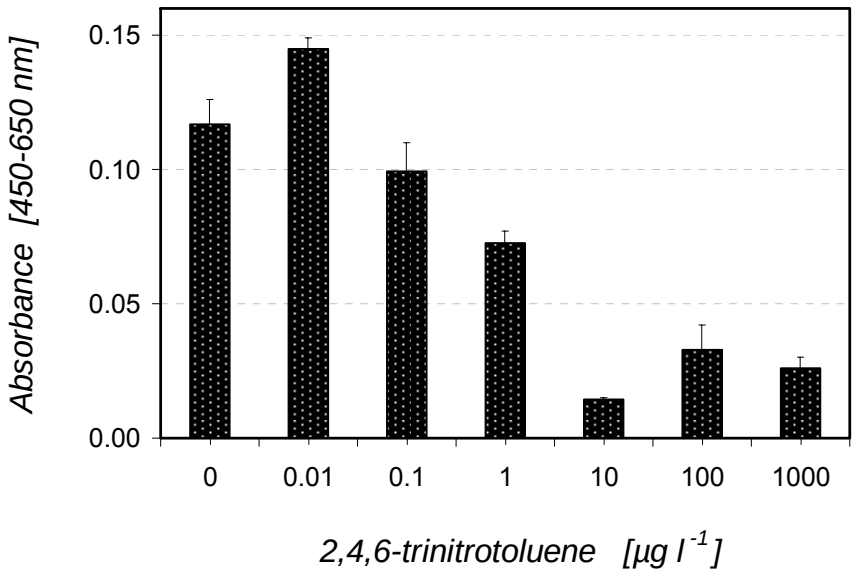

Figure 83. Low dose hook (n = 2) obtained in TNT batch ELISA optimizations (here taller pyramids - structure aspect 2). The amount of incubated antibody was low 0.091 µg / structure (Ab solution: 91 µg l^{-1}, 1 ml / structure). The dilution of the applied Tr was 1: 2,000.

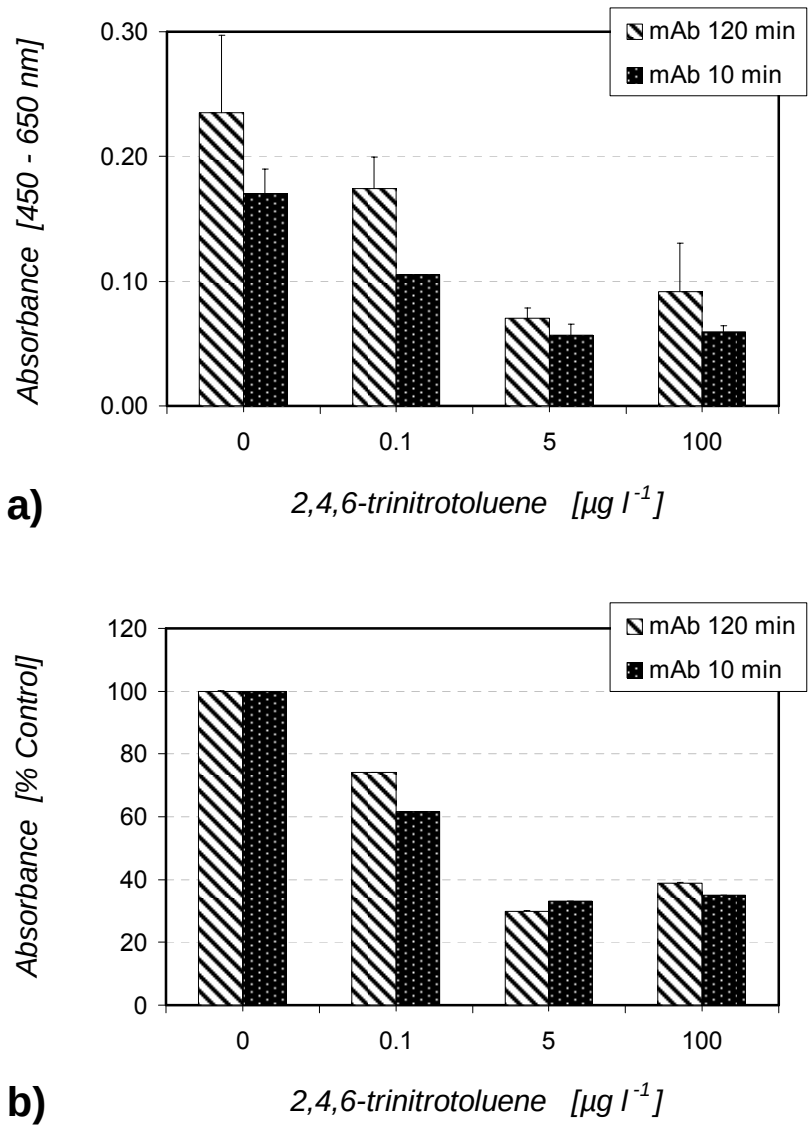

Figure 84. Standard curve (n = 2), obtained with TNT batch ELISA on taller pyramids (structure aspect 2), with 120 min / 10 min antibody (anti-TNT) incubation time. The amount of incubated antibody was low 0.091 µg / structure (Ab solution: 91 µg l^{-1}, 1 ml / structure). The dilution of the applied Tr was 1: 2,000. The signal pattern indicates that 10 min antibody incubation time can be safely applied instead of 120 min.

In the end, all experiments with batch ELISA revealed that among the three pyramid types, the best results were obtained with the intermediate pyramid structures (aspect 1). This structure aspect was further used for batch ELISA for other An integrated into the exchangeable chip of the sensor platform.

Batch TNT-ELISA with covalently immobilized Protein A/G

Immobilization of the catching molecule Protein A/G to the golden surface by covalent attachment to a SAM of MPA was explored during the immunosensor development (method in sub-chapter 2.3.2.2.) The pilot results obtained with this method are presented and compared with the results obtained in parallel with the Protein A/G's adsorption method.

In fig. 85, the signal pattern suggests that covalent attachment of Protein A/G through the described method is possible. Although the number of measurements was limited by the number of golden structure that were available, an inhibition curve should be possible with covalent attachment at least as good as it is possible with adsorption. However, the results obtained with the first measurements could not be maintained from one day to another, because the attained signal decreased very much with the next measurements.

With repeated covalent binding, on fresh golden structures, the initial result was reproduced with the "new" structures but not with the "old" ones (fig. 86). This situation is probably due to the fast degradation of the thioalcane monolayer because of the high temperatures. The amount of incubated antibody was low (Ab solution: 1,060 ng ml^{-1}, 1 ml / structure). The dilution of the applied Tr was 1: 2,000.

As it happens, the discussed experiments were carried out in normal light conditions, at RT (which at that (summer) time mounted 30°C). SAMs tend to be more stable at lower temperatures, but are still stable in air until more than 100°C (Sung and Kim, 2001) but light may render them unstable (Dijksma, 2001).

In principle, stability of SAMs arises from the structure and the pre-treatment of the metal surface (gold, silver or copper), on the solubility of SAM molecules in the reagent (buffer) solution, and of the Van der Waals interactions between these molecules (Dijksma, 2001).

Under certain conditions, thioalcane SAMs form domains (patches) (Suo et al., 2004). With short chain thioalcanes like 3-mercaptopropionic acid (MPA), the surface geometry of the gold layer is critical, the thioalcane molecules being within the dimension range of the surface roughness (e.g. crevices of humps), so that the reactive tail of the thioalcane molecules may be underexposed to covalent binding (Gooding et al., 2001).

Within the thioalcane family, properties vary much with the alkyl chain and the tail group. The van der Waals interactions depend on the length of the alkyl chain and the degree of branching. Recent studies suggest that stability of SAM is higher with longer and less branched chains of thioalcane molecules, and that stability decreases with higher thioalcane solubility in the reagent solution, and in the presence of light (within 0.5 - 2 days) (Dijksma, 2001; Sung and Kim, 2001).

In addition, for biosensors, the covalent immobilization of immunoreagents to the solid surface is a critical aspect, during and after the formation of SAMs, because of possible unexpected (and undesired) interactions between chemicals and solvents and the plastics of the sensor.

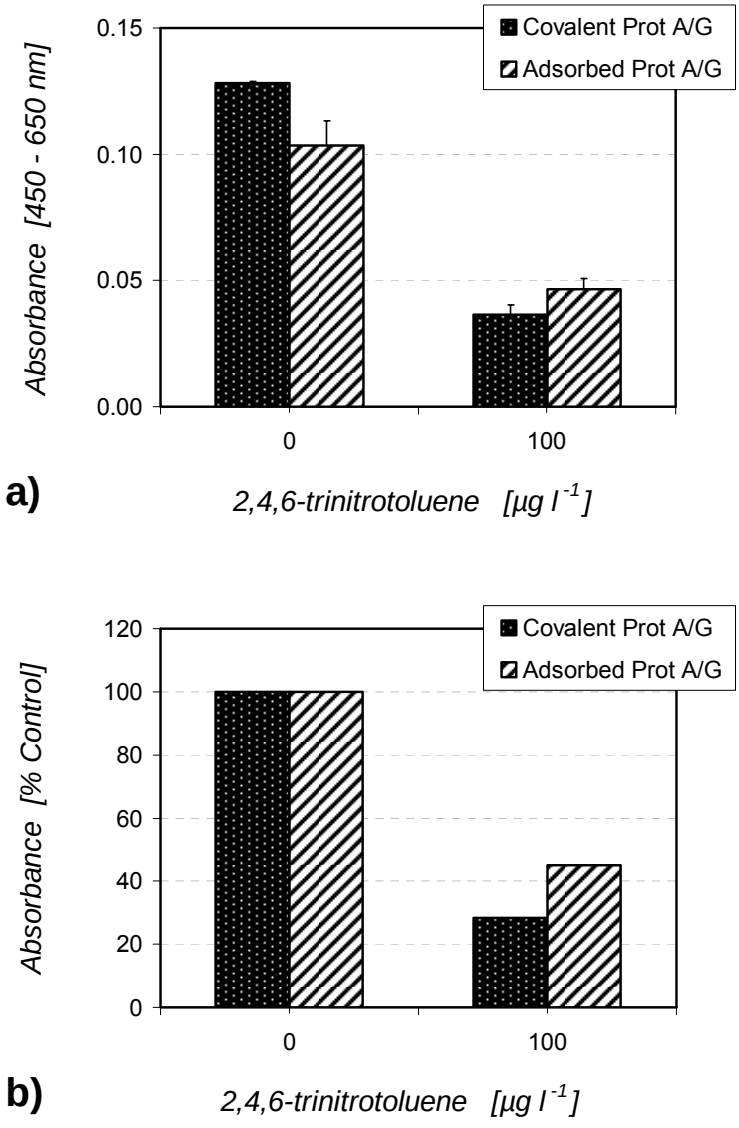

Figure 85. Inhibition pattern (n = 2), obtained with TNT batch ELISA on the same golden structure type that was applied in the biosensors chip, with covalent attachment vs. physical adsorption of Protein A/G. The signal pattern suggests that Protein A/G may be immobilized by covalent attachment as well as by adsorption.

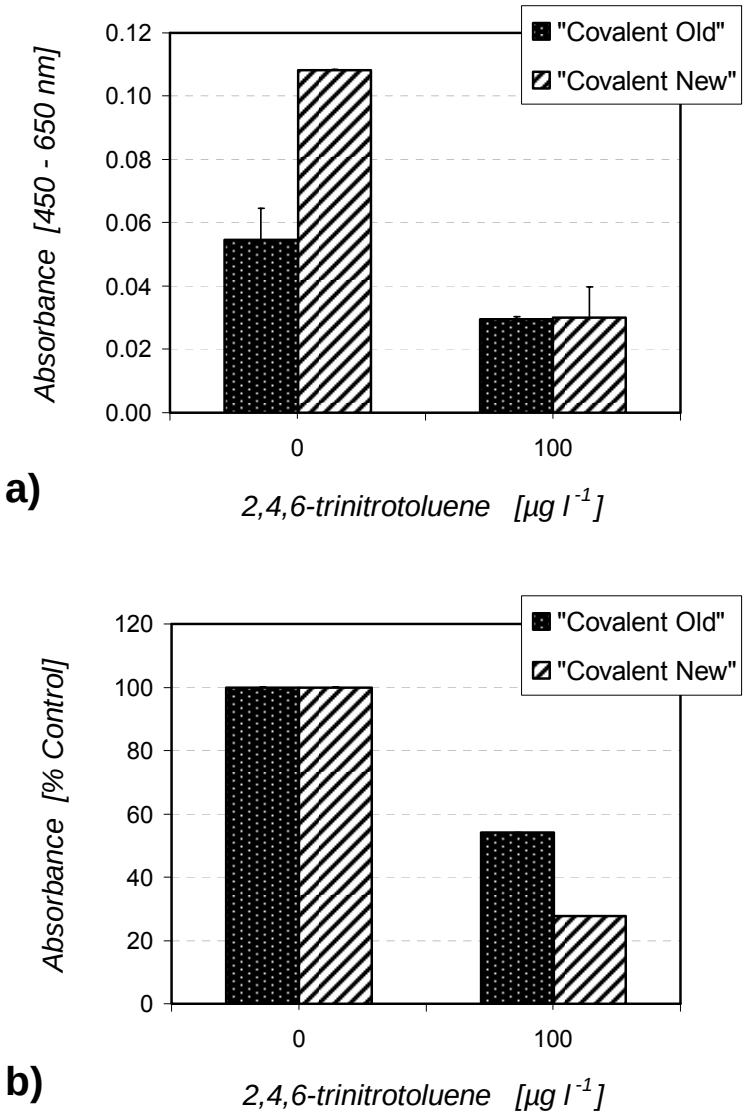

Figure 86. Comparison between the inhibition patterns obtained with TNT batch ELISA (n = 2) by the golden structures onto which Protein A/G was covalently attached anew ("new covalent") and two days earlier ("old covalent"; fig. 83).

For these reasons, future developments with our immunosensor platform should use longer-chain thioalcanes (12-20 methylene units), like ω-mercapto-hexadecanoic acid instead of 3-mercapto-propanoic acid (MPA), with protection from light as much as possible. In addition, the thioalcanes that are least soluble in the experimental buffer (at given pHs) should be preferred. Beside these, silver and copper should be considered as alternative to gold, SAM having also protective effect against copper corrosion (Sung and Kim, 2001).

The fact that high quality SAMs can also control surface properties, e.g. adhesion and wetting (Suo and Kim, 2001), suggest that it can be a barrier against unspecific binding (adsorption) of Tr molecules to the assays solid phase. Basically, the literature indicates

that for well-ordered defect-free SAMs, adsorption times of minimum 15 hours are necessary (Engquist, 1996).

Recently, Lee and collaborators showed that catching proteins (in their case Protein A) can be immobilized in the form of SAMs on a gold surface, without the intermediation of thioalcanes. This was done via modification of Protein A with the thiol (-SH) functional group and subsequent adsorption of the thiol group to the gold (Lee et al., 2003).

Similarly, Fab fragments can be directly and orderly adsorbed to gold through the thiol groups obtained during the Fab preparation by the reduction of the disulfide bonds of the hinge region of the digested Fc fragments (Brogan et al., 2003).

Beside the thioalcane mediated immobilization, SAMs of Protein A/G and other catching proteins, antibodies or antibody fragments represent promising options for future immobilization studies directed towards various immunosensor applications.

4.3.3. Optimized batch ELISA with TNT, atrazine and diuron

Batch ELISA was essential for the biosensor development, because it represented the intermediary step for the transfer of immunochemicals from the microtiter plate to the biosensor platform. The isolated golden structures were kept in glass vials (one structure per vial), and all manipulation was performed with greatest care, to avoid structures' damage or/and contamination.

Batch ELISA involved a lot of manual handling, because no automatic manipulation was possible, like with the microtiter plate or with the sensor platform. For example, automated washing could not be employed, so all washing steps were done by hand, with single-use syringes (for reagent addition) and Pasteur pipettes for reagents' and washing buffer's removal from the glass vials. Similarly, the incubated substrate was transferred from each vial to a corresponding well of a microtiter plate prior to stopping with H_2SO_4 and reading with the absorbance reader. Otherwise, (1) the OD could not be read, and (2) the structures would have been destroyed in the presence of H_2SO_4.

Nonetheless, the sensor manufacturer (IMM Mainz) could produce only a limited amount of golden structures for batch ELISA and for the disposable chip, because of the high costs.

After testing with the TNT assays, out of the three structure types, one has been chosen for final integration in the sensor prototype, more precisely in the disposable chip. This was the structure carrying pyramids of intermediary height (aspect 1).

Batch ELISA with this structure type allowed producing standard curves with good parameters, especially very good sensitivities (fig. 87). Thus, achieved IC_{50}s were: 0.2 µg l^{-1}

with TNT, 2.1 µg l^{-1} with diuron and 0.3 µg l^{-1} with atrazine. These assays could in the end be transferred to the biosensor platform (sub-chapter 4.4.).

A great measure of the flexibility of the developed sensor platform is the fact that several different catching protein/antibody could be employed. These were goat anti-mouse for the monoclonal antibodies against TNT, atrazine and diuron; Protein A/G for the monoclonal antibodies against TNT; and TIB 172 for isoproturon and for the newly developed antibodies against nitroaromatics (Krämer et al., 2004b).

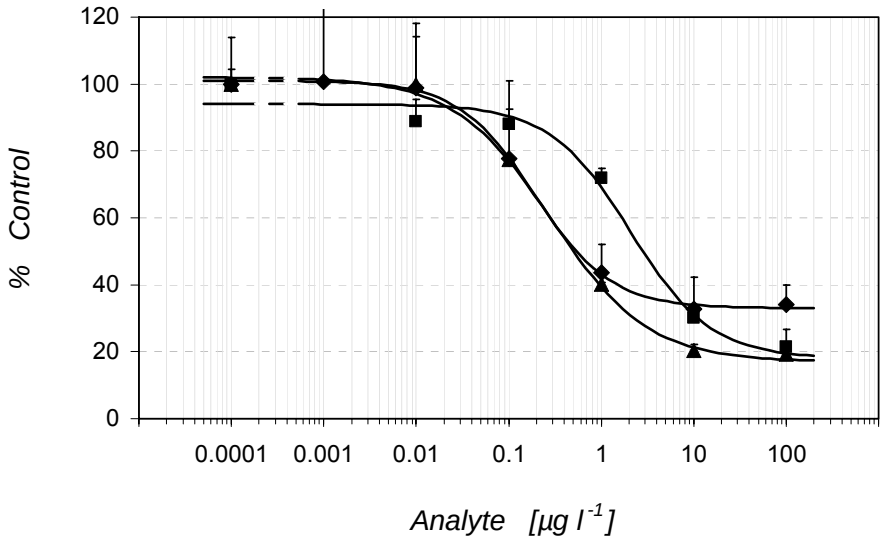

Figure 87. Standard curves for TNT, diuron and atrazine, produced with batch ELISA. Standards and Tr (both in 40 mM PBS) were incubated together. The zero dose is represented as 0.0001 µg l^{-1} and separated from the first real concentration by an interrupted line. The standard curves were fitted according to the 4-parameter equation (eq. 6) with the following values obtained for the curve parameters:

(◆) TNT (n = 9): A = 101; B = 1.05; C = 0.2 µg l^{-1}; D = 33; DL (IC_{20}) = ca. 0.1 µg l^{-1};
(■) diuron (n = 3): A = 94; B = 1.00; C = 2.1 µg l^{-1}; D = 18; DL (IC_{20}) = ca. 0.5 µg l^{-1};
(▲) atrazine (n = 3): A = 102; B = 0.83; C = 0.3 µg l^{-1}; D = 17; DL (IC_{20}) = ca. 0.1 µg l^{-1}.

4.3.4. Batch ELISA developments with isoproturon

The isoproturon assay on microtiter plates proved to be more sensitive when isoproturon was pre-incubated (up to 1 hour at RT) prior to the addition and incubation (30 min at RT) of the Tr (Krämer 2004a). As longer incubation times are not suitable for an immunosensor platform, we compared the inhibition curves obtained with 1h / no An pre-incubation (fig. 88).

The result obtained with no An pre-incubation indicated, as expected, a lower sensitivity. As in TNT batch ELISA, 1% (w/v) milk powder (separate incubation step of 30 min at RT, after antibody incubation step) was an effective blocker.

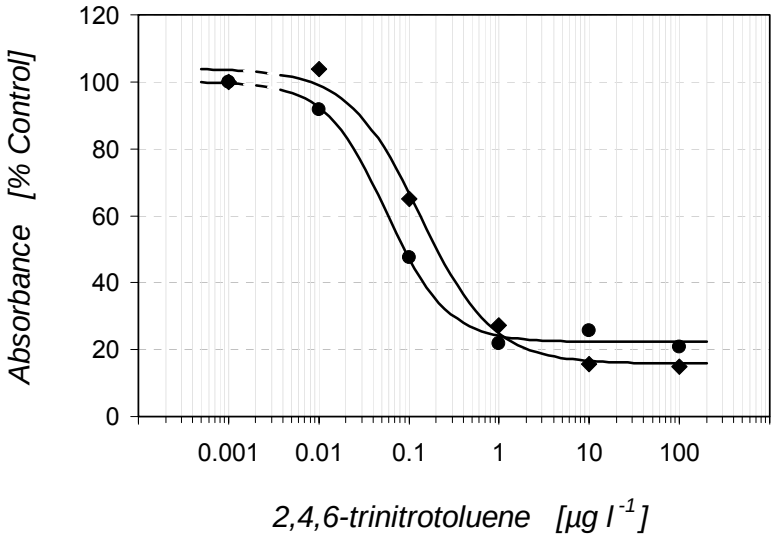

Figure 88. Standard curves (n = 3), obtained with isoproturon batch ELISA on the golden structure type (structure aspect 1) that was employed in the sensor), with 1h / no An pre-incubation time. The amount of incubated anti-isoproturon antibody was 0.75 µg / structure (Ab solution: 750 µg l^{-1}, 1 ml / structure). The dilution of the applied Tr was 1: 200. The zero dose is represented as 0.0001 µg l^{-1} and separated from the first real concentration by an interrupted line. The standard curves were fitted with to the 4-parameter equation (eq. 6) with the following values obtained for the curve parameters (n =2):

(●) 1h pre-incubation: A = 100; B = 1.28; C (IC_{50}) = 0.06 µg l^{-1}; D = 22; R^2 = 0.997;

(◆) no pre-incubation: A = 104; B = 1.08; C (IC_{50}) = 0.13 µg l^{-1}; D = 16; R^2 = 0.994.

The isoproturon batch ELISA reflected well the importance of the washing steps on such a peculiar surface geometry as employed in the herein described development. Thus, washing 2 times (with 4 mM PBST; 1ml / vial) was not sufficient; 3 times was necessary and sufficient (fig. 89).

The signal pattern indicates the An pre-incubation time is not necessary (for only little sensitivity was lost), and even more recommendable (because of higher signal and lower background).

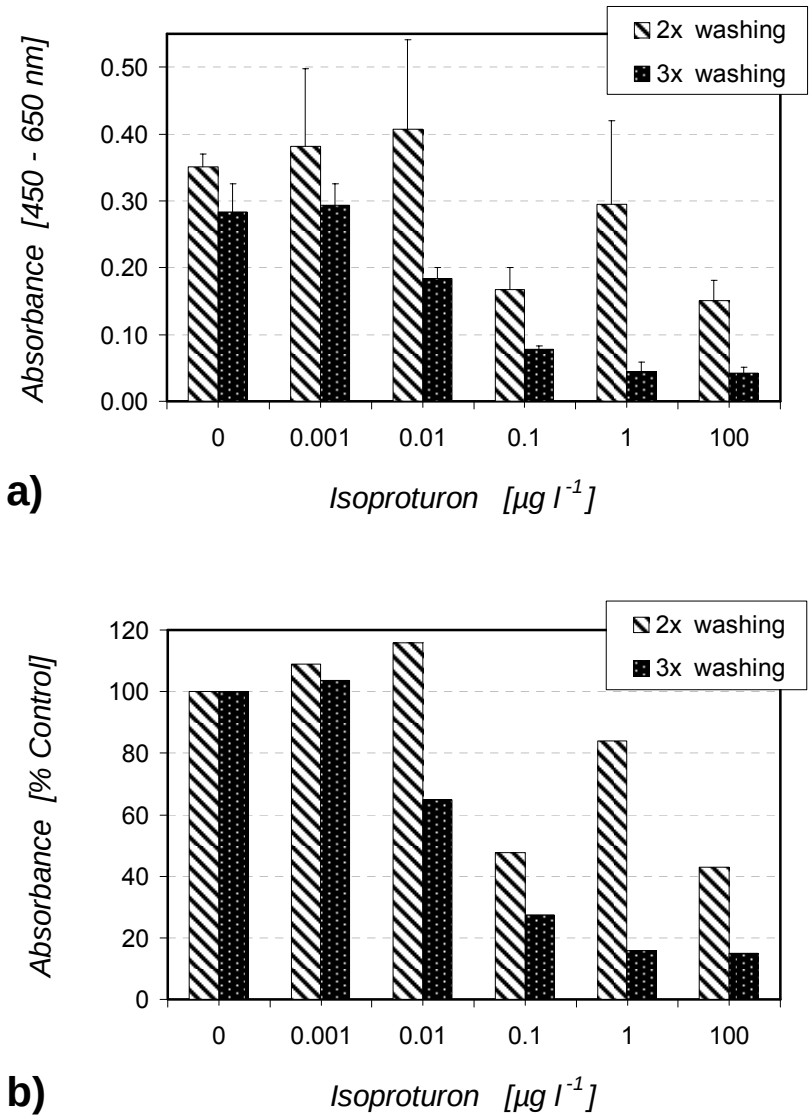

Figure 89. Standard curves (n = 3), obtained with isoproturon batch ELISA on the golden structure type (structure aspect 1) that was employed in the sensor, with 2x / 3x washing (with 4 mM PBST, 1ml/ vial). The amount of incubated anti-isoproturon antibody was 0.75 µg / structure (Ab solution: 750 µg l^{-1}, 1 ml / structure). The dilution of the applied Tr was 1: 200. The signal pattern indicates that 3x washing is necessary and enough for efficient washing of the golden surface of the structures.

4.3.5. Troubleshooting with batch ELISA

In comparison with ELISAs on microtiter plates, with the batch ELISA the principal troubles were: higher unspecific binding of the Tr, poorer and unequal washing, and higher standard deviations.

Higher unspecific binding of Tr molecules is due to the strong binding of proteins to gold surfaces, through physical adsorption. While this property of proteins is welcome for coating proteins and antibodies, it is not desired with Tr. For this reason, efficient blocking is necessary. Albeit, there will always be a minimal unspecific binding, hence a higher background (ca. 15 - 30 % of the specific signal, unlike the usual 1% or so on microtiter plates).

We achieved satisfactory blocking with blocker proteins like bovine serum albumin (BSA), casein and skimmed milk powder. The best was the 1% (w/v) solution of skimmed milk powder in 40 mM PBS, applied as a separate incubation step (10 – 30 min, sometimes up to 60 min) after the step of immobilization of the specific antibody.

4.4. Competitive immunoassays using the immunosensor prototype

4.4.1. Probing measurements with prototypes (demonstrators)

4.4.1.1. General remarks on measuring with the sensor

In principle, the laboratory prototype (with no temperature regulation) was used for explorations and optimizations, and the field prototype (with temperature control system) was employed especially for optimizations.

Two competition formats, with many variations were explored with on-line measurements with the laboratory prototypes (fig. 90): a) sequential incubation of An and Tr *(antigens displacement format) – sequential saturation analysis*, and b) simultaneous incubation of An and Tr *(antigens mixing format) – competitive saturation analysis*, which presupposed on-line mixing (2 volumes An to one volume Tr).

Given the differences in the experimental formats of the biosensor platform as compared to the plate and batch experimental formats, the transfer of the immunochemicals onto the sensor prototypes required still many routine and low-rewarding technical issues.

While running, the lid of the temperature-controlled part must be on, while the instrument is being controlled through the touch-screen interface.

At this proof of principle stage, a set of 10 chips could be measured within one day. One set was first tested for equal binding, and then the set was prepared (each chip the same way, manually performed ELISA steps) for measurement and stored in the freezer overnight. The next morning, each chip was allowed to come first to 4°C (15 min), then to RT (10 min) before starting the measurements.

Figure 90. Scheme of the experimental steps needed for measuring with the sensor prototype. Selected examples (TNT 100 µg/L, chip volumes) with sequential saturation analysis format (A) (results in figs. 91 and 92) and competitive saturation analysis format (B) (results from fig. 94 on, and with the proof of principle).

A)	**sequential saturation analysis**		**25-Aug-03**
overnight	**Protein A/G incubation**	**Adsorption 1: 500 (in Carb. Buffer 50 mM)**	**off-line; 3°C**
60 min	**Anti-TNT mAb incubation**	**1: 1,000 (in PBS 40 mM)**	**off-line; 20°C**
30 min	**Milk powder 1% (w/v) incubation**	**(in PBS 40 mM)**	**off-line; 20°C**
2 min	**Analyte pumping**	**conc. (PBS)**	**on-line**
3 min	**Analyte incubation**		
20 s	**Analyte pumping**		
3 min	**Analyte incubation**		
20 s	**Tracer pumping**	**1: 4,000 (PBS)**	
300 s	**Tracer incubation**		
2 min	**Washing (PBST 4 mM)**		
30 s **60 s**	**Substrate pumping** **Substrate incubation**	**Read at RT 19-20°C**	
3 min	**Washing (PBST 4 mM)**		
3 min	**Washing via V2-V6 (PBST 4 mM)**		**on-line**

B)	**competitive saturation analysis**		19-Aug-03
overnight	**Protein A/G incubation**	**Adsorption 1: 1,000** (in Carb. Buffer 50 mM)	**off-line; 3°C**
60 min	**Anti-TNT mAb incubation**	**1: 1,000** (in PBS 40 mM)	**off-line; 20°C**
30 min	**Milk powder 1% (w/v) incubation**	(in PBS 40 mM)	**off-line; 20°C**
2 min	**Analyte pumping**	**Via V2-V5**	**on-line;**
1 s	**Tracer pumping**	**1: 6,000** (PBS)	
2 s	**Analyte pumping**	**Via V2-V4**	
Previous two steps repeated 19 times			
10 min	**Analyte/Tr Incubation**		
2x3 min	**Washing (PBST 4 mM)**		
25 s **60 s**	**Substrate pumping** **Substrate incubation**	**Read at 20°C**	
3 min	**Washing (PBST 4 mM)**		
3 min	**Washing via V2-V6** (PBST 4 mM)		**on-line**

Immediately before inserting the chip onto the sensor and start of the measurement, the chip was prepared, using plastic syringes: the incubation/measurement cell was flushed with washing buffer, and the tracer reservoir (the meander) was filled with Tr solution.

After inserting the chip onto the ground-plate of the sensor, the sample reservoir, the temperature-controlled part is closed, and the automated, computer-controlled sequence of steps is started. During this time the sensor parameters and performed stages are supervised by the operator though the touch screen interface.

4.4.1.2. Measurements

As anticipated to a certain extent by the results obtained on microtiter plates, with the sequential saturation format, the inhibition was poor if any, both with the laboratory prototype (fig. 91) and the field prototype (fig. 92).

In the optimization trials with the displacement format, the inhibition became slightly visible when the TNT incubation step was repeated 3 times, but it was still too weak. Therefore, mixing the Tr with the standard/sample could not be avoided. Sometime, encouraging results were obtained also with the sequential format, so that with a next generation of sensors, better results are envisioned.

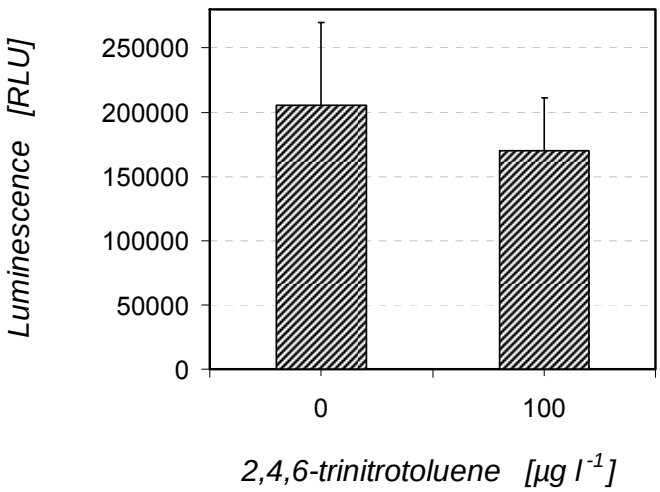

Figure 91. Typically, the inhibition obtained by on-line measurements (n = 3) with the <u>laboratory prototype</u> was very poor, if at all, with the mixing antigen format. In this format the An was incubated first (to allow it bind to the immobilized antibody in the incubation/measurement cell on the exchangeable chip), and the Tr was incubated afterwards, theoretically to bind to the recognition sites left free on the antibody. Additional experimental conditions: blocking step with milk powder 1%; Tr dilution 1: 2,000; antigens incubation 5 min; RT 21°C.

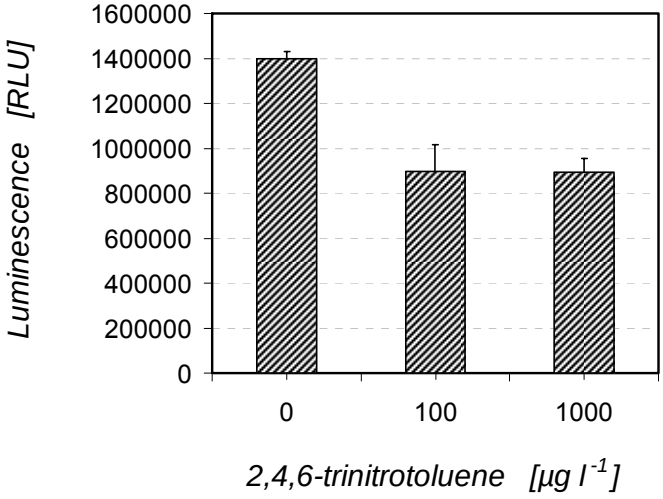

Figure 92. Typically, the inhibition obtained by on-line measurements (n = 2) with the <u>field prototype</u> was very poor, if at all, with the sequential saturation format. In this format the An was incubated first (to allow binding to the immobilized antibody in the incubation /measurement cell on the exchangeable chip), and the Tr was incubated afterwards, theoretically to bind to the recognition sites left free on the antibody. Additional experimental conditions: no blocking; An incubation 3 x 5 min in a row; Tr (1: 25,000) incubation 1 min.

The antigen mixing format needed also many trials and tests before good inhibition could be obtained. In order to check whether the initial lack of inhibition is due to biochemical or to purely technical factors we performed the TNT assay on pairs of sensor chips, but off-line. The only exception was the on-line application of the luminescence signal and the signal reading. We repeated this procedure 4 days in a row, with a zero dose and a TNT concentration of 100 µg l^{-1}.

The result was concluding: 4 times in a row, very good inhibition was possible (fig. 93). The inhibited signal represented less than 10% of the zero dose, in all cases.

These experiments were carried with the final version of the chip, but also with chips in which the volume of the incubation/measurement cell above the golden structure was about 10 times larger.

With the higher volume chips, both the surface to volume ratio and the flow pattern were changed. With high volume chips, inhibition was only slightly weaker.

Thus we established that the biochemistry of the TNT-ELISA works on the chip of the sensor.

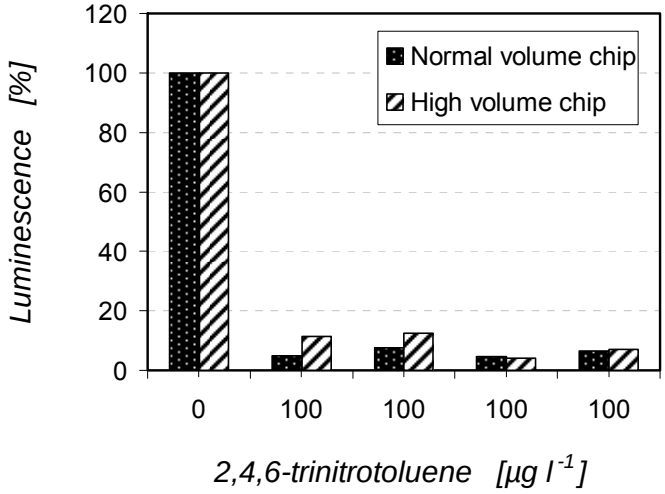

Figure 93. Inhibition obtained with off-line measurements (n = 1), in the mixed antigens format. For each chip type, one pair of chips (zero dose chip and inhibition chip) was measured each day, 4 days in a row. The signal pattern indicates that the involved immunochemical dynamics worked on the sensor chip.

After obtaining inhibition with the off-line TNT assay on the sensor chips, we went to optimizing the experimental conditions for on-line measurements.

With the (adapted) procedure described earlier (fig. 90), good inhibitions were obtained by on-line measurements, with two TNT concentrations: 10 µg l^{-1} (fig. 94) and 100 µg l^{-1} (fig. 95), in each case, with both normal and high volume chips. However, the inhibited signal was higher than with off-line measurements, probably because the washing by hand was stronger (and so more effective) than the on-line washing.

Washing efficiency in the incubation-measuring cell depends on the surface geometry (like with batch ELISA), as well as on the flow rate and duration. In principle, the flow rate can be adjusted by the manufacturer for a value higher than the currently used one of 300 µl s^{-1}. However, higher flow rates are risky, and not essential for our objective.

Higher flow rates are expected to result in different washing pattern, like more turbulent flow, instead of the safer laminar flow. In addition, higher flow rates imply higher sucking pressure of the pump, which may become too high and so cause bubbles to penetrate the system. This phenomenon was confirmed experimentally, when the flow rate was set at 600 µl s^{-1}; no reliable measurements was possible in such conditions (details in the troubleshooting sub-chapter).

Regarding the washing (flow) duration, we observed that 1-3 min should be good enough for obtaining a proof of principle with our experimental prototypes. Again, more flow

optimization would be needed for technical optimizations towards a commercial version of the developed immunosensor prototype.

The practical value of an immunosensor is strongly related to the measuring time. The total measuring time depends on the duration of the automated steps, notably washing steps and incubation steps. Therefore we tested the sensitivity potential of the developed sensor platform with short incubation times, i.e. with 10, 5 and 2 min.

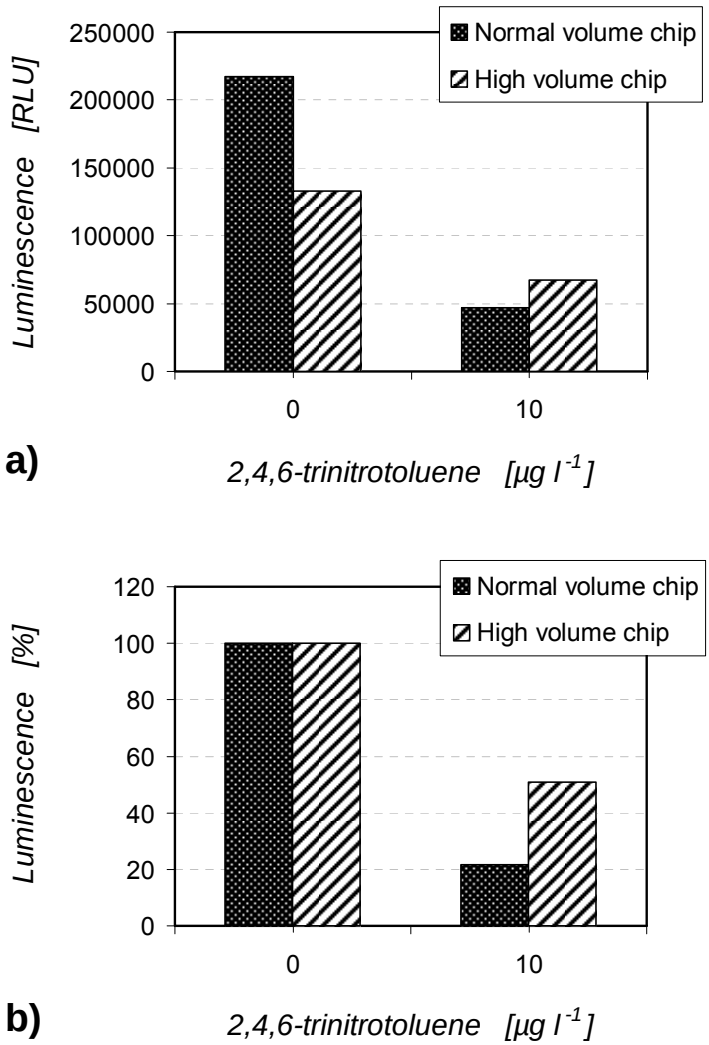

Figure 94. Inhibition obtained with 10 µg l^{-1}, by on-line measurements (n = 1), in the mixed antigens format, with both normal and high volume chips. Dilution of Protein A/G: 1: 1,000. Dilution of Ab: 1: 1,000. Dilution of Tr: 1: 6,000. The signal pattern indicates that the higher volumes chips are less suitable.

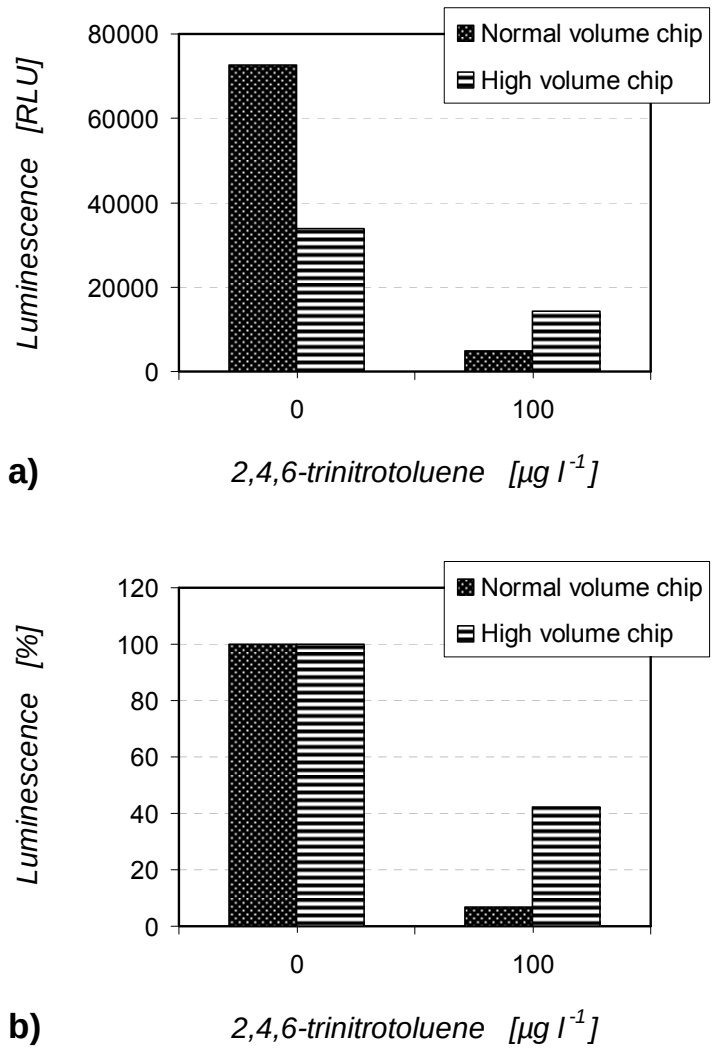

Figure 95. Inhibition obtained with 100 µg l^{-1}, by on-line measurements (n = 1), in the mixed antigens format, with both normal and high volume chips. Dilution of Protein A/G 1: 500. Dilution of Ab: 1: 1,000. Dilution of Tr: 1: 6,000. The signal pattern indicates that the higher volumes chips are less suitable.

In fig. 96, one can observe that inhibition with the used standards (0.1 and 1 µg l^{-1} TNT) decreases significantly with 5 min duration of the step of antigens incubation, when compared with 10 min of incubation. In these measurements, An and Tr were mixed on-line (mixed antigens format), 2 volumes of An (TNT standards) for 1 volume Tr. One volume corresponds to one second pumping at a constant flow rate.

In fig. 97, one can notice that inhibition with 1 µg l^{-1} TNT was possible with 2 minutes incubation time, and this was rather close to the inhibition produced with 5 min incubation time. This suggests that the incubation times may in principle be shortened down to 2 min, with good inhibition.

In fig. 98, one can see that in a sequential saturation format (the An incubated first), inhibition varies with the duration of the Tr incubation; this inhibition is not satisfactory for the biosensor platform.

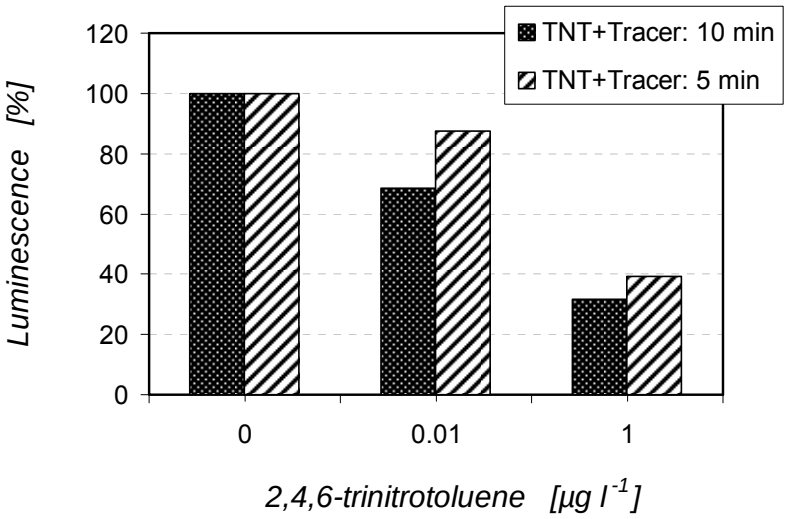

Figure 96. Inhibition obtained with 10 min vs. 5 min duration of the antigens incubation, by on-line measurements (n = 1), in the mixed antigens format. The signal pattern indicates that the 10 min incubation results in better inhibition, hence higher sensitivity.

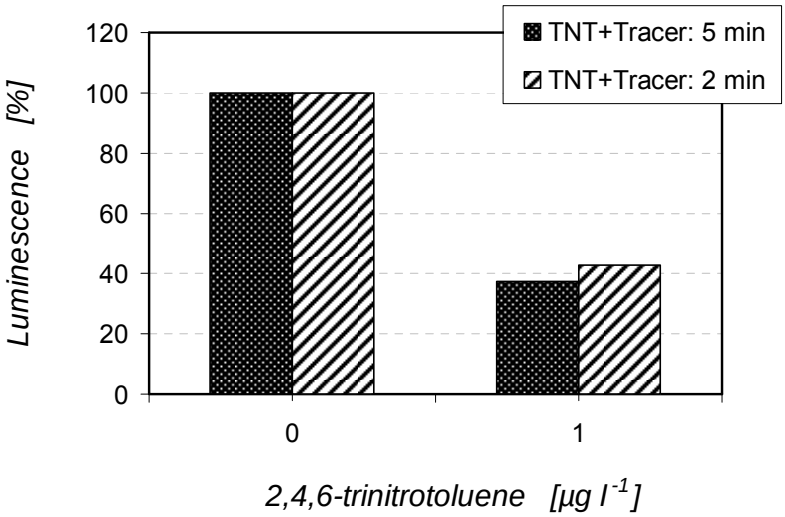

Figure 97. Inhibition obtained with 5 min vs. 2 min duration of the antigens incubation, by on-line measurements (n = 1), in the mixed antigens format. The signal pattern indicates that the 2 min incubation results in slightly weaker inhibition, hence rather lower sensitivity.

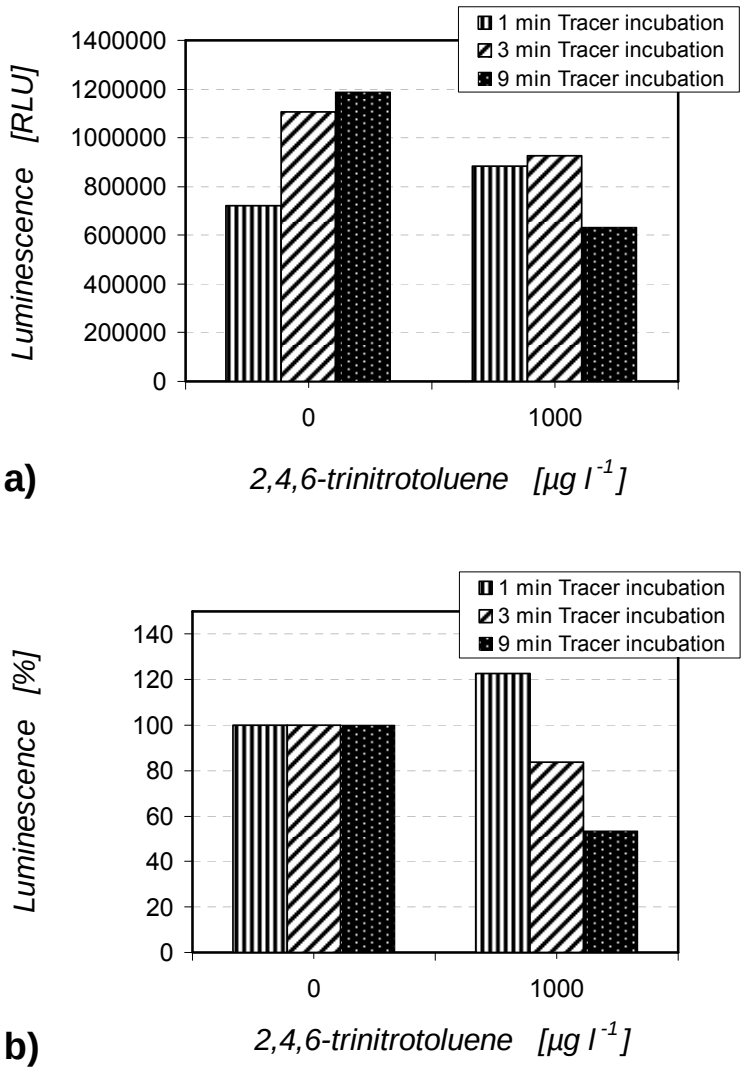

Figure 98. Inhibition obtained with the sequential saturation format (n = 1), by on-line measurements with the field prototype, with the Tr incubations of 1 / 3 / 9 min. The TNT was incubated first, 14x1 min. Other experimental information: incubated mAb solution 10,600 µg l^{-1}; Tr dilution 1: 50,000. The signal pattern indicates that inhibition is absent or poor at shorter Tr incubations, but it can increase when Tr has more time to bind.

4.4.1.3. Preliminary standard curve with on-line measurements

Although inhibition was possible at 5 min and 2 min antigens incubation time, in order to maximize our chance for a sensitive standard curve with TNT and with other less sensitive assays (like the atrazine assay and the diuron assay), we have chosen 10 min incubation as the standard time for subsequent measurements.

One last important aspect in the transfer of the immunochemicals to the biosensor platform is that the luminescence signal (RLU) produced by the Tr is very strong. Therefore,

the Tr must be diluted much more in comparison to absorbance measurements in microtiter plates. Even when the Tr was diluted 2 or 3 times more than in the microtiter plate format, RLU was still very strong (fig. 99). This fact, correlated with a very sensitive luminescence detector, allows wide experimental margins in assays optimisations on the sensor platform.

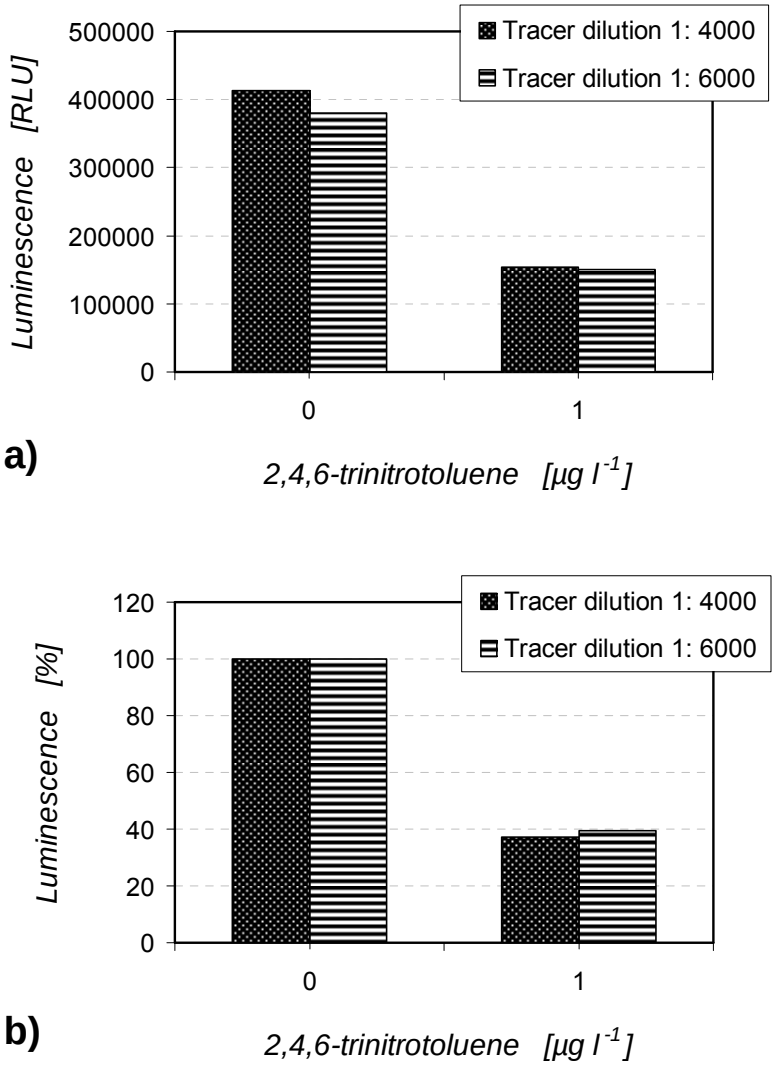

Figure 99. Inhibition obtained with two different dilutions (1: 4,000 and 1: 6,000) of the Tr, by on-line measurements (n = 1), in the competitive saturation (mixed antigens) format. The RLU obtained with the TNT assays was very strong. The two chosen dilution were 2x; 3x higher then the dilution used in the optimized TNT assay on microtiter plate, and the duration of the on-line incubation of the An / Tr mixture was 5 min. The signal pattern indicates that even slightly different tracer dilutions have a visible consequence, especially in the signal height.

After the experimental probing, it was possible to proceed, with the field prototype, to a series of on-line measurements which allowed the calculation of a preliminary standard curve with the TNT assay (fig. 100). For this curve one zero dose and one TNT

concentration were tested, each day, 4 days in a row, each day another TNT concentration. The inhibition slope is present, with a very good sensitivity, and acceptable background.

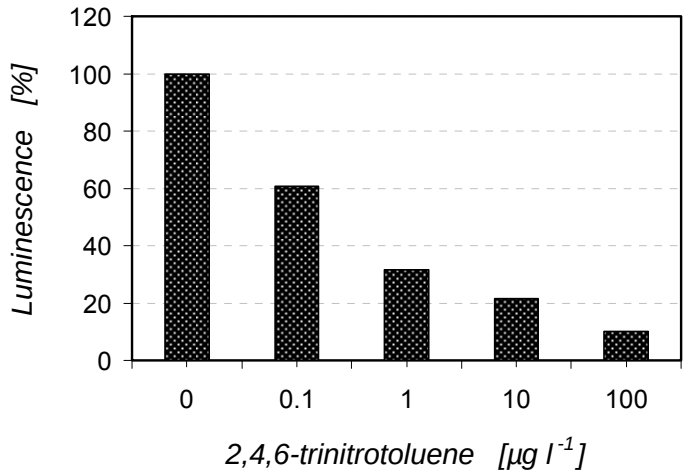

Figure 100. Preliminary standard curve obtained in three different days, by on-line measurements (n = 1), with the competitive saturation format. The duration of the on-line incubation of the An / Tr mixture was 10 min. The signal pattern indicates that the method of on-line measuring of TNT, with the biosensor platform, is very sensitive.

For manufacture and technical reasons, single- or double-measurements (n = 1; 2) were performed with the chips provided by IMM. The chips were not serial products at this stage of first-generation demonstrators. During the probing, the robustness of the obtained results was critically dependent on the good functioning of the sensor machine (trouble-shooting details in sub-chapter 4.4.4.), and less on the number of measurements.

Nonetheless, the validity of the results was conditioned by the careful general handling and chip preparation. When relatively larger series of (6 - 10) chips were provided by the manufacturer, they were tested for evenness in binding capacity and employed in the production of more optimized standard curves, as described in sub-chapter 4.4.2.

4.4.2. Optimizations and proof of principle with TNT, atrazine and diuron

A) Analysis of TNT

To resume, with the optimized TNT-ELISA on microtiter plates the following performance characteristics of the standard curve were obtained: detection limit (DL; IC_{20}) between 0.1–0.2 µg l^{-1}; linear dose-response region (IC_{20}–IC_{80}) from 0.1 to 10 µg l^{-1}; test midpoint (IC_{50}) between 0.3 and 1 µg l^{-1}.

In general, the curve parameters were preserved when the competition step was shortened from 30 to 10, 5, or 3 min. This indicated that the TNT-assay was fast enough to be part of a sensitive field immunosensor.

Compared with the fast TNT-ELISA on microtiter plate (fig. 73), the sensitivity increased roughly by a factor of 2 in the batch ELISA (fig. 87), and by a factor of 10 in the immunosensor, in the latter revealing an IC_{50} of ca. 0.02 µg l^{-1} (fig. 101).

B) Analysis of atrazine

The in-house optimized immunoassay for atrazine, which used mAb AM5D1-3 together with a commercial Tr (Fitzgerald Ind. Int., USA) was also fast in terms of length of the competition step (incubation: 10 min) in microtiter plates: IC_{50} was ca. 5 µg l^{-1} (fig. 73).

Compared with the fast atrazine-ELISA on microtiter plate, the sensitivity increased roughly by a factor of 15 in the batch ELISA (fig. 87), and a factor of 7 in the immunosensor, in the latter reaching an IC_{50} of ca. 0.7 µg l^{-1} (fig. 101).

C) Analysis of diuron

With the previously in-house established immunoassay for diuron an IC_{50} of 1.2-1.7 µg l^{-1} was obtained in microtiter plates, using again only 10 min incubation for the competition step (fig. 73). This proved that we had a fast diuron assay.

In batch ELISA with 10 min incubation in the competition step, a comparable sensitivity (slightly lower) was obtained (fig. 87), while with the immunosensor sensitivity increased by a factor of 3, with an IC_{50} of ca. 0.4 µg l^{-1} (fig. 101). So, the diuron-ELISA was more sensitive in the immunosensor than in both microtiter plate and batch assay.

In the experimental demonstration presented here, 35-40 min were needed for one measurement, corresponding to a maximum of 10 chips per day. This is relatively low frequency for actual on-site measurements, but it was caused by the experimental conditions: starting with the usage of freshly prepared chips without stabilization and ending with the high amount of handling needed with a not (yet) commercial prototype.

The core concept of this development was the flexibility of the approach, meaning in the end, the potential for future applications and validations in the field.

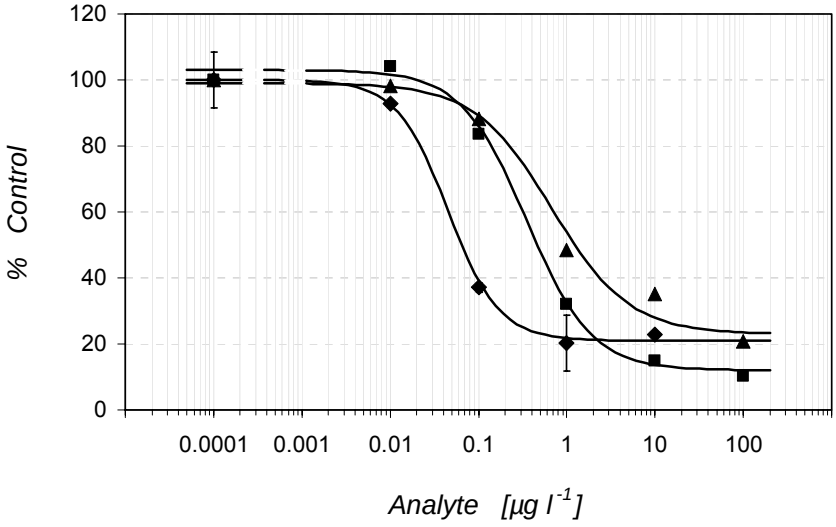

Figure 101. Standard curves ELISA for TNT, diuron and atrazine, produced with the immunosensor field prototype. Standards and corresponding Tr (both in 40 mM PBS) were mixed on-line and incubated together 10 min at 22°C onto the immobilized mAb. The zero dose is represented as 0.0001 µg $l^{-1}$and separated from the first real concentration by an interrupted line. The standard curve was fitted according to the 4-parameter equation (eq. 6), and the values of the curve parameters are:

(◆) TNT (n =2): A = 100; B = 1.50; C = 0.05 µg l^{-1}; D = 21; (DL = IC_{20}) = ca. 0.02 µgl^{-1};

(■) diuron (n = 1): A = 103; B = 1.18; C = 0.40 µg l^{-1}; D = 12; (DL = IC_{20}) = ca. 0.2 µgl^{-1};

(▲) atrazine (n = 1): A = 99; B = 1.00; C = 0.70 µg l^{-1}; D = 23; (DL = IC_{20}) = ca. 0.2 µgl^{-1}.

4.4.3. Further developments

4.4.3.1. Developments with isoproturon

To extend the work further for pesticide screening, work was carried out with additional mAbs, such as anti-isoproturon mAb IOC 7E1 (Krämer et al., 2004a). Although the isoproturon batch ELISA on the golden structure was successful, the assay's further transfer to the biosensor platform could not be achieved.

However, having the experience of the proof of principle with other three assays, we envisage that further efforts will make the transfer possible, on the basis of the knowledge already obtained with the isoproturon assay on microtiter plates and batch formats.

With the isoproturon assay, some sensitivity was sacrificed in order to optimize for shorter incubation times of the competition step, (including no An pre-incubation). Nevertheless, like with the other An presented here, the isoproturon assay remained very sensitive, even when the competition step was shortened to 10 min (details in sub-chapters 4.2.1 and 4.3.4).

In comparison, the conventional ELISA has 1½ hours in the competition step, with 1 hour pre-incubation of the An (Krämer et al., 2004a).

With the fast ELISA the IC_{50} was 0.4 µg l^{-1}, in the isoproturon batch ELISA the IC_{50} was 0.2 µg l^{-1}. Thus, unlike in the TNT assay, shorter incubation times for competitors lead in the isoproturon assay to a loss in sensitivity, but just like in TNT-assay, the sensitivity was higher in the batch ELISA by a factor of two (fig. 102).

These results make a promising basis for a high sensitivity in future applications of this immunoassay in the field immunosensor.

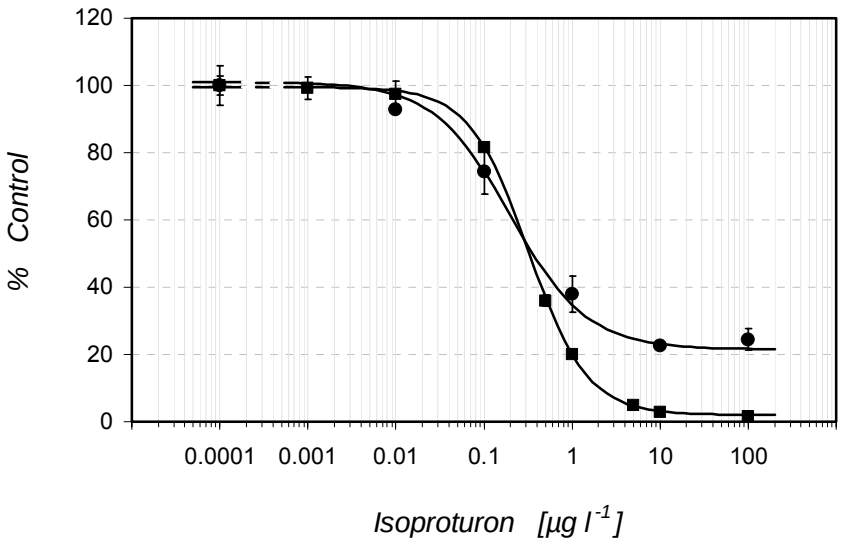

Figure 102. Standard curves with isoproturon in microtiter plate (n=6) and batch ELISA (n=3). The standards and the Tr (both in 40 mM PBS) were incubated together 10 min at RT. The zero dose is represented as 0.0001 µg l^{-1} and separated from the first real concentration by an interrupted line. The standard curve was fitted according to the 4-parameter equation (eq. 6), and the resulted values of the curve parameters are:

(■) in microtiter plate: A = 99.5; B = 1.30; C = 0.32 µg l^{-1}; D = 2.0; DL (IC_{20}) = ca 0.1 µg l^{-1};

(●) in batch format: A = 101; B = 1.00; C = 0.20 µg l^{-1}; D = 22; DL (IC_{20}) = ca 0.1 µg l^{-1}.

4.4.3.2. Covalent immobilization of Protein A/G

First experiments with covalent immobilization of coating protein (Protein A/G) through SAMs of thioalcanes eventually allowed binding and inhibition (fig. 103). These values were not reproduced after the regeneration of the chip, probably because of the instability of SAMs (details at the end of sub-chapter 4.3.2.).

After regeneration, Protein A/G should still be bound to SAMs but free of specific antibodies; in principle the antibodies were allowed to bind anew before the new measurements. This approach should be taken further, because the covalently immobilized

Protein A/G could be easily regenerated, and would therefore be a versatile surface for antibody binding and regeneration.

For such development, however, care must be taken that chemicals needed in the covalent attachment are not harmful to the chip material. Notably, in the practice of SAM, the gold surface is previously cleaned with strong acids like H_2SO_4 and HNO_3, and rinsed with water. Very short (few min) treatments with (diluted) H_2SO_4 can be applied with batch ELISA. But no strong acid can employed on the chip – cleaning should be done only with water, or with other previously tested substances.

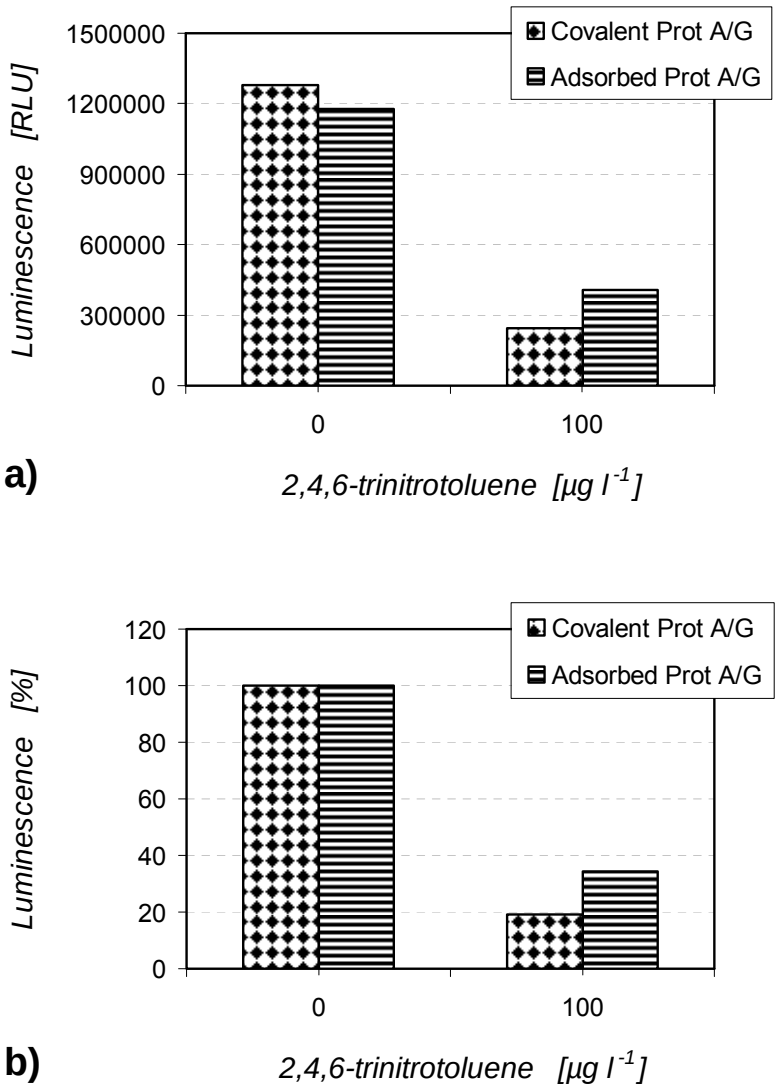

Figure 103. Pilot on-line measurements with the immunosensor (field prototype) with 100 µg l^{-1} TNT, with Protein A/G coated by covalent binding (n = 2) and by adsorption (n = 1). The RLU obtained with the two methods were similar in height (ca 1.2 mil RLU), but the inhibition with 100 µg l^{-1} was better with covalently bound Protein A/G (signal: 19 % control) than with adsorbed Protein A/G (signal: 35 % control).

In principle, antibodies could also be covalently immobilized directly to SAMs, but this option needs addressing two aspects. First, direct covalent immobilization of antibodies may lead to steric hindrance of the Ab-Ag interactions. Second, regeneration of the layer of covalently bound Ab presupposes relatively harsh treatments, which will lead to losses in antigen binding capacity. On the contrary, affinity based immobilization of the mAb (affinity capture by other molecules, e.g. Protein A/G) can avoid such losses (Quinn et al., 1999).

With covalent immobilization coupled with antibody regeneration even higher sensor flexibility is possible (Scheller et al., 2001). To study this technique with a potential next generation of the developed sensor, it would be useful to perform a comparison between covalent and adsorption approaches regarding the surface density and geometry of the immobilized antibody.

For such a surface characterisation one can employ scanning electron microscopy (SEM), ellipsometry, an adapted ELISA, or a combined approach, depending on the established specific objectives (Berney et al., 1997).

In addition, the structure and integrity of SAM can be investigated with scanning tunnelling microscopy (STM), atomic force microscopy (AFM) and infrared spectroscopy, contact angle measurements, surface plasmon resonance, quartz crystal microbalance and electrochemical methods like cyclic voltametry (CV) and impedimetry (Dijksma et al., 2001).

4.4.4. Troubleshooting in sensor measurements

The most experimentally important aspect with such a prototype immunosensor was the different (i.e. much higher) surface to volume ratio. The present study joins the literature (Holt et al., 2000) to make an important point: a higher surface is potentially an advantage, but not a granted one. If at all, this advantage is materialized only through laborious adjustment of the other experimental parameters.

4.4.4.1. Background luminescence

During the transfer of the immunochemicals onto the sensor platform, we observed that there was a background luminescence signal which interfered with the specific signal produced by the Tr. This background could be rather efficiently blocked with a solution of skimmed milk powder, 1% (w/v) in PBS 40 mM, incubated into the chip after the antibody immobilization. Details on the luminescence background are provided in the next paragraphs.

Enzyme tracing by labelling antigens or antibodies with horseradish peroxidase (HRP) is very popular in analytical methods based on immunochemical methods, like immunoassays (Tijssen, 1985) and immunosensors (Eggins, 1996; EWCB, 2004). Luminescent substrates for HRP are already popular, because of the recent improvements of luminescence detectors, and because of the sensitivity of chemiluminescence.

In general with HRP, the enzymatic process consists in the transfer of hydrogen from a hydrogen donor to hydrogen peroxide (H_2O_2). Thus H_2O_2 will be reduced to H_2O, and the hydrogen donor will be oxidized (Sun et al., 2001). The enzyme molecules mediate the proton and electron transfer by forming temporary complexes with the substrate molecules. When the hydrogen donor is luminol, the oxidoreduction by HRP takes place with the emission of energy under the form of photons (luxogenic reaction), and this emission is called chemiluminescence (Roda et al, 2000; Trojanowicz, 2000; Fletcher et al, 2001).

Under normal conditions, when the H_2O_2/luminol mixture reaches the incubation /measurement cell of the sensor chip, measurable luminescence signal results from the catalytic activity of the peroxidase in the Tr conjugate that is bound to the immobilized antibody. The development of both not inhibited (no An) and inhibited (with An) signal, from the start of substrate pumping until the signal is washed away is represented in fig. 104. One can observe that the luminescence signal becomes visible (approximately at second 15 of the 30 seconds of substrate pumping) and then increases until the end of the substrate pumping. The signal continues to increase in the next 60 seconds of substrate incubation. At second 90, it is the measured signal for each chip – indicated in the picture by the number "2". Then, the signal it vanishes abruptly, being washed out with buffer.

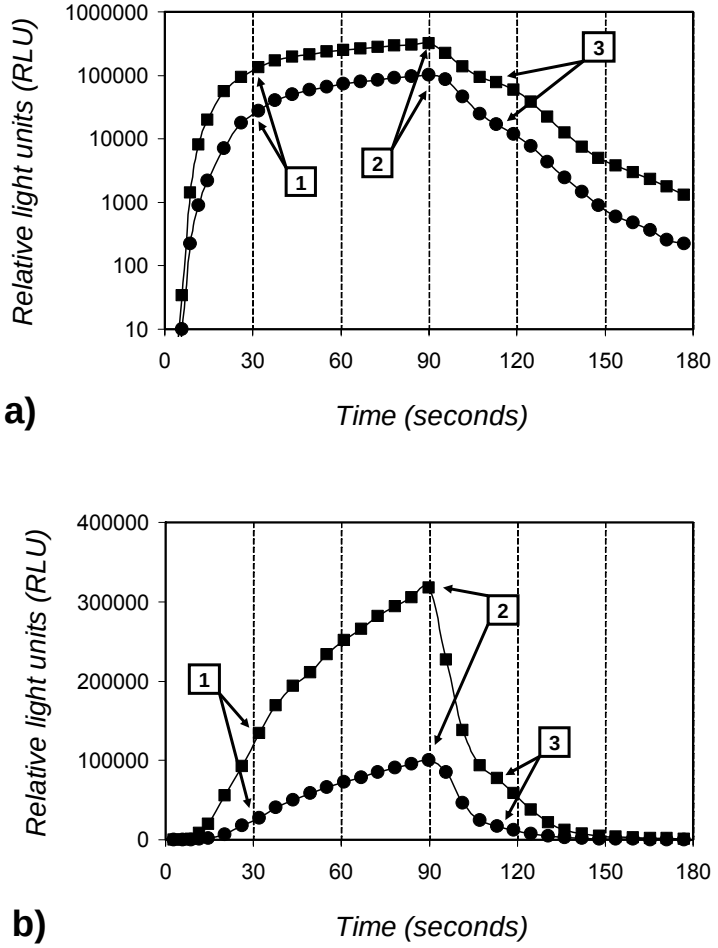

Figure 104. Typical development of luminescence signal on competitively bound Tr on monoclonal anti-TNT antibody. The signal development is represented both **(a)** as semi-log (as displayed by the sensor) and **(b)** as rectangular plot (for easier observation). Different moments in time represent different stages of substrate manipulation in the incubation-measurement cell of the exchangeable chip: substrate pumping (sec 0 – 30); substrate incubation (sec 30 – 90) and washing with system buffer (PBST 4mM). The two signals represent (■) uninhibited RLU (at zero dose) and (●) inhibited RLU, with 1 μg l^{-1} TNT standard. The numbers represent: **1** – end of substrate pumping, start of substrate incubation; **2** – end of substrate incubation; the measured signal for each chip (and taken into calculations); start of washing; **3** – signal hump at 20-30 seconds of washing with buffer.

Background interferences with the specific signal are strong. In order to separate the background signal from the specific one, the substrate mixture was pumped separately (1) on the solid surface alone and coated with catching protein / protein; (2) on caught (immobilized) Ab / catching protein plus caught anti-analyte Ab plus blocker protein (solution of 1% skimmed milk powder in 40 mM PBS). The resulted background signal was very high in the absence of the protein blocker, and had a different pattern of development (fig. 105).

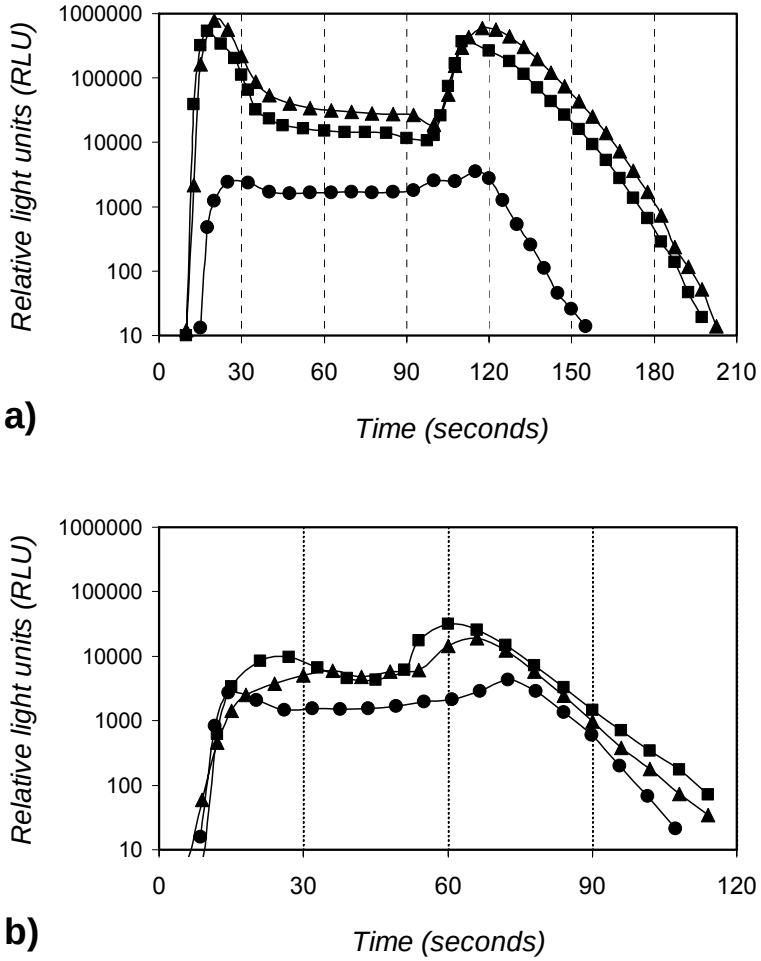

Figure 105. Development of luminescence signal after coating with catching protein /antibody and anti-TNT mAb, in the absence of the Tr. The catching protein is Protein A/G (a) or Gam (b). The three signals represent luminescent substrate brought into contact with: immobilized Protein A/G / Gam alone (■); Anti-TNT mAb immobilized via Protein A/G / Gam (▲); anti-TNT mAb immobilized via Protein A/G / Gam, plus solution of skimmed milk powder (1% in system buffer) as blocker (●). Different moments in time represent different stages of substrate manipulation in the incubation-measurement cell of the exchangeable chip: **(a)** substrate pumping (sec 0 – 30); substrate incubation (sec 30 – 120); washing – new substrate (rest in the channel; sec 120 – ca 150), then followed by washing – with system buffer (4mM PBST) reaching the incubation-measurement cell; **(b)** substrate pumping (sec 0 – 30); no substrate incubation; washing – new substrate (rest in the channel; sec 30 – ca 75-90), then followed by washing: with system buffer reaching the incubation-measurement cell.

The background luminescence signal varied strongly with the temperature (fig. 106a) and decreased with the store time of the coated chip (fig. 106b). The background signal was also different when the An has been incubated or not, in the chip (fig. 107).

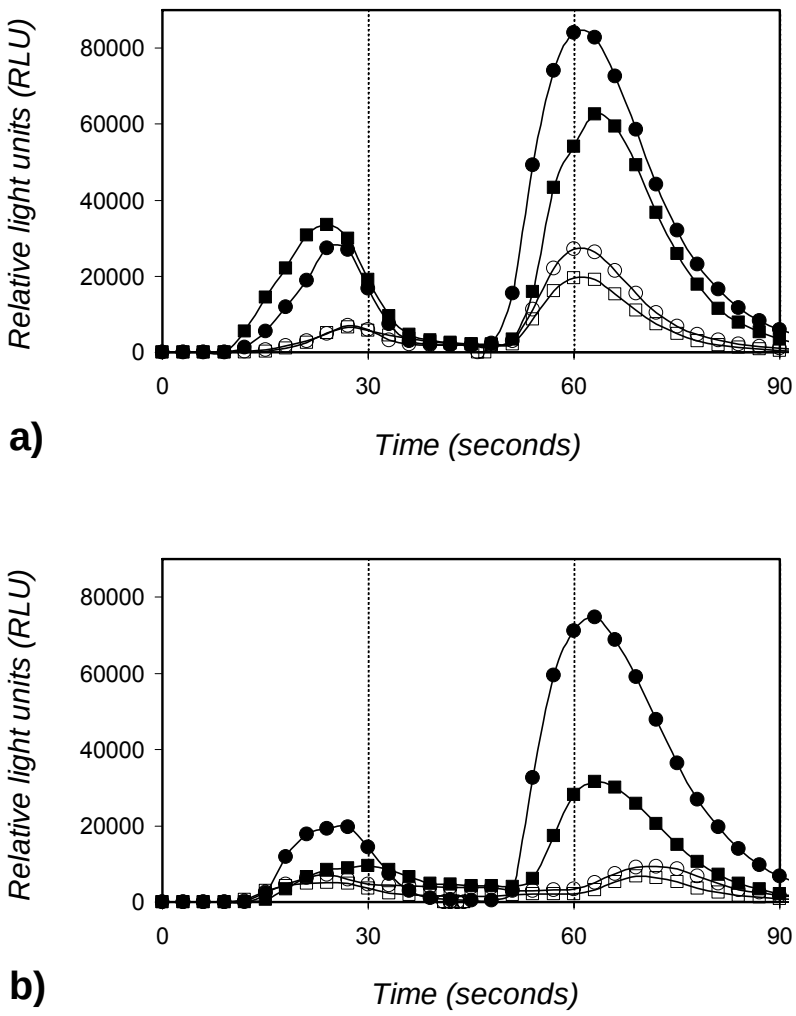

Figure 106. Intensity of luminescence signal produced after coating with Gam decreases with higher process temperature longer (a) and store time (b) Different moments in time represent different stages of substrate manipulation in the incubation-measurement cell of the exchangeable chip: substrate pumping (sec 0 – 30); no substrate incubation; washing – new substrate (rest in the channel; sec 30 – 45-60), then followed by washing – with system buffer (4 mM PBST) reaching the incubation-measurement cell. Here, the substrate was pumped onto and then washed away from the immobilized goat anti-mouse, 3 times in a row; for simplicity, only the first set of signals is shown (the other 2 are just similar). **(a)** Luminescence signal at ca 18-19°C is represented by filled symbols (●;■), while luminescence at ca 21-22°C represented by empty symbols (○;□). **(b)** Luminescence signal after 1 night store time at 3°C is represented by filled symbols (●; ■), while luminescence signal after 3 nights store time at 3°C is represented by empty symbols (○; □).

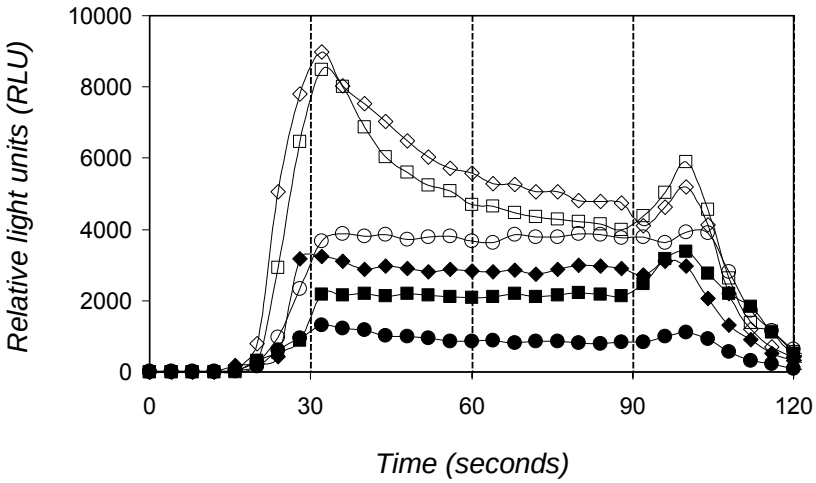

Figure 107. Intensity of luminescence signal produced by antibodies is higher when antibodies bound TNT. Different moments in time represent different stages of substrate manipulation in the incubation-measurement cell of the exchangeable chip: substrate pumping (sec 0 – 30); substrate incubation (sec 30 – 90); washing – new substrate (rest in the channel; sec 90 – 105-120); washing – with system buffer (4 mM PBST) reaching the incubation-measurement cell. In the signal development, filled symbols represent antibodies incubated with the zero dose, while empty symbols represent antibodies incubated with 1000 µg l^{-1}. The measurements are done in successive pairs: first (■) and (□); second (●) and (○); third (◆) and (◇).

4.4.4.2. The low dose hook

In on-line measurements with the immunosensor prototype, low dose hook was superimposed on the (initially unexpected) background luminescence and the unspecific binding of Tr, this complex situation rendering trouble shooting more difficult.

The low dose hook becomes critical at very short incubation times (details in sub-chapter 4.1.3.2). At 10 min incubation time for the An – Tr mixture, the low dose hook was overpassed. At shorter incubation times, the low dose hook effect is distorting the standard curve.

For the sake of the proof of principle, we chose to avoid low dose hook effects by lengthening the incubation time. Yet, there is another solution: ad-hoc spiking all samples and standards with a known concentration of An – that concentration below which no low dose is low enough to induce a low dose hook; then this concentration is subtracted from the concentration measured with the sensor.

4.4.4.3. Unspecific binding of the enzyme-tracer

One basic concern in all biosensor technologies is the stability of the immobilization of the biological molecules. The two main possible approaches in the immobilization of the catching molecules – physical adsorption and covalent binding, both have advantages and drawbacks.

Gold surface is a good option for both approaches, since gold adsorbs well both proteins (as needed for adsorption of catching proteins/antibodies) and sulphur atoms in thioalcanes (as needed for covalent binding of the catching proteins/antibodies).

We chose to apply physical adsorption of the catching protein-antibody. Protein adsorption proved to be strong enough to prevent having all the proteins washed off before needed. Obviously, this was also true for the label protein, meaning higher proportions of (unspecific) binding of the Tr to the solid surface at the expense of (specific) binding to the immobilized antibodies. Therefore an efficient blocking of the unspecific binding was necessary.

The best blocking was obtained with solutions of skimmed milk powder in 40 mM PBS (1%, w/v), applied as separated incubation step after immobilization of the specific monoclonal antibody. Other blockers (solutions), with lower blocking efficiencies, were casein, BSA and the commercial blocker (and protein stabilizer) LowCross™ Buffer.

Another blocker was Tween 20, the non-ionic surfactant currently used in washing buffer 4 mM PBST on all three platforms (plate; batch and sensor). Without Tween 20 in the washing buffer, the unspecific binding could not be stopped.

Beside the classic methods to fight unspecific binding, some other methods might be used in immunosensor applications. For example, electrochemical control of immuno-reagents can minimize nonspecfic adsorption, together with other undesired effects like cross-reactive binding, because of functional effects upon proteins and the Ab-Ag dynamics (Liron et al., 2002).

4.4.4.4. Analyte adsorption to the channel wall

One common problem in analytical systems using thin flow channels is that too much of the sample An can adsorb to the channel before reaching the incubation-measurement cell. The cause of this phenomenon is the high surface / volume ratio in thin cylinders, rendering very important an otherwise marginal phenomenon: physical adsorption of dissolved molecules.

This undesired phenomenon may have two major consequences. First, at very low An concentrations, most (if not all) An molecules in the sample may be prevented from

detection; this results in higher proportions of false negatives in screenings. Second, at very high An concentrations, many An molecules may stick to channel walls and be a source of contamination for next measurements; this results in higher proportions of false positives.

The conduit of the developed sensor was designed for the shortest possible way that the An can go through the ground plate. Therefore, from an engineering perspective, the contamination problem was already reduced to a minimum. The left risk of contamination is manageable by careful design and preparation of the measurements.

We avoided contaminations between successive measurements by applying a washing step (with a washing chip) between any two measurements. A washing step lasted in total 3 min at the normal flow rate, meaning 3 sub-steps of 1 min washing through all the possible flow routes (fig. 108): (1) V3–V4–V7; (2) V3–V5–V7; and (3) V2–V6–V7. A technical description of the necessary steps programming is provided in annex 9, table 16.

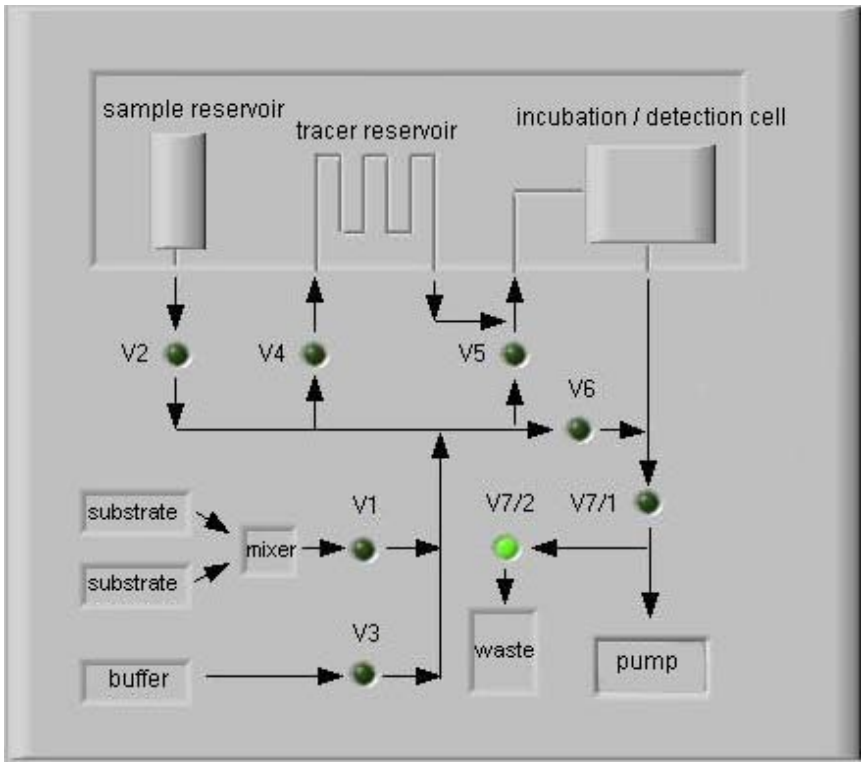

Figure 108. Scheme of the conduit in the sensor platform (ground plate and chip) (IMM Mainz, after Kolb et al. 2003)**.** The arrows indicate the direction of flow, while the balls represent the valves (from V1 to V7). The substrate and buffer reservoirs, the micromixer, the pump and the waste are represented as separated boxes onto the ground plate. The chip, containing sample reservoir, the tracer reservoir and the incubation/detection cell is represented as a separate rectangular area.

Depletions of An at small concentrations cannot be fought through faster washing without experiencing major disruptions of the other system settings, e.g. process temperature, flow rate.

The relevance of the An adsorption to the channel walls is actually dependent on the sensitivity of the employed analytical system (here, the immunochemicals optimized for the immunosensor platform) and the threshold An concentration used in screening. For example, if the immunochemicals' detection limit is very low, it may happen to hit a theoretically detectable amount of An that is actually all adsorbed to the channel wall, i.e. undetectable. Further, this really matters only if the threshold An concentration used for screening is very small, i.e. close to the theoretical detection limit.

The importance of the depletion of An molecules in samples upon the standard curve obtained with the immunosensor should become visible with the most sensitive assays. Thus, in the standard curves obtained with the field prototype (fig. 101), the parameters for sensitivity (IC_{50}) and for slope (B) correlate positively, i.e. higher sensitivity (lower IC_{50} values) associate with steeper slopes: with atrazine, IC_{50} = 0.7 and B = 1; with diuron, IC_{50} = 0.4 and B = 1.2; with TNT, IC_{50} = 0.05 and B = 1.5.

The most probable explanation for this correlation is the following: the fact that the most sensitive curves have higher slopes (i.e. very steep in the dose-response region) is due precisely to increasing relative importance of An depletion with very low standard concentrations. Otherwise, the same steep slope should have been observed with the assay optimizations on the microtiter plates and "batch" structures, which was not the case.

In the developed sensor, An adsorption to the channels wall is limited to a certain extent by using the general 4 mM PBST buffer, which is 4 mM PBS with 0.05% Tween 20 surfactant. Using higher concentrations of surfactant is not justified at the attained sensitivities with atrazine and diuron, but it might be useful with TNT, where the sensitivity was the highest (IC_{50} < 0.1 mg l^{-1}).

However, higher concentrations of surfactant may be harmful especially to the Tr catalytic activity. Higher surfactant concentrations may also lead to desorption of the antibodies (or of the catching proteins) from the solid phase (Colby, 1999). Of course, this would not be a problem if the antibodies would be attached covalently.

Anyway, the fact that this depletion effect can be quantified by the steady changes in the slope parameter is quite useful for the determination of the method limit. Moreover, because of this quantification, the depletion effect can be simply predicted and the standard curve used as such or by statistical corrections. Statistical corrections can be done in a very simple way; this implies a redrawing of the standard curve in the low doses portion through introducing the slope parameter known for the given assay and preserving the maximum inhibition point (An concentration) obtained with the immunosensor. In this case we would have the "de jure" detection limit (IC_{20}) of the corrected curve and the "de facto" detection limit of the experimentally obtained curve.

4.4.4.5. Blocked channels and micromixer

For the correct functioning of the automatic flow system of the sensor, it is primordial that all channels and the other components of the fluidic system be air-free. This is required by the basic physics of the pressure-driven flow systems. The fundamental principle is that fluids are not compressible / extensible, while gases are.

The first critical consequence in systems functioning with negative pressure (drawing pump) as ours is that efficient (i.e. strong enough and constant) liquid propulsion is not possible in the presence of air bubbles in the channels and the adjacent volumes. The working pressure of the flow system depends on the relative hight of the pump and of the conduit, because of the law of communicating vessels. Therefore, careful positioning in space of the pump and of the buffer and reagent reservoirs insures a very good working drawing pressure.

The second critical consequence of the mentioned physical principle is that the flow predictability of fluid (reagents) is lost in the presence of air bubbles in the channels and the adjacent volumes; therefore the desired chemical reaction cannot be controlled anymore in such a non air-free system.

Under these conditions, a foreign body blocking a channel interrupts the transmission of the negative pressure from the pump to the reagent reservoirs, hence forcing pervasion of air into the fluid system through the connections between the system components. Such foreign bodies can be small rubber particles disintegrated from the rubber tubing and stuck inside a channel. Another possibility is that some very thin channels, like those of a micromixer, get clogged by buffer salt and / or other reagents, during some repose periods.

In order to prevent such events, both sensor prototypes were thoroughly washed with ultrapure water after every day of experiments; before starting daily experiments, the prototypes were made air free, again, by controlled washing with Milli-Q water. In principle, minor, temporary obstructions of a flow micro-channel may be overcome naturally, by being removed by the accumulating sucking pressure.

Only after the system was checked air-free, the preparation of the instrument with reagents and buffer for the due measurements may begin.

4.4.4.6. Lose rubber disks (air bubbles)

As mentioned in the previous sub-chapter, when the channels are blocked, the air is forced into the system by the sucking pump. The air can penetrate into the fluidic system by the connections between the components of the fluid delivery system. In principle, these are

the junctions between the flexible (plastic or rubber) tubings and the rigid ends of the channels (metal heads). This is why a visual check of the junctions is recommendable before going to any experiments with the sensor prototypes.

The most sensitive conduit junctions are those between the ground plate and the exchangeable chip. These are five rubber discs placed around the channel metal heads on the chip, and fitting with five corresponding metal heads on the ground plate. The chip (and the channel junctions) is fastened on the ground plate manually, with two-winged screws (one at each corner of the chip). When inserted onto the ground plate, the chip should be tightening moderately; this can be easily done. If the chip is really too tightly squeezed, the junction lumen may be obturated by the dilated rubber disc; if the chip is too soft on the ground plate, the junctions run a risk to sucking-in air during fluid pumping. However, in a commercial future prototype, the chip insertion onto the ground plate has to be done automatically.

Nonetheless, the rubber type in the junction rubber discs is important. The rubber should be not too rigid (so that it can mould around the channel metal heads); not to flabby (so that is resists squeezing between the ground plate and the chip); and not brittle at often repeated chip exchanges (so that rubber particles do not brake away into the channel).

4.4.4.7. Unevenly drawing micromixer

Micromixers are very canny devices, but they are also more sensitive to functional disruptions. The micromixer incorporated into the conduit of the immunosensor developed by IMM (Fig. 109) is made of very fine intertwining lamellae and meanders, which can behave as a grille retaining air bubbles or all kind of accidental physical impurities like the earlier mentioned tiny rubber grains. More, because its geometry, the micromixer can get much easier clogged, e.g. with salts, and it may take longer to get it completely unblocked.

The potential danger with micromixers is that, partial obliteration of the micromixers fluid system is less noticeable in real time than in a common channel. All along this malfunction, the two reagents supposed to be mixed in equal volumes may actually be mixed incorrectly and unpredictably. Therefore, the undesired consequences of a micromixer' perturbation may induce artefact results which pass undetected.

An unwelcome contribution to the event describe above is the sensitivity of the equal-to-be mixing vis-à-vis to the partial pressures (sucking efficiency) in the two reagent-to-mix tubings uphill the micromixer. Thus, a small perturbation in micromixer or in one pre-tubing determines compensatory increase of the partial pressure on the other tubing, i.e. enhanced pressure disequilibrium.

Moreover, while in a normal channel, a minor obstruction is usually removed by the opposing pressure it creates, a minor flow obstruction of between some lamellae tend to be consolidated. This happens because the opposing pressure it creates can easily escape to the other tubing, through the neighbour lamellae.

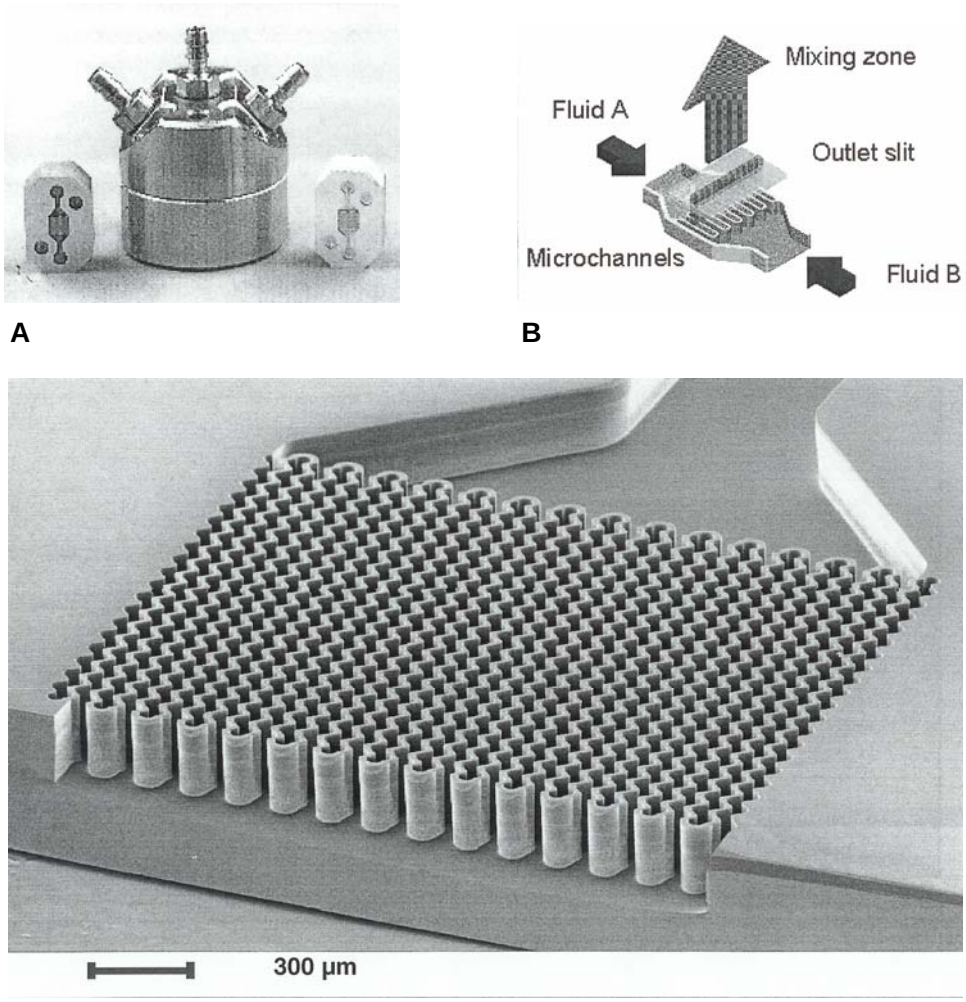

Figure 109. The micromixer manufactured by IMM and incorporated into the developed biosensor: A) General view; B) Mixing principle; C) Lamellae detail
(IMM Mainz, project report; see also Kolb et al. 2003)

However, troubles with micromixers are relevant more to the final stage that is of sensor commercialization than for the sensor development itself. This is because the micromixer was meant to mix the two solutions of the commercial substrate.

In order to circumvent such micromixer troubles, the two solutions were mixed off-line before being used for the on-line measurements. This was possible because the mixture was stable for 8 h, thus being stable enough for our developments in the laboratory.

In the field, with a commercial prototype, the micromixer will be a logistic advantage in that it will allow less handling and longer effective employment time.

4.4.4.8. Process temperature

Beside the general influence of temperature in immunoassays (sub-chapter 4.1.1.4.1.), on-line measurements with the immunosensor prototypes brought the specific problem of background luminescence. This phenomenon appeared to be temperature-dependent, in that it is stronger at lower temperature. Above 22°C, the interferences due to background are lowered down to a manageable level.

In order to minimize the background, we adjusted the process temperature of the (temperature-controlled) field instrument to 22°C. All on-line measurements (finally resulting in standard curves) with the field-instruments were carried at / above this temperature.

Another important aspect in measuring with the developed immunosensor is that the reagents are used in only small amounts; therefore they are more prone to degradation at room / process temperature. Basically, stabilization of immunoreagents is always a critical need in immunoassays (Hock et al., 1999), but this issue is even more sensitive with miniaturized immunosensors.

For this reason, careful stabilization of reagents will be necessary for future applications with the here described immunosensor platform, especially in the field.

For some reagents, stabilization methods are known, and commercial stabilization kits are available (e.g. by Applied Enzyme Technology Ltd). As we observed experimentally (sub-chapter 4.1.1.2), the HRP enzyme-tracer for the TNT assays was stabilized by the commercial SuperFreeze solution, at -20°C. With SuperFreeze, the Tr was stable for at least 30 weeks, while without this stabilizer, the Tr degraded in days.

The horseradish peroxidase itself is stabilized, beside commercial stabilizers, by low temperatures (for years between +2 and +8°C), dark, TMB, and by luminol (Schütz et al., 1997).

5. SUMMARY AND OUTLOOK

The immunosensor development

Effective pollution assessment is dependent upon an increase of real-time, on-site measurements. This is necessary, nowadays, because of an unprecedented number of pollutants, polluted sites and pollution laws. Therefore, the analytical programs tend to require more flexible, on-site, analytical methods and instruments, which must be also environmental- and user-friendly.

The semi-automated, miniaturized, single-use biosensor described here is designed to be a versatile, field screening instrument, with a power-autonomy of 6-8 hours, and temperature controlled. The instrument was based on an earlier laboratory flow-injection immuno-affinity system for laboratory analyses of pesticides in water samples (Krämer et al., 1997). The concept of the instrument was built on the fundamentals both of flow-injection and immunoanalysis, and the main target analytes are TNT, atrazine, diuron, and isoproturon.

The development consisted in transferring a series of immunochemicals from the traditional immunoassay format on microtiter plate (ELISA) onto of the new biosensor platform. This transfer required covering a series of basic steps:

(1) Immunoassay developments and / or optimizations on microtiter plate. This step also presupposed a work of identification of the experimental set-up that may be suitable for flow-injection conditions and sensor automation. Equally important, efforts were made to optimize the immunoassays towards fast analyses (fast ELISAs). This is because, in the end, with the immunosensor platform, short incubation times are necessary for on-site analysis.

(2) Transfer of the immunochemicals from microtiter plate (where the solid phase was the plastic wall of the wells of the microtiter plate) to "batch structures" (where the solid phase is the gold layer covering the solid PMMA structures). In this step, the golden structures were used without the sensor chip, placed in small glass vials, and used in performing the basic ELISA procedure. At the end of this stage, the immunochemicals were proved to work in the batch set-up, including with a fast format.

(3) Transfer of those immunochemicals that were successful in batch ELISA onto the immunosensor platform, where the golden structures were incorporated into an incubation / measuring cell of the exchangeable chip. This step included probing with off-line and on-line set-ups, as well as optimizations towards a standard procedure for each analyte. In this step, two versions of the sensor prototype (demonstrators) were employed: the laboratory prototype (at RT) and the field prototype (portable and temperature-controlled).

The proof of principle consisted in producing standard curves by means of on-line measurements with the field version of the immunosensor. This was achieved with three analytes: TNT, atrazine, and diuron. Additional developments were carried on with the forth analyte - isoproturon, on microtiter plates and batch structure.

Critical aspects

The central concept of the entire development is analytical flexibility. This concept was tackled by using a versatile design for the instrument, and by applying a versatile analytical technique: ELISA.

The developed sensor instrument has the following basic design features:

(1) Exchangeable chips which can be inserted onto the groundplate of the sensor (itself a portable, autonomous box);
(2) The chip can be prepared for whatever desired analyte for which immuno-chemicals exists and was formatted for the sensor conditions, stored and used when in the field;
(3) The chip can be regenerated, and subsequently prepared and used for the same or for another analyte; in the commercial stage, it is envisaged that the chip will be single-use;
(4) The anti-analyte antibody can be immobilized via catching proteins that bind entire classes of monoclonal antibodies.

The ELISA technique is traditionally performed on microtiter plates. The intrinsic dynamics of each assay conditioned the success of the immunochemicals transfer from microtiter plate onto the sensor platform. This was so for two reasons. First, the general analytical requirements with a field instrument must meet the peculiar reaction dynamics and the performances of each applied immunoassay. Second, the experimental conditions in the sensor instrument are very different than on the traditional solid support of ELISA which is the polystyrene.

Therefore, it was expected that the transfer of the immunoassays onto the sensor platform will result in important changes in the obtained analytical parameters. The most important aspects that needed addressing during ELISA transfer were:

(1) Much higher surface to volume ratio in the sensor chip than in the wells of the microtiter plate;
(2) Completely different fluid handling imposed by the miniaturized flow-injection system;
(3) Relatively high unspecific binding of proteins to the employed golden surface;

(4) Completely different detection system (luminescence instead of absorbance) and an important (but manageable) background signal;
(5) Automatization;
(6) Off-line chip preparation and storage.

The study carried on the flexibility of the immunochemicals in the microtiter plate helped to identify which on-line set-up was feasible for each specific analyte. A series of phenomena that may impede on the well functioning of the tested immunosensor were identified as predictions of the law of mass action and exemplified experimentally with short incubation times: facilitated binding of antigens; low dose hook; feed-back inhibition; sampling intensity; and intermediary plateaus on the standard curve.

With the newly developed TNT-assay, the sequential saturation analysis and the competitive saturation analysis, simultaneously performed on microtiter plate, showed that the assay performances were corrupted when the antigens are not incubated together. This effect is particularly strong when the analyte is incubated before the enzyme-tracer; at limit, a standard curve is still possible when the enzyme-tracer is incubated before the analyte.

The same phenomenon was observed with the immunoassays for atrazine and diuron. This result ruled out the possibility to avoid direct contact between samples and enzyme-tracer in the analysis of these analytes. This is valuable information for the sensor applications, since it shows that the risk of false positives (due to sample hazards harming the enzyme-tracer) cannot be removed.

The transfer of the isoproturon reagents onto the developed sensor platform was not possible with the procedure applied with the other three analytes (immunochemicals). A symmetrically opposed displacement pattern was observed with the isoproturon assay, indicating another type of antibody – antigen reaction dynamics.

Batch ELISA provided critical information on the immunoassay behaviour at half-way between the microtiter plate and the biosensor platform.

Proof of principle and general analytical performances

With TNT standards, as it was anticipated with the microtiter plate assay, only the competitive saturation format allowed to obtain a standard curve. Subsequently, the experimental procedure developed on the sensor platform with the TNT assay has been successfully adapted for atrazine and diuron.

As a proof of principle, we produced standard curves for each of the three analytes, using on-line measurements with the tested immunosensor.

The most realistic incubation time for the competition step proved to be 10 min. On microtiter plates, some assays could be optimized down to 3 min (competition step), but in the immunosensor, this duration is not easily applicable, because of the physical constraints of the fluidic system (like small dimensions flow pattern) combined with the antigen–antibody reaction dynamics (ruled by diffusion rates and association /dissociation rates). At this stage, each measurement took ca. 40 min, including all the needed off-line manual handling and on-line procedure.

The three obtained standard curves, displayed a detection limit (defined as IC_{20}) of ca. 0.02 μgl^{-1} for TNT and ca. 0.2 μgl^{-1} for atrazine and diuron. With 10 min of incubation of the An / Tr mixture, compared with the fast ELISA (at IC_{50}) on microtiter plate, the sensitivity of the TNT curve was higher roughly by a factor of 2 in batch ELISA and by a factor of 10 in immunosensor. Similarly, the sensitivity of the atrazine curve was higher roughly by a factor of 15 in batch ELISA and by a factor of 7 in immunosensor. With diuron, the sensitivity was similar in microtiter plate and in batch, but increased by a factor of ca. 3 in immunosensor.

Outlook

Already with the proof of principle, very good sensitivities for all three analytes were achieved. For TNT, the sensitivity of the sensor is comparable with those achieved by conventional methods performed by RP-HPLC-UV (U.S. EPA 8330, 1994) or GC-ECD (U.S. EPA 8095, 2000). Of course, this newly developed platform is made for screening purposes and will not achieve the precision and accuracy of these reference methods.

The applications for this field immunosensor are meant for on-site screening, where it will be necessary to distinguish reliably contaminated and uncontaminated samples at a certain threshold value. Here, the sample preparation will also play a considerable role. It should be easy and well adapted (regarding solvent content, etc.) to the immunosensor.

Continuation in the field of nitroaromatics will be achieved in applying a battery of newly developed mAbs for TNT and its metabolites (Krämer et al., 2004b) to the system. With these mAbs TNT can also be analyzed with the same sensitivity, but in addition the new mAbs show more and higher CRs than mAb A1.1.1.

The developments in batch ELISA described with the antibody against isoproturon, are important because they demonstrate the possibility to optimize various immuno-chemicals for the sensor platform.

On the side of the main sensor development, some limited studies probed the possibility to undertake further applications and developments of the biosensor platform in the future. Thus, the applications of the developed sensor platform can be extended to

screening of TNT and other pollutants in soils. Further, the flexibility of the developed analytical platform can be even more increased by applying covalent attachment of the coating protein to the golden surface via a self-organized layer of thioalcanes, so that the protein layer can be repeatedly regenerated and re-used.

Last, but not least, the stability of immunoreagents will have to be improved in the future. Here, lyophilisations of the enzyme-tracer and immobilized antibody on the chip might be an option. Then the reagents could be dissolved with buffer just before the measurement.

The present development was aimed towards environmental analysis, but once a subsequent prototype generation will have achieved commercial validation, the constituent principles and technology should also be applicable to medical diagnostics, and food analysis.

6. LITERATURE

Aalberse, R.C., Budde, I.K., Stapel, S.O., Van Ree. R., 2001. Structural aspects of cross-reactivity and its relation to antibody affinity. Allergy, 56, Suppl. 67, 27-29.

AB Umwelttechnik (Lägerdorf), 1997. Bodenwäscher für Nitroaromaten (Rüstungs-altlasten). UmweltMagazin, Dezember 1997, 45

Achtnich, C., Pfortner, P., Weller, M.G., Niessner, R., Lenke, H., and Knackmuss, H.-J., 1999. Reductive transformation of bound trinitrophenyl residues and free TNT during a bioremediation process analyzed by immunoassay. Environ. Sci. Technol., 33, 3421-3426.

Achtnich, C., Knackmuss, H.-J., 2000. Perspektiven der biologischen Elimination von trinitroaromaten aus Kriegsaltlasen. Biospektrum 4.2000, 271-273. http://www.biospektrum.de/pdf/591.pdf

Achtnich, C., and Lenke, H., 2001. Stability of immobilized 2,4,6-trinitrotoluene metabolites in soil under long-term leaching conditions. Environmental Toxicology and Chemistry, 20 (2), 280-283.

Adriaens, P., Goovaerts, P., Skerlos, S., Edwards, E., Egli, T., 2003. Intelligent infrastructure for sustainable potable water: a roundtable for emerging transnational research and technology development needs. Biotechnology Advances, 22, 119-134.

Adrian, N., Campbell, E., 1999. TNT and RDX degradation by cell-free extracts of *Clostridium acetobutylicum*. CERL Technical Report 99/102, U.S. Army Construction Engineering Research Laboratory, Champaign, IL. http://owww.cecer.army.mil/techreports/Adrian_clostridium/Adrian_clostridium_tr.pdf

Ahmed, M.T., Loutfy, N., Yousef, Y., 2001. Contamination of medicinal herbs with organ phosphorus insecticides. Bull. Environ. Contam. Toxiol. 66, 241-426.

Albro, P.W., Luster, M.I., Chae, K., Chaudhary, S.K., Clark, G., Lawson, L.D., Corbett, J.T., and McKinney, J.D., 1979. A radioimmunoassay for chlorinated dibenzo-p-dioxins. Toxicol. Appl. Pharmacol. 50, 137-146.

Alter, E., Donnevert, G., Sabel, C., 1998. Analytik sprengstofftypischer Substanzen – Ein Methodenvergleich. UWSF – Z. Umweltchem. Ökotox. 10 (2), 66-74.

Altamirano, M., García-Villada, L., Agrelo, M., Sánchez-Martín, L., Martín-Otero, L., Flores-Moya, A., Rico, M., López-Rodas., V., Costas, E., 2004. A novel approach to improve specificity of algal biosensors using wild-type and resistant mutants: an application to detect TNT. Biosens. Bioelectron. 19, 1319-1323.

Anderson, G.P., Rowe-Taitt, C.A., Ligler, F.S., 2000. Raptor: a portable, automated biosensor. Proceedings of the First Conference on Point Detection for Chemical and Biological Defense, October.

Anderson, G., Rowe-Taitt, C.A., 2001. Water quality monitoring using an automated portable fiber optic biosensor: RAPTOR. SPIE Proceedings 4206, February.

Arrow, K., Daily, G., Dasgupta, P., Levin, S., Maler, K.-G., Maskin, E., Starrett, D., Sterner, T., and Tietenberg, T., 2000. Managing ecosystem resources. Environ. Sci. Technol., 34, 1401-1406.

Bader, M., Göen, T., Müller, J., Angerer, J., 1998. Analysis of nitroaromatic compounds in urine by gas chromatography – mass spectroscopy for the biological monitoring of explosives. Journal of Chromatography B, 710, 91-99.

Baeumner, A.J., 2003. Biosensors for environmental pollutants and food contaminants. Analytical and Bioanalytical Chemistry, 377 (3), 434-445.

Bakhtiar, R., Leung, K.H., Stearns, R.A., and Hop, C.E.C.A., 1997. Evidence for a novel heme addust generated by the *in vitro* reaction of 2,4,6-trinitrotoluene with human hemoglobin using electrospray ionization mass spectrometry. Journal of Inorganic Chemistry, 68, 273-278.

Bakaltcheva, I.B., Ligler, F.S., Patterson, C.H., Shriver-Lake, L.C., 1999. Multi-analyte explosive detection using a fiber optic biosensor. Anal. Chim. Acta 399, 13-20.

Bang Laboratories, Inc., 1997. Adsorption protocols. Tech. Note # 13a. Bang Laboratories, Inc. Fishers, IN. Web site: www.bangslabs.com

Barshick, S. -A., Griest, W.H., 1998. Tracer analysis of explosives in seawater using solid-phase microextraction and gas chromatography / ion trap mass spectroscopy. Anal. Chem., 70, 3015-3020.

Bart, J.C., Judd, L.L., Hoffman, K.E., Wilkins, A.M., Kusterbeck, A.W., 1997. Application of a portable immunosensor to detect the explosives TNT and RDX in groundwater samples. Environ. Sci. Technol. 31, 1505-1511.

Bailey, C.G., and Yan, C., 1998. Separation of explosives using capillary electrochromatography. Analytical Chemistry, 70 (15), 3275-3279.

Behrend, C., Heesche-Wagner, K., 1999. Formation of hydride-Meisenheimer complexes of picric acid (2,4,6-trinitrophenol) and 2,4-dinitrophenol. Applied and Environmental Microbiology, 65 (4), 1372-1377. http://intl-aem.asm.org/cgi/reprint/65/4/1372.pdf

Beltz, L.A., Neira, D.R., Axtell, C.A., Iverson, S., Deaton, W., Waldschmidt, T.J., Bumpus, J.A., Johnston, C.G., 2001. Immunotoxicity of explosives-contaminated soil before and after bioremediation. Arch. Environ. Contam. Toxicol. 40, 311-317.

Berney, H., Roseingrave, P., Alderman, J., Lane, W., Collins, J.K., 1997. Biosensor surface characterization: confirming multilayer immobilisation, determining coverage of the biospecies and establishing detection limits. Sensors and actuators B, 44, 341-349.

Berthe-Corti, L., Jacobi, H., Kleihauer, S, Witte, I., 1998. Cytotoxicity and mutagenicity of 2,4,6-trinitrotoluene (TNT) and hexogen contaminated soil in *S. typhimurius* and mammalian cells. Chemosphere, 3 (2), 209-218.

Best, E.P.H., Miller, J.L., Zappi, M.E., Fredrickson, H.L., Spreacher, S.L., Larson, S.L, Strekfuss, T., 1997. Degradation of TNT and RDX in ground water from the Iowa Army Ammunition Plant in flow-through systems planted with aquatic and wetland plants. (1997) Abstracts Book, 12th Ann. Conf. on Hazardous Waste Research, Kansas City, 19.-22.5.1997. http://www.engg.ksu.edu/HSRC/97abstracts/doc12.html

Best, E.P.H., Sprecher, S.L., Larson, S.L., Fredrickson, H.L., Bader, D.F., 1999. Environmental behavior of explosives in groundwater from the Milan army ammunition plant in aquatic and wetland plant tratments. Removal, mass balances and fate in groundwater of TNT and RDX. Chemosphere, 38 (14), 3383-3396.

Best, E.P.H., tatem, H.E., Geter, K.N., Wells, M.L., Lane, B.K., 2004. Toxicity and metabolites of 2,4,6-trinitrotoluene (TNT) in plants and worms from exposure to aged soil. Report ERCD/EL TR-04-18, October 2004, US Army Corps of Engineers, Engineer Research and Development Center, Vicksburg, MS.

Betts , K.S. 1997. Native aquatic plats remove explosives. Environmental Science and Technology, 31 (7), 304A.

Bhadra, R., Wayment, D.G., Hughes, J.B., and Shanks, J.V., 1999. Confirmation of Conjugation during TNT Metabolism by axenic plant roots. Environ. Sci. Technol., 33, 446-452.

Boopathy, R., Manning, J., Kulpa, C.F., 1997. Optimization of environmental factors for the biological treatment of trinitrotoluene-contaminated soil. Arch. Environ. Contam. Toxicol. 32, 94-98.

Bordelon, N., Washburn, K., He, L.-Y., Donnelly, K.C., 1996. Bioavailability of genotoxic mixtures in soil. Proceedings of HSRC / WERC Joint Conference on the Environment, May, 1996. http://www.engg.ksu.edu/HSRC/96Proceed/bordelon.html

Boyajian, G.E. and Carreira, L., H., 1997. Phytoremediation: A clean transition from laboratory to marketplace?. Nature Biotechnology, 15, Feb. 1997, 127-128.

Boyd, E., Bruce, N., 2002. Defusing the environment. Microbiology Today 29 / May 02. http://www.socgenmicrobiol.org.uk/pubs/micro_today/pdf/050205.pdf

Brannon, J.M., Myers, T.E., 1997. Review of fate and transport processes of explosives. Technical Report IRRP-97-2, U.S. Army Corps of Engineers, Washington, DC, 20314-1000. 30 pages.

Brannon, J.M., Price, C.B., Hayes, C., 1998. Abiotic transfomation of TNT in montmorillonite and soil suspensions under reducing conditions. Chemosphere, 36 (6), 1453-1462.

Brogan K.L., Wolfe, K.N., Jones, P.A., Schoenfisch, M.H., 2003. Directed oriented immobilization of F(ab') antibody fragments on gold. Analytica Chimica Acta, 496, 73-80.

Bromberg, A., Mathies, R.A., 2003. Homogenous immunoassay for detection of TNT and its analogues on microfabricated capillary electrophoresis chip. Anal. Chem., 75, 1188-1195.

Brunet, J.E., Vargas, V., Gratton, E., and Jameson, D.M., 1994. Hydrodynamics of horseradish peroxidase revealed by global analysis of multiple fluorescence probes. Biophysical Journal, 66, 446-453.

Bruns - Nagel, D., Drzyzga, O., Steinbach, K., Schmidt, T.C., Von Löw, E., Gorontzy, T., Blotevogel, K.-H., and Gemsa, D., 1998. Aerobic/ anaerobic composting of 2,4,6-trinitrotoluene-contaminated soil in a reactor system. Environ. Sci. Techn., 32, 1676-1679.

Bruns - Nagel, D., Knicker, H., Drzyzga, O., Butehorn, U., Steinbach, K., Gemsa, D., and Von Löw, 2000. Characterization of ^{15}N-TNT residues after an aerobic/ anaerobic tratment of soil/ molasses mixtures by solid state ^{15}N NMR spectroscopy. 2. Systematic investigation of whole soil and different humic fractions.. Environ. Sci. Techn., 34, 1549-1556.

Burauel, P., and Bassmann, F., 2005. Soils as filter and buffer for pesticides – experimental concepts to understand soil functions. Environmental Pollution, 133, 11-16.

Butler, J.E. 2000. Solid supports in enzyme-linked immunosorbent assay and other solid-phase immunoassays. Methods, 22, 4-23.

Buttner, W.J, Findlay, M., Vickers, W., Davis, W.M., Cespedes, E.R., Cooper, S., Adams, J.W, 1997. *In situ* detection of trinitrotoluene and other nitrated explosives in soils. Anal. Chim. Acta, 341, 63-71.

Cano-Ruiz, J.A., and McRae, G.J., 1998. Environmentally conscious chemical process design. Annual Review Energy & the Environment, 23 (1), 499-536.

Carpenter, D.F., McCormick, N.G., Cornell, G.H., and Kaplan, A.R, 1978. Microbial transformation of ^{14}C-labelled 2,4,6-trinitrotoluene in an activated-sludge system. Applied and Environmental Microbiology, May 1978, 949-954.

Cassada, D.A., Monson, S.J., Snow, D.D., Spalding, R.F., 1999. Sensitive determination of RDX, nitroso-RDX metabolites, and other munitions in ground water by solid-phase extraction and isotope dilution liquid chromatography – atmospheric pressure chemical ionization mass spectrometry. Journal of Chromatography A, 844, 87-95.

Charles, P.T., Gauger, P.R., Patterson Jr., C.H., Kusterbeck A.W., 2000. On-site immunoanalysis of nitrate and nitroaromatic compounds in groundwater. Environ. Sci. Technol 31, 4641-4650.

Chekol, T, Vough, L.R., 2002. Assessing the phytoremediation potantial of Tall Fescue and Sericea Lespedeza for organic contaminants in soil. Remediation Journal, 12 (3) 117-128.

Christopoulos, T.K., and Diamandis, E.P., 1996. Theory of immunoassays. In Diamandis, E.P. and Christopoulos, T.K. (Eds), 1996. Immunoassays. Academic Press. ISBN 0-12-21-214730-8.

Chua, S., 1999. Economic growth, liberalization, and the environment: a review of the economic evidence. Annual Reviews Energy & the Environment, 24 (1), 391-430.

Ciumasu I.M., Krämer P.M., Weber C.M., Kolb G., Tiemann D., Windisch S., Frese I., Kettrup A.A., 2004. Single-use immunosensor for environmental pollutants. Proof of principle for nitroaromatics and pesticide. Poster presentation at 'The Eighth World Congress on Biosensors', Granada, Spain, May 24-26, 2004 (Abstract book P2.4.8).

Ciumasu I.M., Krämer P.M., Weber C.M., Kolb G., Tiemann D., Windisch S., Frese I., Kettrup A.A., 2005 (in press). A new, versatile immunosensor for environmental pollutants. Development and proof of principle with TNT, diuron, and atrazine. Biosensors and Bioelectronics 21: 354-364. http://www.sciencedirect.com/science/journal/9565663

Clement, R.E., Yang, P.W., Koester, C.J., 2001. Environmental analysis. Anal. Chem., 73, 2761-2790.

Craig, H., Ferguson G., Markos, A., Kusterbeck, A., Shriver-Lake, L., Jenkins, T., and P.Thorne: Field demonstration of on-site analytical methods for TNT and RDX in ground water. (1996) Proceedings of the 1996 HSRC WERC Joint Conference on the Environment, Albuquerque, New Mexico, May 21-23, 1996. http://www.engg.ksu.edu/HSRC/96proceed/craig.pdf

Crockett, A.B., Craig, H.D., Jenkins, T.F., and Sisk, W.E., 1996a. Field sampling and selecting on-site analytical methods for explosives in soil. EPA/540/R-97/501, Nov. 1996, U.S. Environmental Protection Agency (EPA), Office of Research and Development (ORD), Office of Solid Waste and Emergency Response (OSWER).

Crockett, A.B., Craig, H.D., Jenkins, T.F., and Sisk, W.E., 1996b. Field sampling and selecting on-site analytical methods for explosives in soil. EPA/540/S-97/501, December 1996, U.S. Environmental Protection Agency (EPA), National Exposure Research laboratory (NERL).

Crockett, A.B., Jenkins, T.F., Craig, H.D., Sisk, W.E., 1998. Overview of on-site analytical methods for explosives in soil. Special Report 98-4, U.S. Army Cold Regions Research and Engineering Laboratory. http://www.crrel.usace.army.mil/techpub/CRREL_Reports/reports/SR98_04.pdf

Crockett, A.B., Craig, H.D., and Jenkins, T.F., 1999. Field sampling and selecting on-site analytical methods for explosives in water. EPA/600/S-99/002. May 1999. U.S. Environmental Protection Agency (EPA), Office of Research and Development (ORD), Office of Solid Waste and Emergency Response (OSWER).

Crumbling, D.A., Groenjes, C., Lesnik, B., Lynch, K., Shockley, J., Van Ee, J., Howe, R., Keith, L., and Mckenna, J., 2001. Applying the concept of effective data to contaminated sites could reduce costs and improve cleanups. Environmental Science & Technology, October 1, 2001, 405A-409A.

Dankwardt, A., 1999. Recommendations about the use of Immunochemical methods for FAO/IAEA training and reference centre for food and pesticide control. Report by Sension GmbH UTG – Centre for environmental technologies Am Mittleren Moos 48, 86167 Augsburg, Germany. http://www.iaea.org/trc/pest-2027_review.pdf

Dankwardt, A., 2000. Immunochemical analysis in pesticide analysis. In Meyers, R.A. (Ed), Encyclopedia of Analytical Chemistry. John Wiley & Sons Ltd, Chichester. ISBN 0471 97670 9. http://www.wiley.co.uk/wileychi/eac/pdf/A1714-W.PDF

Danzer, K., 2001. Selectivity and specificity in analytical chemistry. General considerations and attempt of a definition and quantification. fresenius J. Anal. Chem, 369 (5), 397-402.

Dasgupta, D., and Balachandran, S., 2004. Artificial immune system: a bibliography. Technical Report No. CS-04-002, version 5.2. University of Memphis (USA), Computer Science Division.

Daun, G., Lenke, H., Reuss, M., and Knackmuss, H-.J., 1998. Biological treatment of TNT-contaminated soil. 1. Anaerobic cometabolic reduction and interaction of TNT and metabolites with soil components. Environ. Sci. Technol., 32, 1956-1963.

Davis, L.C., and Chou, N.C., 1996. Metabolism of TNT associated with roots of higher plats. Proceedings of the 1996, HSRC/WERC joint conference on the environment. ISSN 1054-8564. http://www.engg.ksu.edu/HSRC/96Proceed/davis.pdf

Dawel, G., Kastner, M., Michels, J., Poppitz, W., Gunther, W., and Fritsche, W., 1997. Structure of a laccase-mediated product of coupling of 2,4-diamino-6-nitrotoluene to guaiacol. Applied and Environmental Microbiology, 63, Nr.7, 2560-2565. http://intl-aem.asm.org/cgi/reprint/63/7/2560.pdf

Decision No 2455/2001/EC of the European Parliament and of the Council of November 2001, establishing the list of priority substances in the field of water policy and amending Directive 2000/60/EC. Official Journal of the European Communities 15.12.2001, L331/1-5.

DeLorenzo, M.E., Scott, G.I., and Ross, P.E., 2001. Toxicity of pesticides to aquatic microorganisms: A review. Environmental Toxicology and Chemistry, 20 (1), 84-98.

DeSilva, B.S., and Wilson, G.S., Synthesis of bifunctional antibodies for immunoassays. Methods, 22, 33-43.

Dijksma, M., 2001. Development of electrochemical immunosensors based on self-assembled monolayers. PhD thesis at Utrecht University, The Netherlands.

Dindal, A.B., Bayne, C.K., Jenkins, R.A., Koglin, E.N., 2000. Environmental technology verification report. Explosives detection technology. Research International FAST 2000™. U.S. Environmental Protection Agency, report EPA/600/R-00/045.

Dionex Corporation, 1997. Extraction of explosives from soils by accelerated solvent extraction (ASE®). Application Note 328, LPN 0888 5M 1/97. http://www.dionex.com

Directive 80/68/EEC of the Council of 17 December 1979 on the protection of groundwater. Official Journal L 020, 26/01/1980, 0043- 0048

Directive 91/414/EEC of the Council of 15 July 1991 concerning the placing of plant protection products on the market. Official Journal L230, 19.8.1991, 1.

Directive 2000/60/EC of the European Parliament and of the Council of 23 October 2000, establishing a framework for Community action in the field of water policy. Official journal of the European Communities L 327/1-72, from 22/12/2000.

Doppalapudi, R., Dinesh, P., Maloney S.W., Sorial, G., 2000. Electrochemical reduction of energetically contaminated wastewater: Development and testing of pilot scale reactor. (2000) Report Number ERDC/CERL TR-00-38, U.S. Army, Corps of Engineers, CERL, Champaign, IL. http://owww.cecer.army.mil/TechReports/Maloney_Redox_TR/Maloney_Redox_TR.pdf

Dosch, M., Weller, M.G., Bückmann, A., Niessner, R., 1998. Homogeneous immunoassay for the detection of trinitrotoluene (TNT) based on the reactivation of apoglucose oxidase using a novel FAD-trinitrotoluene conjugate. Fresenius J. Anal. Chem. 361, 174-178.

Draper, W.M., 2001. Biological monitoring: Exquisite research probes, risk assessment, and routine exposure measurement. Anal. Chem., 73, 2745-2760.

Echols, R.T., Christiansen, M.M., Krisko, R.M., Altstadt, J.H., 1999. Selective determination of TNT in soil extracts by sequential injection spectrophotometry. Anal. Chem. 71, 2739-2744.

Ecotechniek Bodem (Maarssen, NL), 1997. Schonende Behandlung (Thermische Bodensanierung). UmweltMagazin, Dezember 1997, 45.

Edelman, G.M., 1972. Antibody structure and molecular immunology. Nobel lecture. http://nobelprize.org/medecine/laureates/1972/Edelman-lecture.pdf

Eiceman, G.A., 2000. Instrumentation of gas chromatography, In Meyers, R.A. (Ed), Encyclopedia of Analytical Chemistry. John Wiley & Sons Ltd, Chichester. ISBN 0471 97670 9.

Eikenberg, O., Krämer, P.M., Kettrup, A.A., 1997. Immunochemical screening for TNT in soil. Validation of commercially available test.kits. In: Gottlieb, J., Hötzl, H., Huck, K., Niessner, R. (Eds.), Field Screening Europe. Kluwer Academic Publishers, Dordrecht, The Netherlands, 193-196.

Eldredge, N., 1995. Dominion. University of California Press. 190 pages. Reprinted in 1997. ISBN 0-520-20845-5.

El-hawari, A.M., Hodgson, J.R., Winston, J.M., Sawer, M.D., Hainje, M., and Lee, C.C., 1981. Species differences in the disposition and metabolism of 2,4,6-trinitrotoluene as a function of route of adminitration. Final Report. Midwest Research Institute, Project No. 4274-B, Kansas City, MO. DAMD17-76-C-6066. AD-A114-025 (Cited in U.S. EPA 1990).

Emmrich, M., 2001. Kinetics of the alkaline hydrolysis of important nitroaromatic co-contaminants of 2,4,6-trinitrotoluene in highly contaminated soils. Environ. Sci. Technol., 35, 874-877.

Engquist, I., 1996. Self-assembled monolayers. An introduction on web at: http://www.ifm.liu.se/applphys/ftir/sams.html

Eriksson, J., 2003. Retention and mobilisation of trinitrotoluene, aniline, nitrobenzene and toluene by soil organic Matter, PhD thesis, Swedish University of Agricultural Sciences, Umeå 2003 http://diss-epsilon.slu.se/archive/00000160/01/91-576-6500-1.fulltext.pdf

Ermolenko, D.N., Zherdev, A.V., Dzantiev, B.B., and Popov, V.O., 2002. Antiperoxidase antibodies enhance refolding of horseradish peroxidase. Biochemical and Biophysical Research Comunications, 291 (4), 959-965.

Esser, P., 1997. Edge effect in microwell™ ELISA. Nunc Bulletin, no. 1 (1). Nunc™ Brand Products.

Esteve-Nuñez, A., Lucchesi, G., Philipp, B., Schink, B., Ramos, J.L, 2000. Respiration of 2,4,6-Trinitrotoluene by *Pseudomonas sp.* Strain JLR11. Journal of Bacteriology 182 (5), 1352-1355. http://jb.asm.org/cgi/content/abstract/182/5/1352

Esteve-Nunez, A., Caballero, A., Ramos, J.L., 2001 Biological degradation of 2,4,6-trinitrotoluene. Microbiol Mol Biol Rev. 65 (3), 335-52. http://mmbr.asm.org/cgi/reprint/65/3/335.pdf

Estevez-Alberola, M.-C., and Marco, M.-P., 2004. Immunochemical determination of xenobiotics with endocrine disrupting effects. Analytical and Bioanalytical Chemistry, 378 (3), 563-575.

EU MRLs, 2004. Informal coordination of MRLs established in Directives 76/895/EEC, 86/362/EEC, 86/363/EEC and 90/642/EEC, updated on 3rd November 2004.

EU Commission Report SANCO/3045/99-final from 12 March 2002, on Isoproturon, in view of inclusion of isoproturon in Annex I of Directive 91/414/EEC.

EWCB – The Eight World Congress on Biosensors, 24-26 May, 2004, Granada, Spain. Biosensors and Bioelectronics. Abstract book.

Farber, S., and Griner, B., 2000. Using conjoint analysis to value ecosystem change. Environ. Sci. Technol., 34, 1407-1412.

Feldkamp, C.S., Carey, J.L., 1996. Immune function and antibody structure. In Diamandis, E.P. and Christopoulos, T.K., 1996. Immunoassays. Academic Press. ISBN 0-12-21-214730-8.

Fernando, S.A., Sportsman, J.R., Wilson, G.S., Studies of the low dose hook effect in a competitive homogeneous immunoassays. J. Immunol. Methods., 151, 27-46.

Fernando, S.A., Wilson, G.S., Studies of the hook effect in the one step sandwich immunoassay. J. Immunol. Methods., 151, 47-66.

Fernando, S.A., Wilson, G.S., Multiple epitope interactions in the two-step sandwich immunoassay. J. Immunol. Methods., 151, 67-86.

Fitzpatrick, L.J., and Dean, J.R., 2002. Extraction solvent selection in environmental analysis. Anal. Chim., 74, 74-79.

Fletcher, P., Andrew, K.N., Calokerinos, A.C, Forbes, S., Worsfold, P.L., 2001. Analytical applications of flow-injection with chemiluminescence detection – a review. Luminescence, 16, 1-23.

French, C.E., Nicklin, S., Bruce, N.C., 1998. Aerobic degradation of 2,4,6-trinitrotoluene by *Enterobacter cloacae PB2* and by pentaerythritol tetranitrate reductase. Applied and Environmental Microbiology, 64 (8), 2864-2868. http://intl-aem.asm.org/cgi/reprint/64/8/2864.pdf

French, C.E., Rosser, S.J., Davies, G.J., Nicklin, S., and Bruce, N.C., 1999. Biodegradation of explosives by transgenic plants expressing pentaerythritol tetranitrate reductase. Nature Biotechnology, vol 17., May 1999, 491-494. http://biotech.nature.com

Frese, I., Krämer, P.M., Ciumasu, I.M., Weber, C.M., Kolb, G., Tiemann, D., Development of an optical detection cell for an automated miniaturized immunochemical device for on-site screening of pesticide residues in water. Oral presentation at Sensor 2003, May 13-15, 2003, Nürnberg, F.R.G.

Fu, S., Chu, S., Xu, X., 2001. Organochlorine pesticide residue in soils from Tibet, China. Bull. Environ. Contam. Toxicol., 66, 171-177.

Gabaldon, J.A., Maquieira, Puchades, R., 1999. Current trends in immunoassay-based kits for pesticide analysis. Critical Reviews in Food Sciences and Nutrition, 39 (5), 519-538.

Garrett, S.M., 2003. A paratope is not an epitope: implications for immune network models and clonal selection. ICARIS-2003, Springer-Verlag Lecture Notes in Computer Science, 2787, 217-228.

Gauger, P.R., Holt, D.B., Patterson Jr., C.H., Charles, P.T., Shriver-Lake, L., Kusterbeck, A.W., 2001. Explosives detection in soil using a field-portable continuous flow immunosensor. J. Haz. Mat., 83, 51-63.

Gerdes, M., Meusel, M., Spener, F., 1999. Influence of antibody valency in a displacement immunoassay for the quantitation of 2,4-dichlorophenoxy-acetic acid. Journal of Immunological Methods, 223, 217-226.

Gilcrease, P.C. and Murphy, V.G., 1995. Aerobic biotransformation of 2,4,6-trinitrotoluene (TNT) by *Pseudomonas fluorescens*. Proceedings of the 10th Annual Conference on Hazardous Waste Research 1995. The Great Plains/Rocky Mountains hazardous Substances Research Center.

Gobi, K.V., Mizutani, F., 2001. Amperometric detection of superoxide dismutase at cytochrome c-immobilized electrodes: xantine oxidase and ascorbate oxidase incorporated biopolymer membrane for *in-vivo* analysis. Anal. Sci. 17 (January), 11-15.

Godejohann, M., Preiss, A., Mügge, C. Wünsch, G., 1997. Application of on-line HPLC-^{1}H NMR to environmental samples: Analysis of groundwater near former ammunition plants. Anal. Chem. 69, 3832-3837.

Godejohann, M., Astratov, M., Preiss, A., Levsen, K, Mügge, C., 1998. Application of continuous-flow HPLC – proton nuclear magnetic resonance spectroscopy and HPLC – thermospray-mass spectroscopy for the structural elucidation of phototransformation products of 2,4,6-trinitrotoluene. Analytical Chemistry, 70 (19), 4104-4110.

Goldman, E.R., Pazirandeh, M.P., Charles, P.T., Balighian, E.D., Anderson, G.P., 2002. Selection of phage displayed peptides for the detection of 2,4,6-trinitrotoluene in seawater. Anal. Chim. Acta 457, 13-19.

Goldman, E.R., Anderson, G.P., Lebedev, N., Lingerfelt, B.M., Winter, P.T., Patterson Jr, C.H., Mauro, M., 2003. Analysis of aqueous 2,4,6-trinitrotoluene (TNT) using a fluorescent displacement immunoassay. Anal. Bioanal. Chem. 375, 471-475.

Gong, P., Wilke, B.-M., Fleichmann, S., 1999. Soil-based phytotoxicity of 2,4,6-trinitrotoluene (TNT) to terrestial higher plants. Arch. Environ. Contam. Toxicol., 36, 152-157.

Gooding, J.J., Erokhin, P., Losic, D., Yang, W., Policarpio, V., Liu, J., Ho, F.M., Situmorang, M., Hibbert, D.B., Shapter, J.G., 2001. Analytical Sciences, by The Japan Society for Analytical Chemistry, 17, 3-9.

Gottlieb, J., Huck, K., Maurer, A., 1997. Field Screening – neue Methoden und Strategien by der Umweltanalytik vor Ort. Field screening – new methods and strategies for an environmental on-site analysis. GIT Labor-Fachzeitschrift 1/97, 48-50.

Green, T.M., Charles P.T., Anderson, G.P., 2002. Detection of 2,4,6-trinitrotoluene in seawater using a reversed-displacement immunosensor. Anal. Biochem. 310, 36-41.

Grübler, A., Nakicenovic, N., and Victor, D.G., 1999. Modeling technological change: implications for the global environment. Annual Reviews Enery & the Environment, 24 (1), 545-569.

Hallock, P., Barnes, K., and Fisher, E.M., 2004. Corral-reef risk assessment from satellites to molecules: a multiscale approach to environmental monitoring and risk assessment of coral reeffs. Environmental Micropaleontology, Microbiology and Meiobenthology, 1, 11-39.

Hanazato, T., 2001. Pesticide effects on freshwater zooplancton: an ecological perspective. Environmental Polution, 112, 1-10.

Harper, M., Glowacki, C.R., and Michael, P.R., 1997. Industrial hygiene. Anal. Chem. 69, 307R-327R.

Harvey, S.D., Galloway, H., Krupsha, A., 1997. Tracer analysis of military high explosives (2,4,6-trinitrotoluene and hexahydro-1,3,5-trinitro-1,3,5-triazine) in agricultural crops. Journal of Chromatography A, 775, 117-124.

Haupt, K., and Mosbach, K., 1998. Plastic antibodies: developments and applications. TibTech (Elsevier), 16, 468-475.

Hawari J, Halasz L, Paquet E, Zhou B, Spencer G, Ampleman, Thiboutot S: Characterization of metabolites in the biotransformation of 2,4,6-trinitrotoluene with anaerobic sludge. (1998) Applied and Environmental Microbiology, 64 (6), 2200-2206. http://intl-aem.asm.org/cgi/reprint/64/6/2200.pdf

Hawthorne, S.B., Lagadec, A.J.M., Kalderis, D., Lilke, A.V., Miller, D.J., 2000. Pilot-scale destruction of TNT, RDX, and HMX on contaminated soils using subcritcal water. Environ. Sci. Technol., 34, 3224-3228.

Hayashi, Y., Matsuda, R., Ito, K., Nishimura, W., Imai, K., Maeda, M., 2005. Detection limit estimated from slope of calibration curve: an application to competitive ELISA. Analaytical Sciences 21, 167-169.

Heiss, C., Weller, M.G., Niessner, R., 1999. Dip-and-read test strips for the determination of trinitrotoluene (TNT) in drinking water. Anal. Chim. Acta, 396, 309-316.

Heller, C.A., Grenl, S.R., Erickson, E.D., 1982. Field detection of 2,4,6-trinitrotoluene in water by ion-exchange resins. Anal. Chem., 54, 286-289.

Hewit, A.D, Jenkins, T.F., 1999. On-site method for measuring mitroaromatic and nitramine explosives in soil and groundwater using GC. Special Report 99-9, U.S. Army Cold Regions Research and Engineering Laboratory. http://www.crrel.usace.army.mil/techpub/CRREL_Reports/reports/SR99_09.pdf

Hilmi, A., Luong, J.H.T., Nguyen, A-.L., 1999. Determination of explosives in soil and ground water by liquid chromatography – amperometric detection. Journal of Chromatography A, 844, 97-110.

Hilmi, A., Luong, J.H.T., 2000. Micromachined electrophoresis chips with electrochemical detectors for analysis of explosive compounds in soil and groundwater. Environ. Sci. Technol., 34, 3046-3050.

Hock, B., Rahman, M., Rauchalles, S., Danwardt, A., Seifert, M., Haindl, S., Kramer, K., 1999. Stabilisation of immunoassays and receptor assays. Journal of Molecular Catalysis B: Ezymatic, 7, 115-124.

Hock, B., Rothe, S., and Seifert, M., 2000a. Hormone in der Umwelt – die Tests im Überblick. Nachricht aus der Chemie, 48, 918-924.

Hock, B., Kramer, K., and Seifert, M., 2000b. Environmental analysis using antibody and receptor based techniques. Intern. J. Environ. Anal. Chem., vol. 73 (3-4), Special issue – Proceedings of the 3rd Euroconference on Environmental Analytical Chemistry, Chalkidiki, Greece, 9-15 Oct, 1999, 289-303.

Hoffmann, I., Warrelmann, J., Jastorff, B., Schultz-Berendt, V., Werner, P., 1999. Reinigung sprengstoffbelasteter Wässer durch ein chemisches Reduktionsverfahren. TerraTech, 2, 49-51.

Hofstetter, T.B., Heijman, C.G., Haderlein, S.B., Holliger, C., and Schwarzenbach, R.P., 1999. Complete reduction of TNT and other (poly)nitroaromatic compounds under iron-reducing subsurface conditions. Environ. Sci. Technol., 33, 1479-1487.

Holt, D.B., Kusterbeck, A.W., Ligler, F.S., 2000. Continuous flow displacement immunosensors: a computational studies. Analytical Biochemistry, 287, 234-242.

Holt, D.B., Gauger, P.R., Kustebeck, A.W., Ligler, F.S., 2002. Fabrication of a capillary immunosensor in polymethyl methacrylate. Biosens. Bioelectron. 17, 95-103.

Honeychurch, K.C., Hart, J.P, Pritchard, P.R.J., Howkins, S.J., Ratcliffe, N.M, 2003. Development of an electrochemical assay for 2,6-dinitrotoluene, based on a screen-printed carbon electrode, and its potential application in bioanalysis, occupational and public health. Biosens. Bioelectron. 19, 305-312.

Hooker, B.S., and Skeen, R.S., 1999. Transgenic phytoremediation blasts onto scene. Nature Biotechnology, 17, May 1999, 428.

Horacek, J., and Skladal, P., 2000. Effect of organic solvents on immunoassays of environmental pollutants studied using a piezoelectric biosensor. Analytica Chimica Acta, 412, 37-45.

Hudson, P.J., Souriau, C., 2003. Engineered antibodes. Nature Medicine, 9 (1), 129-134.

Hulpke, H., Müller, G., Wendt, H., 2000. Ökotoxicologie – Basis unserer Chemikaliensicherheit. Nachrichten aus der Chemie, 48, 1066-1068.

Hundal, L.S., Powers, W.L., Shea, P.J., Confort, S.D., McCallister, D.L., 1995. TNT sorption and bound residue formatio in soil. In Proceedings of the 10th Annual Conference on hazardous Waste Research 1995, by the GreatPlains/Rocky Mountain hazardous Substance Research Center, USA. http://www.engg.ksu.edu/HSRC/95Proceed/hundal.html

Hwang, F., Chow, T., Adrian, N.R., 1998. Transformation of TNT to triaminotoluene by mixed cultures incubated under methanogenic conditions. US Army Corps of Engineers. USACERL Technical Report 98/116, September 1998.

Jager, T., Vermeire, T.G., Rikken, M.G.J., Van der Poer, P., 2001. Opportunities for a probabilistic risk assessment of chemicals in the European Union. Chemosphere, 43 (2), 257-264.

Jenkins, T.F., Walsh, M.E., Schumacher, P.W., Miyares, P.H., Bauer, C.F., and Grant, C.L., 1989. Liquid chromatographic method for the determination of extractable nitroaromatic and nitramine residues in soil. Journal of the AOAC, 72, 890-899.

Jenkins, T.F., Walsh, M.E., 1992. Development of field screening methods for TNT, 2,4-DNT and RDX in soil. Talanta 39, 419-428.

Jenkins, T.F., Thorne, P.G., McCormick, E.F., Myers, K.F., 1995a. Preservation of water samples containing nitroaromatics and nitramines. Special Report 95-16, U.S. Army Cold Regions Research and Engineering Laboratory. http://www.crrel.usace.army.mil/techpub/CRREL_Reports/reports/SR95_16.pdf

Jenkins, T.F., Thorne, P.G., Myers, K.F., McCormick, E.F., Parker, D.E., Escalon, B.L., 1995b. Evaluation of the new clean solid phases for extraction of nitroaromatics and nitramines from water. Special Report 95-22, U.S. Army Cold Regions Research and Engineering Laboratory.

http://www.crrel.usace.army.mil/techpub/CRREL_Reports/reports/SR95_22.pdf

Jenkins, T. F., Schumacher, P.W., Mason, J.G., and Thorne, P.G., 1996a. On-site analysis for high concentrations of explosives in soil - extraction kinetics and dilution procedure. Special Report 96-10, U.S. Army Cold Regions Research and Engineering Laboratory. http://www.crrel.usace.army.mil/techpub/CRREL_Reports/reports/SR96_10.pdf

Jenkins, T.F., Grant, C.L., Brar, G.S., Thorne, P.G., Ranney, T.A., Schumacher, P.W., 1996b. Assessment of sampling error associated with collection and analysis of soil samples at explosives-contaminated sites. Special Report 96-15, U.S. Army Cold Regions Research and Engineering Laboratory. http://www.crrel.usace.army.mil/techpub/CRREL_Reports/reports/SR96_15.pdf

Jenkins, T.F., Grant, C.L., Brar, P.G., Thorne, P.G., Schumacher, P.W., Ranney, T.A., 1997a. Sampling error associated with collection and analysis if soil samples at TNT-contaminated sites. Field Anal. Chem. Technol., 1, 151-163.

Jenkins, T.F., Walsh, M.E., Thorne, P.G., Thiboutot, S., Ampleman, G., Ranney, T.A., Grant, C.L., 1997b. Assessment of sampling error associated with collection and analysis of soil samples at a firing range. Special Report 97-22, U.S. Army Cold Regions Research and Engineering Laboratory. http://www.crrel.usace.army.mil/techpub/CRREL_Reports/reports/SR97_22.pdf

Jenkins, T.F., Walsh, M.E., Thorne, P.G., Miyares, P.H., Ranney, T.A., Grant, C.L., and Esparza, J.R., 1998. Site characterization for explosives contamination at a military firing range impact area. Special Report 98-9, U.S. Army Cold Regions Research and Engineering Laboratory. http://www.crrel.usace.army.mil/techpub/CRREL_Reports/reports/SR98_09.pdf

Jenkins, T.F., Pennington, J.C., Ranney, T.A., Berry Jr., T.E., Miyares, P.H., Walsh, M.E., Hewitt, A.D., Perron, N.M., Parker, L.V., Hayes, C.A., and Wahlgren, E.G., 2001. Characterization of explosives contamination at military firing ranges. U.S. Army Corps of Engineers, Technical Report ERDC TR-01-5.

Johnson, M.S., 1998. Development and application of non-traditional Vertebrate models to investigate terrestrial ecological risk to 2,4,6-trinitrotoluene exposure. Virginia Polytechnic Institute and State University, Maryland-Virginia.

http://scholar.lib.vt.edu/theses/available/etd011199140153/unrestricted/dissertation4.pdf

Jortani, S.A., Miller, J.J., Helm, R.A., Johnson, N.A., Valdes, R. Jr., 1996. Suppresion of immunoassay results by cross-reactivity. J. Clin. Ligand Assay, 20, 177-179.

Karu, A.E., Harrison, R.O., Schmidt, D.J., Clarkson, C.E., Grassman, J., Goodrow, M.H., Lucas, A., Hammock, B.D., Van Emon, J.M., and White, R.J., 1991. Monoclonal immunoassay of triazine herbicides: development and implementation. In: Vanderlaan, M., Stanker, L.H., Watkins, B.E., Roberts, D.W. (Eds.), Immunoassays for trace chemical analysis: monitoring toxic chemicals in humans, food and the environment. ACS Symposium Series 451, American Chemical Society, Washington, DC, USA, 59-77.

Karu, A.E., Goodrow, M.H., Schmidt, D.J., Hammock, B.D., Bigelow, M.W., 1994. Synthesis of haptens and derivation of monoclonal antibodies for immunoassay of the phenylurea herbicide diuron. J. Agric. Food Chem., 42, 301-309.

Katagiri, M., Kadoya, T., Miyake, K., Ishibashi, F., Ohkawa, H., 1999. Effects of methanol and temperature on enzyme immunoassay with monoclonal antibodies specific to the insecticide etofenprox. Biosci. Biotechnol. Biochem., 63 (11), 1988-1990.

Keith, L.H., 1997. Environmental endocrine disruptors. A handbook of property data. John Wiley and Sons, New York, 1232 p., ISBN 0-471-19126-4

Kelly, J., 2004. Gunpowder: alchemy, bombards & pyrotechnics. United Dragon Holdings Inc. ISBN 0-465-03718-6.

Kettrup, A., Steinberg, C., Freitag, D., 1991. Ökotoxicologie – Wirkungserfassung und Bewertung von Schadstoffen in der Umwelt. UWSF-Z. Umweltchem. Ökotox., 3 (6), 370-377.

Keuchel, K., Weil., L., Niessner, R., 1993. Development of an enzyme immunoassays for the determination of 2,4,6-trinitrotoluene – probing the influence of humic acids. In Vo-Dinh, T. and Cammenn, K. (Eds). Proceedings of SPIE – volume 1716. International Conference on Monitoring of Toxic Chemicals and Biomarkers, 44-50.

Keuchel, C., and Niessner, R., 1994. Rapid field screening for determination of 2,4,6-trinitrotoluene in water and soil with immunofiltration. Analytical and Bioanalytical Chemistry, 350 (7-9), 538-543.

Kim, H.-Y., Song, H.-G., Transformation of 2,4,6-trinitrotoluene by white rot fungus *Irpex lacteus*. Biotechnology Letters, 22 (12), 969-975.

Kipriyanov, S.M., Little, M., Kropshofer, H., Breitling, F., Gotter, S., Dubel, S., 1996. Affinity enhancement of a recombinant antibody: formation of complexes with multiple valency by a single-chain Fv fragment-core streptavidin fusion. Protein Engineering, 9, 203-211.

Kleinstein, S.H., Seiden, P.E., 2000. Simulating the immune system. Computing in Science & Engineering, July/August 2000, 69-76.

Klibanov, A.M., 2001. Improving enzymes by using them in organic solvents. Nature, vol. 409, 11 Januray 2001, 241-246.

Knicker, H., and Müller, P., 2003. Binding of trinitrotoluene (TNT) to water extractable humus. Environmental Chemistry Letters, 1 (2), 121-125.

Knopp, D., 2000. Antikörper – Biomoleküle zur selectiven Anreichung organischer Analyten. Nachrichten aus Chemie, 48, 1056-1061.

Kohen, F., Kim, J.B., Lindner, H.R., Eshhar, Z., Green, B.S., 1980. Monoclonal immunoglobulin G augments hydrolysis of an ester of the homologous hapten. FEBS Letters 111, 427-431.

Köhne, A.P., Dornberger, U., Welsch, T., 1998. Two-dimentional high performance liquid chromatography for the separation of complex mixtures of explosives and their by-products. Chromatographia, 48 (1/2), 9-16.

Kolb, G., Frese, I., Hessel, V., Ciumasu, I.M., Krämer, P.M., Löwe, H., Tiemann D., 2004. An automated, portable immunochemical flow-injection system for on-site analysis of environmentally hazardous chemicals. Oral Presentation at Lab Automation 2004, 1-5 February 2004, San Jose, CA, USA.

Korte, F., 1980. Chemikalien in Ökotest. Erste Voraussetzung: Bestandsaufnahme. Umschau, 80, Heft 21, 643-648.

Krämer, P.M., 1996. Biosensors for the measurement of pesticide residues in the environment: past, present, and future. J. AOAC Int, 79 (6), 1245-1254.

Krämer, P.M., 1998a. Automated imunochemical analysis of specific s-triazine and phenylurea herbicides in drinking water supplies. Food Technol. Biotechnol., 36 (2), p. 111-118.

Krämer, P.M., 1998b. A strategy to validate immunoassay test kits for TNT and PAHs as a field screening method for contaminated sites in Germany. Anal. Chim. Acta, 376, 3-11.

Krämer, P.M., Baumann, B.A., Stoks, P.G., 1997. Prototype of a newly developed immunochemical detection system for the determination of pesticides residues in water. Anal. Chim. Acta, 347 (1/2), 187-198.

Krämer, P.M., Goodrow, M.H., Kremmer, E., 2004a. Enzyme-linked immuno-sorbent assay based on rabbit polyclonal and rat monoclonal antibodies against isoproturon. J. Agric. Food Chem., 52, 2462-2471.

Krämer, P.M., Weber, C.-M., Ciumasu, I.M., Kremmer, E., Kettrup, A.A., 2004b, Development of monoclonal antibodies for 2,4,6-trinitrotoluene and its metabolites 2-amino-4,6-dinitrotoluene and 4-amino-2,6-dinitrotoluene for their use in immunosensors. Poster presentation at 'The Eighth World Congress on Biosensors', Granada, Spain, May 24-26, 2004 (Abstract book P2.4.60).

Krämer, P.M., Kremmer, E., Weber, C.-M., Ciumasu, I.M., Forster, S., Kettrup., A.A., 2005. Development of new rat monoclonal antibodies with different selectivities and sensitivities for 2,4,6-trinitrotoluene (TNT) and other nitroaromatic compounds. Anal. Bioanal. Chem. 382: 1919-1933. http://www.springerlink.com/(cams0xblxzdzdfjaeuhfquca55)/app/home/isue.asp

Kratz, W., Riesbeck, F., 1998. Die wirkung von Sprengstoffen in Böden einer miltärischen Altlast auf die Populationsentwicklung von *Folsomia candida* (Willem, 1902) (Collembola, Insecta). UWSF – Z. Umweltchem. Ökotox., 10 (3), 143-146.

Krausa, M., Doll, J., Schorb, K., Hambitzer, G., 1996. Elektrochemischer Detektor zur schnellen Bestimmung von Nitro- und Amino-aromaten in Böden und Wässern. TerraTech, 5, 36-38.

Krausa, M., 1998. Schneller Sprengstoff-Detektor. UmweltMagazin, Mai 1998, 94.

Kufer, P., Lutterbüse, R., Baeuerle, P.A., 2004. A revival of bispecific antibodies. Trends in Biotechnology, 22 (5), 238-244.

Kusterbeck, A.W., Charles, P.T.,1998. Field demonstration of a portable flow immunosensor. Field Anal. Chem. Techn. 2(6), 341-350.

Kusterbeck, A.W., Shriver-Lake, L., 2000. Explosives detecting immunosensors. ESTCP cost and performance report. Environmental security technology certification program. U.S. Department of Defense, Environmental Security Technology Certification Program (ESTCP), September 2000, Naval Research Laboratory 6900, Washington DC 20375.

Kypriyanov, S.M., Little, M., Kropshofer, H., Breitling, F., Gotter, S. and Dubel, S., 1996. Affinity enhancement of a recombinant antibody: formation of complexes with multiple valency by a single-chain Fv fragment-core streptavidin fusion. Protein Engineering, 9, 203-211.

Lan, E.H., Dunn, B., Zink, J.I., 2000. Sol-gel incapsulated anti-trinitrotoluene antibodies in immunoassays for TNT. Chem. Mater., 12, 1874-1878.

Larson, R.A., Jafvert, C.T., Bosca, F., Marley, K.A., and Miller, P.L., 2000. Effects of surfactants on reduction and photolysis (>290 nm) of nitroaromatic compounds. Environ. Sci. Technol., 34, 505-508.

Lau, P.C.K., and DeLorenzo, V., 1999. Genetic engineering: the frontier of bioremediation. New molecular tools and an improved understanding of biodegradative processes are slowly increasing prospects for successful technology deployment. Environmental Science & Technology, March 1, 124 A – 128 A.

Lavine, B.K., 2000. Clustering and classification of analytical data. InMeyers, R.A. (Ed.) Encyclopedia of Analytical Chemistry, John Wiley & Sons Ltd, Chichester. ISBN 0471 97670 9.

Lee, W., Oh, B.-K, Bae, Y.M., Paek, S.-H., Lee, W.H., Choi, J.-W., 2003. fabrication of self-assembled protein A monolayer and its application as an immunosensor. Biosensors and Bioelectronics, 19, 185-192.

Lemke, M., 1998. Sanieren ist Vertrauenssache. UmweltMagazin, April 1998, 43.

Lendemann, U., Spain, J.C., Smets, B.F., 1998. Simultaneous biodegradation of 2,4-dinitrotoluene and 2,6-dinitrotoluene in an aerobic fluidized-bed biofilm reactor. Environ. Sci. Technol., 32, 82-87.

Lenke, H., Warrelmann, J., Daun, G., Hund, K., Sieglen, U., Walter, U. and Knackmuss, H-.J., 1998. Biological tratment of TNT-contaminated soil. 2. Biologically induced immobilization of the contaminants and full-scale application. Environ. Sci. Technol., 32, 1964-1971.

Li, J., Cheng, G., Dong, S., 1996. Direct electron transfer to cytochrome c oxidase in self-assembled monolayers on gold electrodes. J. Electroanal. Chem. 416, 97-104.

Liron, Z., Tender, L.M., Golden, J.P., Ligler, F.S., 2002. Voltage-induced inhibition of antigen-antibody binding at conducting optical waveguides. Biosensors and Bioelectronics, 17, 489-494.

Luppa, P.B., Sokoll, L.J., Chan, D.W., 2001. Immunosensors – principles and applications to clinical chemistry. Clinica Chimica Acta, 314, 1-26.

Mallat, E., Barcelo, D., Barzen, C., Gauglitz, G., Abuknesha, R., 2001. Immunosensors for pesticide determination in natural waters. Trends Anal. Chem. 20(3), 124-132.

Manning, J.F., Boopathy, R., and Kulpa, C.F., 1994. A laboratory study in support of the pilot demonstration of a biological soil slurry reactor. U.S Army Environmental Center (USAEC), Aberdeen Proving Ground, Maryland 21010-5401. Report No. SFIM-AEC-TS-CR-94048.

Marion, G.,M., Pelton, D.K., 2000. Frozen soil barriers for explosives containment. U.S. Army Corps of Engineers, Technical Report ERDC /CRREL TR-00-19.

Martin, R.J., 2001. Comparing and contrasting some environmental and experi-mental design problems. Environmetrics, 12, 273-287.

Medary, R.T., 1992. Inexpensive, rapid field screening test for 2,4,6-trinitrotoluene in soil. Anal. Chim. Acta, 258, 341-346.

Medintz, I.L., Goldman, E.R., Lassman, M.E., Hayhurst, A., Kusterbeck, A.W., and Deschamps, J.R., 2005. Self-assembled TNT biosensor based on modular multifunctional surface-tethered components. Anal. Chem., 77, 365-372.

Meharg, A.A., Dennis, G.R., Cairney, J.W.G., 1997. Biotransformation of 2,4,6-trinitrotoluene (TNT) by ectomycorrhizal basidiomycetes. Chemosphere, 35 (3), 513-521.

Meusel, M., Trau D., Katerkamp, A., Meier, F., Polzius, R., Cammann, K., 1998. New ways in bioanalysis -- one-way optical sensor chip for environmental analysis. Sensors and Actuators B, 51, 249-255.

Meyer, R., 1985. Explosiv Stoffe. Sechste, überarbeitete und erweiterte Auflage. VCH VerlAggesellschaft.

Michels, J., 1998. Sprengstoff-Fabrik Werk Tanne. UmweltMagazin, Dezember 1998, 44-45.

Miller, J.J., Levinson, S.S., 1996. Interferences in immunoassays. In Diamandis, E.P. and Christopoulos, T.K., 1996. Immunoassays. Academic Press. ISBN 0-12-21-214730-8.

Miller, J.N., 2002a. Enzymatic analysis methods. In Ullmann's Encyclopedia of Industrial Chemistry., 2002, Wiley-VCH Verlag GmbH & Co. KGaA. Article on-line posting January 15, 2001.

Miller, J.N., 2002b. Enzymes and immunoassays. In Ullmann's Encyclopedia of Industrial Chemistry., 2002, Wiley-VCH Verlag GmbH & Co. KGaA. Article on-line posting January 15, 2001.

Miller, J.N., Niessner, R., Knopp, D., 2002. Enzyme and immunoassays. In Ullmann's Encyclopedia of Industrial Chemistry., 2002, Wiley-VCH Verlag GmbH & Co. KGaA. Revised January, 2001.

Montpas, S., Samson, J., Langlois, E., Lei, J., Pich, Y., Chnevert R., 1997. Degradation of 2,4,6-trinitrotoluene by *Serratia marcescens*. Biotechnology Letters, 19 (3), 291-294.

Morley, M.C., and Speitel Jr., G.E., 1999. Biodegradation of high explosives on granular activated carbon: enhanced desorption of high explosives grom GAC-Batch studies. Amarillo National Resource Center for Plotonium. Report ANRCP-1999-11.

Mörner, J., Bos., Fredrix, M., 2002. Reducing and eliminating the use of organic persistent pesticides. Guidance on alternatives strategies for sustainable pest and vector management. United Nations Environment Programme (UNEP) – Chemicals. http://www.chem.unep.ch/pops

Mueller, W.F., Bedell, G.W., Shojaee, S., Jackson, P.J., 1995. Bioremediation of TNT wastes by higher plants. Proceedings of the 10th Annual Conference on Hazardous Waste Research, by Kansas State University, 222-230.

Myers, K.F., McCormick, E.F., Strong, A.B., Thorne, P.G., Jenkins, T.F., 1994. Comparison of the commercial colorimetric and enzyme immunoassays field screening methods for TNT in soil. U.S. Army Corps of Engineers, Technical report IRRP-94-4.

Naal, Z., Park, J.-H., Bernhard, S., Shapleigh, J.P., Batt, C.A., Abruña, H.D., 2002. Amperometric TNT Biosensor based on the oriented immobilization of a nitroreductase maltose binding protein fusion. Anal. Chem. 74, 140-148.

Narang, U., Gauger, P.R., Ligler, F.S., 1997. A displacement flow immunosensor for explosive detection using microcapillaries. Anal. Chem. 69, 2779-2785.

Nash, J. and Ehrenfeld, J., 1997. Codes of environmental management practice: assessing their potential as a tool for change. Annual Reviews Energy & the Environment, 22 (1), 487-535.

Niessner, R., Knopp, D., 2002. Enzyme and immunoassays. In Ullmann's Encyclopedia of Industrial Chemistry., 2002, Wiley-VCH Verlag GmbH & Co. KGaA. Article on-line posting on January 15, 2001.

Nishino, S.F., Spain, J.C., Lenke, H., Knackmuss, H.-J., Mineralization of 2,4- and 2,6-dinitrotoluene in soil slurries. Environ. Sci. Technol., 33, 1060-1064.

Ntow, W.J., 2001. Organochlorine pesticides in water, sediment, crops, and human fluids in a farming community in Ghana. Arch. Environ. Toxicol., 40, 557-563.

Oehmichen, U., Schmitz, M., Seeliger, P., 2003. Die neue Trinkwasserverordung. Der Kommentar aus rechlicher und technisch-wirtschaftlicher Sicht. ISBN 3-89554-146-x, Wirtschafts- und VerlAggesellschaft Gas und Wasser mbH., 360 pages.

Oh, B.-T., Sarath, G., Shea, P.J., 2001. TNT nitroreductase from *Pseudomonas aeruginosa* strain isolated from TNT-contaminated soil. Soil Biology & Bio-chemistry, 33, 875-881.

Oks, J.P., and Stein, A., 2000. Use of decision trees to value investigation strategies for soil pollution problems. Environmetrics, 11, 315-325.

Opresko, D.M., 2005. Toxicity Sumary for 2,4,6-trinitrotoluene. The Risk Assessment Information System. Prepared for Oak Ridge Reservation Environmental Restoration Program. http://risk.lsd.ornl.gov/tox/profiles/2_4_6_trinitrotoluene.doc

Palazzo, A.J. and Leggett, D.C., 1986. Effect and disposal of TNT in a terrestrial plant. Journal of Environmental Quality 15, 49-52 (cited in Harvey et al., 1997).

PAN UK (Pesticide Action Network UK), 2000. Pesticides in water. Costs to health and the environment. Briefing 1, October 2000. http://www.pan-uk.org

PAN UK (Pesticide Action Network UK), 2001. The list of the lists. A catalogue of the lists of pesticides identifying those associated with particulary harmful health or environmental impacts. Briefing 3, November 2001. http://www.pan-uk.org

Pasti-Grigsby MB, TA Lewis, DL Crawford, and RL Crawford: Transformation of 2,4,6-trinitrotoluene (TNT) by actinomycetes isolated from TNT-contaminated and Uncontaminated Environments. (1996) Applied and Environmental Microbiology, 62 (3), 1120-1123. http://intl-aem.asm.org/cgi/reprint/62/3/1120.pdf

Penalva, L., Puchades, R., Maquieira, A., 1999. Analytical properties of immuno-sensors working in organic media. Anal. Chem., 71, 3862-3872.

Penalva, L., Puchades, R., Maquieira, A., Gee, S., Hammock, B.D., 2000. Development of immunosensors for the analysis of 1-naphtol in organic media. Biosensors & Bioelectronics, 15, 99-106.

Person, J.E., Gill, A., Vadgama, P., 2000. Analytical aspects of biosensors. (Review article) Ann. Clin. Biochem., 37, 119-145.

Pennington, J.C., Zakikhani, M., Harrelson, D.W., and Allen, D.S., 1999. Monitored natural attenuation of explosives in groundwater – Cost and performance. Technical Report EL-99-9. U.S. Army Engineer Waterways Experiment Station, Vicksburg, MS.

Pfortner, P., Weller, M.G., Niessner, R., 1998a. Immunological method for the detection of nitroaromatic residues covalently bound to humic acids. Fresenius J. anal. Chem., 360, 192-198.

Pfortner, P., Weller, M.G., Niessner, R., 1998b. Detection of bound nitroaromatic residues in soil by immunoassay. Fresenius J. anal. Chem., 360: 781-783.

Phelan, J.M., and Barnett, J.L., 2001. Solubility of 2,4-Dinitrotoluene and 2,4,6-trinitrotoluene in water. Journal of Chemical and Engineering Data, 46 (2), 375-376.

Piletsky, S.A., Piletska, E.V., Bossi, A., Karim, K., Lowe, P., Turner, A.P.F. Substitution of antibodies and receptors with molecularly imprinted polymers in enzyme-liked and fluorescent assays. Biosensors and Bioelectronics, 16, 701-707.

Pluckthun, A., Pack, P., 1997. New protein engineering approaches to multivalent and bispecific antibody fragments. Immunotechnology, 3 (2), 83-105.

Porter, R.R., 1972. Structural studies of immunoglobulins. Nobel lecture. http://nobelprize.org/medecine/laureates/1972/Porter-lecture.pdf

Preuss, A., Fimpel, J., Dieckert, G., 1993. Anaerobic transformation of 2,4,6-trinitrotoluene (TNT). Arch. Microbiol., 159, 345-353.

Psillakis, E., Naxakis, G., Kalogerakis, N., 2000. Detection of TNT-contamination in spiked-soil samples using SPME and GC/MS. Global Nest: the Int. J., 2(3), 227-236.

Pyell, H., 1997. MEKC und CEC miniaturisierte Trenntechniken. Nachr. Chem. Tech. Lab., 45 (1), 33-36.

Quinn, J., Patel, P., Fitzpatrick, B., Manning, B., Dillon, P., Daly, S., O'Kennedy, R., Alcocer, M., Lee, H., Morgan, M., Lang, K., 1999. Biosensors and Bioelectronics, 14, 587-595.

Rabbany, S.Y., Marganski, W.A., Kusterbeck, A.W., Ligler, F.S., 1998. A membrane-based displacement flow immunoassay. Biosensors and Bioelectronics, 13, 939-944.

Rabbany, S.Y., Lane, W.J., Marganski, W.A., Kusterbeck, A.W., Ligler, F.S., 2000. Trace detection of explosives using a membrane-based displacement immunoassay. J. Immunol. Methods, 246, 69-77.

Radenberg, T., Sidiropulos, D., 1998. Sanierung einer ehemaliger Sprengstoffabrik in Leverkusen. TerraTech 4/1998, 39-41.

Renner, T., Baumgarten, D., Unger, K.K., 1997. Analysis of organic pollutants in water at trace levels using fully automated solid-phase extraction coupled to high-performance liquid chromatography. Chromatographia, 45, 199-205.

Richardson, S.D., Water analysis. Anal. Chem., 73, 2719-2734.

Riefler, R.G., and Smets, B.F., 2000. Enzymatic reduction of 2,4,6-trinitrotoluene and related nitroarenes: kinetics linked to one-electron redox potentials. Environ. Sci. Technol., 34, 3900-3906.

Roda, A., Pasini, P., Guardili, M., Baraldini, M., Musiani, M., Mirasoli, M., 2000. Bio-and chemiluminescence in bioanalysis. Fresenius J. Anal. Chem., 366, 752-759.

Rodgers, J.D., and Bunce, N.J., 2001. Electrochemical tratment of 2,4,6-trinitrotoluene and related compounds. Environ. Sci. Technol., 35, 406-410.

Rodriguez-Mozaz, S., Marco, M.-P., Lopez de Alda, M.J., and Barcelo, D., 2003. Biosensors for environmental monitoring of endocrine disruptors: a review article. Analytical and Bioanalytical Chemistry, 378 (3), 588-598.

Rogers, K.R., and Gerlach, C.L., 1999. Update on Environmental Biosensors. Scientific understanding and technological development are advancing, but comercialization, with a few exceptions, has been slow. Environ. Sci. Technol., 33 (23), 501A – 506A.

Rogers, K.R., 2000. Principles of affinity-based biosensors. (review). Molecular Biotechnology, 14, 109-129.

Ruppert, T., Weil, L., and Niessner, R., 1992. Influence of water contents on the enzyme immunoassay for triazine herbicides. Vom Wasser, 8, 387-401.

Russell, A.J., Trudel, L.J., Skipper, P.L., Groopman, J.D., Tannenbaum, S.R., Klibanov, A.M., 1989. Antibody-antigen binding in organic solvents. Biochem. Biophys. Res. Commun., 158 (1), 80-85.

Ruzicka, J. and Hansen, E.H., 1975. Flow-injection analysis. Part I. A new concept of fast continuous flow analysis. Anal. Chim. Acta, 78, 145-147.

Sapsford, K.E., Charles, P.T., Petterson, C.H., Ligler, F., 2002, Demonstration of four immunoassay formats using the array biosensor. Anal. Chem., 74, 1061-1068.

Sabljic, A., and Peijnenburg, W., 2001. Modeling lifetime and degradability of organic compounds in air, soil, and water systems. IUPAC Technical Report. Pure Appl. Chem., 73 (8), 1331-1348.

Saupe, A., Garvens, H.J., Heinze, L., 1998. Alkalyne hydrolysis of TNT and TNT in soil followed by thermal treatment of the hydrolysates. Chemosphere, 36 (8), 1725-1744.

Sax, N.I. and Lewis, R.J., 1987. Hawley's Condensed Chemical Dictionary. 11th ed. Van Nostrand Co., New York, 1191.

Schäfer, R.K., 2002. Evaluation of the ecotoxicological threat of amunition derived compounds to the habitat function of soil. PhD thesis, Freien Universität Berlin.

Scheller, F.W., Wollenberger, U., Warsinke, A., and Lisdat, F., 2001. Research and development in biosensors. Current Opinion in Biotechnology, 12, 35-40.

Schmid, R.D. and Künnecke, W., 1990. Flow-injection analysis (FIA) based on enzymes or antibodies – applications in the life sciences. J. Biotechnol, 14, 3-31.

Schmidt, T.C., Steinbach, K., von Low, E., Stork, G., 1998. Highly polar metabolites of nitroaromatic compounds in ammunition wastewater. Chemosphere, 37 (6), 1079-1090.

Schmidt, A., Butte, W., 1999. Photocatalytic degradation of reduction products of 2,4,6-trinitrotoluene (TNT). Chemosphere, 36 (6), 1293-1298.

Schmidt, T.C., Steinbach, K., Buetehorn, U., Heck, K., Vokwein, U., Stork, G., 1999. Synthesis of refference substances for highly polar metabolites of nitroaromatic compounds. Chemosphere, 38 (13), 3119-3130.

Schmitz, M., 2001. Die neue Trinkwasserverordnung. Konsequenzen für Unternehmen, Behörden und Marktpartners. UTA 2/2001, 58-60.

Schneider, P., and Hammock, B.D., 1992. Influence of the ELISA format and the hapten-enzyme conjugate on the sensitivity of an immunoassay for s-Triazin herbicides using monoclonal antibodies. J. Agric. Food Chem., 40, 525-530.

Schneider, P., Gee, S.J., Kreissig, S.B., Harris, A. S., Krämer, P., Pilar Marco, M., Lucas, A.D., and Hammock, B.D., 1995. Troubleshooting during development and use of immunoassays for environmental monitoring. In. New Frontiers in Agrochemical Immunoassays. Kurtz, D.A., Skerritt, J.H., Stanker, L. (Eds). AOAC International, Arlington, VA, USA. Chapter 8, 103-122.

Schneider, U., Weingran, C., Wolf, M., 1996. Einstieg in die Bodensanierung an den hessischen Rüstungsaltstandorten. TerraTech 2/1996, 40-43.

Schobel, U., Barzen, C., Gauglitz, G., 2000. Immunoanalytical techniques for pesticide monitoring, based on fluorescence detection. Fresenius J. Anal. Chem., 366, 646-658.

Schoenmuth, B., 2002. Freilandversuche zur TNT-Dekontamination und [14C]-TNT-Aufnahme durch Gehölze. Teilvorhaben 3.6 des BMBF-Verbundvorhabens Biologische Sanierung von Rüstungsaltlasten. Abschlussbericht, Kurzfassung. http://www.dendroremediation.de/bericht2002/ab-0kurzbericht.pdf

Schrader, P.S., and Hess, T.F., 2004. Coupled abiotic-biotic mineralization of 2,4,6-trinitrotoluene (TNT) in soil slurry. Journal of Environmental Quality, 33, 1202-1209.

Schuster, R., and Gratzfeld-Huesgen, A., 1993. HPLC analysis of explosive constituents in soil samples. Application note. Copyright © Agilent Technologies. http://www.agilent.com/chem

Schütz, A.J., Winklmair, M., Weller, M.G., Niessner, R., 1997. Stabilization of Horseradish peroxidase (HRP) for the use in immunochemical sensors. SPIE, 3105, 332-340.

Schütz, A.J., Winklmair, M., Weller, M.G., Niessner, R., 1999. Selection of hapten structures for indirect immunosensor arrays. Fresenius J. Anal. Chem., 363, 625-631.

Schwendner, A., 1996. Gefärdungsabschätzung für die ehemalige Munitions-anstalt Feucht. TerraTech 2/1996, 24-31.

Schwesinger, F., Ros, R., Strunz, T., Anselmetti, D., Güntherod, H.-J., Honegger, A., Jermutus, L., Tiefenauer, L., Plückthum, A., 2000. Unbinding forces of single antibody - antigen complexes correlate with their thermal dissociation rates. Proc. Natl. Acad. Sci. USA 97, 9972-9977.

Selby, C., 1999. Interference in immunoassays. (Review artice). Ann. Clin. Biochem., 36, 704-721.

Sembries, S., and Crawford, R.L., 1997. Production of *Clostridium bifermentans* spores as inoculum for bioremediation of nitroaromatic contaminants. Applied and Environmental Microbiology, 63 (5), 2100-2104. http://intl-aem.asm.org/cgi/reprint/63/5/2100.pdf

Sequeira, M., Bowden, M., Minogue, E., Diamond, D., Towards autonomous environmental monitoring systems. Talanta, 56, 355-363.

Setford, S.J., Kröger, S., and Turner, A.P.F., 1999. Organic phase immunosensors. Analusis, 27 (7), 600-609.

Setford, S. J., 2000. Immunosensing in organic and mixed aqueous-organic phase environments. Trends in analytical chemistry, 19 (5), 330-339.

Shan, G., Lipton, C., Gee, S.G., Hammock, B.D., 2002. Immunoassay, biosensors and other nonchromatographic methods. In Lee, P.W. (Ed.), Handbook of residue analytical methods for agrochemicals (ISBN 0471 49194 2), John Wiley & Sons, Ltd, Chichester, 2002, 623-679.

Shriver-Lake, L.C., Charles, P.T., Kusterbeck, A.W., 2003. Non-aerosol detection of explosives with a continuous flow immunosensor. Anal. Bioanal. Chem. 377 (3), 550-555.

Sigg, L., Behra, P., Stumm, W., 2001. Chiemie des milieux aquatique. Chimie des eaux naturelles et des interfaces dans l'environment. DUNOD, 3e édition, revisée et augmentée, 567 pages.

Sohn, H., Calhoun, R.M., Sailor, M.J., Trogler, W.C., 2001. Detection of TNT and picric acid on surfaces and in seawater by using photoluminescent poly-siloles. Angew. Chem. Int. Ed., 40 (11), 2104-2105.

Spanggord, R.J., Yao, C.D., and Mill, T., 1997. Investigation of the kinetics and products resulting from the reaction of peroxone with amino-dinitrotoluenes. US Army Corps of Engineers, Cold Regions Research & Engineering Laboratory (CRREL), Special report 97-5.

Spanggord, R.J., Yao, C.D., and Mill T., 2000a. Kinetics of amino-dinitrotoluene oxidations with ozone and hydroxyl radical. Environ. Sci. Technol., 34, 450-454.

Spanggord, R.J., Yao, C.D., and Mill T., 2000b. Oxidation of amino-dinitrotoluenes with ozone: products and pathways. Environ. Sci. Technol., 34, 497-504.

Spiegel, K., and Welsch, T., 1997. Monitoring degradation processes of explosives by HPLC analysis with UV-and amperometric detection. Fresenius J. Anal. Chem., 357, 333-337.

Stadlbauer, E.A., 1999. Analytik und Toxicologie von Rüstungsaltlasten. GIT Labor-Fachzeitscrift 4/99, 405-407.

Stahl, J.D., and Aust, S.D., 1993a. Metabolism and detoxification of TNT by *Phanerochete chrysosporium*. Biochemical and Biophysical Research Communications, 192 (2), 477-482.

Stahl, J.D., and Aust, S.D., 1993b. Plasma membrane dependent reduction of 2,4,6-trinitrotoluene by *Phanerochete chrysosporium*. Biochemical and Biophysical Research Communications, 192 (2), 471-476.

Stefan, R.I., Van Staden, J.F.K., Aboul-Enein, H.Y., 2000. Immunosensors in clinical analysis. Fresenius J. Anal. Chem., 366, 359-668.

Stern, P., 2001. Interference during immunoanlyses (Review). Biomarkers and Environment, 4 (1-2). http://www.cechtuma.cz/bioenv/2001/1-2/11-en.html

Strategic Diagnostics Inc., 1997, Quality control of immunoassays for pesticides residues. Strategic Diagnostics Inc. 128 Sandy Drive, Newark, DE 19713, USA. http://www.sdix.com/TechSupport/bulletins/t00029.pdf

Stockholm Convention on Persistent Organic Pollutants, adopted on 22 May 2001, by the conference of plenipotentiaries, by the invitation of UNEP Governing Council Decision 19/13C, and after being prepared by an Intergovernmental Negotiating Committee (INC).

Stöcklein, W., Scheller, F.W., Abuknesha, R., 1995. Effects of organic solvents on semicontinuous immunochemical detection of coumarin derivatives. Sensors and actuators B, 24-25, 80-84.

Stöcklein, W., Warsinke, A., Micheel, B., Kempter, G., Höhne, W., Scheller, F.W., 1998. Diphenylurea hapten sensing with a monoclonal antibody and ist Fab fragment: Kinetic and thermodynamic investigations. Analytica Chimica Acta, 362, 101-111.

Strachan, G., Whyte, J.A., Molloy, P.M., Paton, G.I, and Porter, A.J.R., 2000. Development of robust, environmental, immunoassays formats for the quantification of poesticides in soil. Environ. Sci. Technol. 34, 1603-1608.

Strandth, M., 2000. Insights into weak affinity antibody-antigen interactions. Studies using affinity chromatography and optical biosensor. University of Kalmar, Sweden. ISBN 91-628-4481-4.

Sun, W., Jiao, K., Zhang, S., Zhang, C., Zhang, Z., 2001. Electrochemical detection for horseradish peroxidase-based enzyme immunoassay using p-amino-phenol as substrate and its application in detection of plant virus. Analytica Chimica Acta, 434, 43-50.

Sung, M.M., and Kim, Y., 2001. Self-assembled monolayers of alkanethiols on clean copper surfaces. Bull. Korean Chem. Soc., 22 (7), 748-752.

Suo, Z., Gao, Y.F., Scoles, G., 2004. Nanoscale domain stability in organic mono-layers on metals. Journal of Applied Mechanics, by The American Society of Mechanical Engineers (ASME), 71, 24-31.

Tan, E.L., Ho, C.H., Griest, W.H., Tyndall, R.L., 1992. Mutagenicity of trinitrotoluene and its metabolites formed during composting. Journal of Toxicology and Environmental Health, 36, 165-175.

Tharakan, J.P., Gordon, J.A., 1999. Cometabolic biotransformation of trinitrotoluene (TNT) supported by aromatic and non-aromatic cosubstrates. Chemosphere, 38 (6), 1323-1330.

Thompson, F.L., Ramer, L.A., and Schnoor, J.L., 1998. Uptake and transformation of TNT by hybrid Poplar trees. Environ. Sci. Technol., 32, 975-980.

Thompson, P.L., Moses, D.D., Howe, K.M., 2003. Phytorestoration at the Iowa Ammunition Plant. In Mc Cutcheon, S.C., and Schnoor, J.L. (Eds), 2003. Phytoremediation. Transformation and control of contaminants. John Wileys & Sons, Inc. ISBN 0471394351.

Thorne, P.G., and Myers, K.F., 1997. Evaluation of commercial enzyme immunoassays for the field screening of TNT and RDX in water. US Army Corps of Engineers, Cold Regions Research & Engineering Laboratory (CRREL), Special report 97-32.

Thorne, P.G., and Leggett, D.C., 1999. Investigations of explosives and their conjugated transformation products in biotreatment matrices. US Army Corps of Engineers, Cold Regions Research & Engineering Laboratory (CRREL), Special report 99-3.

Tijssen, P. 1985. Practice and theory of enzyme immunoassays. Series Laboratory techniques in biochemistry and molecular biology; v15. Elsevier Science Publishers B.V., Amsterdam, The Netherlands.

Tope, A.M., Jamil, K., and Baggi, T.R., 1999. Transformation of 2,4,6-trinitrotoluene (TNT) by immobilized and resting cells of *Arthrobacter sp..* Journal of Hazardous Substance Research, 2, 3-1 – 3-9.

Torrance, L., 1998. Immunological detection and quantification methods. Proceedings of OECD Workshop Molecular Technologies for Safe Drinking Water, Interlaken '98, 5-8 July, Interlaken, Switzerland. http://www.eawag.ch/publications_e/proceedings/oecd.html

Trojanowicz, M., 2000. Flow-injection analysis. Instrumentation and applications. World Scientific Publishing Co. 496 pp. ISBN 981-02-2710-8

Turner, A.P.F., 2005. Biosensors 2004 – The Eight World Congress on Biosensors, 24-26 May, 2004, Granada, Spain. Biosensors and Bioelectronics, 20 (8), 1459-1460.

United Nations Environmental Programs (UNEP). Proceedings of "UNEPworkshop to develop a global POPs monitoring programme to support the effectiveness evaluation of the Stockholm Convention. Geneva, 24-27 May 2003. www.chem.unep.ch/gmn/Files/popsmonprg_proc.pdf

United Nations Environmental Programs (UNEP) – Chemicals, Geneva. Guidance for a global monitoring programme for persistent Organic Pollutants. 1st edition, June 2004. www.chem.unep.ch/gmn/GuidanceGPM.pdf

U.S. Army Center for Health Promotion and Preventive Medicine (USACHPPM), 2000. Wildlife toxicity assessment for 2-amino-4,6-dinitrotoluene and 4-amino-2,6-dinitrotoluene. Project Number 39-EJ1138-01C, Aberdeen Proving Ground,

Maryland, October 2000. Key technical authors: Holdsworth, G., Johnson, M.S., and Janus, E.R.

U.S. ATSDR (U.S. Agency for Toxic Substances and Disease Registry), 2003. Toxicological profile for Atrazine. CAS# 1912-24-9. http://www.atsdr.cdc.gov/toxprofiles/tp81.html

U.S. ATSDR (U.S. Agency for Toxic Substances and Disease Registry), 1995. Toxicological profile for 2,4,6-trinitrotoluene (TNT). CAS# 118-96-7. http://www.atsdr.cdc.gov/toxprofiles/tp81.html

U.S. EPA, 1990. Health and environmental effects document for 2,4,6-trinitrotoluene. Environmental criteria and assessment office, Office of Health and Environmental asesment, Cincinnati, OH, ECAO-CIN-G89.

U.S. EPA Method 8330, 1994. Nitroaromatics and nitramines by high performance liquid chromatography. U.S. Environmental Protection Agency, Office of Solid Waste and Emergency Response, Washington, DC, SW-846, Revision 0.

U.S. EPA Method 4050, 1996. TNT explosives in soil by immunoassay. U.S. Environmental Protection Agency (EPA), Office of Solid Waste and Emer-gency Response, Washington, DC, SW-846, Revision 0.

U.S. EPA 8095, 2000. Explosives by gas chromatography. U.S. Environmental Protection Agency, November 2000.

U.S. EPA 5360 A1, 2000. EPA Quality manual for environmental programs. U.S. Environmental Protection Agency (EPA). Document 5360 A1, May 5, 2000.

U.S. EPA QA/R-2, 2001. EPA Requirements for quality management plans. Document EPA/240/B-01/002. U.S. Environmental Protection Agency (EPA), March 2001.

U.S. EPA NPL, 2005. National priorities list. U.S. Environmental Protection Agency. http://www.epa.gov/superfund/sites/npl/npl.htm

U.S. Department of the Army, 1987, Technical Manual 5-814-8 – Evaluation criteria guide for water pollution prevention, control and abatement programs.

Valdes, R.Jr., Jortani, S.A., 2002. Unexpected suppression of immunoassays results by cross-reactivity: now a demonstrated cause for concern. Clinical Chemistry, 48 (3), 405-406.

Van Bergen, S.K., Bakaltcheva, I.B., Lundgren, J.S., Shriver-Lake, L.C., 2000. On-site detection of explosives in groundwater with a fiber optic biosensor. Environ. Sci. Technol., 34, 704-708.

Van Emon, J.M., 2001. Immunochemical applications in environmental sciences. Journal of AOAC International, 84 (1), 125-132.

Van Regenmortel, M.H.V., 2004. Reductionism and complexity in molecular biology. EMBO Reports, 5 (11).

Vasilyeva, G.K., Kreslavski, V.D., Oh, B-.T., and Shea, P.J., 2001. Potential of activated carbon to decrease 2,4,6-trinitrotoluene toxicity and accelerate soil decontamination. Environmental Toxicology and Chemistry, 20 (5), 965-971.

Vijayendran, R.A., Leckband, D.E., 2001. A quantitative assessment of hetero-geneity for surface-immobilized proteins. Anal. Chem., 73, 471-480.

Vining, R.F., Compton, P., McGinley, R., 1981. Steroid radioimmunoasays – effect of shortened incubation time on specificity. Clinical Chemistry, 27 (6), 910-913.

Vorbeck, C., Lenke, H., Fischer, P., Spain, J.C., and Knackmuss, H.-J., 1998. Initial reductive reactions in aerobic microbial metabolism of 2,4,6-trinitrotoluene. Applied and Environmental Microbiology, 64 (1), 246-252. http://intl-aem.asm.org/cgi/reprint/64/1/246.pdf

Wallenborg, S.R., Bailey, C.G., 2000. Separation and detection of explosives on a microchip using micellar electrokinetic chromatography and indirect laser-induced fluorescence. Anal. Chem., 72, 1872-1878.

Walsh, M.E., Jenkins, T.F., and Thorne, P.G., 1995. Laboratory and analytical methods for explosives residues in soil. Journal of Energetic Materials, 13, 357-383.

Walsh, M.E., Ranney, T., 1998a. Determination of nitroaromatic, nitramine, and nitrate ester explosives in water using solid-phase extraction and gas chromatography – electron capture detection: comparison with high performance liquid chromatography. Journal of Chromatographic science, 36, 406-416.

Walsh, M.E., and Ranney, T.A., 1998b. Determination of nitroaromatic, nitramine, and nitrate ester explosives in water using SPE and GC-ECD. CRREL Report 98-2, U.S. Army Cold Regions Research and Engineering Laboratory. http://www.crrel.usace.army.mil/techpub/CRREL_Reports/reports/CR98_02.pdf

Walsh, M.E., Ranney, T.A., 1999. Determination of nitroaromatic, nitramine, and nitrate ester explosives in soil using GC-ECD. Special Report 99-12, U.S. Army Cold Regions Research and Engineering Laboratory. http://www.crrel.usace.army.mil/techpub/CRREL_Reports/reports/SR99_12.pdf

Wang, Y., Wang, Z., Wang, C., Wang, W., 1999. Uptake of weakly hydrophobic nitroaromatics from water by semipermeable membrane devices (SPMDs) and by goldfish (*Carassius auratus*). Chemosphere, 38 (1), 51-66.

Warrelmann, J., Lenke, H., Daun, G., Walter, U., Hund, K., Knackmuss, H.-J., 1996. Microbiologische Sanierung Explosivstoff-belasteter Böden. Pilotproject auf dem Standort der Rüstungsaltlast Hessisch Lichtenau-Hirschhagen. TerraTech 2/1996, 44-47.

Wattiez, C., 2002. "Sustainable" pesticides strategy for Europe. Agro-Chemicals Report, II (4), 23-24.

Weiss, T., and Angerer, J., Belastung der Bevölkerung der Bundesrepublik Deutschland durch nitroaromatischen Verbindungen. Zwichenbericht anlässlich des Statusseminars des BWPLUS am 28.2 und 1.3.2001 in Forschungszentrul Karlruhe. Programm Lebensgrundlage Umwelt und ihre Sicherung (BWPLUS). IPASUM Erlangen.

Welsch, T., and Block, H., 1997. Separation and enrichment of traces of explosives and their by-products from water by multiple micro liquid extraction for their determination by capillary gas chromatography. Fresenius J. Anal. Chem., 357, 904-908.

Weetall, H.H., 1991. Antibodies in water immiscible solvents. Immobilized antibodies in hexane. J. Immunol. Methods., 136 (1), 139-142.

Weller, M.G., 1992. Strukturelle und kinetische Untersuchungen zur Entwicklung und Optimerung von Hapten-Enzymimmunoassays (ELISAs) am Beispiel der Bestimmung von Triazinherbiziden. PhD thesis at the Technical University Munich, published by Hieronymus Buchreproduktions GmbH, Munich.

Wharton, D.A., 2002. Life at the limits. Organisms in extreme environments. Cambridge University Press, 307 pages.

Wilkström, P., Andersson, A.-C., Nygren, Y., Sjöström, J., and Forsman, M., 2000. Influence of TNT transformation on microbial community structure in four different lake microcosms. Journal of applied Microbiology, 89, 302-308.

Wilson, R., Clavering, C., Hutchinson, A., 2003a, Paramagnetic bead based enzyme electrochemiluminescence immunoassay for TNT. J. Electroanal. Chem. 557, 109-118.

Wilson, R., Clavering, C., Hutchinson, A., 2003b, Electrochemiluminescence enzyme immunoassays for TNT and pentaerythritol tetranitrate. Anal. Chem. 75, 3912-3917. J. Electroanal. Chem., 557, 109-118.

Winklmair, M., Schuetz, A.J., Weller, M., Niessner, R., 1999. Immunochemical array for the identification of cross-reacting analytes. Fresenius J. Anal. Chem., 363, 731-737.

Wisniak, J. 2000. The history os salpeter production with a bit of pyrotechnics and Lavoisier. The Chemical Educator, 5 (4), 4401-4408.

Wolfe, N.L., Ou, T.-Y., Gunnison, D., 1994. Alternative methods for biological destruction of TNT: A preliminary feasibility assessment of enzymatic degradation. U.S. Army Corps of Engineers, Technical Report IRRP-94-3.

Wollin, K.-M., Levsen, K., 1999. Schnelle Vor-Ort-Analytik zur Untersuchung von Rüstungsaltlasten. UWSF – Z. Umweltchem. Ökotox. 11 (6), 353-364.

Won, W.D., Heckly, R. J., Glover, D.J., and Hoffsommer J.C., 1974. Metabolic disposition of 2,4,6-trinitrotoluene. Applied Microbiology, Mar 1974, 513-516.

Workman, J., Creasy, K.E., Doherty, S., Bond, L., Koch, M., Ullman, A., and Veltkamp, D.J., 2001. Process analytical chemistry. Anal. Chem., 73, 2705-2718.

Wu, Y.-C., 2001. Alkaline hydrolysis of TNT – Modeling mass transport effect. PhD thesis at University of California – Los Angeles.

Yau, K.Y.F., Lee, H., Hall, J.C., 2003. Emerging trends in the synthesis and improvement of hapten-specfic recombinant antibodies. Biotechnology Advances, 21, 599-637.

Yin, J., Beuscher, A.E., Andryski, S.E., Stevens, R.C., Schultz. P.G., 2003. Structural plasticity and the evolution of antibody affinity and specificity. J. Mol. Biol., 330, 651-656.

Yinon, J., 1990. Toxicity and metabolism of explosives. CRC Press, Boca Raton, FL, USA.

Zhang, C., Huges, J.B., Nishino, S.F., Spain, J.C., 2000. Slurry-phase biological treatment of 2,4-dinitrotoluene and 2,6-dinitrotoluene: role of bioaugmentation and effects of high dinitrotoluene concentrations. Environ. Sci. Technol, 34, 2810-2816.

Zeck, A., Weller M.G., Niessner R., 1999. Characterization of a monoclonal TNT-antibody by measurement of the cross-reactivities of nitroaromatic compounds. Fresenius J. Anal. Chem., 364, 113-120.

Annex 1.

General properties of TNT, atrazine, diuron and isoproturon

A: Data for 2,4,6-trinitrotoluene (TNT)

Chemical name (IUPAC):	2,4,6-trinitromethylbenzene
Other names:	trinitrotoluol, trinitrotoluéne, trotyl, trilite, tolit, tutol, triton, tri, Füllpulver 02 (Meyer, 1985)
Molecular formula:	$C_7H_5N_3O_6$ (structure shown in annex 4, table 11 - CRs)
Appearance:	light-yellow flakes or needles; dark when exposed to sunshine either monoclinic or orthorhombic crystals
Molecular weight:	227.133
Specific gravity	1.6 (Wu, 2001)
Detonation capacity	6900 m s^{-1}.
Melting / solidification point:	80.9°C
Thermal ignition temperature:	300°C
Stability:	Chemically and thermally stable, in the dark
Sensitivity:	Low sensitivity to impact and friction
Solubility:	Poor solubility in water, sparingly soluble in organic liquids
EU List of Priority Substances:	Not on the list of top 33 water pollutants
USA List of Priority Substances:	On the list in 2003 (i.e. the last one), rank 83 (from 275 hazardous substances)
Uses:	High explosive in the military (shells, bombs and grenades); intermediate in industrial applications
Workplace exposure:	Mostly through breathing dust and vapours and contact with dust on the skin
Contaminated resources:	Soils and waters, including agricultural soils and drinking water reservoirs
Intoxication effects:	Skin allergies, anaemia, liver malfunctions, immunity dysfunctions, cataract; possible negative effects for human reproduction system; possibly carcinogen
Recovery from intoxication:	TNT is broken down in liver and the resulting compounds are eliminated by urine

Review institutions:

U.S. EPA (Environmental Protection Agency) – http://www.epa.gov/, and U.S. ATSDR (Agency for Toxic Substances and Disease Registry), including CERCLA (Comprehensive Environmental Response, Compensation, and Liability Act) Priority List – http://www.atsdr.cdc.gov/clist.html.

Annex 1. (Continuation)

B. Data for atrazine

Chemical name (IUPAC): 2-chloro-4-ethylamino-6-isopropylamino-1,3,5-triazine

Molecular formula and structure: $C_8H_{14}ClN_5$

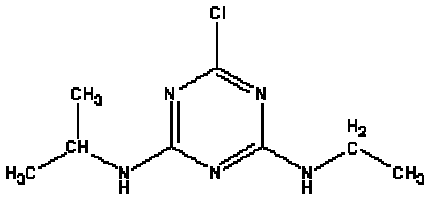

Appearance: White (colourless) powder

Molecular weight: 215.7

Melting / solidification point: 173°-177°C

Stability: Stable in the dry state. Resistant to photolysis

Solubility: 0.03 g l^{-1} in water (20°C), 15 g l^{-1} in methanol (25°C), 52 g l^{-1} in chloroform (27°C), 183 g l^{-1} in dimethyl sulfoxide (27°C)

Uses: Non-agricultural (e.g. landscape maintenance) and agricultural. Pre- and post-emergence broad spectrum herbicide. Selective / total herbicide at low / high levels, respectively. Commonly available as water dispersible granules. Estimated to be the most heavily used pesticide in USA; banned in EU.

EU List of Priority Substances: On the (alphabetic) list of top 33 water pollutants, position 3 USA

List of Priority Substances: Not on the list (of 275 hazardous substances) in 2003.

Exposure: Ingestion, inhalation and skin contact.

Contaminated resources: Soils; surface and groundwaters, including drinking waters

Intoxication effects: Especially reproductive / development negative effects; suspected carcinogen; suspected endocrine-, immuno-, gastro-intestinal-, liver-, neuro- and sense organ-toxicant

Environmental fate: It is not expected to strongly adsorb to sediments; bioconcentration is not expected to be significant. In soils, microbial degradation occurs, with half-live of 40-70 days

Review agencies:

EU Commission, Environment DG – http://europa.eu.int/comm/environment/water/water-dangersub/pri_substances.htm; U.S. EPA (Environmental Protection Agency) – http://www.epa.gov/oppsrrd1/reregistration/atrazine/; U.S. ATSDR (Agency for Toxic Substances and Disease Registry) – http://www.atsdr.cdc.gov/clist.html.

Annex 1. (Continuation)

C. Data for diuron

Chemical name (IUPAC): 3-(3,4-dichlorophenyl)-1,1-dimethylurea

Molecular formula and structure: $C_9H_{10}Cl_2N_2O$

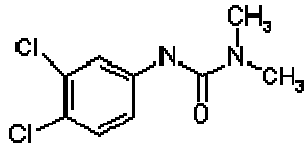

Appearance: White crystalline solid

Molecular weight: 233.1

Melting / solidification point: 158°-159°C

Stability: Stable to hydrolysis and photolysis (but it can be degraded by ultraviolet radiation). Decomposes on heating at 180-190°C

Solubility: 42 mg l^{-1} in water (25°C)

Uses: Both non-agricultural (railways, roadsides, ditches) and agricultural. Pre-emergence, total herbicide in agricultural crops, widely used as an alternative to atrazine and simazine. Available as wettable powder or liquid suspension.

EU List of Priority Substances: On the (alphabetic) list of top 33 water pollutants, position 13

USA List of Priority Substances: Not on the list (of 275 hazardous substances) in 2003.

Exposure: Ingestion, inhalation and skin contact Intoxication effects. Eye and throat irritation; depression of the central nervous system; serious health damage after prolonged exposure; possibly carcinogen

Recovery from intoxication: No specific antidote; treated symptomatically

Toxicity to aquatic system: Very high, including long-term adverse effects; especially toxic to fish and invertebrates

Contaminated resources: Surface waters, groundwaters and soils; serious risk for the drinking waters reservoirs; reduced mobility in certain soils (usually, it is adsorbed to soil organic matter and clay).

Environmental fate: Metabolized by animals, plants and micro-organisms. Moderately mobile; persistent in soils (half time 90-180 days), and in waters (half life of 43 days)

Review agencies:

EU Commission, Environment DG – http://europa.eu.int/comm/environment/water/water-dangersub/pri_substances.htm; U.S. EPA (Environmental Protection Agency) – http://www.epa.gov/oppsrrd1/reregistration/diuron/; U.S. ATSDR (Agency for Toxic Substances and Disease Registry) – http://www.atsdr.cdc.gov/clist.html.

Annex 1. (Continuation)

D. Data for isoproturon

Chemical name (IUPAC):	N,N-dimethyl-N'-[4-(1-methylethyl)phenyl]urea
Molecular formula and structure:	$C_{12}H_{18}N_2O$

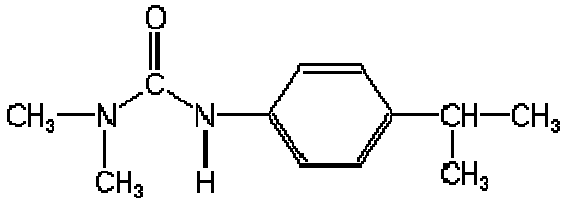

Appearance:	Crystalline solid (white powder)
Molecular weight:	206.29
Melting / solidification point:	156.5°-158°C
Stability:	Stable under anaerobic conditions (92% after 119 days); stable to photolysis (90% after 30 days)
Solubility:	70.2 g l^{-1} in water (20°C); 70 g l^{-1} in methanol (20°C); 30 g l^{-1} in acetone (20°C); 46 g l^{-1} in 1,2-dichloroethane (20°C)
Uses:	Herbicide against weeds in cereals. Commonly available as water dispersible granules
EU List of Priority Substances:	On the list (water pollutants), position 19 (alphabetic order).
USA List of Priority Substances:	Not on the list (of 275 hazardous substances) in 2003.
Contaminated resources:	Soils, surface waters and groundwaters
Exposure:	Ingestion, inhalation and skin contact
Intoxication effects	Haemolytic effects, liver degeneration (hepatocytes) and tumours
Recovery from intoxication:	It is completely metabolized, and the degradation compounds are eliminated through urine
Environmental fate:	10-20% mineralization (ring label) after 100 days, but not readily biodegradable
Toxicity to aquatic system:	High above specific concentrations for various plant and animal species

Review agencies:

EU Commission, Environment DG – http://europa.eu.int/comm/environment/water/water-dangersub/pri_substances.htm, and European Commission, Health & Consumer protection directorate-general. Report SANCO/3045/99-final from 12 March 2002, on Isoproturon, in view of inclusion of isoproturon in Annex I of Directive 91/414/EEC; U.S. EPA (Environmental Protection Agency) – http://www.epa.gov/oppsrrd1/reregistration/atrazine/.

Annex 2.

Table 10. Methods used for the analysis of explosives and their degradation products in water and soil

Table 10 – part A						
Author(s)	**Publ. year**	**Method**	**Analyte**	**Matrix**	**Detection limit**	**Test time**
SW846 Method 8330 (US-EPA)	1994	RP-HPLC-UV	TNT		0.1 µg l^{-1}	
			RDX		0.8 µg l^{-1}	
			HMX		1.0 µg l^{-1}	
			NG		ND	
SW846 Method 8095 (US-EPA)	1996	GC-ECD	TNT		0.01 µg l^{-1}	
			RDX		0.004 µg l^{-1}	
			HMX		0.004 µg l^{-1}	
			NG		0.02 µg l^{-1}	
Medintz et al.	2005	Self-assembled TNT biosensor based on modular multifunctional surface-tethered components; fluorescence resonance energy transfer (FRET)	2-amino-4,6-DNT; TNT (low specificity)		1 mg l^{-1}	
			TNB		3.5 mg l^{-1}	
Wilson et al.	2003	Paramagnetic beads based enzyme electrochemi-luminescence	TNT		31 ppb	
Bromberg and Mathies	2003	Homogeneous immunoassay on microfabricated capillary electrophoresis chip; fluorescence	TNT		1 ng ml l^{-1}	
Goldman et al.	2003	Fluorescent displacement immunoassay	TNT	artificial sea water	0.05 µg l^{-1}	
				PBS	0.5 µg l^{-1}	
Shriver-Lake et al.	2003	Field, portable, continuous flow immunosensor (FAST 2000)	TNT; RDX	ground water	10 ppb	
Gauger et al.	2001					
Charles et al.	2000			soil extracts	50-100 mg kg^{-1}	
Kusterbeck and Charles	1998					
Goldman et al.	2002	Phage displayed peptides that showed specific binding to TNT; continuous flow immunosensor	TNT	artificial sea water	12.5 – 25 mg l^{-1}	
Green et al.	2002	Reversed-displacement immunosensor, using microcolumns with Affi-Gel derivatized with TNB and labelled anti-TNT monoclonal antibody (11B3)	TNT	saline buffer	2.5 ng ml^{-1}	
				96% artificial sea water	25 ng ml^{-1} (ppb)	
Naal et al.	2002	Amperometric TNT biosensor based on the surface immobilization of a maltose binding protein (MBP) nitroreductase	TNT; 2,4-DNT		2 µM	
Sapsford et al.	2002	Array biosensor; immunoassay (Mab A1-1-1)	TNT		10 µg l^{-1}	
			TNP		5 µg l^{-1}	

Annex 2 (Continuation)

Table 10 – part B						
Author(s)	**Publ. year**	**Method**	**Analyte**	**Matrix**	**Detection limit**	**Test time**
Altstein et al.	2001	Immunoassay; Mab (SBS) entrapped in a sol-gel matrix	TNT		0.12 ppb	
Sohn et al.	2001	Sensor with a thin film of photoluminescent polysiloles	TNT	Sea water	50 ppb	
			TNP		6 ppb	
Hilmi and Luong	2000	Micromachined electrophoresis chips; electrochemical detector	TNT	soil and groundwater	110 µg l^{-1}	3 min
			2,4-DNT		150 µg l^{-1}	
			2,6-DNT		160 µg l^{-1}	
			2,3-DNT		150 µg l^{-1}	
			RDX		200 µg l^{-1}	
Lan et al.	2000	Optical detector and sol-gel incapsulated anti-TNT antibody	TNT		0.2 ppm	
Kusterbeck and Shriver-Lake	2000	Field, portable, semi-automatic fiber optic biosensor (Analyte 2000)	TNT; RDX	ground water	10 mg l^{-1}	12-17 min
				soil	100 mg l^{-1}	
Van Bergen et al.	2000			ground water	5 µg l^{-1}	<20 min
Wallenborg and Bailey	2000	Microfabricated chip using micellar electokinetic chromatography (MEKC) and indirect laser-induced fluorescence (IDLIF)	TNT	soil extracts	1 ppm (w/w)	
			TNB			
			DNB			
			2,4-DNT			
			2,6-DNT			
			2-Amino-4,6-DNT			
			4-Amino-2,6-DNT			
			Tetryl			
Rabbany et al.	2000; 1998	Membrane based displacement immunoassay	TNT; RDX		450 fmol (100 µl, 1 ng/ml)	5 min
Balkatcheva et al.	1999	Fiber optic biosensor; single and multi analyte detection	TNT		5 µg l^{-1}	30 min
			RDX		2.5 µg l^{-1}	
Echols et al.	1999	Sequential injection spectrophotometry (very selective)	TNT		500 µg l^{-1}	
				soil extracts	80 µg g^{-1}	
Heiss et al.	1999	Dip-and-read test strips (apoenzyme reactivation immunoassay system – ARIS)	TNT	drinking water	0.7 µg l^{-1}	15-20 min
Barshick and Griest	1998	Solid-phase microextraction and gas chromatography / Ion trap mass spectrometry (SPME + GC / ITMS)	TNT	sea water	210 ppt	20 min
			RDX		1900 ppt	
Darrach et al.	1998	Solid phase microextraction and Reversal electron attachment detection (SPME / READ)	TNT	lab samples; water	10 ppt	
Dosch et al.	1998	Homogeneous immunoassay based on the reactivation of apoglucose oxidase	TNT		5 µg l^{-1}	<30 min

Annex 2 (Continuation)

Table 10 – part C						
Author(s)	**Publ. year**	**Method**	**Analyte**	**Matrix**	**Detection limit**	**Test time**
Marquette and Blum	1998	Electrochemiluminescence; optical immunosensing; flow-injection	2,4-DNT		0.2 µg l^{-1}	
Walsh and Ranney	1998	Solid-phase extraction and gas-chromatography – electron capture detection (SPE and GC-ECD)	TNT		0.01 µg l^{-1}	
			Amino-DNTs		0.003 µg l^{-1}	
Narang et al.	1997	Displacement flow immunosensor for explosives using microcapillaries	TNT		440 amol (100 µl, 1 pg ml^{-1})	
Bart et al.	1997	Continuous flow immunosensor (CFI)	TNT	ground water	50 ppb	<10 min
			RDX		20 ppb	
Thorne et al.	1997	D Tech test-kit (ELISA)	TNT	natural water	5 µg l^{-1}	
Craig et al.	1995	Ohmicron test-kit (ELISA) CRREL /EnSys test-kit (ELISA)	TNT	ground water	0.07 µg l^{-1}	
			RDX		3.8 µg l^{-1}	
Jenkins and Walsh	1992	Potassium hydroxide and sodium sulphide; anion indicator resin; absorbance	TNT	soil (extr. by acetone)	1 µg g^{-1}	
			2,4-DNT		2 µg g^{-1}	
			RDX		2 µg g^{-1}	
Medary	1992	Rapid field testing; sodium hydroxide	TNT	soil (extr. by methanol)	4-8 ppm	
Heller et al.	1982	Indicator tube containing CaO – coated beads and an anion indicator resin (alkyl quaternary amine chloride exchange resin)	TNT or TNT plus its photo-degradation compounds	effluent water from ammunition plants	0.1 ppm	

Annex 3.

Figure 110.

View of the developed sensor field prototype (lid on; in the GSF-IÖC laboratory).

Figure 111. View of a set of 10 chips which could be measured in one day

Annex 4.

Table 11. Nitroaromatic compounds used in ELISA, with molecular structures and measured cross-reactivity (CR).

table 11 – part A			
No.	**Compound**	**Molecular structure**	**CR (%)**
1.	2,4,6-Trinitrotoluene (TNT)	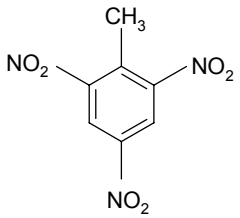	100
2.	1,3,5-Trinitrobenzene	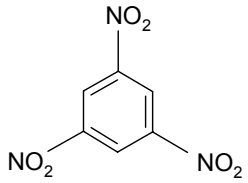	13.2
3.	2,4,6-TNP-Glycylglycine (hapten conjugated to HRP)	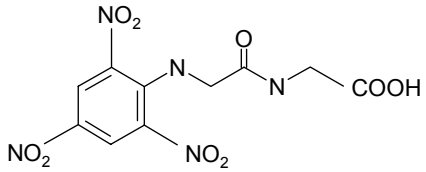	12.2
4.	2-Amino-4,6-Dinitrotoluene	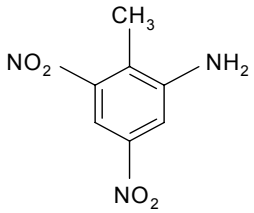	5.4
5.	2,4,6-TNP-Glycine (hapten conjugated to HRP)	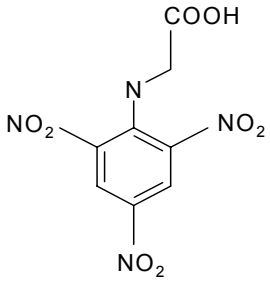	3.6
6.	2,4-Dinitrotoluene	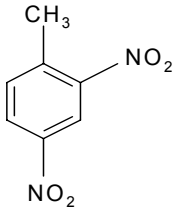	3.2

Annex 4. (Continuation)

table 11 – part B			
No.	**Compound**	**Molecular structure**	**CR (%)**
7.	2,4,6-TNP-α-Aminobutyric Acid (hapten conjugated to HRP)	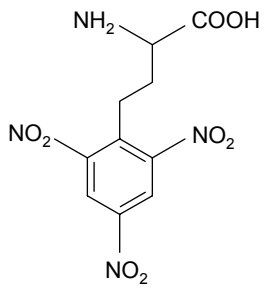	1.6
8.	3,5-Dinitroaniline	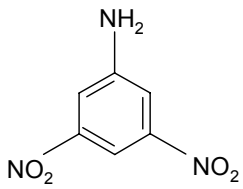	1.1
9.	2,4-DNP-γ-Aminobutyric Acid (hapten conjugated to HRP)	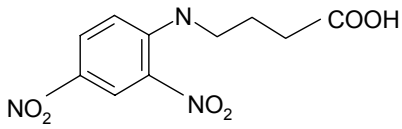	0.5
10.	2,4-DNP-ε-Aminocaproic Acid (hapten conjugated to HRP)	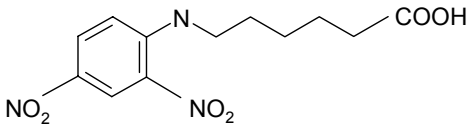	0.3
11.	1,3-Dinitrobenzene	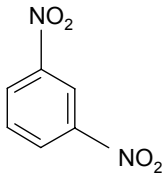	0.3
12.	2,6-Dinitroaniline	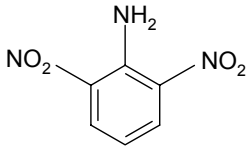	0.3
13.	4-Amino-2,6-Dinitrotoluene	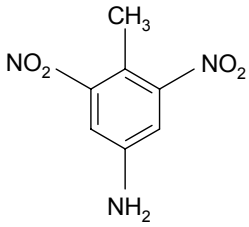	0.2

Annex 4 (Continuation)

table 11 – part C			
No.	**Compound**	**Molecular structure**	**CR (%)**
14.	2,6-Dinitrotoluene	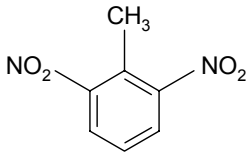	0.1
15.	2,4-DNP-Glycine (hapten conjugated to HRP)	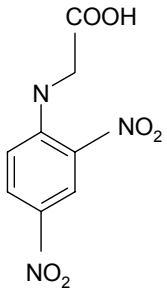	< 0.1
16.	2,4-Diamino-6-Nitrotoluene	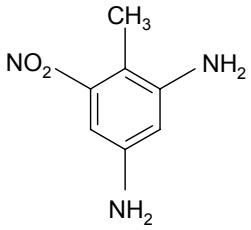	< 0.1
17.	2-Nitrotoluene	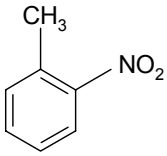	< 0.1
18.	3-Nitrotoluene	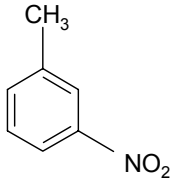	< 0.1
19.	4-Nitrotoluene	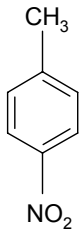	< 0.1
20.	Nitrobenzene	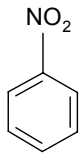	< 0.1

Annex 5.

Figure 112. Example of two-dimensional titration with three concentrations of the anti-TNT antibody and eight dilutions of the enzyme-tracer TNP-glycylglycine – HRP: lower tracer dilutions.

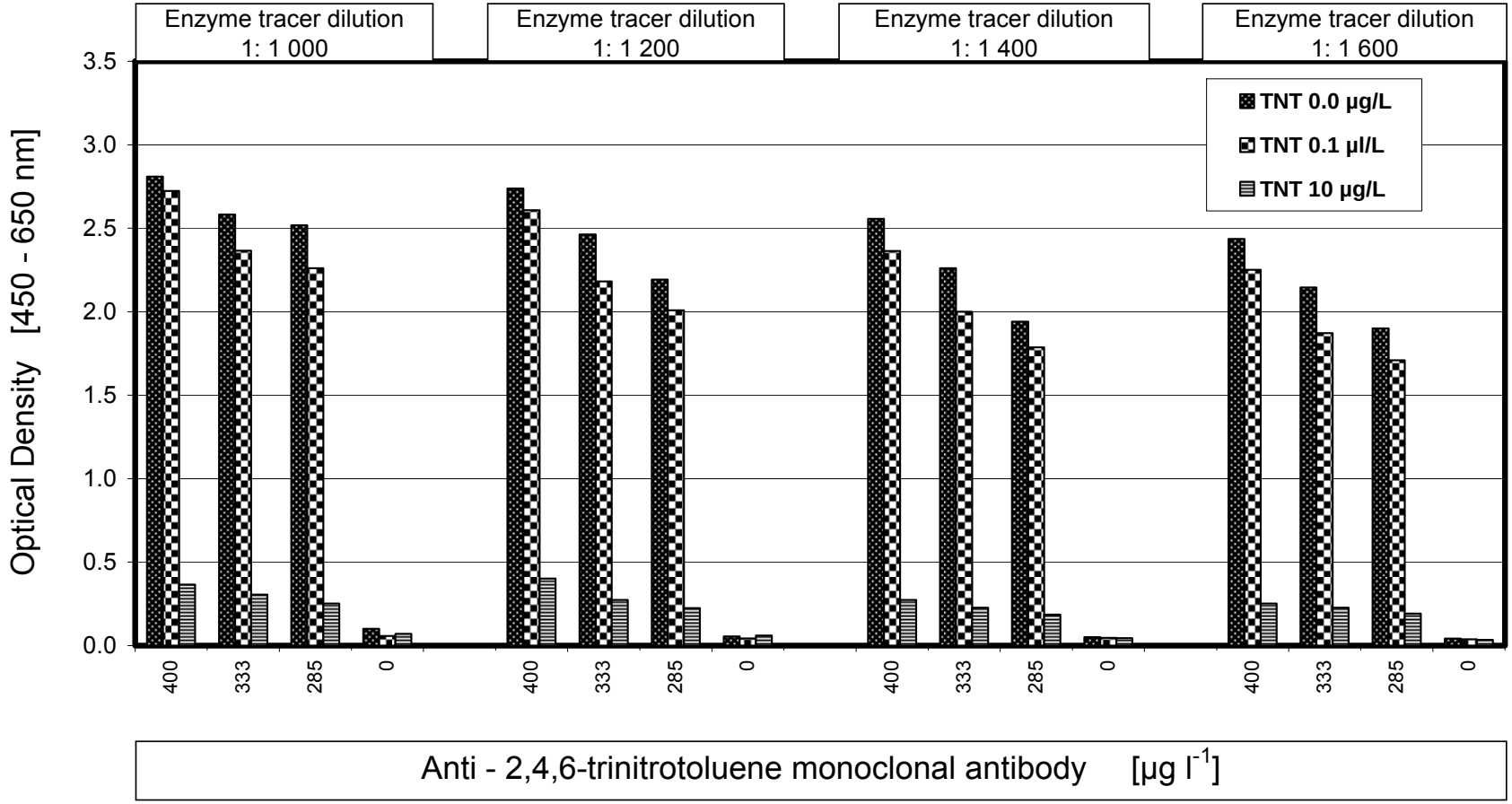

Annex 5. (Continuation)

Figure 113. Example of two-dimensional titration with three concentrations of the anti-TNT antibody and eight dilutions of the enzyme-tracer TNP-glycylglycine – HRP: higher tracer dilutions.

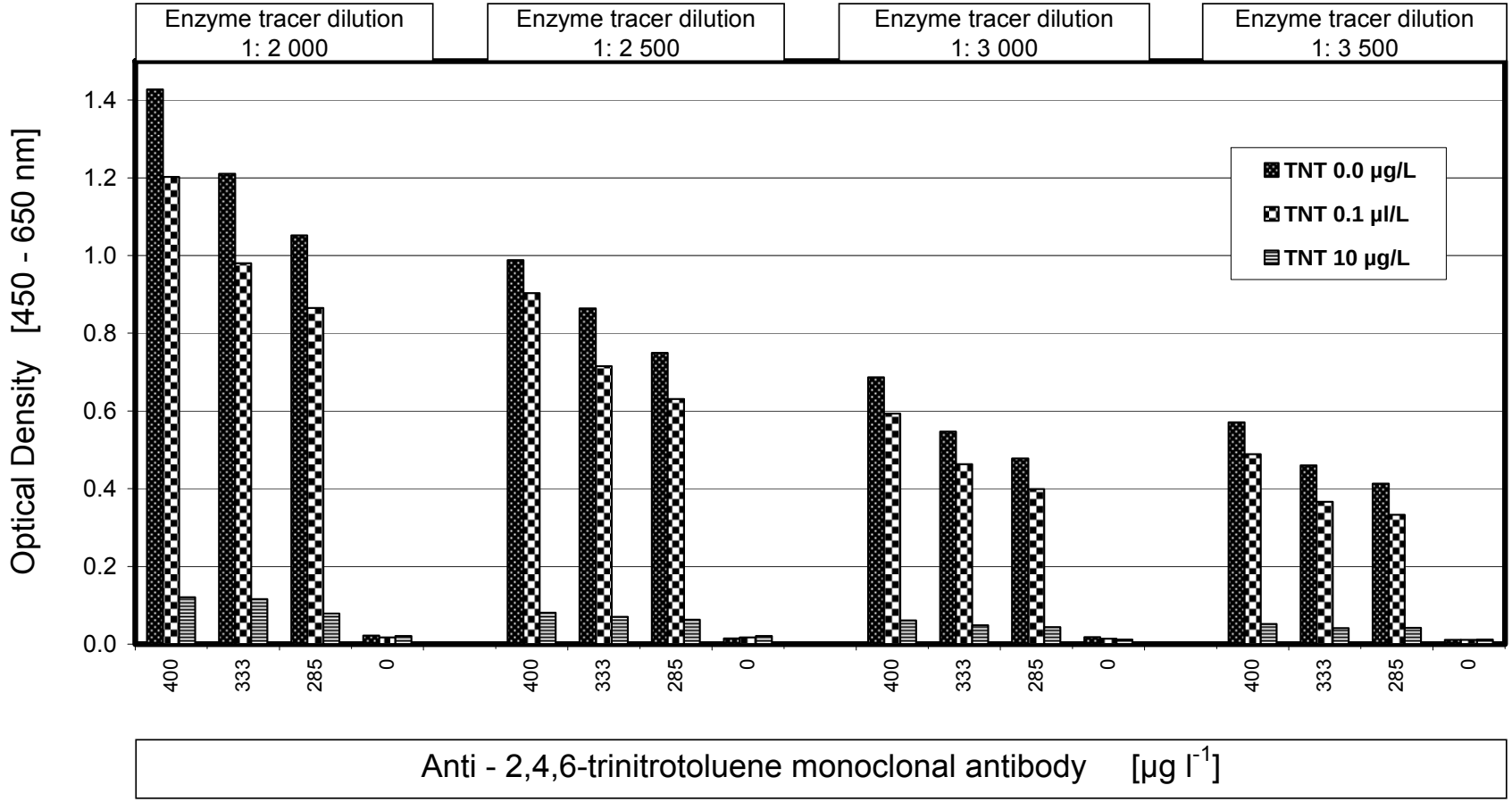

Annex 6.

Table 12. Comparative table with standard curve parameters obtained with various catching proteins in TNT-ELISA

Date y/m/d & Plate	Coating solution		mAb dil.	Nr of repl. (wells)	Enzyme tracer (incubation duration: 30 min)	Tr Dil	TNT	H_2O_2 / TMB pre-inc. (min)	A	B	C (IC50)	D	R^2	Notes
	Name													
02/04/2022	**Gam**	**1000**	**35000**	**3**	TNP-Glycylglycine-HRP-220102 (Aglyc3)-sf	**2000**	**10**	**10**	**0.596**	0.791	**0.373**	0.010	0.990	RT; An in water
02/04/2024	**Gam**	**1000**	**35000**	**3**	TNP-Glycylglycine-HRP-220102 (Aglyc3)-sf	**2000**	**10**	**10**	**1.547**	0.959	**0.769**	0.019	0.999	Re-do 02.04.22
02.02.12-2	**Gam**	**1000**	**35000**	**4**	TNP-Glycylglycine-HRP-220102 (Aglyc2)	**1600**	**3**	**30**	**0.443**	0.801	**0.679**	0.033	0.997	An in water
02.02.12-2	**Gam**	**1000**	**35000**	**4**	TNP-Glycylglycine-HRP-220102 (Aglyc2)	**1600**	**3**	**30**	**0.476**	0.852	**0.515**	0.034	0.994	An in PBS
02.04.16-5	**Gam**	**1000**	**35000**	**4**	TNP-Glycylglycine-HRP-220102 (Aglyc3)	**2000**	**30**	**30**	**0.916**	0.879	**0.583**	0.028	0.998	An in PBS
02.04.19-1	**Gam**	**1000**	**35000**	**3**	TNP-Glycylglycine-HRP-220102 (Aglyc3)-sf	**2000**	**30**	**10**	**1.709**	1.008	**0.603**	0.020	0.999	An in PBS
02.04.19-2	**Gam**	**1000**	**35000**	**3**	TNP-Glycylglycine-HRP-220102 (Aglyc3)-sf	**1000**	**30**	**5**	**1.354**	0.972	**0.628**	0.020	0.999	An in PBS
02.08.08-1	**Gam**	**1000**	**35000**	**4**	TNP-Glycylglycine-HRP-030402 (Aglyc3-sf)	**2000**	**2**	**10**	**1.008**	0.911	**0.803**	0.016	0.999	
02.08.20-4	**Gam**	**1000**	**15000**	**4**	TNP-Glycylglycine-HRP-030402 (Aglyc3-sf)	**2000**	**2**	**10**	**0.566**	0.833	**1.036**	0.008	0.992	
02.08.20-6	**Gam**	**1000**	**25000**	**4**	TNP-Glycylglycine-HRP-030402 (Aglyc3-sf)	**2000**	**2**	**10**	**0.585**	0.461	**0.439**	-0.016	0.985	
02.02.12-1	**Prot. A**	**1000**	**35000**	**4**	TNP-Glycylglycine-HRP-220102 (Aglyc2)	**1600**	**3**	**30**	**0.160**	0.871	**0.546**	0.015	0.999	An in water
02.02.12-1	**Prot. A**	**1000**	**35000**	**4**	TNP-Glycylglycine-HRP-220102 (Aglyc2)	**1600**	**3**	**30**	**0.233**	0.970	**0.512**	0.016	0.989	An in PBS
02.04.16-5	**Prot. A**	**1000**	**35000**	**4**	TNP-Glycylglycine-HRP-220102 (Aglyc3)	**2000**	**30**	**30**	**0.064**	1.068	**0.407**	0.029	0.910	An in PBS
02.04.16-6	**Prot. A**	**1000**	**35000**	**4**	TNP-Glycylglycine-HRP-220102 (Aglyc3)	**1500**	**30**	**30**	**0.062**	0.346	**2.74E+07**	-1.260	0.725	An in PBS
02.04.16-6	**Prot. A**	**1000**	**35000**	**4**	TNP-Glycylglycine-HRP-220102 (Aglyc3)	**2500**	**30**	**30**	**0.053**	0.737	**0.299**	0.026	0.865	An in PBS
02.04.19-1	**Prot. A**	**1000**	**35000**	**3**	TNP-Glycylglycine-HRP-220102 (Aglyc3)-sf	**2000**	**30**	**10**	**0.048**	0.764	**0.442**	0.014	0.986	An in PBS
02.04.19-2	**Prot. A**	**1000**	**35000**	**3**	TNP-Glycylglycine-HRP-220102 (Aglyc3)-sf	**1000**	**30**	**5**	**0.037**	1.009	**0.732**	0.013	0.983	An in PBS
02.08.08-2	**Prot. A**	**1000**	**35000**	**3**	TNP-Glycylglycine-HRP-030402 (Aglyc3-sf)	**2000**	**2**	**30**	**0.054**	1.624	**0.589**	0.022	0.979	
02.08.20-5	**Prot. A**	**1000**	**15000**	**3**	TNP-Glycylglycine-HRP-030402 (Aglyc3-sf)	**2000**	**2**	**10**	**0.063**	0.359	**0.049**	0.009	0.982	
02.08.20-7	**Prot. A**	**1000**	**25000**	**3**	TNP-Glycylglycine-HRP-030402 (Aglyc3-sf)	**2000**	**2**	**10**	**0.046**	0.642	**0.780**	0.016	0.934	

Annex 6. (Continuation)

Table 12. (Continuation)

Date y/m/d & Plate	Coating solution		mAb dil.	Nr of repl. (wells)	Enzyme tracer (incubation duration: 30 min)	Tr Dil	TNT	H_2O_2 / TMB pre-inc. (min)	A	B	C (IC50)	D	R^2	Notes
	Name	Dil.												
02.04.22	**Prot. A/G**	**1000**	**35000**	**3**	TNP-Glycylglycine-HRP-220102 (Aglyc3)-sf	**2000**	**10**	**10**	**0.205**	1.026	**0.469**	0.009	0.997	Coating 2h
02.04.24	**Prot. A/G**	**1000**	**35000**	**3**	TNP-Glycylglycine-HRP-220102 (Aglyc3)-sf	**2000**	**10**	**10**	**0.456**	0.837	**0.474**	0.006	0.998	As on 02.04.22
02.04.30-1	**Prot. A/G**	**1000**	**25000**	**3**	TNP-Glycylglycine-HRP-030402 (Aglyc3-sf)	**1500**	**2**	**15**	**0.660**	0.959	**0.574**	0.015	0.999	
02.04.30-1	**Prot. A/G**	**1000**	**30000**	**3**	TNP-Glycylglycine-HRP-030402 (Aglyc3-sf)	**1500**	**2**	**15**	**0.606**	0.938	**0.560**	0.013	0.998	
02.04.30-2	**Prot. A/G**	**1000**	**25000**	**3**	TNP-Glycylglycine-HRP-030402 (Aglyc3-sf)	**2000**	**2**	**30**	**1,116**	1,042	**0.656**	0.017	1.000	
02.04.30-1	Prot. A/G	**1000**	**30000**	**3**	TNP-Glycylglycine-HRP-030402 (Aglyc3-sf)	**1500**	**2**	**15**	0.606	0.938	**0.560**	0.013	0.998	
02.04.30-2	Prot. A/G	**1000**	**25000**	**3**	TNP-Glycylglycine-HRP-030402 (Aglyc3-sf)	**2000**	**2**	**30**	1,116	1,042	**0.656**	0.017	1.000	
02.04.30-2	Prot. A/G	**1000**	**30000**	**3**	TNP-Glycylglycine-HRP-030402 (Aglyc3-sf)	**2000**	**2**	**30**	1,083	1,031	**0.563**	0.029	0.999	
02.08.08-2	Prot. A/G	**1000**	**35000**	**2**	TNP-Glycylglycine-HRP-030402 (Aglyc3-sf)	**2000**	**2**	**30**	0.666	0.863	**0.635**	0.009	0.995	
02.08.20-5	Prot. A/G	**1000**	**15000**	**2**	TNP-Glycylglycine-HRP-030402 (Aglyc3-sf)	**2000**	**2**	**10**	0.247	0.737	**0.582**	0.009	0.991	
02.08.20-7	Prot. A/G	**1000**	**25000**	**2**	TNP-Glycylglycine-HRP-030402 (Aglyc3-sf)	**2000**	**2**	**10**	0.251	0.477	**0.316**	0.004	0.977	
02.08.08-1	Prot. G	**1000**	**35000**	**4**	TNP-Glycylglycine-HRP-030402 (Aglyc3-sf)	**2000**	**2**	**10**	0.148	0.887	**0.627**	0.015	0.998	
02.08.08-2	Prot. G	**1000**	**35000**	**3**	TNP-Glycylglycine-HRP-030402 (Aglyc3-sf)	**2000**	**2**	**30**	0.411	0.845	**0.495**	0.015	0.998	
02.08.20-4	Prot. G	**1000**	**15000**	**4**	TNP-Glycylglycine-HRP-030402 (Aglyc3-sf)	**2000**	**2**	**10**	0.247	0.855	**0.684**	0.011	0.994	
02.08.20-5	Prot. G	**1000**	**15000**	**3**	TNP-Glycylglycine-HRP-030402 (Aglyc3-sf)	**2000**	**2**	**10**	0.248	0.636	**0.386**	0.007	0.989	
02.08.20-6	Prot. G	**1000**	**25000**	**4**	TNP-Glycylglycine-HRP-030402 (Aglyc3-sf)	**2000**	**2**	**10**	0.241	0.536	**0.299**	0.003	0.989	
02.08.20-7	Prot. G	**1000**	**25000**	**3**	TNP-Glycylglycine-HRP-030402 (Aglyc3-sf)	**2000**	**2**	**10**	0.215	0.596	**0.373**	0.013	0.991	

Annex 7.

Specific programs for the automatic steps carried with the developed sensor

Table 13.
Automatic steps: Program for fluid handling and measurement of one chip

Assay format: competitive saturation (fig. 90B: from 19 August 2003)

V1…V7: valves; P1 = pump
0 = off (valve closed; pump stay); 1 = on (valve opened; pump go)
Psample = pumping sample; PTr = pumping enzyme tracer;
Isatr = incubation of the analyte / enzyme-tracer mixture;
wash1 = wash via valves V3-V4-V7; wash2 = washing via valves V3-V5-V7
Psubstr = pumping substrate; Isubstr = incubating substrate
wash3 = washing via V3-V5-V6; Empty pump = emptying the pump (to waste)
End = end of the automatic sequence of steps; 1000 = as long as needed; 1001 = stop

Job no	Job title	V1	V2	V3	V4	V5	V6	V7	P1	Duration(s)
1	Psample	0	1	0	0	1	0	1	1	120
2	PTr	0	1	0	1	0	0	1	1	1
3	Psample	0	1	0	0	1	0	1	1	2
4	PTr	0	1	0	1	0	0	1	1	1
5	Psample	0	1	0	0	1	0	1	1	2
6	PTr	0	1	0	1	0	0	1	1	1
7	Psample	0	1	0	0	1	0	1	1	2
8	PTr	0	1	0	1	0	0	1	1	1
9	Psample	0	1	0	0	1	0	1	1	2
10	PTr	0	1	0	1	0	0	1	1	1
11	Psample	0	1	0	0	1	0	1	1	2
12	PTr	0	1	0	1	0	0	1	1	1
13	Psample	0	1	0	0	1	0	1	1	2
14	PTr	0	1	0	1	0	0	1	1	1
15	Psample	0	1	0	0	1	0	1	1	2
16	PTr	0	1	0	1	0	0	1	1	1
17	Psample	0	1	0	0	1	0	1	1	2
18	PTr	0	1	0	1	0	0	1	1	1
19	Psample	0	1	0	0	1	0	1	1	2
20	PTr	0	1	0	1	0	0	1	1	1
21	Psample	0	1	0	0	1	0	1	1	2
22	PTr	0	1	0	1	0	0	1	1	1
23	Psample	0	1	0	0	1	0	1	1	2
24	PTr	0	1	0	1	0	0	1	1	1
25	Psample	0	1	0	0	1	0	1	1	2
26	PTr	0	1	0	1	0	0	1	1	1
27	Psample	0	1	0	0	1	0	1	1	2
28	PTr	0	1	0	1	0	0	1	1	1
29	Psample	0	1	0	0	1	0	1	1	2
30	PTr	0	1	0	1	0	0	1	1	1
31	Psample	0	1	0	0	1	0	1	1	2
32	PTr	0	1	0	1	0	0	1	1	1
33	Psample	0	1	0	0	1	0	1	1	2
34	PTr	0	1	0	1	0	0	1	1	1
35	Psample	0	1	0	0	1	0	1	1	2
36	PTr	0	1	0	1	0	0	1	1	1
37	Psample	0	1	0	0	1	0	1	1	2
38	PTr	0	1	0	1	0	0	1	1	1
39	Psample	0	1	0	0	1	0	1	1	2
40	PTr	0	1	0	1	0	0	1	1	1
41	Isatr	0	0	0	0	0	0	0	1	600
42	wash1	0	0	1	1	0	0	1	1	180
43	wash2	0	0	1	0	1	0	1	1	180
44	Psubstr	1	0	0	0	1	0	1	1	25
45	Isubstr	0	0	0	0	0	0	0	0	60
46	wash3	0	0	1	0	1	0	1	1	180
47	Empty pump	0	0	0	0	0	0	0	0	1000
48	End	0	0	0	0	0	0	0	0	1001

Annex 7. (Continuation)

Table 14.
Automatic steps: Program for preparation washing (for making the conduit air-free) before starting any measurement and after finishing all the measurements

Automatic steps and duration										
Wash1 = washing via V1-V5-V7; Wash2 = washing via V3-V4-V7; Wash3 = washing via V2-V6-V7; Empty pump = emptying the pump (to waste); End = end of the steps sequence; 1000 = as long as needed; 1001 = stop										
Job no	**Job title**	**V1**	**V2**	**V3**	**V4**	**V5**	**V6**	**V7**	**P1**	**Duration (s)**
1	Wash1	1	0	0	0	1	0	1	1	120
2	Wash2	0	0	1	1	0	0	1	1	120
3	Wash3	0	1	0	0	0	1	1	1	120
4	Empty pump	0	0	0	0	0	0	0	0	1000
5	End	0	0	0	0	0	0	0	0	1001

Table 15.
Automatic steps: Program for substrate set-up before measurements

Automatic steps and duration										
Psubstr = pumping substrate; Wash1 = washing via V3-V6-V7; Wash2 = washing via V2-V6-V7 Empty pump = emptying the pump (to waste); End = end of the steps sequence; 1000 = as long as needed; 1001 = stop										
Job no	**Job title**	**V1**	**V2**	**V3**	**V4**	**V5**	**V6**	**V7**	**P1**	**Duration (s)**
1	Psubstr	1	0	0	0	0	1	1	1	100
2	Wash1	0	0	1	0	0	1	1	1	120
3	Wash2	0	1	0	0	0	1	1	1	120
4	Empty pump	0	0	0	0	0	0	0	0	1000
5	End	0	0	0	0	0	0	0	0	1001

Table 16.
Automatic steps: Program for the washing of the ground plate in between measurements (to avoid inter-measurements contamination).

Automatic steps and duration										
Wash1 = washing via V2-V6-V7; Wash2 = washing via V1-V5-V7; Wash3 = washing via V3-V4-V7; Empty pump = emptying the pump (to waste); End = end of the steps sequence; 1000 = as long as needed; 1001 = stop										
Job no	**Job title**	**V1**	**V2**	**V3**	**V4**	**V5**	**V6**	**V7**	**P1**	**Duration (s)**
1	Wash1	0	1	0	0	0	1	1	1	120
2	Wash2	1	0	0	0	1	0	1	1	120
3	Wash3	0	0	1	1	0	0	1	1	120
4	Empty pump	0	0	0	0	0	0	0	0	1000
5	End	0	0	0	0	0	0	0	0	1001

Annex 8.

The edge effect observed with TNT-ELISA mounted ca 10% of the zero dose

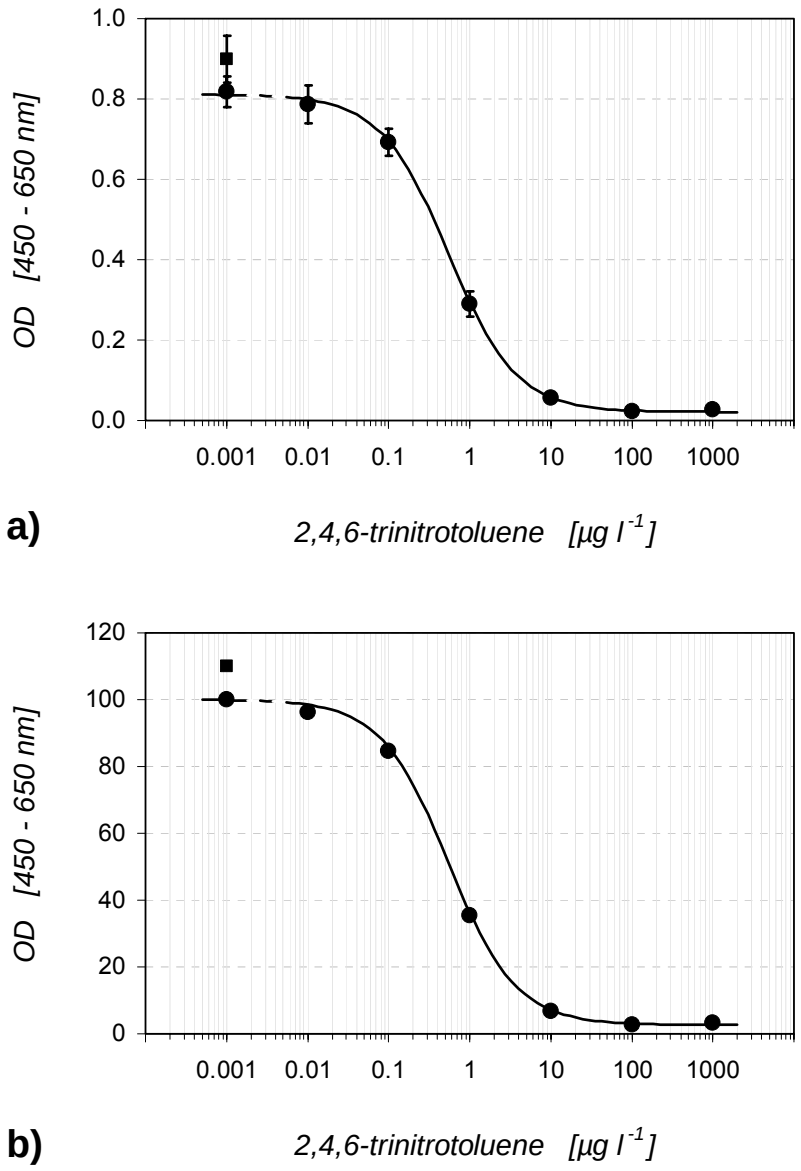

Figure 114. Standard curve (●) and edge effect (■) with TNT-ELISA. The number of measurements (n) was 5 for standards, 30 for the zero dose and 30 for the edge zero dose. The zero dose is represented as 0.001 µg l^{-1} and separated from the first real concentration by an interrupted line. The standard curve was fitted with the 4-parameter equation (eq. 6), with the following values obtained for the curve parameters:

a) OD: A = 0.81; B = 1.04; C (IC_{50}) = 0.54; D = 0.02; R^2 = 1.00;

b) %Control: A = 100; B = 1.04; C (IC_{50}) = 0.54; D = 2; R^2 = 1.00.

CURRICULUM VITAE

Personal data

Name and last name:	Ioan Manuel Ciumasu
Birth date / place:	September 17, 1975 / Roman, Neamt county, Romania
Citizenship:	Romanian

Pre-University education

1982-1990: Primary and secondary school in Roman (general education)

1990-1994: "Roman Voda" Theoretical High School, specialization chemistry-biology

Undergraduate studies

1994-1998: "Alexandru Ioan Cuza" University of Iasi, Faculty of Biology, Iasi, Romania.

1997: 18.08-15.09: Bi-lateral exchange scholarship at "Aristotle" University of Thessaloniki, Greece, summer school in Modern Greek.

1998: Licence in Biology (diploma; B.Sc.). Thesis title: Flora and vegetation of the environs of town Roman, Neamt County.

1998: 06-18.06, Franco-Romanian summer school in biochemistry: "Glycobiology, Glycotechnology and Glycopathology", at "Alexandru Ioan Cuza"University of Iasi, with the collaboration of French government and University of Lille, France.

Graduate studies

1998-2000: "Alexandru Ioan Cuza" University of Iasi, Iasi, Romania. Thorough studies in biology - biological resources

2000: EU Socrates scholarship: one semester at the University of Groningen, Groningen, the Netherlands, Institute of Biology

2001: Master of Science (diploma of thorough studies; MSc). Thesis title: The importance of spatial scale in the study of the effects of grazing upon plant diversity in the salt marshes of the Dutch Wadden Sea area.

2001-2005: PhD student (promotion biology) at the Technical University of Munich, WZW Centre for Life and Food Sciences, Department of Ecological Chemistry and Environmental Analysis, Univ. Professor Dr. Antonius A. Kettrup.
2001-2004: guest scientist at the GSF – National Research Centre for Environment and Health, Neuherberg, Institute of Ecological Chemistry.